An investigation in the *in vitro* and *in vivo* use of microcarrier beads to support keratinocytes and the effect on wound contraction

Mohamed Eldardiri MB Bch MSc MRCS (Ed)

Thesis submitted to UCL University College London 2014

Declaration

I, Mohamed Eldardiri confirm that the work presented in the thesis is my own. Where information has been derived from other sources, I confirm that this has been indicated in the thesis.

Signature:

Date:

Abstract

Full thickness burns and trauma resulting in extensive full thickness skin loss or devitalisation gives rise to the need for skin replacement therapy. Cultured epithelial autologous keratinocytes application has been the main stay treatment over the last three decades. Different methods for cultured epithelial autologous keratinocytes delivery exist with thin epithelial sheet application and sprayed cell culture the most commonly used methods; each method has its advantages and drawbacks.

Microcarrier beads for the culture of cells have been utilised in a number of different applications over the last forty years as they allow rapid cell culture and expansion in a controlled environment. More recently microcarrier commercially available gelatin microcarrier beads "Cultispher G®" have demonstrated the potential to support keratinocyte cell culture and proliferation *in vitro*.

Wound contraction is a physiological component of wound healing and occurs within the proliferation phase of wound healing between 4 days to 3 weeks following the inflammatory phase. Wound contraction is a function of myofibroblasts leading to approximation of the wound margins and reduction in wound size. The migration of keratinocytes from the intact epithelium around the wound edges leads to epithelial closure and completes the process of wound healing.

This study aimed to assess the use of microcarriers for supporting keratinocyte growth *in vitro* and evaluate the effect of keratinocyte delivery using microcarriers on wound contraction using a porcine wound model. In this study, *in vitro* assessment of keratinocyte expansion on microcarriers demonstrated sustainable expansion rates with data being comparable to traditional keratinocyte cell culture. Animal experiments utilising an *in vivo* porcine model have shown that keratinocytes delivered to the wound bed using gelatin microcarriers migrated off the beads and were shown to survive on the wound bed.

In the same animal model, autologous keratinocytes cultured on microcarrier beads reduced wound contraction when applied to full thickness wounds in combination with widely meshed autologous split skin graft compared with split thickness skin graft (STSG) alone or control wounds.

The use of allogeneic cultured keratinocytes on microcarriers in combination with dermal regeneration template "Integra®" demonstrated a reduction in wound contraction compared with Integra® and STSG or Integra® alone. The use of autologous cultured keratinocytes and fibroblasts on microcarriers in combination with Integra® reduced wound contraction compared with Integra and cultured keratinocytes or Integra and STSG. The reduction in wound contraction maintained a large area of the original wound surface area, hence reducing the possibility of contracture formation.

The use of microcarrier beads for culture and delivery of keratinocytes has the potential to overcome the disadvantages of the traditional methods of keratinocyte culture and delivery. It can also play a role in the reduction of wound contraction resulting in the retention of skin mobility and providing favourable functional and aesthetic outcomes.

Table of Contents

List of figures

List of tables

Acknowledgement

I would like to thank my supervisors Justin Sharpe and Dr Paul Sibbons for their support and guidance during the course of this thesis. Very special thanks to Prof Tony Metcalfe (Director of research, Blond McIndoe Research Foundation) for all his time and effort in checking the final amendments of the thesis.

In addition, I would also like to thank all the staff at Blond McIndoe research foundation for their help with 3T3 cells preparation, cell culture maintenance, and the histology of the animal experiments.

My thanks go to all the staff at NPIMR (Northwick Park Institute for medical research) for all their help with the animal procedures. This work was generously funded by "SPARKS" charity for children's health.

Finally, I would like to thank my wife Sobia for her encouragement and support during the whole time of this project.

Chapter 1: Introduction

1.1 Anatomy and functions of human skin

The skin covers the entire interface between the human body and the outside environment. “The integument” is the term used to describe the skin and its appendages. These appendages include hair follicles, sebaceous glands, sweat glands, and the nail apparatus.

The skin plays an important role in the interaction of the body with the outside environment. It covers an average surface area of more than 1.5 m^2 in an adult making up in total about 6-8 % of total body weight (Slominski *et al.* 2008).

The multiple functions of skin include acting as a barrier to physical, biological and chemical agents, as well as to ultraviolet (UV) radiation. The barrier function of skin prevents dehydration by controlling loss of fluid (Frodin and Skogh 1984). Other functions include sensory and thermoregulatory role through sweat secretion, vitamin D synthesis, and excretion of metabolic waste products through sweat glands (Sato *et al.* 1989). Another important role of skin is the change in appearance produced by the action of underlying muscles controlled by the sympathetic nervous system and related to emotional expression (Roosterman *et al.* 2006).

Two types of skin are found: non-hairy “glabrous” skin (covering the palms of the hands and soles of the feet) and hairy skin (covering the majority of the body surface area). The skin is formed of two distinctive layers: the outer epidermal layer and the inner dermal layer (Mackenzie 1969).

The combined thickness of the epidermis and dermis is around 0.5 to 4 mm depending on the anatomical site and type of skin. Thick skin is found in the palms of the hand and soles of the feet (4 mm thick), while thin skin (0.5 mm thick) is found on the eyelids. The epidermis is firmly attached to the underlying dermis through the basement membrane. Epidermal projections into the dermis are formed known as ‘rete ridges’ or

'pegs'. Complementary projections of the dermis into the epidermis are called dermal papillae.

The epidermis is a stratified squamous epithelium, which includes several cell types. These cell types include keratinocytes, melanocytes-which produce melanin pigment-Langerhans cells-which have an immune function-and Merkel cells which have a sensory function (Gottschaldt and Vahle-Hinz 1981). Keratinocytes, which are the predominant cells within the skin, make up at least 80% of the epidermis cellular population (Prunieras 1979).

The epidermis is arranged into four distinct layers, each showing a pattern of keratinocyte proliferation, differentiation and maturation. The four main layers are: stratum basale (germinal layer), spinosum, granulosum and corneum. In glabrous skin, a fifth layer called the stratum lucidum is found between the granular and the cornified layers. These layers reflect the differentiation of keratinocytes as they are displaced from the basal layer to the outermost cornified layer. The process of terminal differentiation involves a series of biochemical and morphological changes, which result in the production of an anucleate cornified keratinocyte layer forming the stratum corneum.

The stratum basale is a single layer of cuboidal basal cells attached to the basement membrane by hemi-desmosomes containing integrins. Adjacent cells are attached by desmosomes containing cadherins. The majority of the cells in this layer are mitotically active and their role in the renewal of the epidermis is through upward displacement, replacing the outermost superficial layer lost during normal epidermal turnover (Prunieras *et al.* 1976).

Above the stratum basale is the stratum spinosum consisting of several layers of irregular, polyhedral shaped cells that display spiny projections. Cells from the previous layer lose contact with the basement membrane and are subsequently pushed up to form this layer (Ehrlich 2004). Cells become progressively flattened as they move up towards

the epithelial surface. Cells contain lamellar granules, which provide the epidermal lipids responsible for the barrier properties of the skin.

Above the stratum spinosum is the stratum granulosum, which is comprised of three to five layers of flattened cells. In this layer, lamellar granules containing lipids and keratohyalin granules are present within the cells cytoplasm. The appearance of the keratohyalin granules signifies the loss of the nuclei and cytoplasm of keratinocytes (Prunieras 1979). The keratohyaline granules contain proteins that promote hydration and cross-linking of keratin, and along with the desmosomal connections help to form the waterproof barrier of the skin.

The stratum corneum consists of several layers of flattened cells without nuclei or organelles, and a keratin rich cytoplasm. This cornified layer consists of anucleated and highly keratinised cells called “corneocytes” which are metabolically inactive.

Type I and II intermediate filaments are two keratin subfamilies found predominantly in keratinocytes and epithelial cells. Their main function is to act as a structural frame for keratinocytes. Epithelial cells contain 20 types out of the total 30 different types of keratin polypeptides identified (Moll *et al.* 1982). Expression of keratin polypeptides is linked to cellular differentiation and its regulation is dependent on various intracellular and extracellular stimuli, and also pathological disease processes.

Moll *et al.* (1982) established a numerical tagging system subdividing keratin polypeptides into acidic type (K10-K20 molecular weight 56.5-46 kilo Daltons-kD), and basic-neutral type (K1-K9 molecular weight 67-64 kD). Filaments within the cells are pairings of one acidic and one basic-neutral polypeptides of similar weight.

Sun *et al.* (1983) introduced the theory of tissue-specific expression of keratins in pairs. Specific types of epithelium and stages of differentiation are characterised by specific pairings of Type I-Type II keratins. The variation is likely to be due to the different physiological role of various types of cells within the epithelium.

In the epidermis, all basal keratinocytes synthesise Keratins K5 and K14, while K15 and K17 are occasionally present. Throughout the process of keratinocyte differentiation, secondary keratins are expressed depending on cell type. In normal epidermis, K1 and K10 are expressed; K6 and K16 are expressed in keratinocytes within tissue culture and in the epidermis during wound healing. Keratinocytes within tissue culture may differ in their keratin expression from epidermal keratinocytes in normal skin (Wu *et al.* 1982). Keratin expression is dependant on the degree of differentiation achieved by cells during the culture process influenced by culture conditions such as the composition of the culture media and the presence of fibroblasts.

Other types of cells within the epidermis include; melanocytes, which are pigment-melanin-producing cells, which protect the body from ultraviolet radiation. Melanin pigment is found inside intracellular organelles 'melanosomes', their number and melanin content varies with different skin types (Ebanks *et al.* 2011). Melanocytes are present in variable ratios to keratinocytes (Pelle *et al.* 2005). Their ratio to basal keratinocytes is 1:36 on average across the total body surface area, in sun–exposed areas it is 1:5 and 1:20 on the trunk.

Langerhans cells are dendritic cells, which play a role in the immune function of the skin barrier. Their role is mainly to induce immune response following infection, which is reduced following burn injuries and skin barrier damage (van den Berg *et al.* 2011). Other cells within the epidermis include Merkel cells, which are responsible for tactile sensation through tactile discs, which are amalgamated groups of Merkel cells attached to keratinocytes through desmosomes.

The basement membrane (BM) zone lies at the interface between the epidermis and the dermis, also known as the "dermal-epidermal" junction. As the epidermis is mainly avascular, the basement membrane serves as a support for the avascular epidermis. The basement membrane zone is formed of four layers: the plasma membrane of the basal keratinocyte, lamina lucida, lamina densa, and lamina fibro-reticularis.

The lamina lucida contains laminin and anchoring filaments bridging the gap between the basal keratinocytes and the lamina densa underneath. The lamina lucida is electron lucent (i.e. appears transparent under electron microscopy) and has an absence of hemidesmosomes. The lamina densa contains collagen type IV and proteoglycans, and the lamina fibro-reticularis contains anchoring fibrils and collagen Type I, III, VI, and VII (Ko and Marinkovich 2010).

The basement membrane is the natural barrier for nutrient delivery to keratinocytes, and a selective filter for plasma proteins, which influence the metabolism of keratinocytes within the basal layer of the epidermis (Prunieras *et al.* 1983). Dermal extracellular matrix (ECM) proteins also penetrate the basement membrane to reach epidermal keratinocytes.

The dermis lies below the epidermis and acts as support and mould for the epidermis. Three distinctive layers form the dermis: the papillary dermis, the reticular dermis, and the hypodermis. The dermis is formed mainly of dermal cells and connective tissue matrix surrounding the skin appendages such as hair follicles, sweat glands, and sebaceous glands. Fibroblasts are the main cells in the dermis along with collagen and elastin fibres forming the extracellular matrix connective tissue. Other cells within the dermis include: monocytes, macrophages, and dendritic cells, which have an immune function similar to Langerhans cells within the epidermis (Warfel *et al.* 1993).

The papillary dermis forms projections from the dermis into the epidermis and is highly vascular. Underneath the papillary dermis and above the reticular dermis lies the sub-papillary plexus of blood vessels. This plexus is of significant importance as it represents the main blood supply to the avascular epidermis (Braverman and Keh-Yen 1981). The structure of the collagen and elastin fibres changes from fine to coarse through the transition from the papillary to the reticular dermis. The hypodermis is the deepest layer of the dermis and it represents the integration of the dermis into the underlying adipose and subcutaneous tissue (Braverman and Keh-Yen 1981).

Collagen is the main component of the dermis and more than 20 types of collagen have been identified (Kadler *et al.* 1996). Fibroblasts produce procollagen molecules which are secreted into the extracellular matrix, where metalloproteinases modify the procollagen into collagen molecules (Kadler *et al.* 1996). Collagen molecules then become cross-linked and aligned into collagen fibrils and filaments having a high tensile strength. Types I, III and V collagens are the most common collagens of the human dermis, with type I contributing 90% of the dermis collagen content (Han *et al.* 2008). The dermis 'ground substance' consists of glycoproteins, glucosaminoglycans and proteoglycans. The ground substance maintains the structure of the dermis and supports cellular attachment and migration within the dermis. The proteoglycans within the 'ground substance' influence tissue repair through binding of growth factors and cytokines, which in turn control cellular proliferation during wound healing (Pineau *et al.* 2008).

Fibroblasts are the main cell type within the dermis and they produce dermal connective tissue matrix proteins. Fibroblasts have an important role in wound healing through interaction with keratinocytes resulting in stimulation of epithelialisation and epithelial differentiation (Tobin 2006). Following epithelial breakdown or loss, fibroblasts produce extracellular matrix proteins acting as scaffolds for cellular migration during wound healing. Hypertrophic scarring or keloid formation, are considered pathological end results of this process. During the wound healing process, the presence of mechanical tension due to epithelial disruption or loss leads to fibroblasts acquiring a characteristic phenotype. This phenotype is a α smooth muscle actin (α-SMA) expressing phenotype and at this stage fibroblasts are called myofibroblasts (Watsky *et al.* 2010). Wound contraction is primarily a function of myofibroblasts, which remain active until wound closure is achieved. Continuous proliferation of myofibroblasts beyond wound closure gives rise to hypertrophic scarring and keloid formation.

Other cells within the dermis include monocytes and macrophages, which play a role in the immunological functions of the skin. Their functions include phagocytosis of dermal cells, and they play a role in the inflammatory phase of wound healing. They produce cytokines and growth factors such as transforming growth factor β1 (TGF β1) and interleukin 1 and 6 (IL-1 & 6) during wound healing regulating both cellular activities and tissue remodelling (Powell *et al.* 1999).

1.2 Skin barrier breakdown or loss and its management

Skin loss or damage to the skin barrier function can result from different types of trauma including burns. Burn injuries affect 48 per 100 000 children and 18 per 100 000 adults every year in England and Wales (Khan *et al.* 2007). In comparison to wartime, burn injuries represent around 5% of the total number of trauma casualties as in the Iraq conflict since 2003 (Foster *et al.* 2011, Kauvar *et al.* 2006). This is compared to less than 1% of trauma injuries in general population (Khan *et al.* 2007). Burn injuries can result from thermal, chemical, electrical or radiation injury. Burn injuries produce coagulative necrosis of the skin and possibly underlying tissues as well as systemic effects. The systemic effects of burn injuries, depending on the extent and depth of the injury, could be life threatening (Baron *et al.* 1994).

The depth of the burn injury can be classified as: superficial epidermal, superficial dermal, deep dermal, and full thickness burns.

In superficial epidermal burns, the epidermis is damaged and the underlying dermis remains intact, and epidermal regeneration occurs through keratinocyte migration.

Figure 1: Superficial dermal burn
Area of erythema, which blanches on application of pressure involving anterior aspect of right knee and upper leg in an adult, blisters covering the anterior leg have been removed. Distance between arrows is 5cm.

In superficial dermal burns (figure 2), the epidermis is damaged along with the superficial layers of the dermis. These wounds are characterised by pain, blanching on pressure and blistering. Healing occurs through regeneration from the dermal appendages. In the absence of infection, superficial dermal burns will heal in around two weeks. If more than 10% of the total body surface area is involved, healing may take longer or surgical intervention is required.

In deep dermal burns (figure 3), the majority of the dermis is involved in the injury. These wounds are usually painless injuries, where blistering is uncommon, and are characterised by 'fixed-staining' red colour resulting from capillary blood vessel damage. Deep dermal burns, if left to heal without intervention, can take more than three weeks to heal. This results in excessive scarring and contracture formation.

In full-thickness burns, all skin components are damaged to the level of subcutaneous fat or fascia. Full thickness burns require surgical intervention to allow healing due to the lack of keratinocyte source for regeneration. Small areas of full thickness burns (less than 2-3 cm in diameter) could possibly heal by keratinocyte migration from the wound edges.

Figure 2: Deep dermal burn
"Fixed staining" involving the left hand in an adult in a deep dermal burn injury. The burn is seen affecting the left hand and forearm with no blistering.
"Fixed staining" refers to the red areas in the palm, which are red stained and do not blanch on application of pressure. Distance between arrows is 2.5cm.

Jackson (1953) studied the extent of skin and surrounding tissue damage caused by burn injuries. He described three distinctive zones, which are: Zone of coagulation or 'necrosis', zone of stasis, and zone of hyperaemia. The zone of coagulation is the central area of tissue destruction caused directly by the burn injury. The zone of stasis is the area surrounding the zone of coagulation; this area could convert to an area of necrosis or progress to recovery. Fluid resuscitation and early reversal of the physiological deficit resulting from the burn injury can prevent the progression to

necrosis. This effect can also be achieved using different types of early interventions reversing the local and systemic effects of the burn injury (Zawacki 1974, Battal *et al.* 1996, Isik *et al.* 1998, Shupp *et al.* 2010). The zone of hyperaemia surrounds the zone of stasis. It represents the systemic reaction to the burn injury, which is dependent on the extent of body surface area involved. The zone of hyperaemia is localised in small burn injuries. In extensive burns involving more than 25% of total body surface area, the zone of hyperaemia extends to involve the whole of the body (Baxter 1993). Different toxins released from the zone of coagulation or 'necrosis' can lead to a systemic inflammatory response, which can progress to multiple organ failure depending on the burn total body surface area. Therefore, the aim of burn management is to prevent infection, promote healing in the zone of necrosis, and prevent conversion of the zone of stasis to necrosis and the inflammatory response in the zone of hyperaemia.

The management of burn injuries has changed as the understanding of the dynamics of the injury evolves. Sir Archibald McIndoe (1900-1960) introduced saline (0.9-1.8% sodium chloride) wound irrigation for burns after noticing the increased likelihood of survival of RAF pilots who sustained severe burns, but fell into the sea before their rescue in World War II. Seawater, which contains 3.5% sodium chloride acted as a cleaning agent for the burns and provided a cooling effect. Baxter and Shires (1968) introduced fluid resuscitation based on the understanding of fluid loss and hypovolemia following burns. The need to prevent infections and use anti-microbial topical applications such as silver nitrate were later introduced (Ross and Hulbert 1940, Clowes *et al.* 1943). Since these early efforts, advances are made everyday in the types of topical agents and dressings used in burns management. Further understanding of the metabolic requirements of the burn victims and the need for nutritional support improved burns survival. Advances in the anaesthetic care and rehabilitation support, has also led to improved survival rates in recent years.

Burn tissue or ‘eschar’ consists of purulent exudate produced by the immigrating inflammatory cells and organisms, dried blood and denatured skin proteins. The ‘eschar’ is quickly colonised by endogenous bacteria derived from skin appendages. Therefore, rapid excision of the dead tissue leaving behind viable tissue only followed by early wound coverage, are the fundamental factors in the reconstruction of severe burns injuries.

Early excision of burn eschar is known to improve survival in full thickness burns (Farmer *et al.* 1955, Macmillan and Artz 1957, Macmillan 1958). One of the significant improvements to burns management in recent times has been the introduction of tangential excision of burn tissue (Janzekovic 1970). Tangential excision, which is the repeated use of the skin graft knife to shave the burn eschar down to viable tissue, reversed the zone of stasis and reduced the inflammatory response in the zone of hyperaemia. Early excision and skin grafting reduces mortality and hospital stay in extensive burn injuries involving more than 20% total body surface area (Ong *et al.* 2006). However, early excision of burns presented a different challenge in extensive burns covering more than 50% of the total body surface area.

Early excision of burn eschar requires simultaneous skin coverage in the form of skin grafting. In extensive burns, the lack of suitable areas for skin graft harvesting results in a delay in treatment, which can seriously affect the outcome. Also donor sites from skin graft harvesting add to the total area of skin loss. Local and potential systemic complications during wound healing of donor sites can add to the already existing challenges of burn injuries management. The time needed for re-epithelialisation of the donor site prolongs hospital stay and extends the time intervals between grafting sessions (Andreassi *et al.* 2005).

1.3 Alternatives to skin grafting (Biological dressings)

Skin loss following burn injuries, ideally requires replacement of the lost skin with skin harvested from another anatomical area. Therefore skin grafting continues to be the standard treatment following deep dermal or full thickness burn injuries.

Tanner *et al.* (1964) introduced meshing of skin grafts i.e. passing the skin graft sheet through a 'mesher' to punch holes within the graft sheet to expand the coverage surface area (figure 4). The meshing ratio is controlled by the size of the roller in the mesher, as size increases, a proportionate increase in the meshing ration is seen (figure 4).

Figure 3: Meshed skin graft 1:1 (left) compared to 5:1 (right)

Wider meshing ration allows expansion of the skin graft size as shown to allow coverage of a larger surface area

http://www.gatewaymed.com/products.aspx?productId=17

This is done in fixed ratios ranging from 1:1.5 (also known as mini-meshing) up to 1:6 depending on donor site availability and wound area treated (figure 5). Progressive keratinocyte migration from the skin graft islands into the mesh defects leads to wound healing. Nevertheless, the wider the meshing ratio, more keratinocyte migration and wound contraction are needed to achieve healing and close the gaps within the meshing pattern. This can lead to delayed wound healing and possibly secondary breakdown and extensive scarring (Gangemi *et al.* 2008).

Based on the fact that in extensive burns, the surface area of intact skin available for skin graft harvesting is limited, the development of skin alternatives became a priority.

The idea of developing skin alternatives became a necessity for patient survival in extensive burns when there is minimal donor site area available for skin grafting.

Skin alternatives or 'Biological dressings' would be able to provide temporary or permanent cover in extensive cases of skin loss following burns or trauma. Girdner (1881) first described the use of cadaveric human skin as a biological dressing. The wide spread use of skin grafts of variable thickness was popularised by Thiersch in 1886 (Thiersch 1886) and Schone in 1906 (Schone 1906) (Leon-Villapalos *et al.* 2010, Schone 1906).

Further research in the 1950s and 1960s led to the foundations of the current use of allograft as a biological skin treatment for major burns (Mowlem 1952, Jackson 1953, Zaroff *et al.* 1966). Allografts are harvested from deceased donors in longitudinal sheets and used as fresh, or cryopreserved at -80°C for up to six months (Pianigiani *et al.* 2005). The allografts can be lyophilised using dry freezing or glycerol to prolong their shelf life to around 6 months.

The use of deceased donor allograft skin for burns has very clear advantages and disadvantages (Leon-Villapalos *et al.* 2010). The advantages include allograft skin providing temporary cover of the burn wound when autograft is not available in both partial thickness and full thickness burns; in addition, it can be used as a cover layer for widely meshed grafts (Alexander *et al.* 1981). Other applications include exfoliative skin loss disorders such as; toxic epidermal necrolysis and staphylococcal scalded skin syndrome, and as temporary cover following burn excision prior to autografting. The use of deceased donor allograft has been shown to improve wound healing and reduce heat and fluid loss (Brychta *et al.* 2002).

The disadvantages of using allografts include their eventual rejection due to immunogenic rejection and the possibility of transmission of blood born infection.

The need to establish an adequate and successful method to preserve allograft skin led to the development of preservation by refrigeration over variable periods of time as

performed by Wentscher in 1903. This was followed by the addition of glycerol as a cryopreservant (Billingham *et al.* 1955). The same authors also described the phenomenon of "second-set" rejection of allogeneic tissue because of the presence of humoral antibodies from prior exposure to the same allogeneic source.

The pathological immunosupression present in the early stages of a severe burn injury protects allografts from rejection during the early period following their application.

Clearly the role of allografts as a biological replacement is temporary, and their use is limited to the early phase of skin loss injuries.

Spurred by the limitations of the use of allografts, the need for skin replacement products has become a priority over the last fifty years. The idea of developing a skin substitute has been a focus of many researchers with variable degrees of success.

Biological skin substitutes are products that are capable of replacing the damaged skin barrier either on a temporary or permanent basis. All biological skin substitutes ideally should have the following criteria: be clinically safe, replace the skin barrier, easy handling and application.

MacNeil (2007) reviewed the ideal properties for biological skin replacements, they should not be immunogenic, toxic, activate an inflammatory response or transmit disease. The skin replacement should also be biodegradable, support the regeneration of normal skin, and prevent fluid and heat loss from the wound surface.

Currently, there is no available skin replacement fulfilling all of the above-mentioned criteria. However, there are few bioengineered skin replacement products in the market, which can address some of the complications following the loss of the skin barrier.

The materials currently available include; Xenografts (Porcine skin), allogeneic cells combined with synthetic/xenogenic scaffold such as Apligraf® (Novartis, Switzerland), TransCyte® (Advanced BioHealing, California, USA), and "Recell®" (Avita Medical, Cambridge, UK) freshly harvested keratinocytes sprayed on burn wounds. Occlusive dressings temporarily restoring the skin barrier function in partial thickness burns and

providing wound cover in full thickness burns include; Biobrane® (Smiths and Nephew, Hull, UK) and Duoderm® (ConvaTec, Middlesex, UK).

Over the last three decades, recent advances have produced dermal replacement products such as Integra® (Integra Life Science, New Jersey, USA) and Matriderm® (Eurosurgical Limited, Surrey, UK). Dermal replacement therapies, as the name implies, provide a dermal substitute which following successful re-vascularisation would still require epidermal cover. The only procedure available until the emerging of keratinocyte cell culture has been a split skin graft. The possibility of isolating epidermal keratinocytes and expanding them *in vitro* opened the door for a new era in the management of burns and skin loss injuries.

The efforts of Rheinwald and Green (1975a) provided the breakthrough with the introduction of keratinocyte cell culture *in vitro*. They were able to isolate epidermal keratinocytes and expand the cells in culture using 3T3 cells (lethally-irradiated Swiss mouse fibroblasts). Further efforts through the addition of epidermal growth factor led to successful repeated expansion of keratinocytes *in vitro* (Rheinwald and Green 1977). Further additions to the culture medium, such as Cholera endotoxin (Green 1978), hydrocortisone, and insulin (Tsao *et al.* 1982) led to the use of defined medium and the optimisation of culture conditions. Following repeated expansion over a period of 3-4 weeks, keratinocyte colonies form thin confluent sheets, which can be re-applied to the wound (Boyce and Hansbrough 1988).

The early applications of cultured keratinocytes included the treatment of venous leg ulcers (Leigh *et al.* 1987, Marcusson *et al.* 1992) and severe burn injuries (Bettex-Galland *et al.* 1988, Ronfard *et al.* 1991). In cases using cultured keratinocytes to treat severe burns' injuries, variable success rates were reported (Williamson *et al.* 1995, Caruso *et al.* 1996, Caruso *et al.* 1999). The success rate was measured against different variables; including re-epithelialisation, wound healing and patient survival. The most commonly reported outcome measure is the percentage of take of the cultured

keratinocyte sheet graft to the wound bed. The percentage of take reported in literature varies from 15% (Blight *et al.* 1991) to 95% (Compton 1992). The variation arises from patient factors, wound bed preparation; different methods of graft application, dressings, and post-operative wound care protocols.

Fraulin *et al*. (1998) introduced the use of freshly harvested sprayed keratinocytes in a pig model to promote wound healing. This method was adopted as an alternative to the use of cultured epithelial sheet grafts in the treatment of skin loss. The use of sprayed cultured keratinocytes in combination with fibrin glue was reported to successfully promote re-epithelisation (Currie *et al.* 2003). Although cultured keratinocytes appear to be the ideal alternative to skin grafting (Boyce 1996, Boyce 2001, Boyce *et al.* 2006a), particularly in extensive cases of skin loss when no donor sites are available for skin graft harvesting, they have clear disadvantages.

The disadvantages include the lack of dermal cellular support, as the epithelial sheets are mainly keratinocytes lacking any dermal components. The absence of dermal cells, mainly fibroblasts, contributes to the fragility of the epithelial cell sheets (Boyce and Hansbrough 1988), early wound breakdown post-operatively, and unpredictable scarring in the long-term (Desai *et al.* 1991). Other factors contributing to the fragility of the epithelial sheets include the repeated use of trypsin to harvest keratinocytes during the *in vitro* expansion process (LaFrance and Armstrong 1999). Repeated trypsinisation can affect keratinocyte cell-to-cell adhesion *in vivo* and leads to the formation of fragile epithelium (LaFrance and Armstrong 1999).

Efforts to address the fragility of epithelial sheet grafts include the use of *in vitro* tissue constructs such as collagen (Boyce 1998, Boyce *et al.* 1988) and de-cellularised dermis (Atiyeh and Costagliola 2007). Also synthetic membranes were used to support the grafts during transfer and wound application including polyurethrane (Rennekampff *et al.* 1996) and silicone (Hernon *et al.* 2006). The use of support membranes allows easy handling of the fragile sheets.

The length of time required for the culture process is another disadvantage; patients with extensive burns are usually critically ill facing a life threatening injury. Early wound coverage following burn excision has been shown to improve survival. This is difficult to achieve as the cycle of keratinocyte culture and expansion takes around 3-4 weeks, which could be crucial time lost before the cultured cells are available for wound application. The use of lethally irradiated mouse fibroblasts (3T3) in keratinocyte cell culture is also another disadvantage. The use of xenogenic cells raises theoretical concerns about the possibility of disease transmission from mice.

1.4. Microcarrier beads in tissue engineering

Researchers over the last 20 years have explored various methods to improve the process of keratinocyte cell culture. Improvements were required to reduce the time needed to reach cell confluence, fragility of the epithelial cell sheets, delivery methods and dermal-alternatives to support the cultured epithelial sheet graft.

Van Wezel (1967) introduced the use of microcarriers "small particles with diameters ranging between 100 and 400 μm in tissue culture. He described the use of the beaded ion exchange medium DEAE (Diethylaminoethyl) Sephadex™A-50 as a microcarrier to facilitate the growth of mammalian cells. He further developed the system for large-scale viral vaccine production (van Wezel 1976).

Four decades later, microcarriers are available from a variety of materials including; cellulose, chitosan, collagen, dextran, gelatin, glass, polyethylene, and polystyrene.

The use of microcarriers in tissue engineering has many advantages; cell expansion can be rapidly achieved using bioreactors, and using microcarriers allows close monitoring and modification of culture conditions. Also, cells expanded on microcarriers can be transplanted *in vivo* and their ability to regenerate lost or damaged tissue assessed experimentally and clinically (Martin *et al.* 2011).

The applications of microcarriers depend on cellular attachment, and many factors influence the attachment of cells to the surface of microcarriers. These factors include; the chemical composition of the microcarriers, surface structure, degree of porosity, and charge density of the particle. In addition, the number of cells that can attach to the microcarrier depends on the particle diameter and the resulting surface area.

The advantages of the use of microcarriers in cell culture include the large surface area provided by microcarriers in a relatively small volume. This large surface area allows cell culture and culture conditions assessment within confined space in a bioreactor-type environment. For example, 1 g of Cytodex™1 microcarriers provides a surface area of 4400 cm^2, the surface area approximately equivalent to 58 "75 cm^2 culture flasks" (Martin *et al.* 2011). This clearly demonstrates that using microcarriers for tissue culture is space saving and cost effective, as well as less time and labour intensive than standard culture methods.

A review of the literature published in PubMed, Embase®, and Cochrane reviews database revealed numerous applications for the use of microcarriers in tissue engineering, some of these applications are referred to in the table 1. The examples of application represent a summary of common applications and are not inclusive.

In addition, cell culture on microcarriers allows adjustment of culture conditions such as medium and culture composition, and mechanical forces in stirred culture. The use of culture medium additives and adjusting the rotation of stirred culture can be achieved due to the versatile attachment of cells to the microcarriers' surface compared to normal culture. Other advantages are that serial culture samples can be analyzed from the culture and thus cell differentiation can be regulated in large scale bio-reactor models (Freed *et al.* 1993).

Table 1: Commercially and Non-commercially available types of microcarrier beads (Martin *et al.* 2011). The examples of application represent a summary of common applications and are not inclusive.

Microcarriers can also be used as cell delivery systems, as cells on microcarriers can either be directly applied to a specific anatomical site or biological background, or incorporated into a larger scaffold and subsequently transplanted. The potential for using microcarriers for tissue engineering applications is extensive (table 1), and successful culture methods have been reported for a range of different cell lineages.

Bone-forming osteoblasts have been shown to proliferate on a range of microcarriers and have been used in both *in vitro* and *in vivo* investigations (Howard *et al.* 1983,

Shima *et al.* 1988). In recent years, various types of microcarriers have been investigated for bone tissue engineering such as polycaprolactone microcarriers seeded with rat bone marrow-derived stem cells (Hong *et al.* 2009) and gelatin microcarriers seeded with mouse embryonic stem cells (ESCs) or dermal fibroblasts (Sommar *et al.* 2010).

New developments in cartilage tissue engineering involve the seeding of chondrocytes on biomaterials such as collagen membranes (Vinatier *et al.* 2009, van Osch *et al.* 2009). Chondrocytes have been shown to alter their phenotype to fibroblasts in monoculture, along with a change in collagen production from type II to type I (Frondoza *et al.* 1996, Freed *et al.* 1993). Microcarriers with surface modifications to enhance cell attachment have recently been reported. These included poly (L-lactide) (PLLA) with chitosan surface coating (Lao *et al.* 2008), poly(D/L-lactide-co-glycolide) (PLGA) microcarrier with positive charge surface modification (Chun *et al.* 2004), and PLLA microcarrier with RGD (arginine-glycine-aspartic acid) surface modification (Chen *et al.* 2006). All of these microcarriers were shown to support the growth and proliferation of chondrocytes.

The use of microcarriers for endothelial cell culture helped to identify endothelial cell growth dynamics, and factors involved in capillary network formation. Endothelial cell attachment to microcarriers within a fibrin matrix led to the development of a three-dimensional angiogenesis model (Wissemann and Jacobson 1985).

Another area of tissue engineering where microcarrier culture has expanded is Parkinson's disease treatment, which may be aided by the use of microcarriers. Rats with hemi-parkinsonism were treated with adrenal chromaffin cells on Cytodex™ microcarriers (Cherksey *et al.* 1996, Saporta *et al.* 1997, Borlongan *et al.* 1998).

The use of microcarriers for the expansion of Adipose-derived stem cells (ADSCs) has been under investigation in recent years (Choi *et al.* 2008, Chung and Park 2009, Serra *et al.* 2009). Recent animal work utilised rabbit bone marrow-derived mesenchymal

stem cells (MSCs) transfected with green fluorescent protein (GFP). The MSCs were attached to PLGA microcarriers following differentiation then injected into the cervical region of mice. Four weeks post-transplantation, newly formed fat pads containing GFP-positive cells were observed.

Another frontier where the use of microcarriers for cell culture is promising is hepatocyte cell culture. The culture of adult rat hepatocytes on microcarriers was initially used to investigate hormone metabolism *in vitro* (Athari *et al.* 1988). Further *in vivo* studies demonstrated metabolic improvements over a period of 30 days following the injection of hepatocytes cultured on microcarriers into rats with a defective bilirubin or albumin metabolism (Demetriou *et al.* 1986a, Demetriou *et al.* 1986b).

Further reports showed a significant increase in survival rate in rats with partial hepatectomy which received hepatocytes transplanted on microcarriers when compared with control groups (Demetriou *et al.* 1988). As an alternative to transplantation into the liver, hepatocytes cultured on microcarriers can be used in extra-corporal bio-artificial liver devices.

1.5. Microcarriers in keratinocyte cell culture

Cultured keratinocytes are most frequently used in the form of confluent epidermal sheets or sprayed single-cell suspensions are harvested from culture flasks using trypsin prior to application to the wound bed.

The use of trypsin to harvest keratinocytes from culture flasks has been reported to damage anchoring basement membrane proteins. Such damage results in mechanical instability and deficient dermal–epidermal adhesion at the level of the basement membrane (Desai *et al.* 1991).

The use of microcarriers for keratinocyte cell culture does not require the application of trypsin for cell harvest, as keratinocytes are cultured on biodegradable microcarriers that can be applied directly to the wound. Furthermore, the utilisation of microcarriers in keratinocyte culture reduces culture time and costs (Atiyeh and Costagliola 2007).

Voigt *et al.* (1999) first reported the use of microcarriers for skin cell culture, where human keratinocytes were shown to proliferate on Cytodex™ 3 dextran microcarriers. Microcarriers and keratinocytes were cryopreserved and remained viable following thawing. In a mouse wound model, new epithelium was observed following application of microcarriers and keratinocytes. Dextran beads were incorporated in the scar tissue, and elicited an inflammatory reaction, as the microcarriers were not biodegradable.

LaFrance and Armstrong (1999) expanded porcine fibroblasts and keratinocytes on biodegradable PLLA microcarriers in separate cultures. A mixture of both microcarriers was applied to a pig wound model and migration of cells from the microcarriers as well as re-establishment of dermal and epidermal elements were observed.

Kim *et al.* (2005) reported similar results using keratinocytes expanded on PLGA microcarriers in an athymic mouse model. However, PLGA microcarriers were reported to produce a mild foreign body reaction. In both studies, no estimate of the percentage of keratinocytes' survival *in vivo* was available as no biomarker was used to trace the cultured keratinocytes.

The concept of using biodegradable gelatin-based microcarriers for keratinocyte culture has become more popular as the drawbacks of using non-biodegardable microcarriers are overcome. Cultispher® microcarriers (gelatin-based) have been investigated for supporting keratinocyte culture and results have shown that they are capable of supporting the growth of keratinocytes and fibroblasts (Gustafson *et al.* 2007, Seland *et al.* 2011, Liu *et al.* 2006, Borg *et al.* 2009). These studies focused on optimising conditions for supporting effective growth of keratinocytes on microcarriers including: preconditioning of culture media and the use of defined media.

Conventional keratinocyte cell culture relies on the presence of a layer of lethally irradiated mouse 3T3 fibroblasts. Theoretically, the xenogenic origin of the 3T3 cells could pose a risk of cross-species disease transmission following clinical application. Liu *et al.* (2006) seeded Cultispher® microcarriers with dermal autologous fibroblasts,

the cells were later removed using freezing in liquid nitrogen while preserving extracellular matrix and other growth factors secreted by fibroblasts. The modified microcarriers were then inoculated with keratinocytes, which showed an increase in proliferation and viability when compared with keratinocytes grown on unmodified microcarriers. In addition, the keratinocytes remained viable at room temperature and upon refrigeration, indicating the possibility of this bioreactor system being suitable for future clinical application.

In another study, keratinocytes grown on Cultispher® microcarriers in defined media were applied to full-thickness wounds in mice, and contributed to the development of a neo-epidermis. The microcarriers degraded in 2-3 weeks time, and the epidermis was thicker compared to the epidermis developing following single-cell suspension treatment (Seland *et al.* 2011).

Borg *et al*. (2009) demonstrated that in an *in vitro* skin equivalent model, keratinocytes grown on Cultispher® in standard media without the addition of feeder cells were able to form an epidermis. Zhang *et al.* (2009) reported that fibroblasts grew on porcine acellular dermal matrix microcarriers. The dermal matrix material was under investigation as a dermal substitute in full thickness wound treatment. Application of these microcarriers in a full-thickness wound mouse model demonstrated a higher rate of wound healing when compared with mice receiving no treatment following wound formation.

In a small clinical study, autologous human keratinocytes cultured on Cultispher® microcarriers were used to treat chronic venous leg ulcers (Liu *et al.* 2004). Partial or full re-epithelialisation was observed in all wounds treated with either single or serial applications of microcarriers plus keratinocytes. No inflammatory response was noted following the degradation of the microcarriers over a period of 2-3 weeks. Based on this evidence microcarriers used for autologous keratinocyte culture could be used to treat skin defects such as chronic non-healing wounds or full-thickness skin loss.

In microcarrier culture, cells grow as monolayers on the surface of the small spheres or as multi-layers in the pores of macro-porous spheres which are usually suspended in media using a gentle stirring action. This allows maximisation of the culture surface area and reduces space and culture cost. In traditional keratinocyte culture, epidermal sheet grafts are required to cover extensive areas of skin loss, in case of severe burns with tens of plastic culture flasks being used to produce these sheet grafts. A bioreactor model utilising microcarriers and occupying a considerable smaller volume could substitute for a large number of tissue culture flasks. The use of microcarriers in cell culture generally has many advantages; such as improved control of culture media, increasing the production capacity of the culture and protection against physical stress (Giard *et al.* 1977, Mered *et al.* 1980). The risk of contamination in cell culture is related to the number of handling steps required to produce a given quantity of cells or products, microcarrier cell culture reduces the number of handling steps (Meignier 1979). There is a much reduced risk of infection in cell culture using microcarriers compared to traditional methods (Meignier 1979).

Hence, microcarriers could represent an improved culture and delivery method for autologous keratinocytes when compared with traditional cell culture. Microcarriers clearly have great potential in keratinocyte cell culture and this potential could be extended to clinical applications. Clinically, microcarriers and cultured keratinocytes could be used as an effective treatment to full-thickness skin loss in the future.

1.6. *In vivo* animal wound models

Any biological or chemical products intended for clinical use have to undergo extensive investigations for safety, efficacy, and adverse effects. Serial clinical trials in multiple phases (Phase I-IV) are designed to investigate all these aspects. Phase I and II are usually in healthy volunteers to assess biocompatibility, safety and adverse reactions. Phase III and IV involve studies in patients to assess therapeutic effects on specific

diseases or disorders. An important stage prior to the start of clinical trials is the pre-clinical testing in a relevant animal model.

An *in vivo* animal model is essential for an accurate assessment of the biological integration and performance of any skin replacement treatment. Animal models used to assess skin substitutes or similar products can help to predict biocompatibility, efficacy, and the immune reaction of the biomaterials when applied in humans. Therefore, the choice of such an animal model is very important to reflect enough similarities in treatment outcomes when compared to humans.

Sullivan *et al.* (2001) provided evidence in support of the use of pig animal model for skin substitutes and wound healing research. Similarities in anatomy, structure, physiology and immunological properties of human and pig skin support the use of a pig wound model (Sullivan *et al.* 2001). Small animals e.g. mice, rats, and guinea pigs are often used for *in vivo* biomedical studies because of the reduced housing requirements, and the low cost overall compared to larger animals. The use of small animals is useful for specific studies, where immune-compromised or transgenic mice are used to demonstrate wound healing concepts. The data obtained is often limited and can only serve to prove or disprove a hypothesis. The limitation is related to the fundamental difference in the wound healing process of small animals. Thin epidermis, dermis, and a "panniculosus carnosus" layer (thin muscle) promote wound healing through contraction, rather than keratinocyte migratory activity (Wong *et al.* 2011).

In comparison, pig skin in general and the dermis in particular are very similar to human skin. The human epidermis thickness is between 50 μm-120 μm comparable to porcine epidermis thickness of 30-140 μm. Both types of epidermis have a similar turnover period of 28-30 days (Vardaxis *et al.* 1997). Both the porcine and human dermis have similar structure, with the dermis being clearly differentiated into papillary and reticular layers (Vardaxis *et al.* 1997). The porcine reticular dermis has reduced

elastin fibre content compared to human dermis and the porcine dermis contains apocrine glands as opposed to eccrine sweat glands in humans.

The immunological and enzymatic properties of human and porcine skin, cytokeratin distribution and basement membrane components are very similar (Sullivan *et al.* 2001). The pig is the only animal which has a comparable number of skin hair follicles to humans (Vardaxis *et al.* 1997). This is of significant value in wound healing research, as re-epithelialisation can progress from hair follicle remnants following partial skin loss in humans, and re-epithelialisation occurs in a similar fashion in porcine skin. Taking into consideration the similarities between porcine and human skin, porcine models are considered the most appropriate and relevant animal model for skin wound healing studies (Vodicka *et al.* 2005)

In conclusion, the pig animal model appears to be the best available tool for experimental studies for human skin regeneration and wound healing. The pig wound model allows the reproduction of consistent experimental results, which can assist in future clinical applications. It can also reduce the time required for the introduction of new treatments for skin loss and wound healing to clinical practice, with a recognisable benefit to all patients.

Hypotheses for investigation

Human and pig keratinocytes will attach to microcarrier beads *in vitro* and proliferate under *in vitro* culture conditions

Cultured autologous pig keratinocytes on microcarrier beads will migrate from the microcarrier beads and integrate into neo-epithelium when applied to porcine full thickness wounds

Green fluorescent protein is a long-term retroviral genetic marker in cultured pig keratinocytes on microcarrier beads when applied to full thickness wounds

Cultured autologous pig keratinocytes on microcarrier beads will form permanent epithelium when applied to full thickness wounds

Cultured autologous pig keratinocytes on microcarrier beads will reduce wound contracture when applied to full thickness wounds in combination with widely meshed split skin graft

Cultured allogeneic pig keratinocytes on microcarrier beads in combination with two-stage artificial dermal regeneration template and artificial skin replacement will produce epithelial closure when applied to full thickness wounds

Cultured allogeneic pig keratinocytes on microcarrier beads in combination with two-stage artificial dermal regeneration template and artificial skin replacement will reduce wound contracture when applied to full thickness wounds

Cultured autologous pig keratinocytes and fibroblasts on microcarrier beads in combination with two-stage artificial dermal regeneration template will form a permanent functional epithelium when applied to full thickness wounds

Cultured autologous pig keratinocytes and fibroblasts on microcarrier beads in combination with two-stage artificial dermal regeneration template will reduce wound contraction in full thickness wounds.

Experimental Aims

To assess the proliferation of human keratinocytes on microcarrier beads *in vitro* compared with conventional culture (Chapter 3)

To compare different types of gelatin microcarrier beads to support the growth and proliferation of human keratinocytes *in vitro* (Chapter 3)

To assess the proliferation of porcine keratinocytes on microcarrier beads *in vitro* compared with conventional culture (Chapter 3)

To compare the application of cultured autologous keratinocytes on microcarrier beads with cultured sprayed keratinocytes on re-epithelisation of full thickness wounds (Chapter 4)

To compare the use of Green Fluorescent Protein as a marker of cultured keratinocytes on microcarrier beads with cultured sprayed keratinocytes in full thickness wounds (Chapter 4)

To compare the effect of cultured keratinocytes on microcarrier beads and sprayed keratinocytes in reducing the rate of wound contraction in full thickness wounds (Chapter 5)

To compare the effect of allogeneic cultured keratinocytes on microcarrier beads and allogeneic cultured sprayed keratinocytes in combination with artificial dermal regeneration template in reducing the rate of wound contraction in full thickness wounds (Chapter 6)

To compare autologous cultured keratinocytes on microcarrier beads alone or in combination with autologous cultured fibroblasts on microcarrier beads in reducing the rate of wound contraction in full thickness wounds (Chapter 7)

To compare cultured allogeneic and autologous keratinocytes on microcarrier beads with cultured allogeneic and autologous sprayed keratinocytes in combination with two-stage artificial dermal regeneration template in re-epithelisation of full thickness wounds (Chapter 6-7)

To compare cultured autologous keratinocytes on microcarrier beads with cultured autologous keratinocytes and fibroblasts in combination with two-stage artificial dermal regeneration template in re-epithelisation of full thickness wounds (Chapter 7)

To compare cultured autologous keratinocytes and fibroblasts on microcarriers with cultured autologous sprayed keratinocytes in combination with two-stage artificial dermal regeneration template in re-epithelisation of full thickness wounds (Chapter 7)

Chapter 2: Materials and methods

2.1 Materials

2.1.1 Human keratinocytes cell culture

Cell lines

Swiss 3T3 mouse embryo fibroblasts, passage number 24 (The Imperial cancer research fund (ICRF), London, UK)

Media and supplements

Source: GIBCO BRL, Life technologies, Paisley, Scotland

⇒ Dulbecco's Modified Eagle's Media (DMEM) with 1000 mg/l D-glucose

⇒ Hanks Balanced Salt Solution (HBSS)

⇒ Penicillin/ Streptomycin 5000 units ml^{-1}/5000 μg ml^{-1}

⇒ F12 + GlutaMAX™ Nutrient Medium

Source: Sigma-Aldrich Ltd., Dorset, UK

⇒ Hydrocortisone (Cortisol, 17-Hydrocorticosterone)

⇒ Cholera Toxin

Source: Austral Biologicals, USA

⇒ Human recombinant EGF 50 μg/ml stock

Source: Imperial Laboratories Ltd, West Portway, Andover, England

⇒ Foetal bovine serum (Foetal calf serum)

Source: Sigma-Aldrich Ltd., Dorset, UK for Percell Biolytica, Sweden

⇒ Cultispher S® microcarriers

⇒ Cultispher G® microcarriers

Reagents

Source: Boehringer Mannheim, Lewes, Sussex, England

⇒ Dispase®

Source: Difco Laboratories, Detroit, Michigan, USA

⇒ Trypsin (0.25%)

Source: GIBCO BRL, Life Technologies, Paisley, Scotland

⇒ Trypsin 0.05%/ EDTA 0.02%

Tissue culture consumables

Source: Greiner Bio-One Ltd, Gloucestershire, England

⇒ 175 cm^2 canted neck filter cap tissue culture flasks

⇒ 75 cm^2 canted neck filter cap tissue culture flasks

⇒ 30 ml sterile universal tubes

Source: Becton Dickinson Labware, NJ, USA supplied by Marathon Laboratory Supplies, Park Royal, London, England

⇒ Falcon® 5 ml, 10 ml, 25 ml, and 50 ml sterile tubes

⇒ 20 ml sterile universal tubes

⇒ Sterile Petri dishes 90 x 15 mm (D x H)

⇒ 200 ml sterile pots

Source: Fisher Scientific UK, England

⇒ Manually programmable cell rotator

⇒ Pre-plugged and non-plugged glass Pasteur pipettes

2.1.2 Porcine keratinocyte and fibroblasts cell culture

Porcine keratinocytes

In vitro studies: Isolated from skin grafts harvested from white pigs donated by Plumpton College, near Lewes, East Sussex, UK.

In vivo studies: Isolated from skin grafts from white pigs used in experimental work (Northwick Park Institute Medical Research (NPIMR), Harrow, London)

Cell lines

⇒ Swiss 3T3 mouse embryo fibroblasts, passage number 24 (The Imperial Cancer Research Fund (ICRF), London, UK)

⇒ PT67 retroviral producer cell line PT67pFB-hrGFP A2 clone from PT67 packaging cell line (BD Biosciences Clontech, Oxford, UK) and ViraPort™ retroviral reporter vector (Stratagene, La Jolla, California, USA) supplied by Agilent Technologies UK Ltd., Cheshire, UK.

Media and supplements

Source: GIBCO BRL, Life Technologies, Paisley, Scotland

⇒ Dulbecco's Modified Eagle's Media (DMEM) with 1000 mg/l D-glucose

⇒ Opti-MEM®(calcium-free) reduced serum media with GlutaMAX®

⇒ Hanks Balanced Salt Solution (HBSS)

⇒ Penicillin/ Streptomycin 5000 units ml^{-1}/5000 μg ml^{-1}

⇒ Amphotericin B 250 μg ml^{-1} (to prevent fungal infection and no effect on keratinocytes expansion was noted following the addition of Amphotericin B)

⇒ Calcium chloride (0.1M)

⇒ Lipofectamine Plus™ reagent for PT67 cell line

Source: Sigma Alddrich Co Ltd, Poole, Dorset, England

⇒ Rat Tail Collagen (type 1)

Source: Imperial Laboratories Ltd, West Portway, Andover, England

⇒ Foetal bovine serum (Foetal calf serum)

Reagents

Source: Boehringer Mannheim, Lewes, Sussex, England

⇒ Dispase®

Source: Difco Laboratories, Detroit, Michigan, USA

⇒ Trypsin (0.25%)

Source: GIBCO BRL, Life Technologies, Paisley, Scotland

⇒ Trypsin 0.05%/ EDTA 0.02%

Tissue culture consumables

Source: Greiner Bio-One Ltd., Gloucestershire, England

⇒ 75 cm^2 canted neck filter cap tissue culture flasks

⇒ 175 cm^2 canted neck filter cap tissue culture flasks

⇒ 30 ml sterile universal tubes

Source: IBS Integra Biosciences, Switzerland

⇒ Cellspin™ magnetic stirrer

⇒ Cellspin™ magnetic stirrer flasks (100 ml and 250 ml)

2.1.3 Animal anaesthesia and theatre consumables

Anaesthesia and per-operative drugs

Source: Parke-Davies Veterinary Ltd, Pontypool, Gwent, Wales

⇒ Ketamine (Vetalar®)

Source: Bayer UK Ltd, St Edmunds, Suffolk, England

⇒ Xylazine (Rompun®)

Source: Zeneca Ltd, Macclesfield, Cheshire, England

⇒ Halothane (Fluothane®)

Source: BOC Ltd, Guilford, Surrey, England

⇒ Nitrous Oxide

⇒ Oxygen

Source: Astra Pharmaceuticals Ltd, Kings Langley, Hert's, England

⇒ Bupivicaine (Marcaine®)

Source: Biorex Laboratories Ltd., Enfield, UK

⇒ Lignocaine Gel B.P. 2%

Source: Smith Kline Beecham Animal Health, Surrey, England

⇒ Ampicillin "Ampifen LA™" (long acting penicillin)

Source: Veterinary Products, Grampian Pharmaceuticals, Lancashire, England

⇒ Caprofen®

Theatre equipment and consumables

Source: Depuy Healthcare Ltd, Leeds, England

⇒ Chlorhexidine (4%) (Hydrex®)

Source: Steripak Ltd, Rancorn, Cheshire, England

⇒ Normal Saline (sodium chloride 0.9%)

⇒ Sterile alcohol (70%)

Source: Seton Healthcare, Oldham, Lancashire, England

⇒ 10% povidine iodine in aqueous solution (Betadine®)

Source: Northwick Park Hospital Pharmacy, Harrow, England

⇒ Liquid Paraffin

Source: Swann Morton•, Sheffield, England

⇒ Scalpel Blades size 10 and size 15

⇒ Silvers™ skin graft knife and blades

Source: Smith and Nephew, Hull, England

⇒ Elastoplast® adhesive roll bandages

⇒ Paraffin Gauze dressings "Jelonet®"

⇒ VISITRAK™ Digital, digital wound measuring device

⇒ VISITRAK™ Grid, single use 3 layer tracing grid

Source: Johnson & Johnson, Ascot, Berkshire, England

⇒ Velband® wool bandage

Source: Ethicon Ltd, Edinburgh, Scotland

⇒ 2/0 and 3/0 silk sutures

Source: Zimmer Ltd., South Marston Park, Swindon, England

⇒ Zimmer® Air Dermatome

⇒ Disposable dermatome blades

⇒ Skin graft adjustable mesher

⇒ Plastic skin graft holders 1:3 and 1:6

Source: 3M United Kingdom plc, Bracknell, England

⇒ 3M Vista™ skin stapler

Source: The Bioengineering Department, Northwick Park Institute for Medical Research, Harrow, England

⇒ Percutaneous poly-tetrafluroethylene (PTFE) wound isolation chambers

Source: Promedics Ltd, Blackburn, Lancashire, England

⇒ Protective pig thermoplastic jackets secured with Velcro® straps

Source: Southern Foam, Crawley, Sussex, England

⇒ Foam support for protective pig jackets

⇒ Foam adhesive

Source: Kendall Healthcare part of Covidien Ltd., Fareham, Hampshire, UK

⇒ Telfa Clear™ Non-adherent wound dressing

2.1.4 Histology, immunohistochemistry and image analysis

Source: GIBCO BRL, Life Technologies, Paisley, Scotland

⇒ MTT (3-[4,5-dimethylthiazol-2-yl]-2,5-diphenyltetrazolium bromide) for staining and cell assay

⇒ Acridine orange dye

Source: QIAGEN UK, Manchester, UK

⇒ RNeasy™ universal kit

⇒ Oligotex™ mini RNA kit

⇒ SYBR green™ Real Time-PCR kit

⇒ Qubit® 2.0 Fluorometer

⇒ Step One Plus™ Real Time PCR System

Source: Digitron, Torquay, Devon, UK

⇒ Pneumatic actuator controller

⇒ Pneumatic piston

Source: Surgipath Europe Ltd., Poole, Peterborough, England

⇒ Microtome blades

Source: Raymond A Lamb Ltd., England

⇒ Menzel-Glaser® Microscope slides

⇒ Twin Frost Microscope slides

⇒ Microscope Glass cover slips

Source: BOC gases, Shoreham-by-Sea, West Sussex, UK

⇒ Compressed nitrogen

Source: BDH laboratory supplies, Poole, Dorset, England

⇒ Formaldehyde

⇒ Gluteraldehyde

⇒ Haematoxylin (Gill's/Harris')

⇒ Eosin

⇒ DPX mountant

⇒ Xylene

⇒ Methanol

Source: Vector Laboratories Ltd, Peterborough, England

⇒ VECTABOND® reagent

⇒ VECTASTAIN® ABC Standard Kit

⇒ VectaMount® permanent mounting medium

⇒ D.A.P.I (4', 6-diamidino-2-phenylindole) fluorescent stain

⇒ Dylight™ staining kit (FITC, flourescine isothiocyanate)

Source: abcam, Cambridge, UK

⇒ K14, Laminin, and α smooth muscle actin secondary antibodies

Source: BMRF Histopathology Lab, Queen Victoria Hospital, East Grinstead, England.

⇒ Trypan blue

⇒ Sodium Chloride

⇒ Sodium Acetate Anhydrous

⇒ Triton X 100

⇒ Acetic Acid

⇒ Diaminobenzidine Tetrachloride dihydrate

Source: Genta Medical, York, UK.

⇒ I.M.S. (Industrial Methylated Spirit)

Source: Sakura Finetek Europe, The Netherlands

⇒ Tissue-Tek® OCT (Optimal cutting temperature) compound, embedding medium for frozen tissue specimens

Source: Canon UK Inc., Reigate, Surrey, UK

⇒ Canon EOS 300D digital camera

Source: Carl Zeiss Ltd., Welwyn Garden City, Hertfordshire, UK

⇒ Zeiss Axioscope microscope

⇒ Axiovision® software for image analysis

2.2 Methods

Human keratinocyte cell culture handling was performed in class II microbiology safety cabinet (Jouan LC2.12, Thermoscientific, NY, United States) and the human keratinocyte were kept in a humidified incubator (LEEC research® CO_2 incubator, LEEC, Nottingham, UK) at 37°C, relative humidity 98% and 5% CO_2 in a separate laboratory from the porcine cell culture.

Porcine keratinocyte and fibroblast cell culture handling was performed in class II microbiology safety cabinet (Jouan LC2.12) and all porcine cell cultures were kept in a humidified incubator (LEEC research® CO_2 incubator) at 37°C, relative humidity 98% and 5% CO_2.

2.2.1 Human keratinocyte isolation

Split thickness skin grafts were obtained from skin samples from discarded tissue (e.g. following breast reduction or abdominoplasty) from the Plastic Surgery Department, Queen Victoria Hospital, East Grinstead with patients' consent for skin use *in vitro*.

The surface of skin samples were prepped using the antimicrobials "Betadine®" and "Hydrex®" prior to harvesting a small split skin graft under sterile conditions using either mini Zimmer® electric dermatome with large specimens or Silvers™ skin graft knife (Swann Morton®, Sheffield, England) with small specimens. Both methods of skin graft harvest produce the same thickness of skin graft so no difference was noted in culture following the use of either method for skin graft harvest.

2.2.2 Human keratinocyte culture media

Human skin graft transport solution

⇒ Hanks Balanced Salt Solution (HBSS)

⇒ Penicillin/Streptomycin 100 units ml^{-1}/100 μg ml^{-1}

Human keratinocyte culture medium with Cholera Toxin

- DMEM with GlutaMAX™ 1000 mg/l D-glucose
- Foetal calf serum 20%
- Hydrocortisone 0.4 μg/ml
- Nutrient F 12 Medium 20%
- Human Recombinant Epidermal Growth Factor 10 μg/ml
- Cholera Toxin 10^{-10} M
- Penicillin/Streptomycin 100 units ml^{-1}/100 μg ml^{-1}

3T3 growth medium

- DMEM with GlutaMAX™ 1000 mg/l D-glucose
- Foetal calf serum 10%

2.2.3 Maintenance of 3T3 cells in human keratinocyte culture

Swiss 3T3 fibroblasts irradiated with 60 Gray from a Caesium-137 source (Blond McIndoe research foundation, East Grinstead, West Sussex, UK) were cultured in 75 cm^2 flasks using 10 ml of 3T3 growth medium. The medium was aspirated and the cells washed in 10 ml of HBBS solution when the flasks were 75% confluent. The HBSS solution was aspirated and the cells were dispersed using 2.5 ml 0.05% trypsin / 0.02% EDTA incubated for 5 minutes at 37°C. 2.5 ml of 3T3 growth medium were used to neutralize the trypsin.

Then the cells were centrifuged at 1000 rpm for 5 minutes and the supernatant discarded. The cells were re-suspended in 5 ml of 3T3 growth medium and a haemocytometer (Neubauer haemocytometer, Camlab, Cambridge, UK) used to perform a cell count. The cells were either re-seeded in a ratio 1:10 into 75 cm^2 flasks for 3T3 cell culture or used in human or porcine keratinocyte cell culture.

A layer of fibroblasts is essential for keratinocyte cell culture (Human or porcine), as the fibroblasts produce growth factors essential to support keratinocytes. Fibroblasts are

pre-irradiated with a sub-lethal dose of irradiation to suppress their growth within the culture, whilst allowing them to continue to produce growth factors.

2.2.4 Human keratinocyte cell culture

In the class II safety cabinet, a sterile petri dish (90 x 15 mm, D x H) was opened and the skin sample was placed on the inside using sterilised forceps. In between each use the forceps were stored in a 20 ml universal container containing sterile alcohol. The forceps were left to air dry before further use.

The skin was washed three times in separate 50 ml Falcon® tubes each containing 25 ml of Hanks buffered saline with Penicillin/Streptomycin 100 units ml^{-1}/100 $\mu g ml^{-1}$.

The skin was then placed into a 50 ml Falcon® tube containing 20 ml of 2 mg/ml Dispase®, sealed and transferred to an orbital shaker at 37°C/30 rpm. The skin was incubated for about 1 hour then the Falcon® tube was cleaned with sterile alcohol and placed back in the safety cabinet. Dispase® was used to separate the epidermis from the dermis and trypsin was used to breakdown the epidermis. The skin was placed onto a clean petri dish and the epidermis was gently peeled off the dermis using two pairs of forceps. The epidermis was then placed into a 50 ml Falcon® with 25 ml of trypsin, and placed in the orbital shaker at 37°C/30 rpm. The epidermis was incubated for another hour and the tube cleaned with sterile alcohol and placed back in the safety cabinet.

10 ml of human keratinocyte culture medium was added to the Falcon® tube and gently shaken. The epidermis was then removed and placed onto a clean petri dish with the skin surface facing down. The cells on the inferior surface of the epithelium were gently scraped using the back of a pair of curved forceps. 5 ml of human keratinocyte culture medium were trickled over the scraped surface of the skin twice, aspirated and added to the Falcon® tube. The Falcon® tube was then centrifuged at 400*g* for 4 minutes. The supernatant was removed and the cells re-suspended in 10 ml of fresh human keratinocyte culture medium. A cell count was undertaken using a haemocytometer and

the keratinocytes were seeded at a density of 4 x 10^6 with 2 x10^6 freshly harvested irradiated 3T3 cells as described in 2.2.3 into each 75 cm^2 flask. The flasks were then incubated at 37°C with 98% humidity and 5% CO_2.

2.2.5 Human keratinocyte cell culture maintenance

The flasks were removed from the incubator to the safety cabinet, gently shaken to remove the dead cells and human keratinocyte culture medium was added to the flasks 10 ml/ 75 cm^2 flask. Freshly irradiated 3T3 calls were added (1 x 10^6/75 ml flask) 3 times/week. When the colonies were 80-90% confluent they were split into new flasks.

The medium was removed and the cells washed with HBSS three times to remove traces of foetal calf serum and non-viable cells. Trypsin was added to the flasks (2 ml/ 75 cm^2) and the flasks placed back in the incubator at 37° C with 5% CO_2 for 10 minutes. The flasks were then removed from the incubator and gently tapped on the side to release the cells. The flask was held upright for 5 minutes to allow the cells to settle down to the bottom of the flask. Human keratinocyte culture medium was added to the flask (8 ml/ 75 cm^2) and the contents pipetted gently for a minute to form an even solution. The solution was re-seeded into new flasks (from one 75 cm^2 flask, 2 ml was aliquoted into each of 4 new 75 cm^2 flasks). Fresh irradiated 3T3 cells were added to each flask (2 x10^6 3T3/ 75 cm^2 flask) and further human keratinocyte culture medium (10 ml/ 75 cm^2 flask). A "T" number is allocated to each flask to indicate the number of times the cells were trypsinised i.e. T1 indicating the first passage.

The cells were harvested between the T2 and T4 stage in a sub-confluent density. In the 2-3 days prior to harvesting, no 3T3 cells were added to the culture flasks to avoid difficulties in removing them prior to keratinocyte harvest. The medium change was carried out every 48 hours.

2.2.6 Porcine keratinocyte transport and culture media

Porcine keratinocyte growth medium

- Opti MEM 1 with GlutaMAX™
- Foetal calf serum 10%
- Penicillin/Streptomycin 100 units ml^{-1}/100 μg ml^{-1}
- Final [Ca^{2+}] 0.5 mM

Porcine keratinocyte transport solution

- Hanks Balanced Salt Solution (HBSS)
- Amphotericin B 1.25 μg/ml
- Penicillin/Streptomycin 200 units ml^{-1}/200 μg ml^{-1}

3T3 growth medium

- DMEM with GlutaMAX™ 1000 mg/l D-glucose
- Foetal calf serum 10%

PT67 growth medium

- DMEM with GlutaMAX™ 4500 mg/l D-glucose
- Foetal calf serum 10%
- Penicillin/Streptomycin 100 units ml^{-1}/100 μg ml^{-1}

2.2.7 Maintenance of 3T3 cells in porcine keratinocyte culture

3T3 cells for porcine keratinocyte culture were maintained as previously described in section 2.2.3 maintenance of 3T3 cells for human keratinocyte culture but in a different laboratory.

2.2.8 Collagen coating of culture flasks

Pig keratinocytes were grown *in vitro* in culture flasks coated with rat tail collagen type I. A stock solution of rat tail collagen was made by dissolving 10 mg of rat tail collagen type I in 40 ml of 0.1 M acetic acid and left on a stirrer for 2 hours.

160 ml of tissue culture grade distilled water were added to make 200 ml in total. Chloroform was then used to sterilise the solution by dripping the chloroform liquid on a glass rod touching the bottom of the container, and this was left overnight at 4°C. In the morning, the sterile rat tail type I collagen solution was pipetted from underneath the chloroform.

75 cm^2 tissue culture flasks were coated by contact with 10 ml of collagen solution for 2 hours. The collagen solution was aspirated and the flasks were allowed to dry with the caps off for 4 hours.

The flasks could be stored at room temperature for up to one month and the collagen solution could be used up to 3 times before discarding. Immediately prior to use the culture flasks were rinsed with 10 ml of Hanks Balanced Salt Solution (HBSS).

2.2.9 Porcine keratinocyte isolation

A different isolation protocol was used for porcine keratinocyte isolation to address the higher risk of contamination and culture infection in porcine keratinocyte culture.

Porcine split thickness skin grafts were wrapped in a sterile gauze swab and placed into a 50 ml Falcon® tube containing 20 ml of porcine keratinocyte transport solution. Following transport to the laboratory, the skin was divided into small pieces measuring about 3 x 3 cm using a sterile disposable size 15 scalpel in a sterile petri dish. The skin samples were washed 5 times using transport solution in 5 different 50 ml Falcon® tubes, each tube is placed on a shaker for 1 minute at 200 rpm. Once removed the skin was placed into a solution of 20 ml of 2 mg/ml filtered Dispase® containing 200 units/ml Penicillin, 200 µg/ml Streptomycin and 1.25 µg/ml Amphotericin at 4°C overnight.

The following day at room temperature, a further 5 ml of Dispase® were added and the tube placed in an orbital shaker at 37°C for one hour at 30 rpm. The epidermis was then separated gently from the dermis. The epidermis was then washed using the transport

solution and placed into 10 ml of 0.25% trypsin solution containing 200 units/ml Penicillin, 200 μg/ml Streptomycin. This was left in the orbital shaker at 37°C for one hour. The epidermis was removed from the trypsin solution and the inferior surface abraded using sterile curved forceps to remove the keratinocytes. The trypsin was inactivated using 10 ml Optimem® and 10% foetal calf serum and centrifuged for 5 minutes at 400*g*. The supernatant was aspirated and the cell pellet re-suspended in porcine keratinocyte growth medium and a cell count performed using a haemocytometer.

2.2.10 Porcine keratinocyte cell culture

The 75 cm^2 flasks previously coated with rat tail collagen were washed with HBSS and seeded with 2 $x10^6$ irradiated 3T3 cells in porcine keratinocyte culture medium. The flasks were incubated for 2 hours at 37°C prior to isolating the pig keratinocytes. The pig keratinocytes were seeded at a density of 4 $x10^6$ per 75 cm^2 flask in 10 ml of growth medium. The medium was replaced every 48 hours and 90% confluence was reached after one week. Confluence was estimated by the size of newly formed colonies within 10 fields (x5) magnification in each flask.

When 90% confluence was reached, the keratinocytes were passaged using 0.05% trypsin / 0.02% EDTA. The flasks were washed three times with HBSS and then HBSS was aspirated. 5 ml of trypsin were added to each 75 cm^2 flask and the flasks incubated at 37°C for 10 minutes. The trypsin was neutralized with 5 ml growth medium and a cell count performed using a haemocytometer. The keratinocytes were then sub-cultured in a ratio of 1:4 into rat tail collagen coated flasks pre-seeded with irradiated 3T3 cells 2 hours before the addition of porcine keratinocytes. These secondary cultures reached 90% confluence in 3-4 days. Over a period of 3 weeks, after the cultures are passaged for about 4 times, the keratinocytes were harvested at 50% confluence the day prior to application to reduce the effect of contact inhibition on proliferation post application.

For cell spray suspension preparation, a cell count was performed using a haemocytometer and the keratinocytes re-suspended in growth medium (without foetal calf serum) at a concentration of 10^7 cells/ml.

2.2.11 Porcine fibroblast isolation

Pig skin samples were harvested, transported and stored overnight as described in 2.2.9 Porcine keratinocyte isolation.

The following day at room temperature, a further 5 ml of Dispase® were added and the tube placed in an orbital shaker at 37°C for one hour at 30 rpm. The epidermis was then separated gently from the dermis. The dermis was then washed using the transport solution and placed into 5 ml of collagenase (defrosted just before use). This was left in the orbital shaker at 37°C for 2 hours. 5 ml of 3T3 growth medium were added to dermis and collagenase and pipetted through a cell strainer into a Falcon® tube containing further 5 ml of 3T3 growth medium. Another 10 ml of 3T3 growth medium were added and the tube centrifuged for 5 minutes at 400*g*. The supernatant was aspirated and the cell pellet re-suspended in 10 ml of 3T3 growth medium and a cell count performed using a haemocytometer. The fibroblasts were seeded 1 x 10^6 cells/75 cm^2 flask and incubated at 37°C 5% CO_2.

2.2.12 Porcine fibroblast cell culture

The 3T3 growth medium was replaced after the first 24 hours and then every 48 hours and 90% confluence was reached after 4-5 days.

When 90% confluence was reached, the fibroblasts were passaged using 0.05% trypsin/0.02% EDTA. The flasks were washed three times with HBSS and then HBSS was aspirated. 5 ml of trypsin were added to each 75 cm^2 flask and the flasks incubated at 37°C for 5 minutes. The trypsin was neutralized with 5 ml 3T3 growth medium and a cell count performed using a haemocytometer. The fibroblasts were then sub-cultured in a ratio of 1:10 into 75 cm^2 flasks. These secondary cultures reached 90% confluence in

3-4 days. The fibroblasts were harvested at 50% confluence the day prior to application. For cell spray suspension preparation, a cell count was performed using a haemocytometer and the fibroblasts re-suspended in 3T3 growth medium.

2.2.13 Maintenance of the retroviral cell producer line

The retroviral producer cell line PT67pFB-hrGFP A2 clone cell line was maintained as the Swiss mouse 3T3 fibroblasts in section 2.2.3 using PT67 growth medium.

2.2.14 Retroviral transduction of porcine keratinocytes with the GFP gene vectors

The ViraPort™ retroviral vector pFB-HrGFP (Stratagene), containing the humanised form of the green fluorescent protein (GFP) from the "sea pansy Renilla Reniformis", was used to transfect a RetroPack PT67 packaging cell line (Clontech) according to the manufacturer's instructions using Lipofectamine Plus™ reagent.

Cells were cultured under selective pressure in DMEM with GlutaMAX™, sodium pyruvate, 4.5 gm/l glucose, and 10% foetal calf serum. Fluorescent colonies were isolated, expanded and screened for production of the virus containing the hrGFP protein. Screening was done using fluorescent microscopy by inspection of 10 fields (x20) magnification and counting fluorescent colonies. The PT67pFB-hrGFPClone A2 cell line was maintained as described in section 2.2.113. The cells were stored in liquid nitrogen and then thawed one week prior to the start of the porcine keratinocyte cell culture.

Following the PT67pFB-hrGFPClone A2 cell harvest as described in section 2.2.3 maintenance of 3T3 cell culture, a cell count was performed using a haemocytometer. The medium was then removed and DMSO (Dimethyl Sulphoxide) 10% v/v added to give a final concentration of 3 x 10^6/ml. DMSO was used to reduce intracellular metabolism prior to freezing, and to act as "antifreeze" to protect cells from ice crystals

formation during freezing or thawing. 1 ml of the cell suspension was added to each freezing vial. The vials were labeled with cell line, number of passage, cell count, project number, and date. The freezing vials were placed in a beaker containing ice then in a freezing plastic vessel (BiCell® freezing vessel, Osaka, Japan) at freezing rate of approximately -1°C per minute prior to storage in a -70°C freezer overnight. The next day the freezing vials were transferred to a liquid nitrogen storage tank.

When required, the PT67pFB-hrGFPClone A2 cells were thawed after removal from liquid nitrogen tank to around 37°C in a warm water beaker, taking care the cells did not touch the cap of the vial. The cells were pipetted from each vial and placed in a universal tube. 10 ml cold DMEM were slowly dripped on the cells. The total volume was topped to 20 ml using cold DMEM and the cells spun at 400g for 4 minutes. The medium was aspirated from above the cells, and the cell pellet re-suspended in 20 ml DMEM and 10% foetal calf serum. The cells were again spun at 400g for 4 minutes, medium aspirated, and the cell pellet re-suspended in warm PT67 growth medium. A cell count was performed using a haemocytometer and the PT67pFB-hrGFPClone A2 cell density seeding in the flasks was; 1 x 10^6 in 75 cm^2 flask and 2.5 x 10^6 in 175 cm^2 flask. PT67 growth medium was added; 10 ml in 75 cm^2 flask and 30 ml in 175 cm^2 flask. The flasks were incubated at 37°C humidity 98% and 5% CO_2.

Once the porcine keratinocytes had undergone their first passage, the medium in the PT67pFB-hrGFPClone A2 flask was changed to the porcine keratinocyte growth medium and placed into an incubator at 37°C and 5% CO_2 for 2 hours. The flask was then transferred to a 32°C incubator for 48 hours. The medium was removed from the flasks and spun down at 3600 rpm for 10 minutes. The supernatant was then removed and pooled.

The medium in the porcine keratinocytes flasks was then removed and replaced with the pooled medium. These flasks were placed back into the 37°C incubator and 5% CO_2 for 2 hours. They were then transferred to a 32°C incubator for 48 hours. Following this the

flasks were rinsed with HBSS twice and fresh porcine keratinocyte growth medium and 3T3 cells were added. The porcine keratinocyte cell culture continued as described in section 2.2.10. The transduction frequency was then calculated as in section 2.2.15, and the process repeated following the next passage prior to keratinocyte cell harvest for *in vivo* application.

2.2.15 Calculation of transduction frequency

The flasks containing the transduced keratinocytes were examined using the inverted fluorescent microscope. The keratinocytes expressing Green Fluorescent protein (GFP) in each flask were counted in ten areas (field width 2 mm) at x40 magnification. This was compared with the total number of keratinocytes in similar ten areas (field width 2 mm) using the same magnification; a percentage was calculated to give an estimate of the transduction rate.

Following keratinocyte harvest for *in vivo* application, after the cell count was performed, a second cell count was performed using the inverted fluorescent microscope to again confirm the transduction frequency. Transduction frequency was found to be around 75% prior to *in vivo* application.

2.2.16 Keratinocyte cell seeding on microcarrier beads

2 g of Cultispher G® microcarrier beads were reconstituted in 100 ml PBS for one hour and sterilised in autoclave. The beads were stored at 4°C refrigerator for up to two weeks.

Prior to use, the microcarriers were washed three times, twice in PBS and once using keratinocyte growth medium. When cultured keratinocytes reached 80–90% confluence, the cells were harvested from culture flasks using 0.05% trypsin.

The keratinocytes were transferred to a 100 ml Cellspin™ magnetic stirrer flask at a seeding density of 5 x 10^6 cells per 5 ml of microcarrier stock solution in a total volume of 40 ml keratinocyte growth medium. No 3T3 cells were added to the culture flask. As

described by Borg *et al.* (2009) cultures were left static for 24 hours, and then stirred at 45 rpm for 5 minutes with 40 minute static intervals. 50% of the growth medium was replaced three times per week after stopping the stirrer and allowing the beads to settle in the bottom of the flask. At day 7, the total volume was increased to 100 ml and the speed to 50 rpm with continuous stirring.

2.2.17 MTT staining of keratinocytes on microcarrier beads

1 ml was pipetted from the culture vessel (either Falcon® tube or stirrer flask) containing keratinocytes on microcarrier beads. MTT was dissolved in Ca^{++} and Mg^{++} free PBS to a final concentration of 5 mg/ml. MTT was then added to the 100 µl culture aspirate 1:10 to a final concentration of 0.5 mg/ml, followed by incubation at 37°C for 45 minutes.

The medium was then removed from the beads and replaced with HBSS. The viable cells attached to the microcarrier beads were visible using phase-contrast microscopy. Enzymes within viable keratinocytes reduce MTT to formazan, which has a distinctive blue colour.

2.2.18 Acridine orange staining of keratinocytes on microcarrier beads

Acridine orange is a nitrogen heterocyclic chromophore containing the acridine nucleus, which binds to DNA and RNA by intercalation between successive base pairs to produce a broad emission band in the green to red wavelength region (Kimmel *et al.* 1986). Acridine orange is excited by blue-green laser light (488 nm) or by ultraviolet, violet, and blue interference filters coupled to an arc-discharge lamp (mercury or xenon).

1 ml was pipetted from the culture vessel (either Falcon® tube or stirrer flask) containing keratinocytes on microcarrier beads. Acridine orange was dissolved in distilled water to a final concentration of 1 mg/ml. Acridine orange was then added to the 1 ml culture aspirate 1:10 to a final concentration of 0.1 mg/ml, followed by incubation at 37°C for

15 minutes. The medium was then removed from the beads and replaced with HBSS. The cells attached to the microcarrier beads were visible using ultraviolet microscope. Acridine orange is excited by blue-green laser light (488 nm) or by ultraviolet, violet, and blue interference filters coupled to an arc-discharge lamp (mercury or xenon). Excitation maximum shifts to 460 nm (blue), and the emission maximum shifts to 650 nm (red). RNA staining within keratinocytes produced an orange colour.

2.2.19 Keratinocyte cell count using Trypan blue

Trypan blue chromophore penetrates the damaged wall of non-viable cells staining the cells blue. A cell count using a haemocytometer was done following Trypan blue application.

The magnetic stirrer was switched off and the flask carefully moved to the safety cabinet. 1 ml of keratinocyte cell suspension was aspirated from the stirrer flask after gentle pipetting to avoid the microcarriers settling down the stirrer flask. The 1 ml suspension was placed in a screw cap tube and spun for 4 minutes at 1500 rpm. The microcarriers were dissolved and the cells dissociated using 0.25 ml trypsin and incubated at 37°C for 10 minutes. After 10 minutes, all the beads were dissolved as observed visually and the keratinocytes were preserved. 1 ml of keratinocyte growth medium was added and the tube re-spun for 2 minutes at 1500 rpm. The medium is aspirated and the cell pellet re-suspended in 100 μl of keratinocyte growth medium prior to the addition of 0.25 ml Trypan blue. A haemocytometer was used for cell count using the microscope, where both stained and non-stained (i.e. viable) cells were counted. Each cell count was repeated 3 times and an average cell count calculated.

2.2.20 Sample preparation for Scanning Electron Microscopy (SEM)

Porcine keratinocytes were isolated as described in 2.2.9, cultured as described in 2.2.10, and seeded on microcarrier beads as described in 2.2.16.

On day 8, the stirred culture was switched to static for 15 minutes and the microcarriers allowed to settle down the stirrer flask. Inside the safety cabinet, 2 ml of microcarriers and keratinocytes were pipetted from the bottom of the flask. The microcarriers and keratinocytes were washed twice using PBS and fixed with 2.5% glutaraldehyde in 0.1M Cacodylate buffer (pH 7.2-7.4) for 40 minutes at 4ºC.

The microcarriers and keratinocytes were rinsed using 0.1M Cacodylate buffer twice. This was followed by dehydration with graded series (increasing concentration) of ethanol for 5 minutes each; 25%, 50%, 75%, 90%, and 100% (twice). The microcarriers and keratinocytes were dried using Hexamethyldisilasane (HMDS). The samples were immersed in HMDS for 3 minutes, left to air dry in a fume cupboard overnigh. The next morning, the samples were mounted on SEM aluminium stubs (Agar scientific, Stansted, Essex, UK).

The samples were sputter coated to ensure a conductive pathway for the electron beam through the non-conductive specimens using Leit-C conductive carbon cement (Agar scientific, Stansted, Essex, UK). Then the samples were coated a very thin coating of palladium metal using a sputter coater (Polaron SC7640, Quorum Technologies Ltd., Lewes, East Sussex, UK). The samples were viewed using SEM (JEOL JSM-6310 with spatial resolution 1-2.5 nm), University of Brighton, East Sussex, UK.

2.2.21 MTT assay of porcine keratinocytes on microcarrier beads

MTT (3-[4,5-dimethylthiazol-2-yl]-2,5-diphenyltetrazolium bromide) reduction assay was used to quantify porcine keratinocyte proliferation.

Porcine keratinocytes were isolated as described in 2.2.9, and cultured as described in 2.2.10. The keratinocytes were seeded on microcarrier beads in stirred culture as described in 2.2.16. The magnetic stirrer was stopped and microcarriers left to settle at the bottom of the flask. The flask was placed inside the safety cabinet.

500 µl samples containing microcarriers and cells in duplicates were aspirated from the stirrer flask. The medium was replaced with fresh medium containing 10% MTT. Samples were incubated for 4 hours at 37°C and washed with PBS to remove unbound MTT. The resulting formazan crystals were dissolved using vortex spinner in 1 ml of dimethyl sulfoxide. 100 µl of each sample was plated in triplicates in 96-well plates, followed by reading the absorbance at 590 nm (Reference filter 620 nm, Sunrise plate reader, Tecan® group, Switzerland). Absorbance readings were plotted against a standard curve obtained using a serial dilution of porcine keratinocytes.

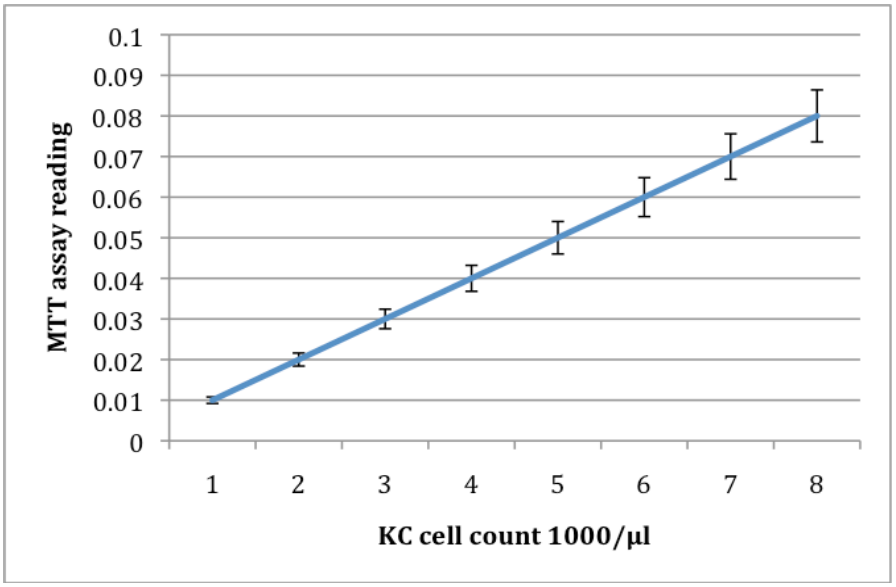

Figure 4: Standard curve for MTT assay against KC cell count
MTT assay results used to calculate KC cell count, a linear relationship between MTT assay readings and the KC cell count within stirred culture was seen

Keratinocyte cell count was calculated using MTT assay readings from serial porcine keratinocyte cell counts isolated from stirred microcarrier culture previously. The readings showed a linear relationship up to sample count of 10 000 cells (figure 6). Using a standard equation (Tecan® product information) in Microsoft Excel® sheet using the assay reading for the sample, the cell count within the sample was calculated.

2.2.22 RNA isolation from porcine keratinocytes on microcarrier beads

Porcine keratinocytes were isolated as described in 2.2.9, cultured as described in 2.2.10, and seeded on microcarriers in stirred culture as described in 2.2.16.

On day 10, the magnetic stirrer was stopped and the microcarriers allowed settling for 15 minutes prior to aspiration of 10 ml of microcarriers and keratinocytes. The beads were incubated with 0.25 ml trypsin at 37°C for 10-15 minutes to dissolve the beads and dissociate the keratinocytes. Trypan blue cell count was performed and the total number of keratinocytes/ml calculated. The medium was gently aspirated using pipette. 5 ml HBSS were added to wash beads, left to settle and aspirated as before.

The beads were covered with 5 ml 0.5% trypsin/HBSS solution and left for 10-15 minutes at 37°C until the beads were dissolved. 5 ml culture medium were added and centrifuged at 1500 rpm for 4 minutes. The culture medium was aspirated and fresh 5 ml medium added, final cell count confirmed, and centrifuged at 1500 rpm for 4 minutes. The culture medium is then aspirated and 350 µl Buffer RLT® (proprietary name) were added and homogenised by pipetting up and down.

Qiagen RNeasy mini kit® was used and buffers were adjusted according to cell count. The lysate was homogenised by centrifuging for 2 minutes at 1500 rpm then 350 µl of 75% ethanol were added and homogenised by pipetting up and down. The 700 µl sample was transferred to a collection tube and the tube was labelled on the side and the top. The tube was spun in a mini-centrifuge at 10 000 rpm for 15 seconds (The 15 seconds were counted after 8000 rpm). The flow-through was aspirated and discarded and 350 µl of Buffer RLT® (proprietary name) added. The tube was spun again at 10 000 rpm for 15 seconds, and the flow-through aspirated and discarded. 350 µl wash Buffer RWI® (proprietary name) were added and the sample spun at 10 000 rpm for 15 seconds, the flow-through aspirated and discarded. 500 µl of Buffer RPE® (proprietary name) were added and sample was spun at 10 000 rpm for 15 seconds, the flow-through aspirated and discarded. 500 µl of Buffer RPE® were added and the sample spun at 10 000 rpm for 2 minutes, the flow-through aspirated and discarded. The sample was transferred to a new tube and 30 µl RNase® free water were added, and sample was

spun at 10 000 rpm for 1 minute. Another 30 μl RNase® free water were added and sample was spun at 10 000 rpm for 1 minute.

SYBR Green II gel kit® was used to ensure purity of RNA sample initially then Quant-iT RNA assay kit® was used to quantify RNA concentration. Two 200 μl of working solutions were prepared (1 μl RNA reagent: 199 μl RNA buffer) for each standard and each sample. Two RNA standards were prepared each in 190 μl working solution: 10 μl standard. The samples were prepared in 199 μl working solution: 1 μl sample. RNA measurement was done using Qubit® Flurometer measuring 2 x standards followed by measurement of RNA in each sample.

2.2.23 Real-time quantitative PCR (qPCR) K14 mRNA from porcine keratinocytes on microcarrier beads

Porcine keratinocytes were isolated as described in 2.2.9, and cultured as described in 2.2.10. The keratinocytes were seeded on microcarrier beads in stirred culture as described in 2.2.16. On day 10, the samples were prepared for RNA isolation as described in 2.2.19. SYBR Green II kit® was used for generating full-length cDNA from RNA and K14 mRNA measurement using QuantiTect SYBR Green PCR Kit®. cDNA synthesis reactions were performed in duplicates and then used as a template for thermal cycling. cDNA synthesis mix was prepared for 1 reaction in a total volume of 20 μl as shown below (table 2):

Component	Volume
Enzyme mix	1 ul
5x cDNA synthesis buffer	4 ul
RNA primer (Mouse K14 F & R)	1 ul
dNTP mix (Promega: U1511)	2 ul
Water	11 ul
Template	1 ul
Total	**20 ul**

Table 2: Preparation of cDNA synthesis mix

The volumes of the components were added to a pre-chilled sterile vial, which was kept on ice at all times. Following mixing 20 µl of each reaction was transferred to two empty replicate wells and the tubes sealed. The tubes were incubated at 42°C for 30 minutes followed by reverse transcription (RT) inactivation at 95°C for 2 minutes (pre-programmed in SYBR Green II®-Step 1 programme). The duplicates were pooled together to produce 40 µl of cDNA sample. The concentration of the sample was measured using Quant-iT ssDNA assay kit® for use with Qubit® Flurometer.

For SYBR Green II®-Step 2, working mixes were prepared in triplicates for each cDNA dilution and non-template control (NTC). The volume of each component for 1 reaction was 25 µl; 24 µl were prepared as shown below:

Component	**Volume**
QPCR Master Mix	12.5 ul
Primer Forward (Mouse K14-F)	2.5 ul
Primer Reverse (Mouse K14-R)	2.5 ul
Water	6.5 ul
Total	**24 ul**

Table 3: Preparation of SYBR Green II®-Step 2 working mix

Optimisation of SYBR Green II® qPCR reactions was performed as per manufacturers' instructions to exhibit good amplification efficiency over a broad dynamic range. The optimal annealing temperature was identified for each assay through running pre-assay samples on agarose gel. 24 µl of working mix were added to each well of PCR plate, 1 µl of template was added to each set of triplicates and 1 µl of water to each set of NTC. The plate was sealed using heat seal and centrifuged briefly to ensure reaction mix in the bottom of each well. The plate was then placed in the Bio-Rad Cycler.

For thermal cycling, the following conditions were pre-programmed in the SYBR Green II®-Step 2 programme:

Cycle	Step	Temperature	Duration
Cycle 1 (1x)	Step 1 (activation step)	95°C	15 mins
Cycle 2 (50x)	Step 1 (denaturation)	95°C	15 secs
	Step 2 (annealing)	60°C	20 secs
	Step 3 (extension)	72°C	20 secs
Data collection and real-time analysis			
Cycle 3 (1x)	Step 1	95°C	30 secs
Cycle 4 (1x)	Step 1	55°C	30 secs
Cycle 5 (80x)	Step 1	55°C	10 secs
Increase set point temperature after cycle 4 by 0.5˚C			
Melt Curve data collection			

Table 4: Thermal cycling SYBR Green II®-Step 2 programme

Relative expression of the target gene was calculated using the 2 ΔCT method described by Livak and Schmittgen (2001). Relative K14 mRNA expression was assessed on days 14 and 21 of microcarriers culture.

2.3 *In vivo* animal wound model

2.3.1 Animals

Female out-bred white pigs aged 4-5 weeks and weighing 20-25 kg, were supplied by Bury Farm, Edgware, England.

2.3.2 Animal husbandry

Animal experiments were carried out under the UK Home Office project license PPL80/2215 and personal license PIL80/11190 in accordance with the Animals (Scientific Procedures) Act 1986. The animal studies were performed at Northwick Park Institute for Medical Research (NPIMR), Harrow, London.

The pigs were delivered 7-10 days prior to the first operative procedure to allow the animals to become familiar with their surroundings according to the rules of good husbandry. The animals were initially housed during the acclimatization period in pens accommodating up to 6 pigs at a time.

Following the first procedure (skin graft harvesting), the animals were placed in individual pens in order to avoid trauma to the wounds and disruption of dressings.

At the start of each procedure the animals weighed between 20-30 kg. Animals were kept starved pre-operatively overnight as with standard general anaesthesia. There were no unplanned animal deaths during the *in vivo* studies.

2.3.3 Animal anaesthesia and euthanasia

All *in vivo* procedures were performed under general anaesthesia. Animals were enticed into a mobile covered container where they were pre-medicated with an intramuscular injection of Xylazine® 1 mg/kg and Ketamine® 5 mg/kg. The animals were then transported to the operating theatre and given inhalation anaesthesia using an animal specific face mask. This was a combination of 2-5% halothane and 3-5 l/min of nitrous oxide and oxygen (1:1) and this was used to maintain anaesthesia during the procedure.

Pressure points (flexed knee joints of all four limbs) were protected throughout the procedure with appropriate cotton wool padding.

Antibiotic prophylaxis was given on induction for all procedures including dressing changes by a single intramuscular injection of Ampicillin® 25mg/kg. Postoperative analgesia included the application of topical 2% Lignocaine® gel to skin graft donor sites, and a subcutaneous injection of Carprofen (Xenecarp®) 4 mg/kg once daily for 2-3 days after the procedure. An anti-parasitic "Ivermectin" (Ivomec®, Merial Animal Health Ltd) 1 ml subcutaneous injection into the neck was given after the first procedure only.

Euthanasia was carried out after wounds excision for histological analysis; the animal was put under general anaesthesia followed by an intramuscular injection of 140 mg/kg Pentobarbitone (Expirol®).

2.3.4 Harvesting of split thickness skin grafts

Spilt thickness skin grafts were harvested either for harvesting porcine keratinocytes for cell cultures or for application alone or in combination with other treatments as part of the *in vivo* experiments.

The para-vertebral area on the animal back was shaved and cleaned with a scrubbing brush using chlorhexidine 4% scrub (Hydrex®). Then, the skin was prepared using 0.5% chlorhexidine in alcohol; normal saline (sodium chloride 0.9%) was used to wash it off. Then a further prep with povidine iodine 10% in aqueous solution (Betadine®) was done. This was left for five minutes and then washed off with sterile alcohol 70% and allowed to evaporate. The animal was then draped with sterile surgical drapes.

The skin was then coated in sterile liquid paraffin to allow easy glide of the dermatome. A single skin graft sheet (8 x 8 cm) was harvested from each animal using the Zimmer® air dermatome at a standard setting to achieve thickness of 600 μm.

The skin graft for harvesting keratinocytes was wrapped in sterile gauze, placed into a sterile container soaked in the transport medium.

The donor site was then dressed with topical 2% Lignocaine® gel, paraffin gauze dressing (Jelonet®) and Betadine® soaked gauze. The donor site was healed in 2-3 weeks time and could be harvested again if required.

2.3.5 Creation of full thickness wounds with PTFE chambers

Six full thickness wounds were made on each pig, three on each flank. Skin grafts were harvested previously from each animal, and the wounds were sited away from the donor site for skin graft harvesting. The flanks of each animal were prepared first by shaving with an electric clipper and then a hand held razor and then prepared as described in section 2.3.3. The animal was draped with sterile surgical towels.

Full thickness wounds were made on the flanks using a sterile cardboard template (4 cm in diameter) and cut out using a size 10 scalpel. The wounds were made through the

epidermis, dermis, subcutaneous fat and the "panniculus carnosus" layer; hence the fascia overlying the muscle was the wound bed.

In order to prevent wound healing from the edges and keratinocyte migration from the wound edges, Polytetrafluoroethylene (PTFE) chambers were inserted into the wounds. To allow the insertion of the wound chambers, the wound edges were undermined by 1cm and a 1 cm incision was made in the edge of the wound at the 3 o'clock margin. A preset hole in the chamber edge at the 3 o'clock margin was used to secure it in position using 2/0 silk sutures. The wounds either had cultured keratinocytes on microcarrier beads or as cell spray with/without meshed split skin graft applied or were left untreated a control group. The wounds were dressed with Telfa clear™ and covered with Jelonet® and lightly packed gauze. The outermost gauze was soaked with Betadine® and gauze soaked in Betadine® was wrapped around the outside of the chamber. The flanks were wrapped in Velband® cotton wool bandage and secured with Elastoplast® and Mefix® adhesive tape. Custom-made foam jackets were applied and secured using Velcro® tape. Throughout the *in vivo* animal experiments, the foam jackets remained secured in place, and there was no incidence of the animals removing them between dressing changes.

2.3.6 Creation of square wounds for assessment of wound contraction

The animals were anaesthetised as described in 2.3.3. Three square-shaped wounds were created on the flank of each animal measuring 4 x 4 cm using a sterile plastic template. STSG was harvested from one flank (not previously used for STSG harvesting for keratinocyte culture) using Zimmer® air dermatome (800 μm thick) and meshed 6:1 using carriers and Zimmer® mesher. The STSG was applied to the wounds and inset using 3M™ skin staples and treatments applied according to a preoperative randomised allocation.

2.3.7 Measurement of wound surface area using Visitrak™ system

For the assessment of wound contraction in square wounds, the surface area of each wound was directly traced using Visitrak™ transparent sheet, and the surface area measured on Visitrak™ device at each dressing change.

The sheet was held in place by an assistant to trace the wound on the animal's back maintaining contact with the wound edges during the process. For each wound, the tracing was repeated 3 times and an average calculated at each time point.

2.3.8 Tissue processing

A whole wound excision biopsy after removal of the PTFE chamber was performed following termination of the animals, at fixed time periods throughout the study. After terminal anaesthesia with a lethal dose of barbiturates the PTFE chamber was removed and whole wounds were excised. The time between initiation of anaesthesia and wound excision did not exceed one hour. The wound biopsy was then divided into four quadrants. Each of these sections was placed into folded aluminum foils, with the relevant sectioning face marked. The folded aluminum foils were filled with optimal cutting temperature compound (OCT) and frozen by immersing in liquid nitrogen.

The sections were stored at -40°C. 15µm thick frozen sections were cut using a cryotome in an insulated cabinet at -20°C.

2.4 Histology

2.4.1 Haematoxylin and Eosin staining (H&E)

Haematoxylin and Eosin (H&E) staining was performed for basic assessment of re-epithelialisation *in vivo*. Slides were air dried overnight then stained in haematoxylin for 1 minute, washed in running tap water for 5 minutes. The slides were then stained in 0.5% aqueous eosin for 5 minutes and dehydrated in ascending concentrations of

alcohol (30%, 70%, and absolute by volume). The slides were immersed in xylene and agitated for 2 minutes then immersed for further 4 minutes in static xylene. The slides were mounted in Distyrene Plasticiser and Xylene (DPX). OCT allowed a greater surface area for the section to stick and provided a slight temperature difference between the slide and the section to improve adherence. The sections were sealed with 50mm coverslips and left to air-dry flat overnight.

2.4.2 Immunohistochemistry

Immunohistochemistry was performed using nickel enhancement of the avidin-biotin complex (ABC) method. This was used to visualise specific cell structure within the tissue sections. The primary antibody attaches to the targeted protein, the secondary antibody couples to the primary antibody and is then visualised under standard microscopy.

Immunohistochemistry was used to visualise **cytokeratin 14 (K14)**, a marker for basal keratinocytes (Abcam, UK, 1:250), **laminin**, an early marker of basement membrane formation (Abcam, UK, 1:250), **collagen VII**, a late marker of the basement membrane (Abcam, UK, 1:200), and **alpha-smooth muscle actin (α SMA)** (Sigma, UK, 1:200), a marker for myofibroblasts. Positive controls were prepared from pig skin specimens away from the experiment wounds. Negative controls were prepared from muscle fascia underneath the skin specimens used for positive controls.

Optimal antibody concentration was judged as being the concentration at which the greatest contrast was seen in the expected structures or areas of the cell or tissue. The final concentration was selected after producing positive staining in more than 5 out of 10 positive control sections, while no staining was noted in the negative sections.

Collagen VII was detected using ABC staining kit, K14, laminin and alpha-smooth muscle actin were detected using DyLight secondary antibodies and mounted in Vectamount with DAPI.

Prepared sections 12 - 15 μm-thick as described in section 2.3.6, and 200 μl of serum/antibody solution were required to cover each slide. The tissue sections were fixed in acetone/methanol (1:1) for 20 minutes at room temperature, rinsed in phosphate buffered saline (PBS) 3 times for 3 minutes each time. The sections were then placed into a humidified chamber and incubated for 30 minutes at 20°C (room temperature) with normal serum of the species used for secondary antibody preparation (Serum diluted 1:30 with PBS). After incubation, serum was blotted off without rinsing and the primary antibody, one of listed earlier, was applied at optimal dilution (1:200 or 1:250). Slides were incubated with primary antibody in a dark humidified chamber at 20°C for one hour. After incubation, the tissue sections were rinsed in PBS for 5 minutes. The secondary antibody was applied (ABC 1:100 and Dylight 1:150) then the sections incubated at 20°C for one hour. The secondary antibodies were optimized previously using serial dilutions (1:50, 1:100, 1:150, 1:200 and 1:250) followed by comparing the quality of staining. The sections were rinsed in PBS for 5 minutes and 3,3'-Diaminobenzidine (DAB) substrate added and then further incubated for 10 minutes at room temperature until suitable staining developed.

The DAB substrate (Vector labs, Ca, USA) was prepared as per manufacturer's instructions using standard dropper (supplied with DAB kit, drop = 0.25 ml) by adding 2 drops of buffer stock solution to 5 drops distilled water and mixed well. Then 4 drops of DAB stock solution were added and mixed well followed by adding 2 drops of hydrogen peroxide solution and mixed well. Since grey-black stain was desired, 2 drops of nickel solution were added and mixed well. The tissue sections were dehydrated in 70% industrial methylated spirit (IMS) for 30 seconds then 100% IMS twice for 2 minutes, then the sections were immersed in xylene and agitated for 2 minutes, then immersed for further 4 minutes in static xylene. The slides were mounted in DPX or DAPI (4',6-diamidino-2-phenylindole) anti-fade mountant (for immunofluorescence), and sealed with 50 mm coverslips and left to air-dry flat overnight.

2.5 Data analysis

2.5.1 Clinical analysis

During each *in vivo* experiment, wounds were macroscopically assessed for infection, epithelialisation, graft take, granulation tissue formation or any other complications. Wound photographs were taken with a Canon EOS 300D digital camera during dressing changes to document wound appearance for qualitative assessment.

2.5.2 Image analysis

Digital photographs of histological sections for image analysis were taken with a Spot 1.1.0 (Diagnostic Instruments Inc., USA) and Olympus DP71 microscope-mounted camera (Olympus UK Ltd., UK) using standard settings from positive controls (standard settings for light intensity, gain, exposure time and offset were used in all experiments). Images were analysed using ImageJ® (National Institute of Health, USA) to detect the GFP-positive area in five random standard areas per section. For statistical analysis, multiple measurements were compared between different treatment groups using ANOVA (all pair-wise comparison).

2.5.3 Statistical analysis

Statistical analysis of data was performed and graphically represented using SigmaStat® 3.5 (Systat Software UK Ltd., UK) and Microsoft Office Excel® 2003 (Microsoft Corporation, USA) software packages. Experimental groups were analysed using one-way analysis of variance (ANOVA) and mixed model analysis of variance (t-test, Kruskal-Wallis test, and Holm-Sidak post hoc test) using Sigmastat® (Systat Software Inc., California, USA).

Chapter 3: An investigation into *in vitro* keratinocyte cell culture on microcarrier beads

3.1 Comparative analysis of two types of gelatin microcarrier beads for the culture of keratinocytes *in vitro*

3.1.1 Study objectives

The aim of this study was to establish a consistent and reliable method for keratinocyte cell culture *in vitro* on microcarrier beads. The use of biodegradable microcarriers would negate the need for trypsinisation prior to keratinocyte transferral to the wound bed. Trypan blue was used to compare keratinocyte cell count *in vitro* on microcarrier beads with standard culture.

3.1.2 Keratinocyte cell culture in cell rotator and magnetic stirrer

Keratinocytes were isolated from the skin samples as described in 2.2.4, and the keratinocyte cell cultures were maintained as described in 2.2.5.

Following primary expansion for 7-10 days, keratinocytes were isolated from tissue culture flasks and seeded onto either Cultispher G® or Cultispher S® in static culture in 15 ml Falcon® tubes; 1.25 x 10^5 cells, 2.5 ml of medium and 2.5 ml of microcarriers. Tubes were incubated at 37°C in 5% CO_2 in a rotator (Fisher Scientific UK Ltd., Loughborough, UK) (figure 7) programmed to rotate full 360° 32 times in 24 hours (minimum rotation setting in 24 hours).

Cultispher G® was used for keratinocyte culture in Cellspin™ magnetic stirrer flasks (figure 8). The seeding density was 1 x 10^6 cells/5 ml of microcarrier beads solution (2 gm/100 ml) in a total of 40 ml of culture medium as described in 2.2.16.

Figure 5: Keratinocyte cell culture in Falcon• tubes in a rotator.
The rotator was kept in an incubator and set at the minimum setting for rotation in 24 hours to minimise culture agitation

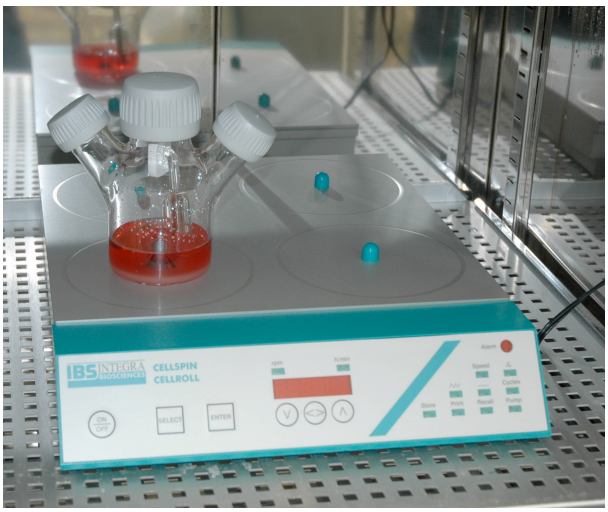

Figure 6: Keratinocyte cell culture in stirrer flask on a magnetic stirring unit.
The stirrer flask and the stirring unit were kept in an incubator during the period of the experiment

On Days 4, 8, 12, 18, 24 and 30, 100 μL of beads were removed using a sterile pipette, the beads were then added to 1:10 of either MTT as described in 2.2.17 (figure 9), or acridine orange as described in 2.2.18 (figure 10). MTT was used to detect metabolically active cells and acridine orange for general cell visualisation.

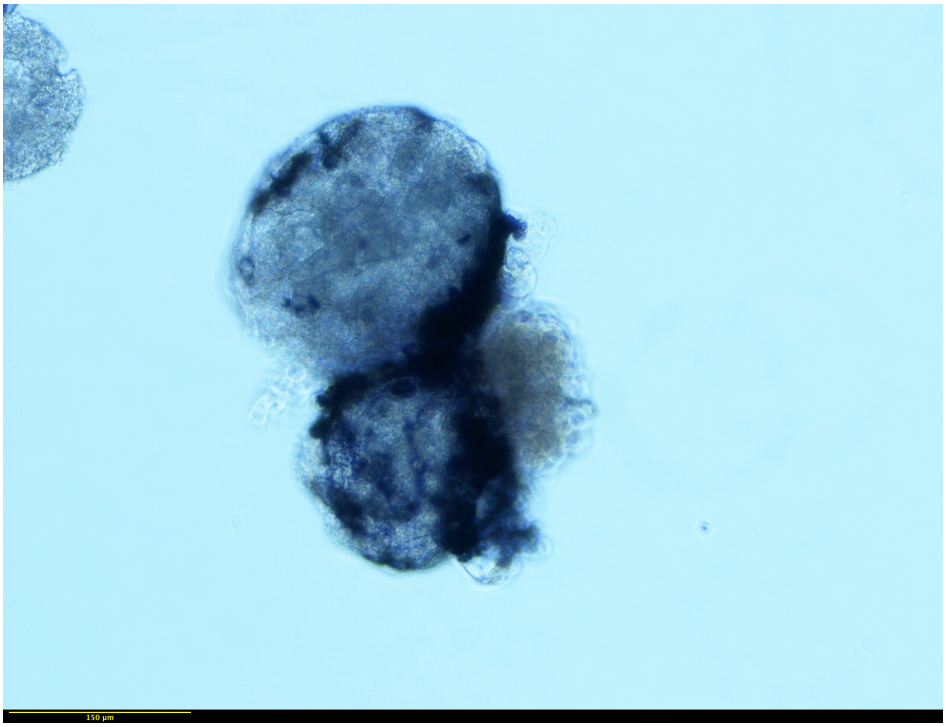

Figure 7: MTT staining keratinocyte cell culture on microcarrier beads day 4
Dark stained keratinocytes following MTT staining seen attached to the surface of Cultispher G® microcarriers (x40 magnification, field width 0.9 mm)

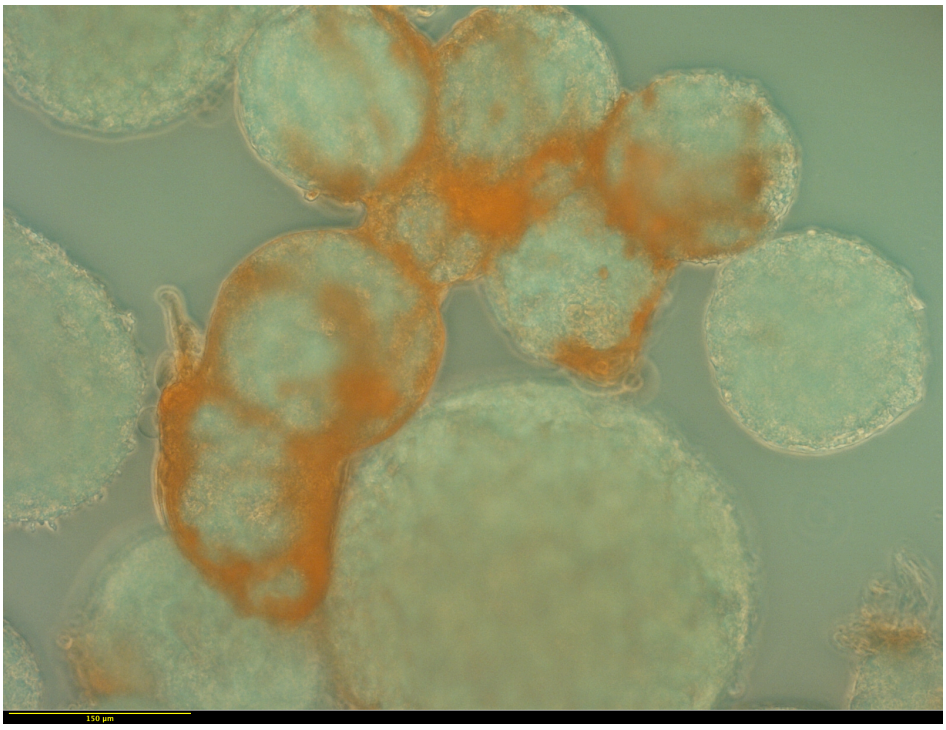

Figure 8: Acridine orange staining keratinocyte cell culture on microcarrier beads day 4
Orange stained keratinocytes following Acridine orange staining seen attached to the surface of Cultispher G® microcarrier (x40 magnification, field width 0.9 mm)

Alamar Blue® can successfully evaluate cellular health and is an indicator of cell viability. Alamar Blue® was added to 0.1 ml of keratinocytes and microcarrier beads

(1:10) then incubated at 37°C for 3 hours. 100 µl of each sample was plated in triplicates in 96-well plates, followed by reading the absorbance at 570 and 600 nm (Sunrise plate reader, Tecan® group, Switzerland). Negative control 96-well plate containing culture medium and microcarriers only was used initially to confirm zero absorbance in absence of keratinocytes. The reading was proportional to the number of viable cells and corresponded to the cellular metabolic activity. Finally, results were analysed by plotting fluorescence intensity (or absorbance) at different time points as percentage of Alamar Blue® reduction (fluorescence intensity) above control reading.

3.1.3 Viable keratinocyte cell count using Trypan blue

Keratinocytes were isolated from the skin samples and cultured as described in 2.2.1 and 2.2.4, and maintained as described in 2.2.5.

Following primary expansion for 7-10 days, keratinocytes were isolated from tissue culture flasks and seeded onto microcarriers as described in 2.2.16. Two tissue culture flasks were maintained as described before to compare cell counts with stirred culture. Cell count was performed at the following time points: day 6, day 10 and day 14.

3.1.4 Results

Standardisation of microscopy was performed as per Blond Mcindoe Research Foundation standard operating procedure using the same microscope with identical settings. Cultispher G® and S® supported Keratinocyte cell culture in cell rotator as demonstrated by MTT and acridine Orange staining. Figure 11 shows Cultishper G® and S® MTT staining at days 4 and 18. Clusters of dark stained keratinocytes were observed attached to the microcarriers indicating cellular attachment.

Figure 12 shows similar findings as keratinocytes are seen attached to Cultispher G® and S® following staining with Acridine Orange at days 4 and 18. The orange colour of stained RNA within keratinocytes is seen attached to the surface of the microcarriers with increasing density from day 4 to day 18.

Day 4 **Day 18**

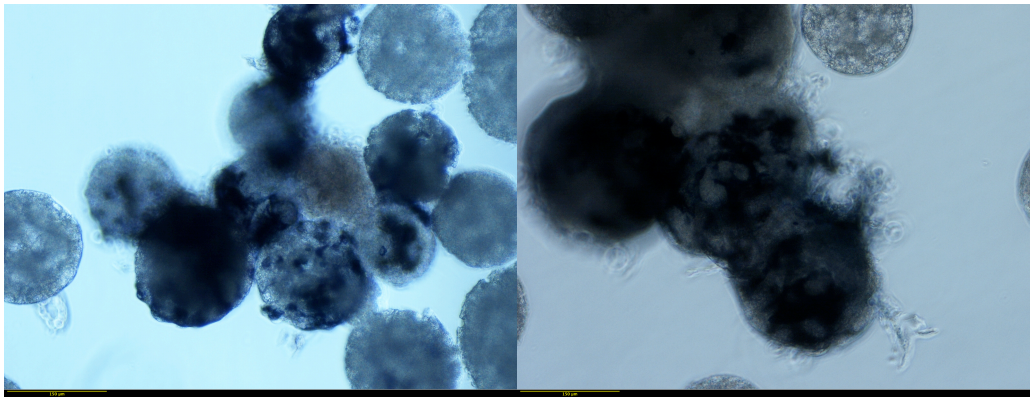

Cultispher G® + keratinocyte cell culture in cell rotator D4 and D18
Dark stained keratinocytes on microcarriers surface showing increase in cell attachment and distribution across beads' surface from day 4 to day 8 (x20 magnification, field width 1.8 mm)

Day 4 **Day 18**

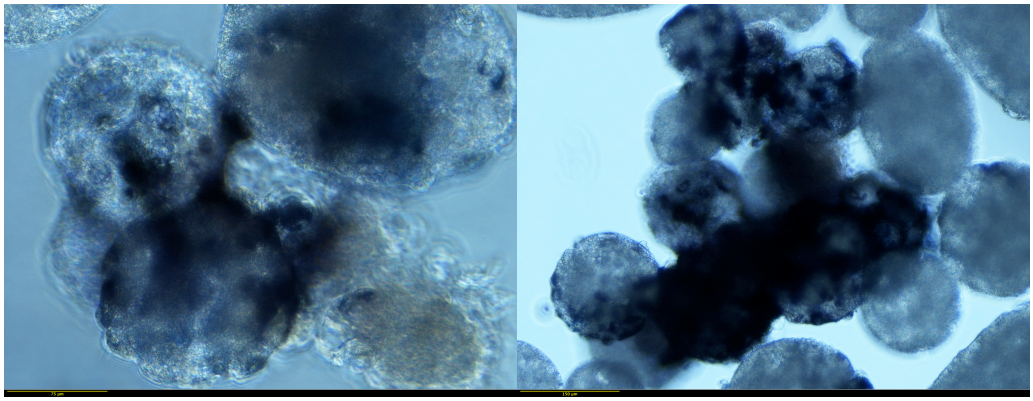

Cultispher S® + keratinocyte cell culture in cell rotator D4 and D18
Dark stained keratinocytes on microcarriers showing increase in cell numbers and distribution on beads' surface (left x40 and right x20 magnification, field width 0.9 mm and 1.8 mm respectively)

Figure 9: Cultispher G® & S® + cultured keratinocytes MTT staining days 4 and

Day 4 **Day 18**

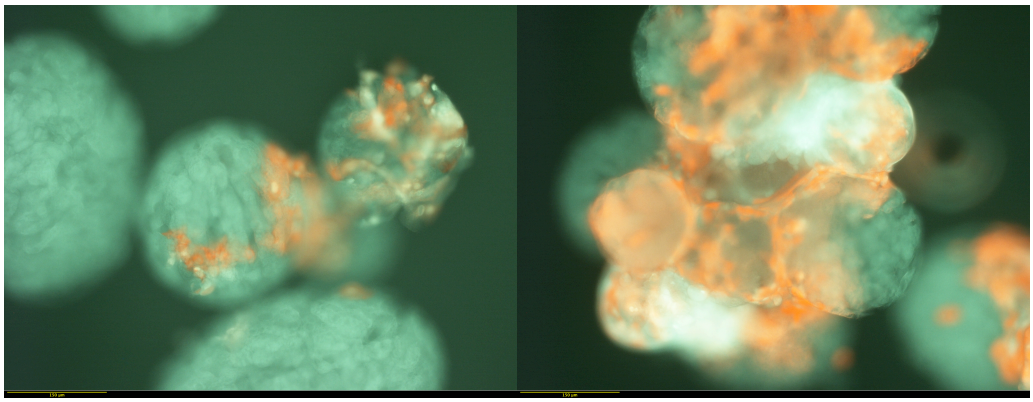

Cultispher G® + keratinocyte cell culture in cell rotator D4 and D18
Orange stained RNA within keratinocytes attached to the surface of microcarriers showing increase in cells attachment and distribution on beads' surface from day 4 to day 18 (left x40 and right x20 magnification, field width 0.9 mm and 1.8 mm respectively)

Day 4 **Day 18**

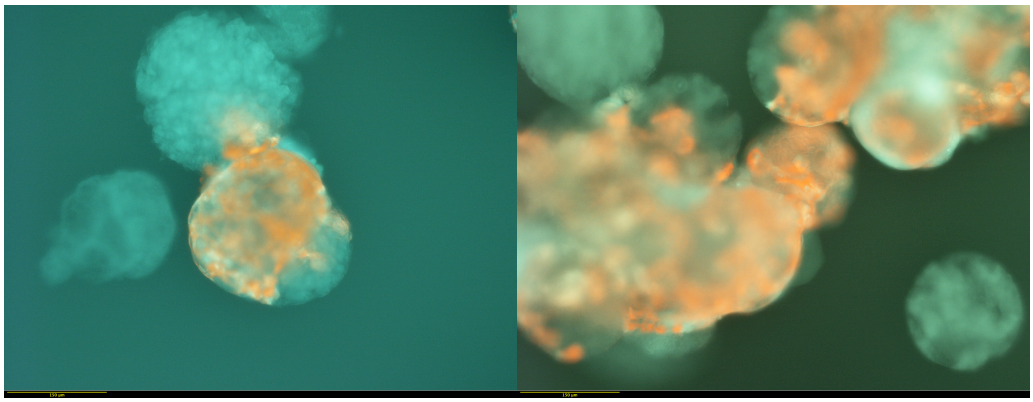

Cultispher S® + keratinocyte cell culture in cell rotator D4 and D18
Orange stained RNA within keratinocytes attached to the surface of microcarriers showing increased cell attachment and distribution on beads' surface from day 4 to day 18 (x20 magnification, field width 1.8 mm)

Figure 10: Cultispher G® & S® + cultured keratinocytes acridine orange staining days 4 and 18

Successful keratinocytes attachment to both types of microcarrier beads started from as early as day 4 and continued throughout the following time points up to day 30.

Alamar Blue® is a cell viability indicator that uses the natural reducing power of living cells to convert resazurin to the fluorescent molecule, resorufin. The active ingredient of Alamar Blue® (resazurin) is a nontoxic, cell permeable compound that is blue in colour and virtually non-fluorescent. Upon entering cells, resazurin is reduced to resorufin, which produces bright red fluorescence. Viable cells continuously convert resazurin to resorufin, hence generating a quantitative measure of viability.

Alamar Blue® reduction as percentage of increased reading compared to similar volumes of culture medium and microcarriers without keratinocytes indicated progressive increase in viable cells (figure 13).

Around day 18 to day 20, a decrease in keratinocyte population was observed followed by an increase (figure 13). The reduction in viable keratinocytes could be explained by the turnover of keratinocytes within the culture, which occurs around 21 days.

Based on the initial qualitative and quantitative data, no significant difference was shown between the two types of Cultispher® microcarriers.

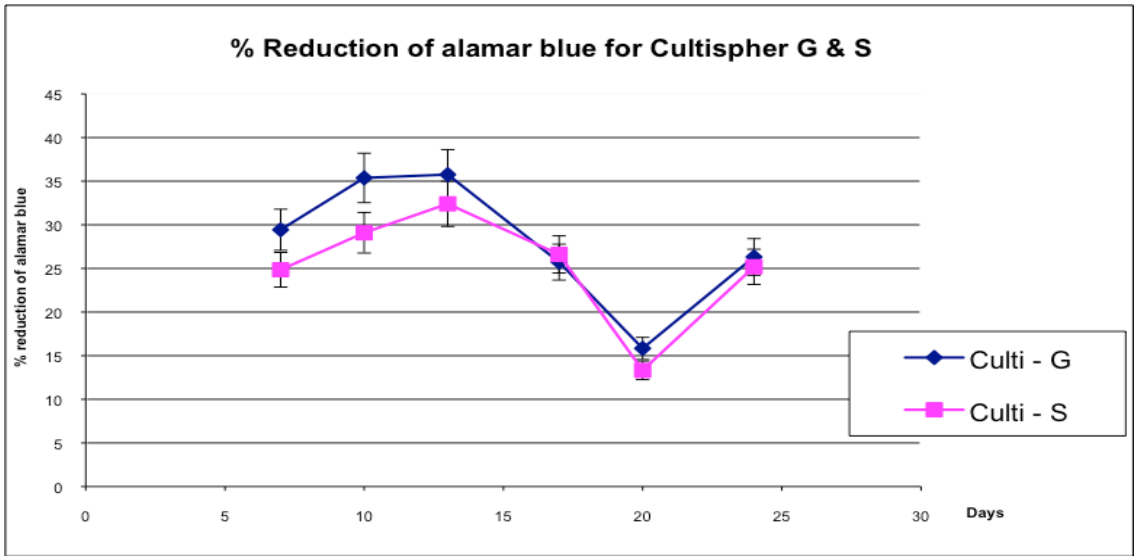

Figure 11: Alamar Blue® reduction keratinocyte cell culture on Cultispher G® & S® in cell rotator (Error bars refer to standard deviation).

Day 4 **Day 18**

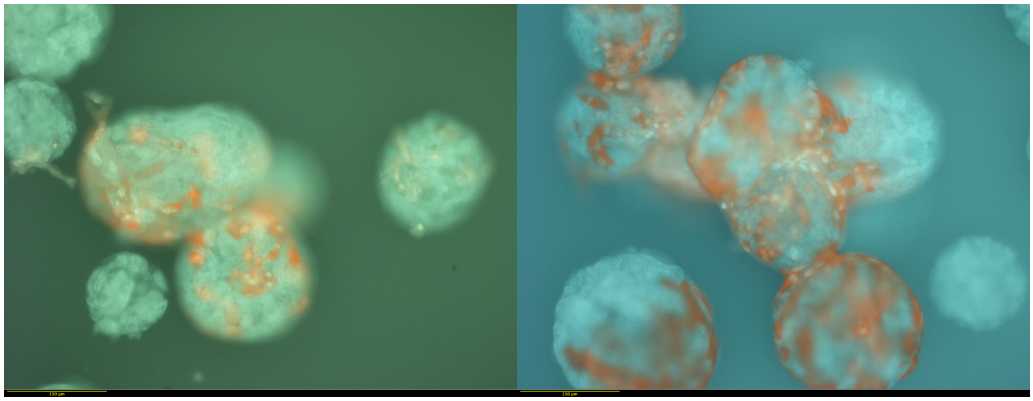

Cultispher G® + keratinocyte cell culture in magnetic stirrer (AO staining) D4 and D18
Orange stained RNA within keratinocytes attached to the surface of microcarriers showing increased cell attachment and distribution on beads from day 4 to day 18 (x20 magnification, field width 1.8 mm)

Day 4 **Day 18**

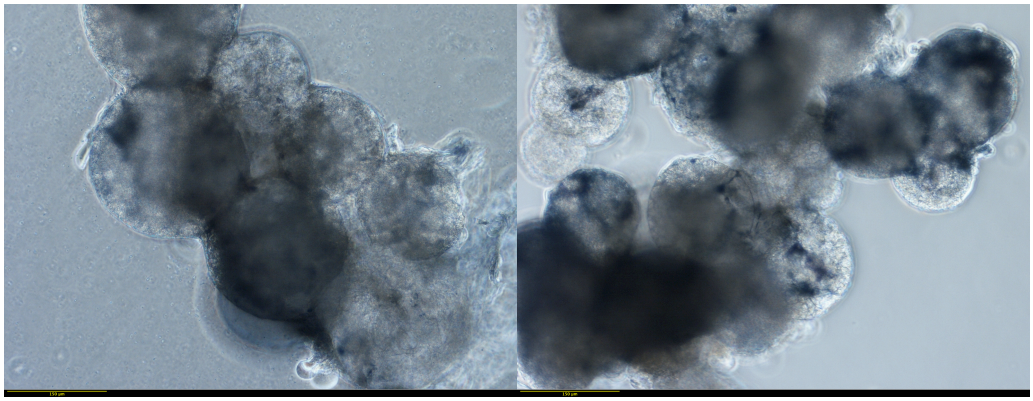

Cultispher G® + keratinocyte cell culture in magnetic stirrer (MTT staining) D4 and D18
Dark stained keratinocytes on microcarriers surface showing increased cell attachment and distribution on beads' surface from day 4 to day 18 (x20 magnification, field width 1.8 mm)

Figure 12: Acridine orange & MTT staining Cultispher G® + keratinocyte cell culture in magnetic stirrer flask D4 and D18

Since according to the manufacturer's information sheet, Cultispher G® microcarriers have more uniform pores and more suitable for anchorage dependent cells, Cultispher G® was chosen for keratinocyte culture in a magnetic stirrer flask.

Using the magnetic stirrer culture, MTT and Acridine orange staining demonstrated keratinocyte attachment and distribution across Cultispher G® microcarriers surface throughout different time points in stirred culture as shown in figure 14.

Alamar Blue® assay was performed as described previously, with samples in triplicates compared to readings from negative controls of culture medium and microcarriers only.

Alamar Blue® assay demonstrated increased reduction percentage in comparison with rotator culture throughout the culture period. A slight decrease in proliferation was noticed at day 18, which was followed an increase at later time points as shown in figure 15. As previously observed with the rotator culture, this could be possibly explained by the keratinocytes turnover within the culture around day 21.

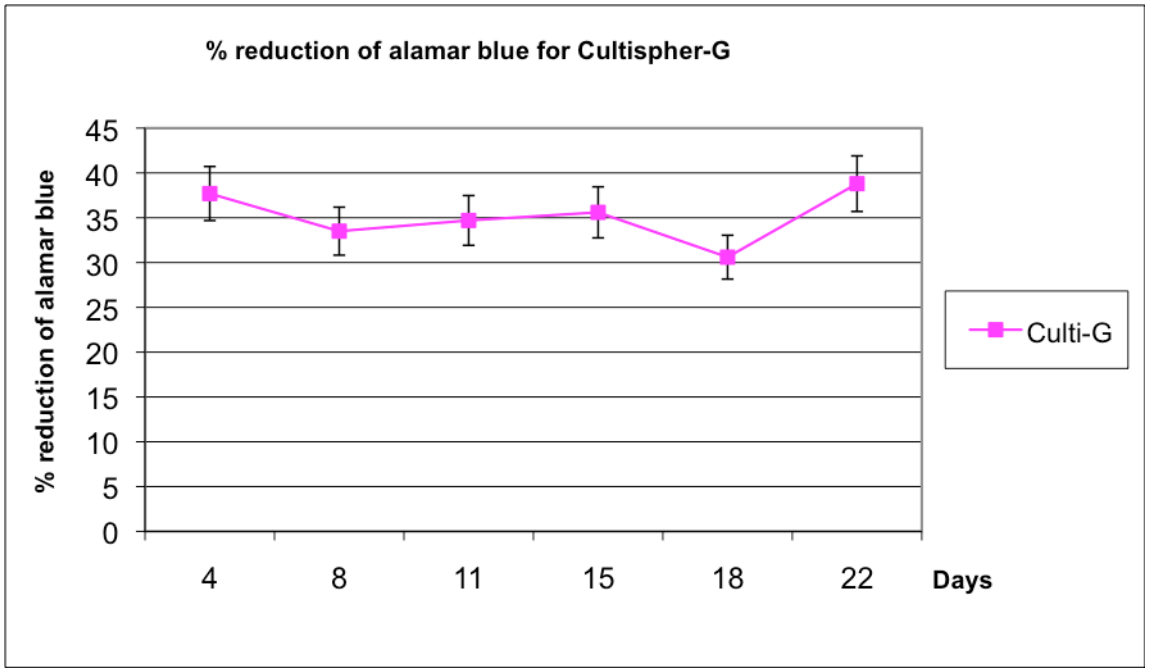

Figure 13: Alamar Blue® reduction keratinocyte cell culture on Cultispher G• in stirrer flask (Error bars refer to standard deviation)

Quantitative and qualitative data demonstrated keratinocytes attachment to microcarriers and an increase in viable cell populations within both static and stirred culture over different time points. Viable keratinocyte cell count doubled at consecutive

time points (day 6 and 10). By day 14, keratinocyte cell number was comparable to similar cell populations obtained from tissue culture flasks (table 5). Cell counts were repeated 3 times for each time point and an average calculated.

The presence of microcarrier beads within the stirred culture provided a large surface area for keratinocyte attachment. This compensates for the change in culture conditions compared to the traditional keratinocyte cell culture in tissue flasks. Keratinocytes in culture flasks showed an increased cell count of around 1 x 10^6 between days 10 to 14.

Time point	Human KC in Culture flasks	Human KC on Microcarriers
Day 0	5*	5
Day 6	15.9*	15.5
Day 10	41.2*	40.1
Day 14	63.4*	62.2

*** Cell count from tissue culture flasks (175 cm^2). All counts x 10^6**

Table 5: Cell count using Trypan blue comparing keratinocytes in culture flasks vs. keratinocytes on microcarriers

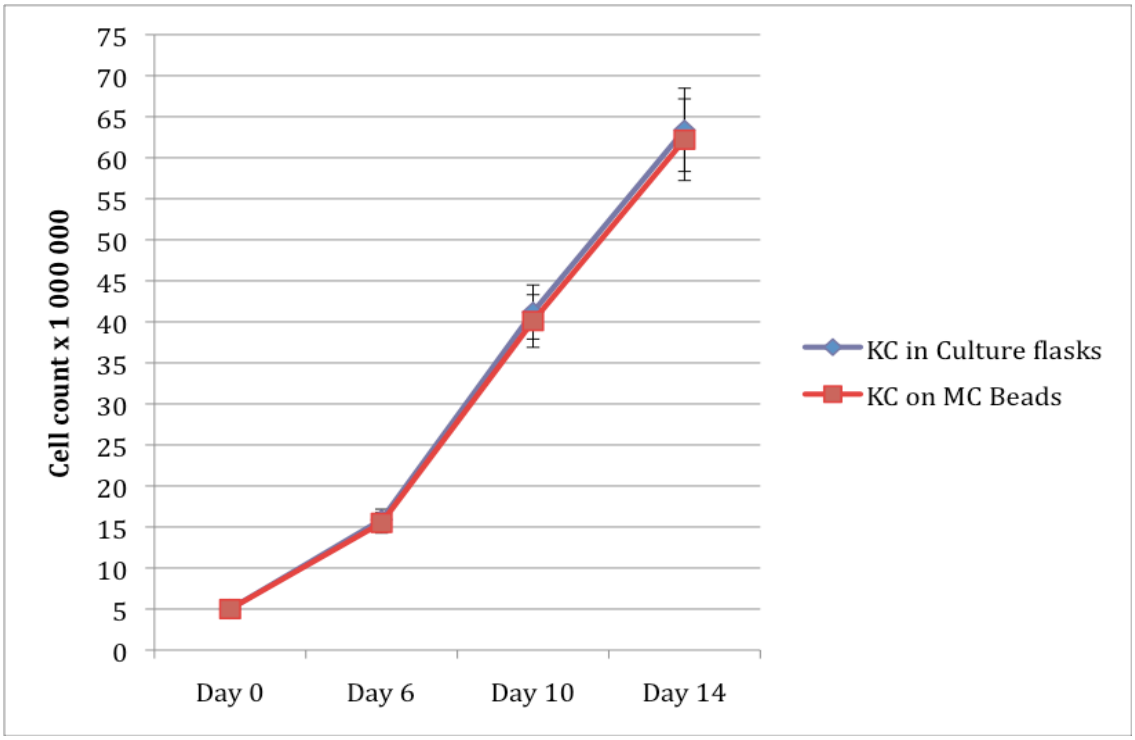

Figure 14: Cell count using Trypan blue comparing keratinocytes in culture flasks vs. keratinocytes on microcarriers (Error bars refer to standard deviation)

3.2 Assessment of *in vitro* migration of porcine keratinocytes from microcarrier beads to monolayer tissue culture

3.2.1 Study objectives

The aim of this study was to assess the ability of porcine keratinocytes to migrate off the microcarriers' surface while retaining their ability to proliferate in culture conditions. The biodegradation of the microcarriers can be assessed in static culture conditions as an indicator for future application on wounds *in vivo*.

3.2.2 Porcine keratinocytes migration from microcarrier beads to tissue culture flasks

Porcine keratinocytes were isolated from the porcine skin samples as described in 2.2.9 and maintained as described in 2.2.10. Porcine keratinocytes were seeded on microcarrier beads in stirred culture as described in 2.2.16.

On Day 8 of the stirred culture, the continuous stirring was stopped for 10 minutes and the microcarrier beads allowed to settle in the lower half of the flask. 1 ml of microcarrier beads was pipetted from the flask inside a safety cabinet. This was seeded into 75 ml tissue culture flask as described before and maintained as in 2.2.10.

Images were taken at days 3, 6, and 10 to assess keratinocytes migration, colony formation, and confluence.

3.2.3 Results

Microcarrier beads seeded with porcine keratinocytes transferred to tissue culture flasks biodegraded without causing infection within the culture. The presence of the microcarrier beads did not influence the migration of the keratinocytes from the beads to the tissue culture flasks' surface.

The ability of porcine keratinocytes to form colonies in culture flasks and further confluence demonstrated cell migration from microcarriers to the surface of the culture flasks.

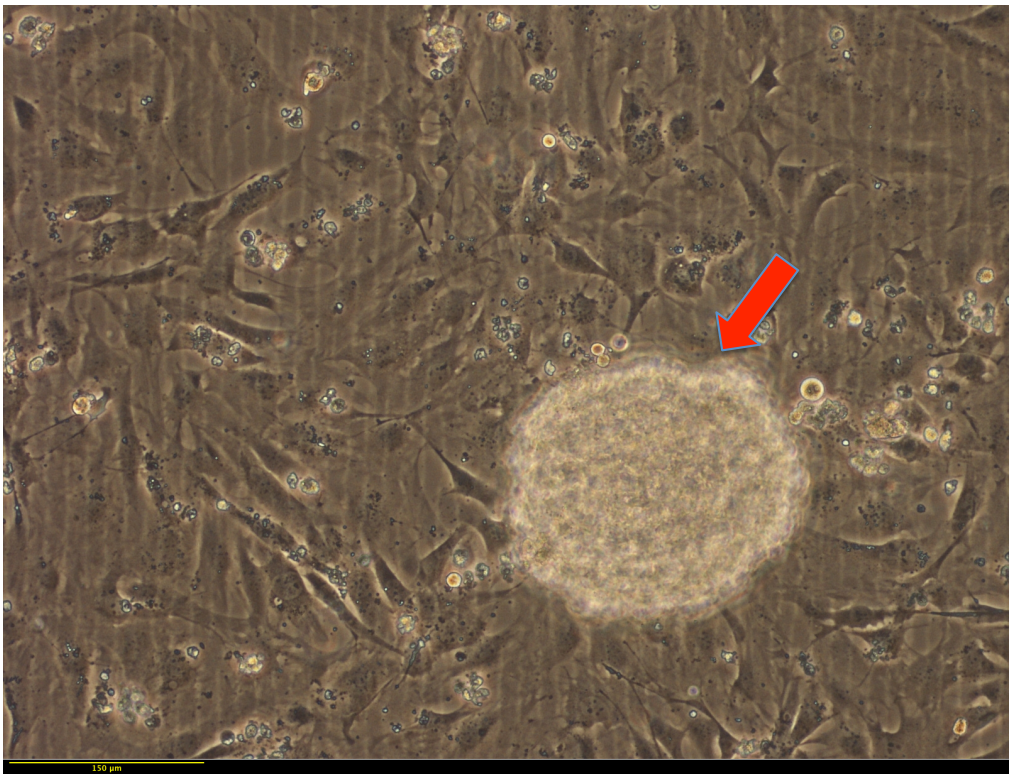

Figure 15: Cluster of microcarriers seeded with porcine keratinocytes in tissue culture flask (day 3) Microcarrier bead (red arrow) with keratinocytes attached to the surface surrounded by 3T3 cells attached to the surface of the culture flask day 3 (x40 magnification, field width 0.9 mm)

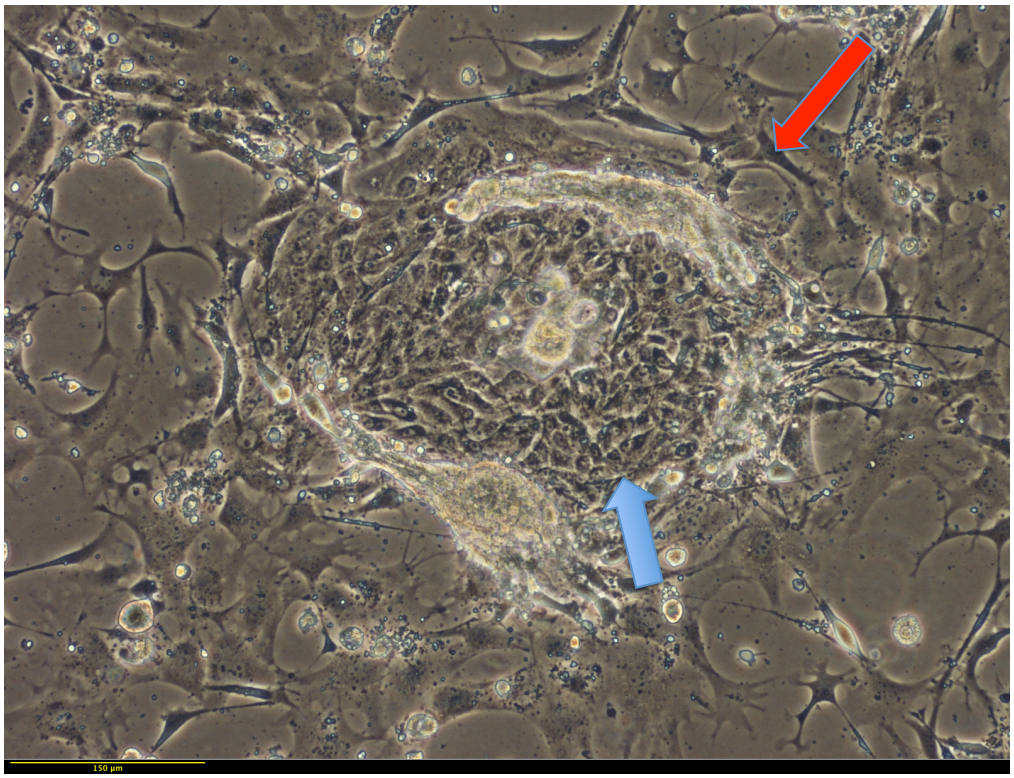

Figure 16: Microcarriers seeded with porcine keratinocytes in tissue culture flask (day 6). Keratinocyte colony (blue arrow) and 3T3 cells (red arrow) attached to the surface of the culture flask, remnants of microcarrier bead seen surrounding the keratinocytes colony day 6 (x40 magnification, field width 0.9 mm)

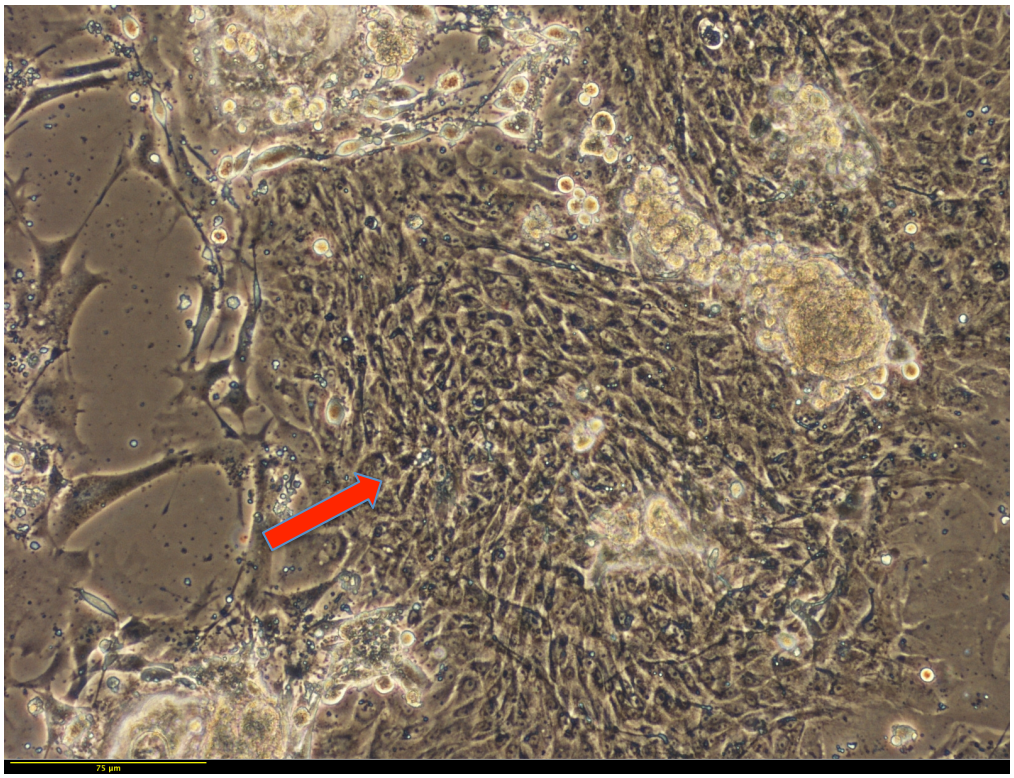

Figure 17: Microcarriers seeded with porcine keratinocytes in tissue culture flask (day 9). Keratinocytes colony (red arrow) and remnants of microcarrier beads seen surrounding the keratinocytes colony day 9 (x40 magnification, field width 0.9 mm)

These observational findings were limited in outlining the effect of microcarriers on the migration of keratinocytes in static culture. Further studies are required to thoroughly investigate the effect of microcarriers on keratinocyte migration *in vitro*.

As seen in figure 17, the microcarrier bead was seen surrounded by 3T3 cells and no porcine keratinocyte colonies on day 3. In figure 18, by day 6, microcarrier beads started to dissolve, and a porcine keratinocyte colony was seen surrounded by the remnants of the microcarrier beads. In figure 19, by day 9, the keratinocytes were 80-90% confluent following the beads dissolution having migrated successfully from the surface of the beads to the tissue culture flask. Representative images in the previous figures were selected which were typical of the cell behaviour observed.

There was no evidence available to describe the exact number of keratinocytes, which migrated from the microcarriers' surface to the culture flask. From the observational

findings, sufficient numbers of keratinocytes expanded in the culture flasks, survived the migration process, and formed confluent colonies (figure 19).

Cultispher G® gelatin microcarrier beads can be biologically inert as they safely dissolved in static culture allowing keratinocyte migration to the surface of the culture flask. The expansion of keratinocytes in culture was maintained and keratinocytes were able to achieve early signs of confluence.

3.3 Assessment of porcine keratinocyte attachment on microcarrier beads using Scanning Electron Microscopy (SEM)

3.3.1 Study objectives

The aim of this study was qualitative assessment of cellular attachment of porcine keratinocytes to the porous surface of the gelatin microcarriers. The study would provide an examination of the relationship between keratinocytes, which are anchorage dependent cells, in cell culture and the surface of microcarriers in stirred culture.

3.3.2 Assessing porcine keratinocyte attachment on microcarrier beads using Scanning Electron Microscopy (SEM)

Porcine keratinocytes were isolated as described in 2.2.9, cultured as described in 2.2.10, and seeded on microcarrier beads as described in 2.2.16.

The samples were prepared as described in 2.2.20, and viewed using SEM (JEOL JSM-6310 with spatial resolution 1-2.5 nm), University of Brighton, East Sussex, UK. The resolution of the SEM depends on the size of the electron spot, which in turn depends on both the wavelength of the electrons and the electron-optical system that produces the scanning beam.

Image is generated by an electron beam focused by one or two condenser lenses to a spot about 1-2.5 nm in diameter. The beam passes through pairs of scanning coils or pairs of deflector plates in the electron column, typically in the final lens, which deflect the beam in the x and y axes scanning over a rectangular area of the sample surface.

The energy exchange between the electron beam and the sample results in the reflection of high-energy electrons by elastic scattering, emission of secondary electrons by inelastic scattering and the emission of electromagnetic radiation, each of which can be detected by specialized detectors. Electronic amplifiers of various types are used to amplify the signals, which are displayed as variations in brightness on a computer monitor. Each pixel of computer is synchronized with the position of the beam on the specimen in the microscope, and the resulting image is therefore a distribution map of the intensity of the signal being emitted from the scanned area of the specimen.

3.3.3 Results

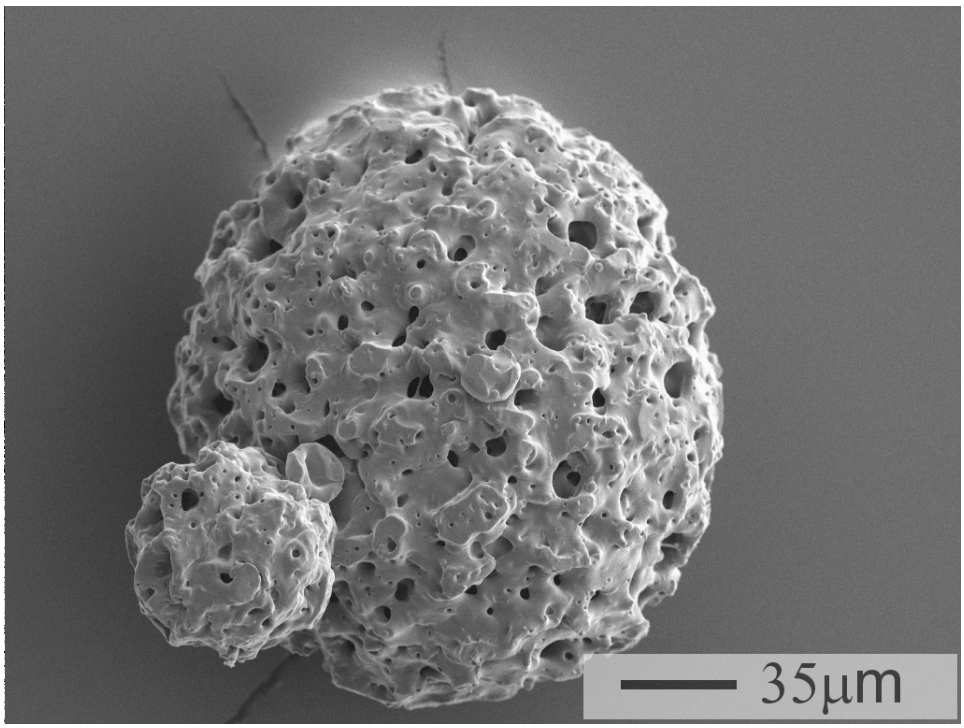

Figure 18: Cultispher G® microcarrier SEM
The porous surface of the microcarrier bead can be seen clearly allowing expansion of the surface area available for cell attachment

Figure 20 and 21 demonstrate the average size of microcarrier beads between 150-200 µm (The range of Cultispher G® micorcarriers is 130-380 µm)

http://www.percell.se/products.htm

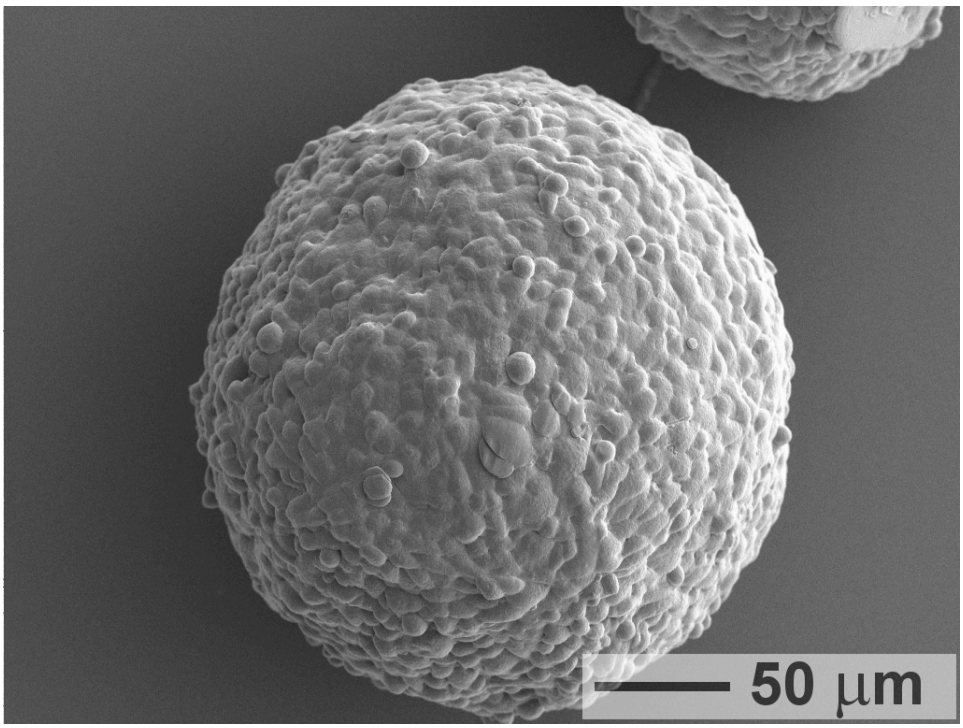

Figure 19: Cultispher G® seeded with porcine keratinocytes day 8 SEM
The porous surface of the microcarrier bead was obscured by the porcine keratinocytes attached to the surface of the microcarrier

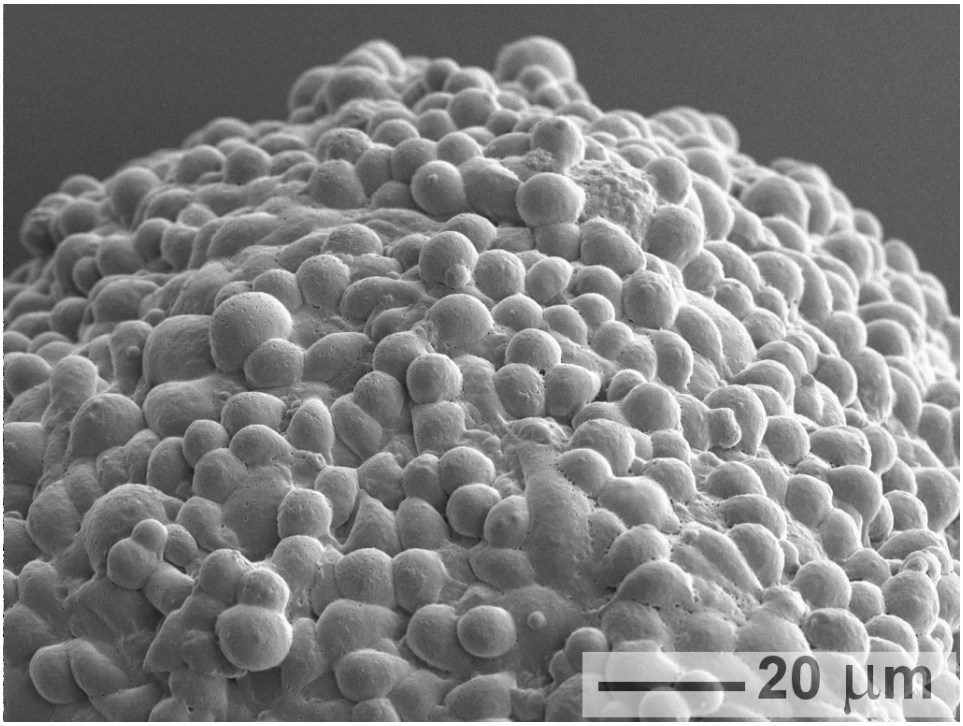

Figure 20: Cultispher G® surface seeded with porcine keratinocytes day 8 SEM
A closer image of the porcine keratinocytes (spherical cells) attached to the surface of the microcarrier

Cultispher G® gelatin microcarriers have a porous surface with pores range approximate 1-10 μm, which expands the surface available for keratinocyte attachment as seen in figure 20. SEM images of microcarriers and porcine keratinocytes at day 8 showed a

confluent layer of porcine keratinocytes attached to the surface of the microcarrier obscuring the porous surface (figure 21). At higher magnification the microcarrier surface (figure 22) showed the attachment of the porcine keratinocytes to the microcarrier surface possibly in multi-layers.

Although not visible by SEM, the porosity of the microcarriers could increases the surface area available for cellular attachment in a confined space compared to tissue culture flasks. Porcine keratinocytes attached to the microcarrier surface in stirred culture utilising the external porous surface as demonstrated using SEM images. Cultispher G® microcarrier beads supported porcine keratinocyte attachment and provided a suitable alternative to traditional tissue culture flasks.

Many factors are essential for cells to adhere to the surface of a culture vessel; divalent cations and growth factors within the culture medium are two examples (Grinnell 1978). Foetal calf serum within the culture medium is the main source of proteins within the culture medium. The microcarriers were washed in the porcine keratinocyte growth medium prior to seeding with keratinocytes and the beads' surface is negatively charged during the manufacturing process. Hence keratinocyte attachment to the microcarriers' surface was possible as demonstrated by the SEM images (figure 22).

3.4 Comparative analysis of porcine keratinocyte proliferation with/without feeder 3T3 cells in stirred culture

3.4.1 Study objectives

The aim of this study was to assess porcine keratinocytes growth and expansion in stirred microcarrier culture with and without the use of feeder 3T3 cells. The comparison of data would allow planning for cell application in a porcine wound model. Porcine keratinocytes growth and expansion was assessed using Acridine orange staining, MTT staining, and Trypan blue cell count at specific time points.

3.4.2 Porcine keratinocyte proliferation with/without feeder 3T3 cells in stirred culture

Porcine keratinocytes were isolated as described in 2.2.9, cultured as described in 2.2.10, and seeded on microcarrier beads as described in 2.2.16. A second 100 ml Cellspin™ magnetic stirrer flask was set up with same seeding density and 2 x 10^6 freshly harvested 3T3 cells. Both flasks were maintained as described before and the second flask containing 3T3 cells was maintained as described in 2.2.7.

Qualitative assessment of keratinocyte growth in the two flasks was undertaken using Acridine orange staining, MTT staining, and Trypan blue cell count at days 3, 6, 9, and 12. The time points were related to the culture stirring protocol described in 2.2.16. Day 12 was the final time point prior to discarding the cultures and terminating the study.

3.4.3 Results

Microcarriers were found to support the growth of porcine keratinocytes with or without 3T3 feeder cells in stirred suspension culture, following initial expansion of keratinocytes in tissue culture flasks.

Acridine orange staining at days 3, 6, 9, and 12 showed porcine keratinocytes cultured in the presence or absence of 3T3 cells populating the surface of the microcarrier beads (figures 23 & 24). MTT staining at days 3, 6, 9, and 12 showed porcine keratinocytes cultured in the presence or absence of 3T3 cells populating the surface of the microcarrier beads (figures 25 & 26). Both sets of qualitative assessment through cellular attachment to the surface of the microcarriers showed expansion of porcine keratinocytes with or without 3T3 cells in the culture medium in the stirred culture. 3T3 feeder cells were used for the initial expansion of the keratinocytes in tissue culture flasks prior to seeding on microcarrier beads.

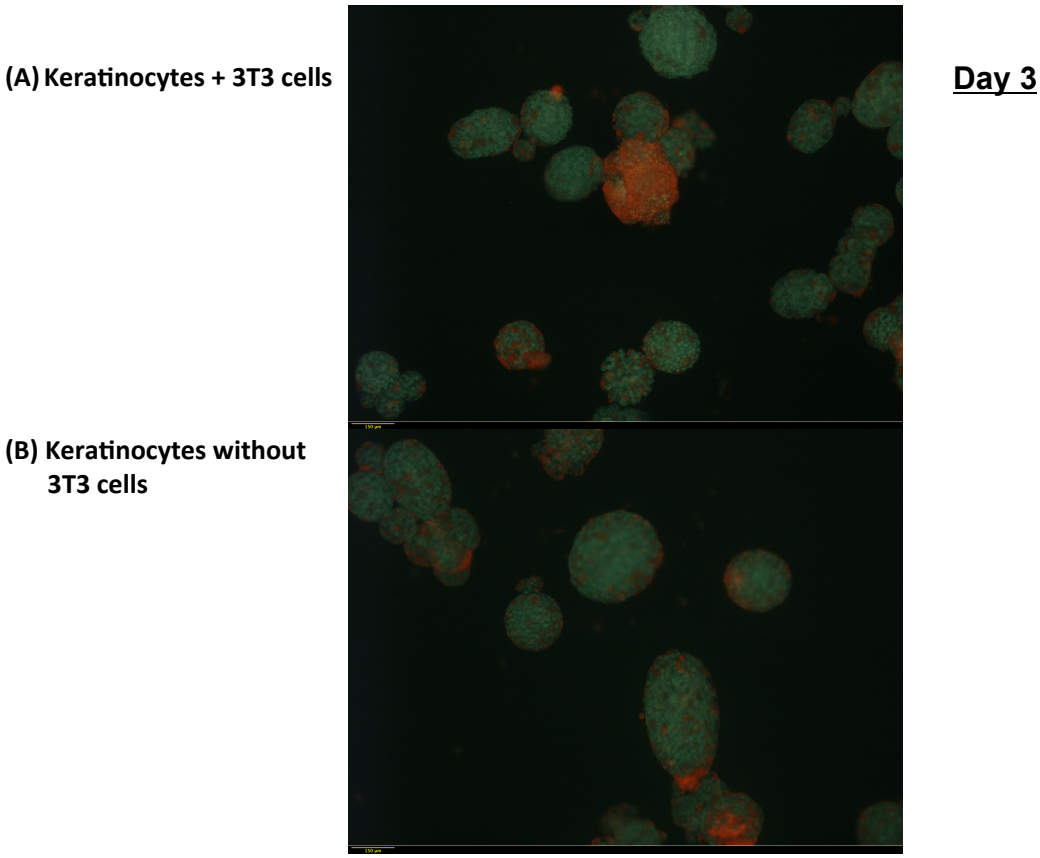

Figure 21: AO staining day 3; keratinocytes + 3T3 (upper) & keratinocytes without 3T3 (lower)
Orange stained RNA within keratinocytes attached to the surface of microcarriers in the presence of 3T3 cells (above) and without 3T3 (below) (x10 magnification, field width 3.6 mm)

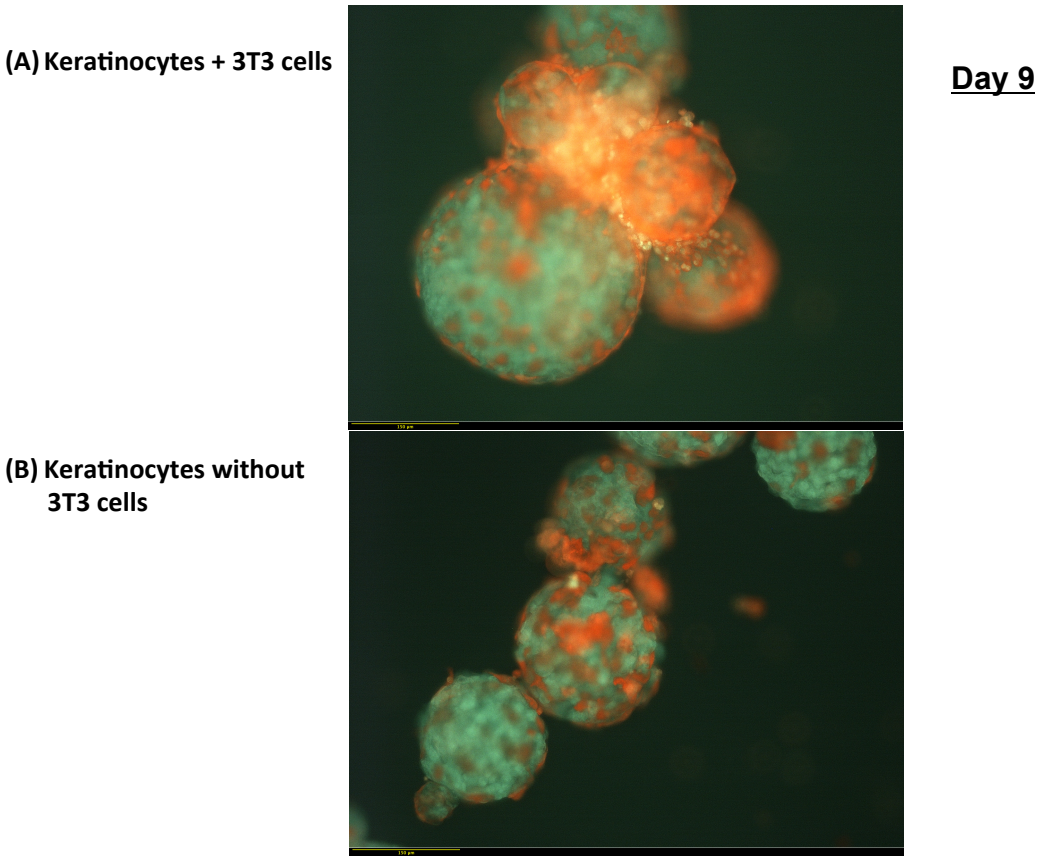

Figure 22: AO staining day 9; keratinocytes + 3T3 (upper) & keratinocytes without 3T3 (lower)
Orange stained RNA within keratinocytes attached to the surface of microcarriers, more cells attached compared to day 3 (x40 (top) and x20 (lower) magnification, field width 0.9 and 1.8 mm respectively)

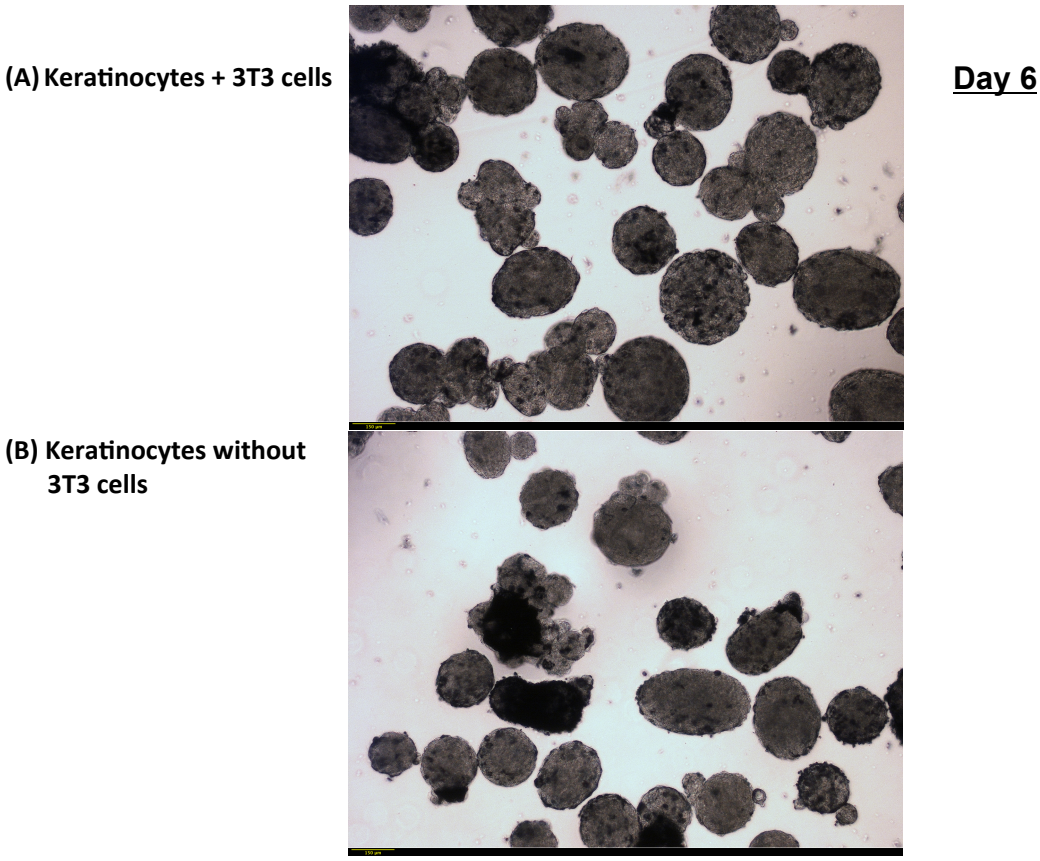

Figure 23: MTT staining day 6; keratinocytes + 3T3 (upper) & keratinocytes without 3T3 (lower)
Dark stained keratinocytes (containing reduced formazan) attached to the surface of microcarriers in the presence of 3T3 cells (above) and without 3T3 (below) (x10 magnification, field width 3.6 mm)

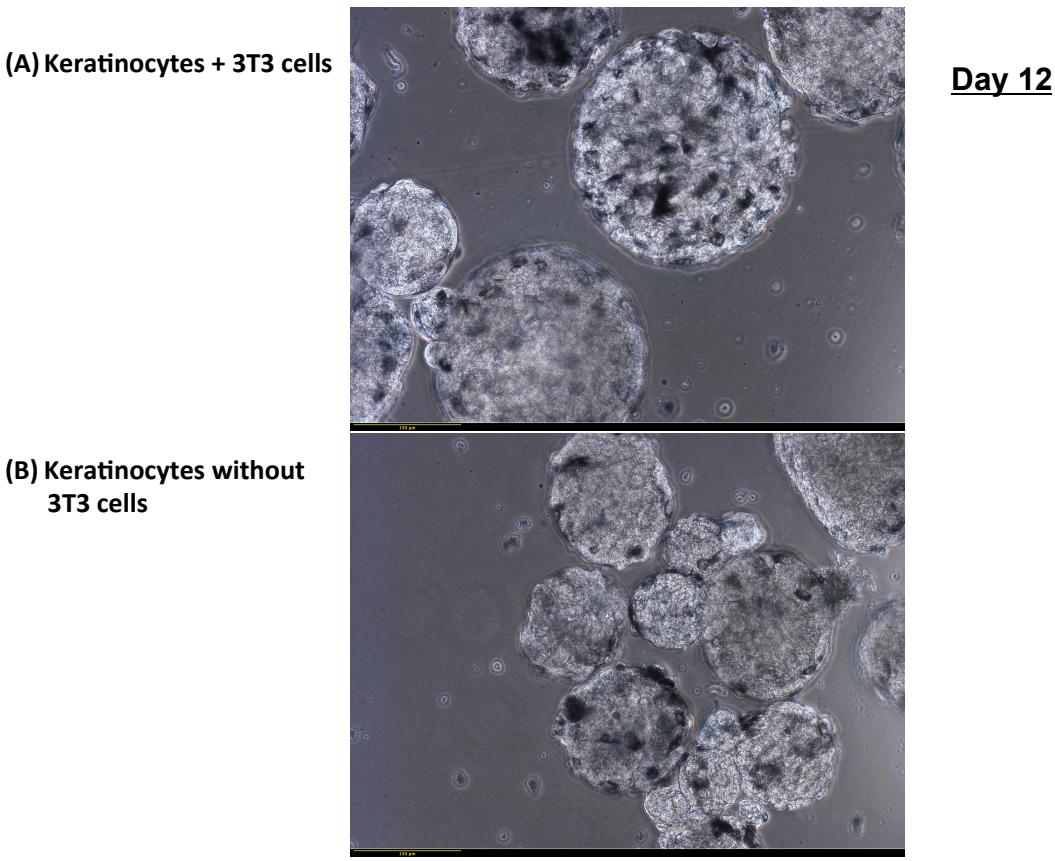

Figure 24: MTT staining day 12; keratinocytes + 3T3 (upper) & keratinocytes without 3T3 (lower)
Dark stained keratinocytes (containing reduced formazan) attached to the surface of microcarriers (x40 magnification (top) and x20 magnification (lower), field width 0.9 mm and 1.8 mm respectively)

Trypan blue was used for keratinocytes counts after dissolving microcarriers on days 3, 6, 9, and 12 as shown in figure 27, the cell count was done 3 times and an average calculated. Keratinocyte cell counts in both stirrer flasks in the presence or absence of 3T3 cells in stirred culture (figure 27) was similar with slightly more cells in the culture without 3T3 cells. Keratinocyte expansion was also similar with matching cell count increasing over the same period of time. The increase in cell counts seen in culture without 3T3 cells averages from < 1 x 10^6 at day 3 to around 3 x 10^6 at day 12. Both porcine keratinocytes cultured with and without 3T3 demonstrated expansion of the keratinocytes during the culture period.

The cell counts from both groups were compared using t-test, the results demonstrated 95% confidence interval for difference of means -49.42 to 45.17, and the power was 0.05 (below desired power of 0.8). The difference in the mean values of the two groups was not great enough to reject the possibility that the difference was due to random sampling variability. The difference was not statistically significant with a p value of 0.916.

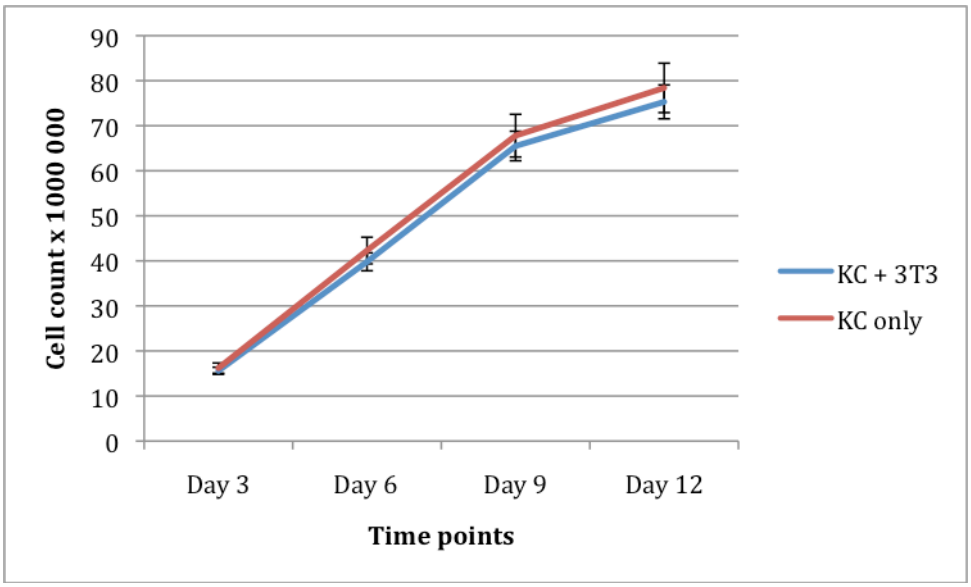

Figure 25: Comparison between KC cell count +/- 3T3 at days 3, 6, 9, and 12 (Error bars refer to standard deviation)

Human keratinocytes have been cultured on microcarrier beads without 3T3 cells (Borg *et al.* 2009) following initial expansion in tissue culture flasks containing 3T3 cells. Porcine keratinocytes expansion occurred in stirred culture in the absence of 3T3 cells and cell counts were slightly higher when compared to cultures containing 3T3 cells.

The ability to expand porcine keratinocytes in the absence of 3T3 cells would negate the use of 3T3 cells in cultures for *in vivo* animal models as it would reduce the risk of infection, culture contamination, and reduce culture maintenance requirements.

3.5 Quantitative assessment of porcine keratinocyte proliferation on microcarrier beads (MTT assay, RNA isolation and real-time quantitative PCR)

3.5.1 Study objectives

The aim of the study was to quantify porcine keratinocyte proliferation on microcarriers using MTT assay and K14 expression using total RNA isolation followed by real-time quantitative PCR.

3.5.2 MTT assay of porcine keratinocytes on microcarrier beads

Porcine keratinocytes were isolated as described in 2.2.9, cultured as described in 2.2.10, and seeded on microcarrier beads as described in 2.2.16.

MTT assay was performed as described in 2.2.21 on days 7, 14, and 21. A standard curve was used for comparison as described in 2.2.21.

3.5.3 RNA isolation from porcine keratinocytes on microcarrier beads

Porcine keratinocytes were isolated as described in 2.2.9, cultured as described in 2.2.10, and seeded on microcarrier beads as described in 2.2.16. RNA isolation was performed as described in 2.2.22 on day 10.

3.5.4 Real-time quantitative PCR (qPCR) K14 mRNA from porcine keratinocytes on microcarrier beads

Porcine keratinocytes were isolated as described in 2.2.9, cultured as described in 2.2.10, and seeded on microcarrier beads as described in 2.2.16. Real-time qPCR isolation was performed as described in 2.2.23 on day 14 and 21.

3.5.5 Results

MTT assay results:

Initially, For MTT assay, at each time point, the samples were processed in triplicate wells and an average reading for each volume calculated.

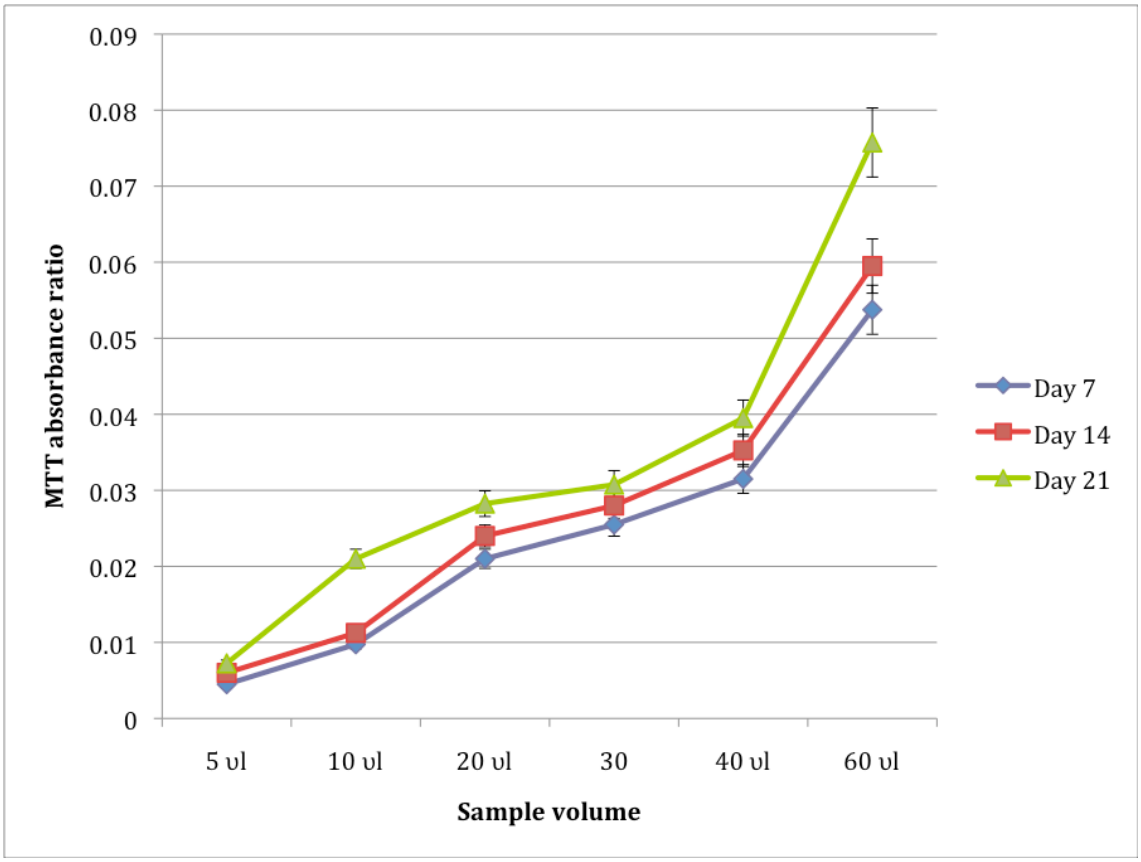

Figure 26: MTT assay vs. sample volumes Days 7, 14, and 21
(Error bars refer to standard deviation)

MTT assay reading plotted versus sample volume with increased assay readings from day 7 to day 21 demonstrating keratinocytes expansion and possibly proliferation across increasing sample volumes from 5 µl to 60 µl (figure 28).

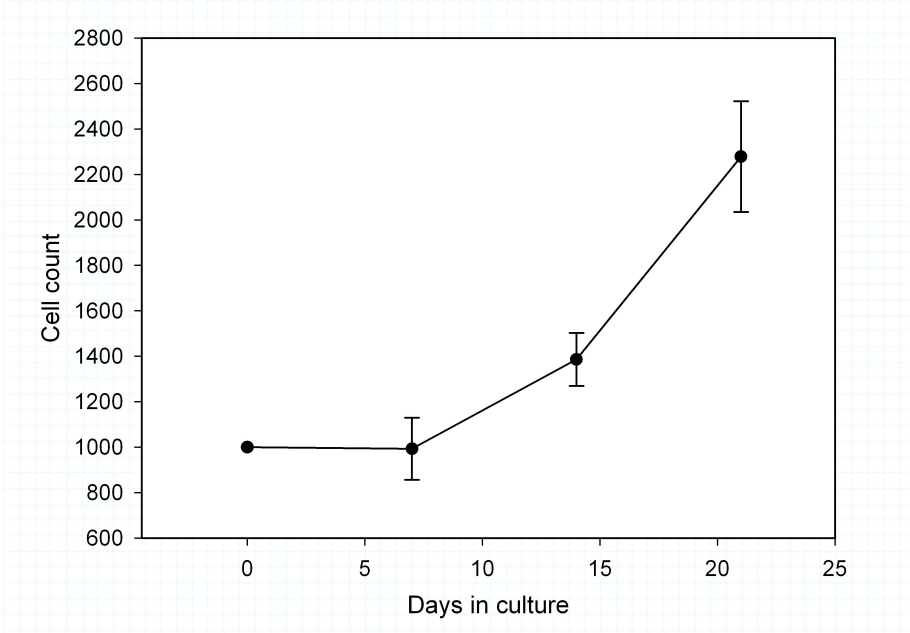

Figure 27: Porcine keratinocyte cell count x 10^6 calculated using MTT assay results

Using Tecan® reader software (Tecan group Ltd., Theale, Reading, UK), the assay reading from different sample volumes was used to calculate the total number of cells in culture at different time points (figure 29). Cell counts increased from 1 x 10^6/ml on day 1 to 2.2 x 10^6/ml on day 21 (figure 29). No keratinocytes expansion was noted up to day 7 followed by notable increase in cell count on days 14 and 21.

Total RNA isolation results:

For quantifying RNA, readings were taken at wavelength 260 nm. The readings allowed calculation of the concentration of nucleic acid in the sample.

Volume (ml)	Standard sample ng/µl	Diluted sample ng/µl
0.1	215	43
0.25	130	25.9
0.5	174	34.8
0.75	209	41.7
0.85	180	55.9
0.95	483	96.6
1	364	72.9
1.25	487	97.5
1.5	522	104.3

Table 6: RNA isolation measurement microcarriers + porcine keratinocytes day 10

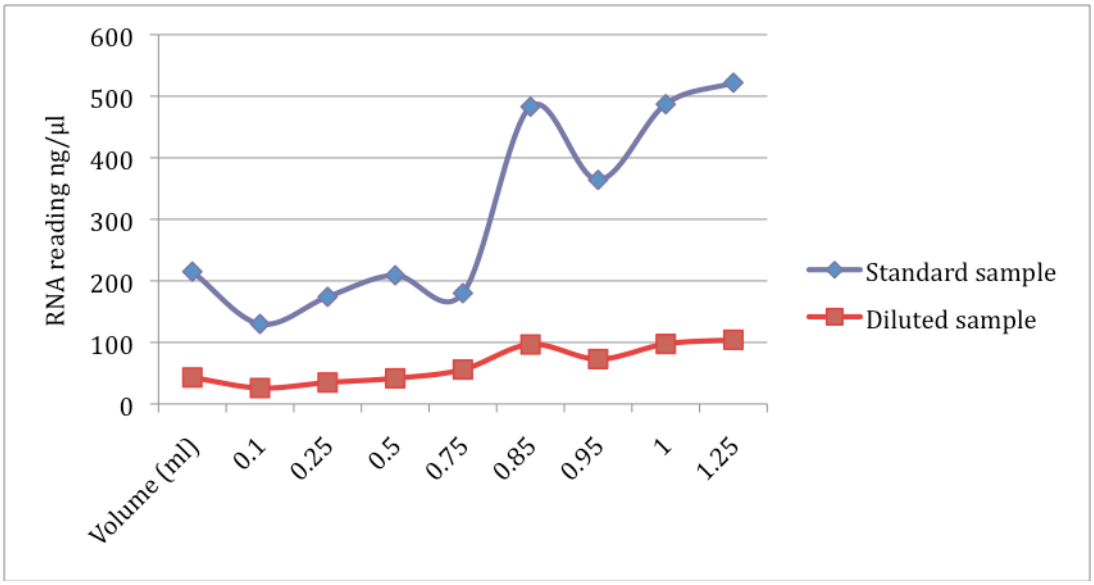

Figure 28: Chart representation of RNA isolation measurements in standard and diluted samples porcine keratinocytes + keratinocytes day 10

For assessment of RNA integrity, the intensity of the RNA was analysed in diluted samples 1:5 for example; 20 µl from 0.1 ml (100 µl) sample. The readings from the diluted samples were 1:5 of the standard sample readings, with the exception of readings from 0.85 ml sample which was equivalent to 1:3. Since it was a single inconsistent reading, it was attributed to sample degradation or possible contamination of the standard sample. Total RNA measurement from porcine keratinocytes culture on microcarriers on day 10 was 255 ng/µl in 10 ml sample from 100 ml spinner flask.

Figure 30 demonstrates the relation between the standard and diluted RNA isolation samples. RNA isolation measurements on day 10 were used as a baseline for RNA isolation on days 14 and 21, as it was used in the preliminary stages of real-time qPCR.

Real-time quantitative PCR (qPCR) K14 results:

K14 is a marker of basal keratinocytes, which can be used to monitor keratinocytes proliferation. As basal keratinocytes differentiate and migrate towards the skin surface, down regulation of K14 occurs (Alam *et al.* 2011).

Relative expression of K14 mRNA was calculated using the 2 ΔCT method described by Livak and Schmittgen (2001) where relative expression = $2^{-\Delta CT}$, where ΔCT = $CT^{Target\ gene} - CT^{GAPDH}$ (GAPDH Glyceraldehyde 3-phosphate dehydrogenase).

Relative quantification relates the PCR signal of the target transcript in a treatment group to that of another sample such as an untreated control. The 2 ΔCT method is a convenient way to analyze the relative changes in gene expression from real-time quantitative PCR experiments (Livak and Schmittgen 2001). Normalizing to an endogenous reference provides a method for correcting results for differing amounts of input RNA. The 2 ΔCT method uses data generated as part of the real-time PCR experiment to perform the normalization function. This method was chosen, as it was not practical to measure the amount of input RNA by other available methods.

Real-time qPCR assay of K14 was done on days 14 and 21 since the day 14 time point would represent the future end point for porcine keratinocytes culture for *in vivo* animal studies. Day 21 was chosen as a comparable time point to the harvest of epithelial sheets from traditional keratinocytes culture in culture flasks.

On the melt curve, one peak was observed and the PCR amplification curve and melt curve were saved (figure 31). The fold change in the target gene relative to the GAPDH endogenous control gene was calculated using Excel.

The fold change was calculated by applying the equation $2^{-\Delta(\Delta CT)}$. K14 assay was positive using qRT-PCR confirming porcine keratinocyte proliferation in microcarrier beads culture. Quantitative K14 assay showed significant increase from day 14 to day 21, which reflected proliferation of porcine keratinocytes in stirred microcarriers culture.

The results of qRT-PCR of K14 in day 14 and 21 showed increase in K14 expression demonstrating keratinocyte proliferation (figure 32). The results of qRT-PCR were different from the MTT assay, as the MTT assay demonstrated keratinocyte expansion in the stirred culture over the same period.

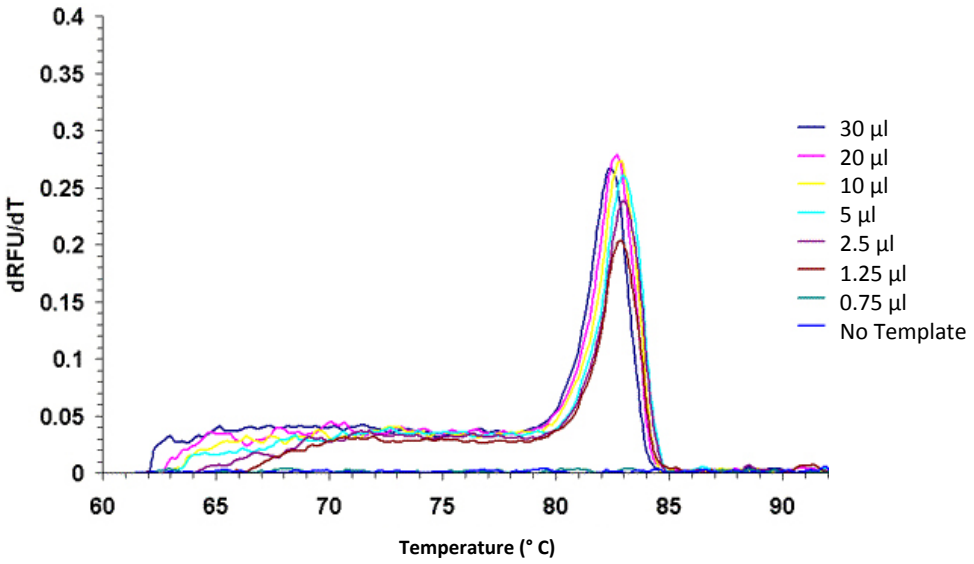

Figure 29: Melting curve SYBR Green 2 qRT-PCR K14
The melting curve demonstrates K14 peaking at 80-85°C in different sample volumes versus change in fluorescence with temperature (dRFU/dT) confirming the detection of K14

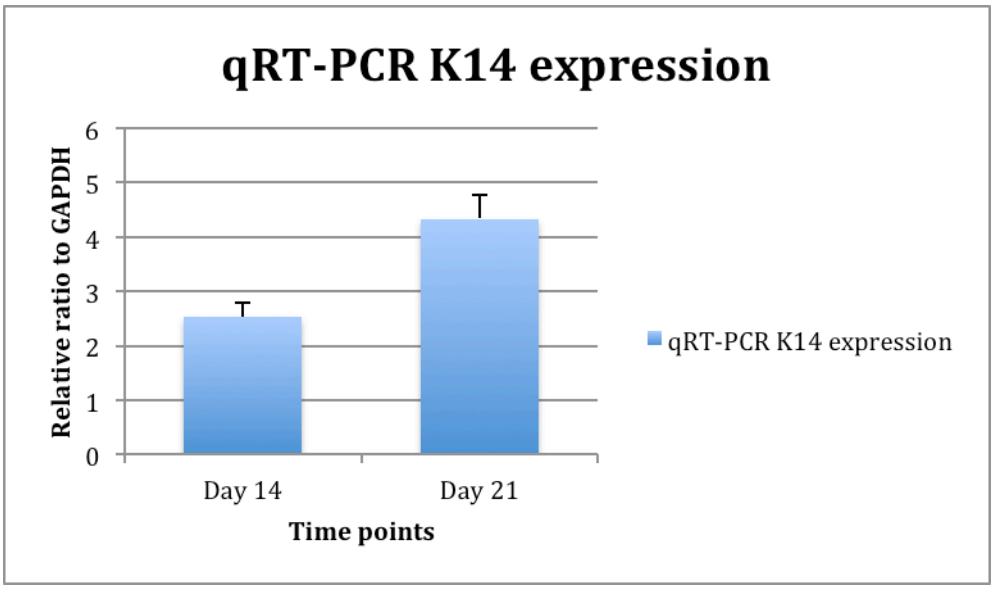

Figure 30: qPCR K14 mRNA expression relative to GAPDH days 14 and 21
Increase in K14 mRNA expression from D14 to D21 demonstrating basal keratinocytes proliferation

Combining the two sets of data together demonstrated that porcine keratinocytes expand and proliferate well on microcarriers in spinner flask culture *in vitro*.

3.6 Assessment of *in vitro* porcine keratinocytes and fibroblasts co-culture on microcarrier beads

3.6.1 Study objectives

The aim of the study was to assess qualitative and quantitative porcine keratinocyte growth and proliferation in co-culture with autologous fibroblasts on microcarrier beads. Qualitative assessment was done using fluorescent microscopy after GFP labelling of porcine keratinocytes. Quantitative assessment was done using MTT assay at days 7 and 14.

3.6.2 Porcine keratinocytes and fibroblasts co-culture on microcarrier beads

Porcine keratinocytes were isolated as described in 2.2.9, cultured as described in 2.2.10, GFP labelled as described in 2.2.14, and transduction frequency calculated as described in 2.2.15. Porcine fibroblasts were isolated as described in 2.2.11, and cultured as described in 2.2.12. Keratinocytes and fibroblasts were seeded on microcarrier beads in ratio 6:1 similar to human keratinocyte-fibroblast co-culture (Jubin *et al.* 2011) as described in 2.2.16. GFP labelled keratinocytes were inspected using epifluorescent microscopy (blue range) days 3,6, and 9. MTT assay was used to quantify porcine keratinocyte proliferation in co-culture as described in 2.2.21.

3.6.3 Results

Porcine keratinocytes expansion was demonstrated in co-culture with porcine fibroblasts as shown by presence of GFP positive keratinocytes on microcarriers.

GFP positive keratinocytes were seen attached to the surface of microcarriers on day 3 (figure 33) using contrast phase and epifluorescent microscopy (blue range).

Qualitative assessment showed that porcine keratinocytes formed colonies in the presence of fibroblasts on microcarriers in stirred culture.

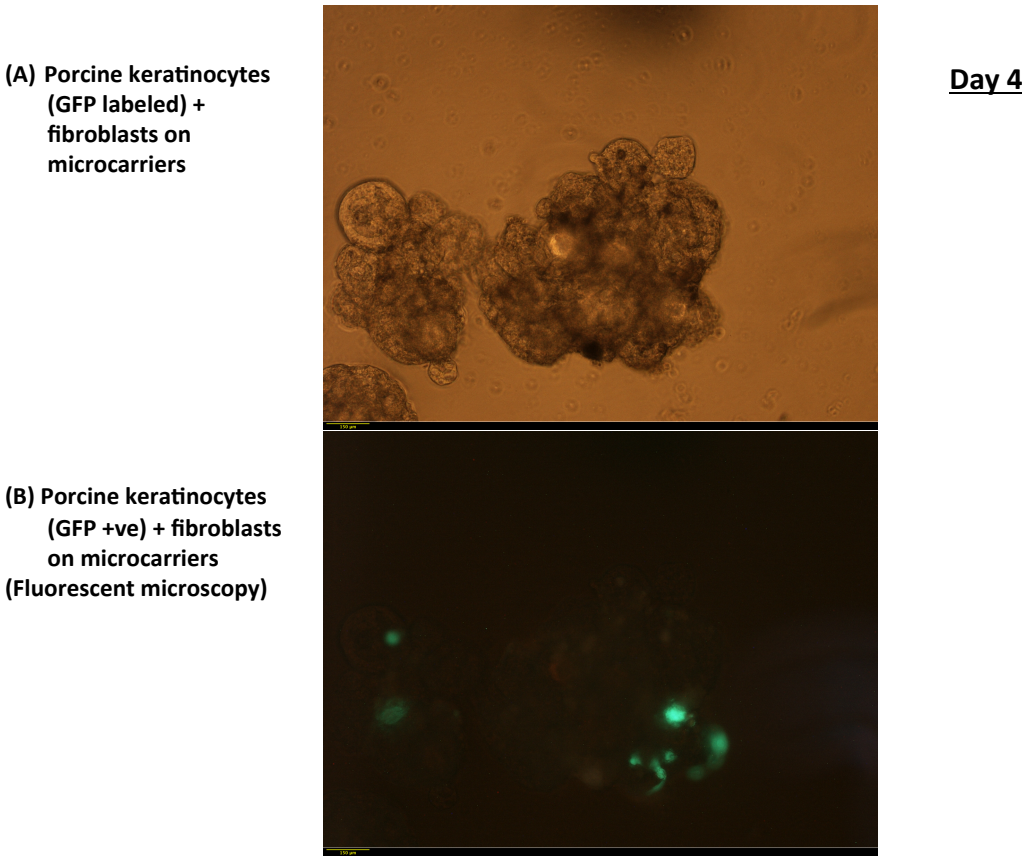

Figure 31: Porcine keratinocytes (GFP labelled) + porcine fibroblasts on microcarriers day 3
(A) Keratinocytes and fibroblasts (dark colour) attached to microcarriers (Contrast phase)
(B) Same field using epifluorescent microscopy demonstrating GFP +ve keratinocytes (green) attached to microcarriers (Both x10 magnification, field width 3.6 mm)

The fibroblast: keratinocyte ratio of 6:1 allowed controlled expansion of both types of cells without fibroblasts overtaking the cultures.

Fibroblasts supported the attachment and growth of keratinocytes in similar manner to irradiated 3T3 cells. The attachment of porcine keratinocytes to microcarrier beads and proliferation in culture at days 3 and 9 was similar to keratinocyte attachment to microcarriers in the absence of fibroblasts. GFP labelled porcine keratinocytes attached to microcarriers as demonstrated at different time points and the presence of fibroblasts did not have a negative impact on keratinocytes attachment or proliferation.

(A) Porcine keratinocytes (GFP labeled) + fibroblasts on microcarriers

Day 9

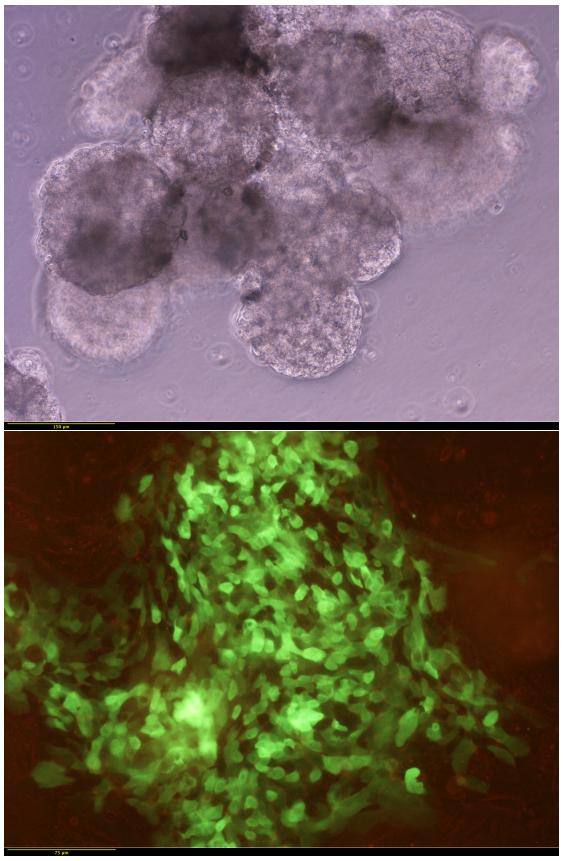

(B) Porcine keratinocytes (GFP +ve) + fibroblasts on microcarriers (Fluorescent microscopy)

Figure 32: Porcine keratinocytes (GFP labelled) + porcine fibroblasts on microcarriers day 9
(A) Keratinocytes and fibroblasts (dark colour) attached to microcarriers (Contrast phase)
(B) Same field using epifluorescent microscopy demonstrating GFP +ve keratinocytes (green) attached to microcarriers (Both x20 magnification, field width 1.8 mm).

MTT assay results;

The results were compared to the porcine keratinocytes' assay readings from 3.5.3 on days 7 and 14.

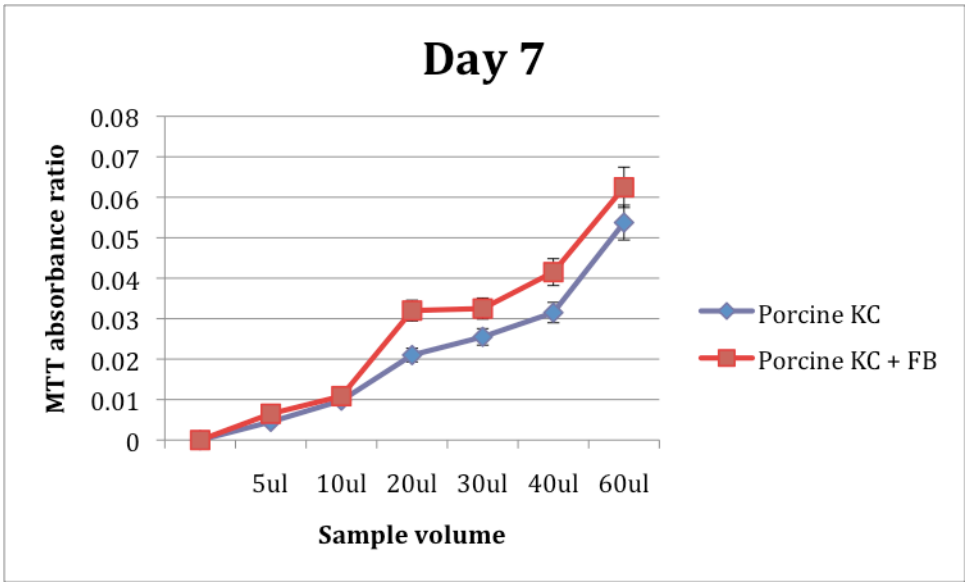

Figure 33: MTT assay results day 7 porcine keratinocytes and keratinocytes + fibroblasts (Error bars refer to standard deviation)

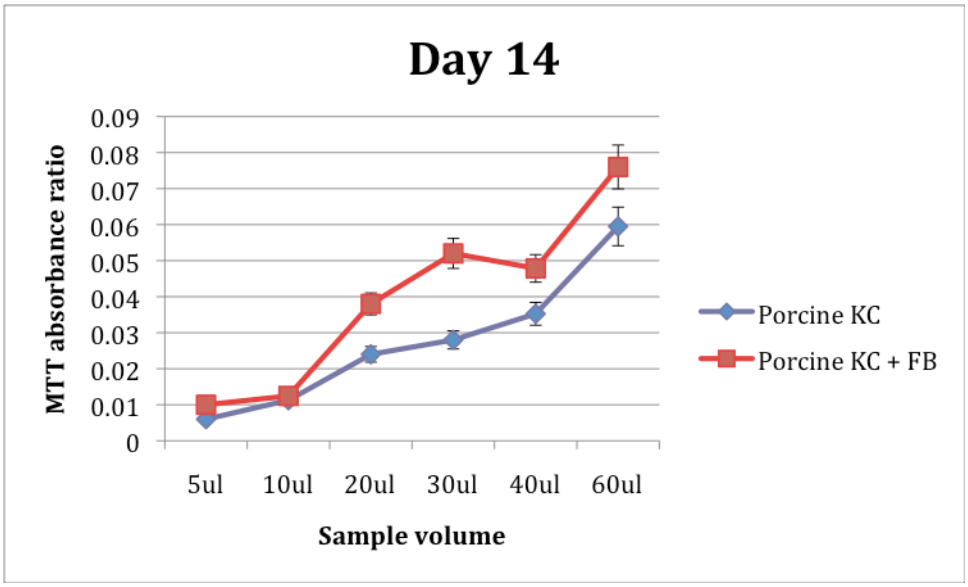

Figure 34: MTT assay results day 14 porcine keratinocytes and keratinocytes + fibroblasts (Error bars refer to standard deviation)

MTT assay results comparing porcine keratinocytes (P-KC) expansion to porcine keratinocytes combined with fibroblasts (P-KC+FB) showed similarly comparable results. Comparing the results from day 7 and day 14, P-KC+FB showed higher MTT assay results compared to P-KC alone. The difference in MTT assay was undetectable in small sample volumes 5-10 µl, and became more detectable in larger sample volumes > 30 µl and up to 60 µl. The gap in MTT assay results increased from day 7 to day 14 in sample volumes between 20-40 µl.

MTT assay results from both groups on day 7 were compared using t-test, the results demonstrated 95% confidence interval for difference of means -0.03 to 0.02, and the power was 0.05 (below desired power of 0.8). The difference in the mean values of the two groups was not great enough to reject the possibility that the difference was due to random sampling variability. The difference was not statistically significant with p value 0.556. MTT assay results from both groups on day 14 were compared using t-test, the results demonstrated 95% confidence interval for difference of means -0.04 to 0.02, and the power was 0.05 (below desired power of 0.8). The difference in the mean values

of the two groups was not great enough to reject the possibility that the difference was due to random sampling variability. The difference was not statistically significant with p value 0.357.

These results demonstrated the expansion of porcine keratinocytes in co-culture with porcine fibroblasts in stirred microcarriers culture. Quantitative assessment demonstrated expansion of porcine keratinocytes in the presence of porcine fibroblasts compared to keratinocytes alone. Porcine fibroblasts co-cultured with autologous keratinocytes (1:6) did not expand uncontrollably to overtake the culture as demonstrated by the survival of the GFP positive keratinocytes in co-culture. Therefore co-culture of porcine keratinocytes and fibroblasts in stirred microcarrier culture allowed keratinocyte expansion *in vitro*.

Chapter 4: An investigation into the survival of retroviral GFP labelled porcine keratinocytes on microcarrier beads compared to sprayed keratinocytes in full thickness animal wound model

4.1 Study objectives

PTFE (Polytetrafluroethylene) wound chambers were used to isolate the full-thickness wounds created in pigs against epidermal cell migration from the skin edge and wound contraction. The design of the PTFE wound chambers allows an extension from the outside rim of the chamber to sit underneath the wound skin edge. Hence, the chamber prevents epithelial migration from the wound edges and allows assessment of wound healing within the chamber in isolation.

Figure 35: PTFE wound chamber

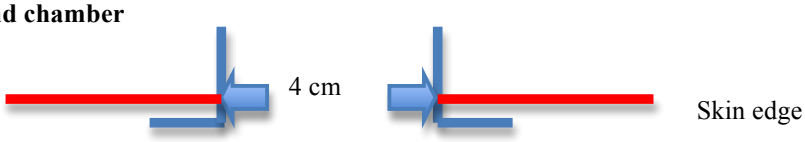

The PTFE chamber has an edge sitting underneath the free skin edge to prevent migration of keratinocytes from the skin edges

The aim of this study was to assess the rate of survival of porcine keratinocytes cultured on microcarriers in a full thickness porcine wound model. These were compared with sprayed cultured keratinocytes grown in traditional culture flasks. Also, the study aims to investigate the migration of porcine keratinocytes off microcarriers when applied to the porcine wound model and the effect on formation of permanent epithelium.

GFP retroviral labelling was used to trace the cultured keratinocytes and their possible contribution to newly formed epithelium. Immunohistochemical staining for K14, laminin, and collagen VII will be used to assess the rate of epithelial formation.

4.2 Study design

Two pigs were used in this study and prior to the beginning of the study; the animals as described in 2.3.1 were admitted to NPIMR according to 2.3.2.

In the first stage of the study, the animals were anaesthetised as described in 2.3.3 in a fully equipped theatre for animal surgical procedures (figure 38).

One sheet of split skin graft measuring about 8 x 8 cm was harvested from each animal from the posterior part of the para-spinal area as described in 2.3.4 using Zimmer® air-driven dermatome (figure 39). The skin graft was wrapped in saline soaked gauze and transported back to the lab in porcine keratinocyte transport medium the same day.

Figure 36: Operating theatre NPIMR, Northwick Park, London
The theatre is fully equipped with a surgical operating table and an anaesthetic machine (monitor/ventilator) for animal surgery

Porcine keratinocytes were isolated as described in 2.2.9, and cultured as described in 2.2.10. The flasks from each animal were clearly labelled and kept in separate shelves in an incubator at 37°C.

After keratinocyte expansion for one week, GFP labelling of porcine keratinocytes was undertaken as described in 2.2.14. This was repeated again in the same week and the frequency of transduction calculated as described in 2.2.15.

At the end of the second week, the flasks from each animal were divided and keratinocytes from half the flasks were seeded on microcarriers as described in 2.2.16.

Figure 37: Zimmer® dermatome ready for use.
(©http://emedicine.medscape.com/article/876290-overview#aw2aab6b6)
The dermatome is fitted with the blade (left) and a suitable sized guard is fitted (right) and secured in place using screwdriver.

The keratinocytes on microcarriers remained in stirred culture for one week until 24 hours prior to application in the second stage of the study. The magnetic stirrer was stopped and the flask transferred to a tissue culture hood, where the culture medium was aspirated. Cells were counted using a haemocytometer after dissolving the beads using trypsin. Keratinocytes were also harvested from the tissue culture flasks using trypsin, and counted. The cells were transferred to small Falcon® tubes in a concentration of 1 x 10^7 in each tube ready for spray application. The microcarriers seeded with keratinocytes were transferred to universal tubes, each containing 1 x 10^7 cells in total. The cells from both groups were stored in a cool bag overnight prior to application the next morning.

Three weeks after harvesting the skin grafts, the animals were anaesthetised as described in 2.3.3. Three wounds were created on the flank of each animal and PTFE wound chambers inserted as described in 2.3.5 as shown in figure 40 (3 on each flank). Treatments were applied accordingly as shown in figure 41.

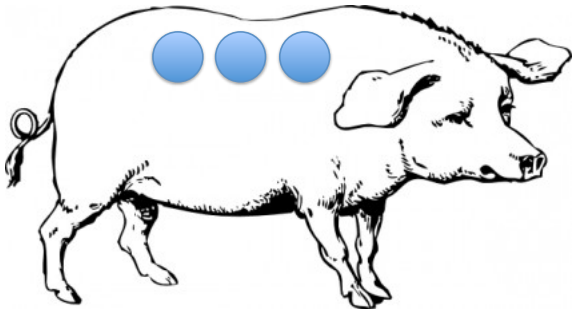

Figure 38: Diagrammatic representation of the site of the PTFE wound chambers on the flank of the animal
(3 wound chambers were located on each flank of each animal as shown)

Microcarriers and keratinocytes, and the control group (microcarriers only) were applied using sterile pipettes. The sprayed keratinocytes were applied evenly using a sterile 5 ml syringe and a disposable sterile nozzle (Syringe spray nozzle, Coster Aerosols Ltd, Stevenage, UK) from a distance of about 10 cm. Wounds were dressed as described in 2.3.5 (figure 42).

A dressing change was done under anaesthesia one week later using the same dressings and photographs taken. There was no incidence of dressings being removed by the animals or wound infections through the period of the study.

The animals were terminated two weeks (Day 15) following treatment as described in 2.3.3. Photographs were taken prior to extracting the wound chambers (from standard distance of 30 cm using the same camera with standard settings), the wounds were excised along the edges, and the specimens processed as described in 2.3.6.

Histological examination of the specimens was done using Haematoxylin and Eosin as described in 2.4.1, and Immunohistochemistry for K14, laminin, and collagen VII was done as described in 2.4.2. Analysis of images from the tissue sections was done as described in 2.5.2.

There was 12 wounds in total; divided into 3 groups (4 wounds each) as follows;

Group 1	Microcarriers and autologous keratinocytes
Group 2	Sprayed autologous keratinocytes
Group 3 (Control)	Microcarriers only

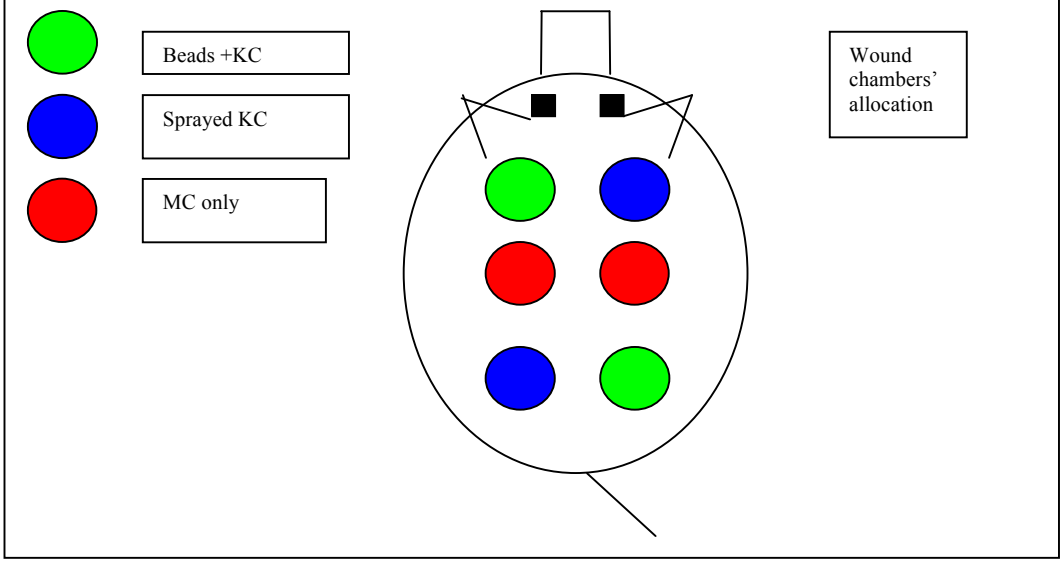

Figure 39: Wound chamber allocation Pig 1 (Exp 1.09)
The allocation was decided on random basis, where pig 2 had the control wounds (red) allocated to different sites

(A) **(B)**

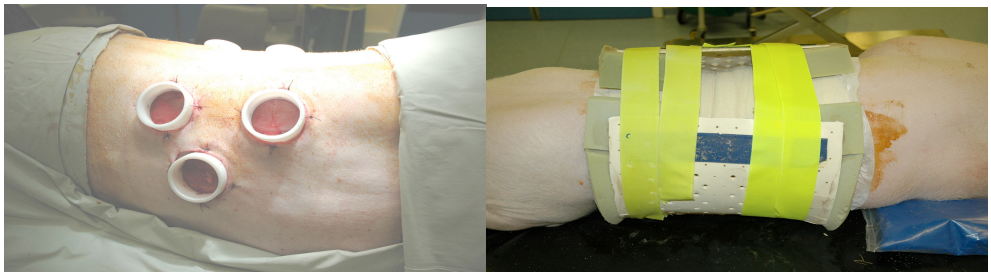

Figure 40: (A) Wound chambers post insertion (B) Dressings and foam jackets applied post procedure
The wound chambers are secured in place using Silk suture (left) and foam jackets were applied to protect the underlying dressings (right)

4.3 Results

This preliminary study was designed to compare the rate of survival of autologous keratinocytes on microcarriers (MCAK) when introduced onto full thickness wounds compared to autologous-sprayed keratinocytes (SAK).

The wounds were isolated within wound chambers to prevent re-epithelialisation from the wound margins and wound contraction. Hence, any newly formed epithelium within the chambers followed the application of either MCAK or SAK.

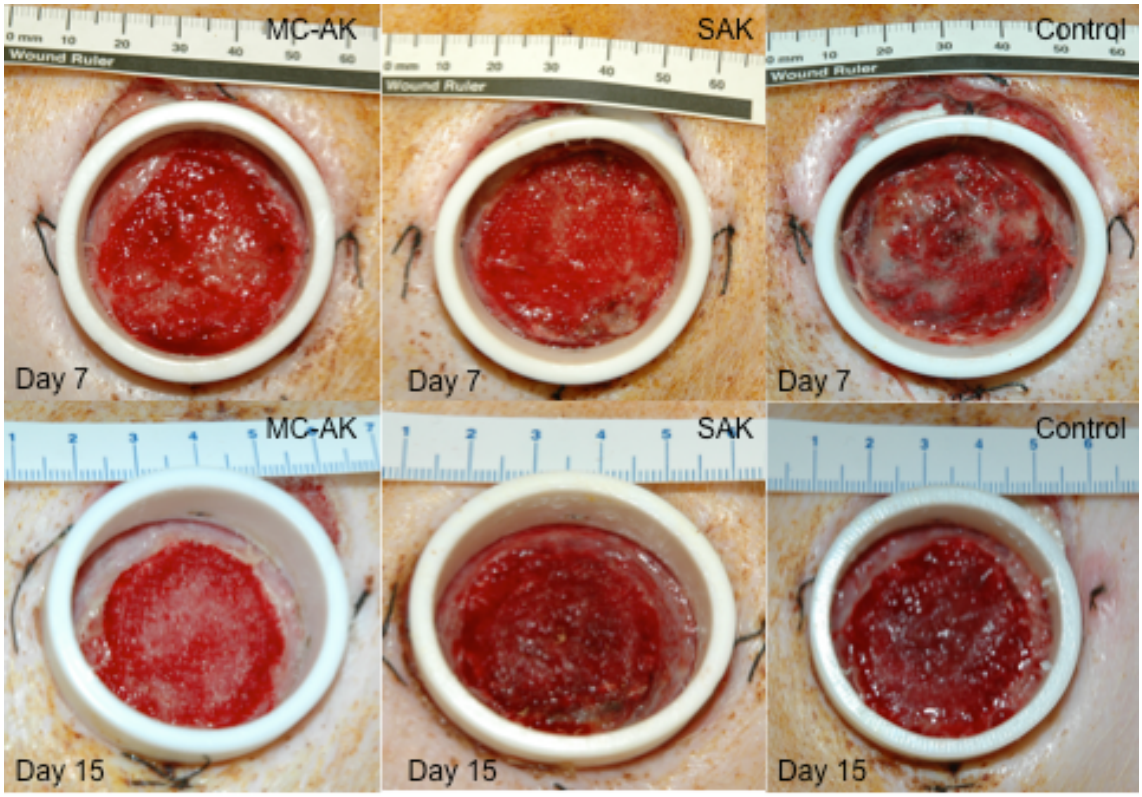

Figure 41: The 3 treatment groups Days 7 and 15
At day 15, MC-AK showed early signs of epithelial formation noted around the edges of the central granulating wound (left), while the control group showed granulation tissue without any signs of epithelial formation (right)

The biocompatibility of the gelatin microcarriers "Cultispher G®" in the wound was assessed in the control group, where only microcarriers were applied. Degradation of the microcarriers in the control group would indicate the suitability for future application *in vivo*. The three treatment groups, microcarriers did not produce any adverse reactions. There was no incidence of wound infection and by 15 days, therefore it was assumed that all microcarriers either degraded, dissolved, or were processed within the 3 wound groups. There were no microcarriers retrieved from any of the wounds indicating that no gelatin microcarriers were still present within any of the wounds.

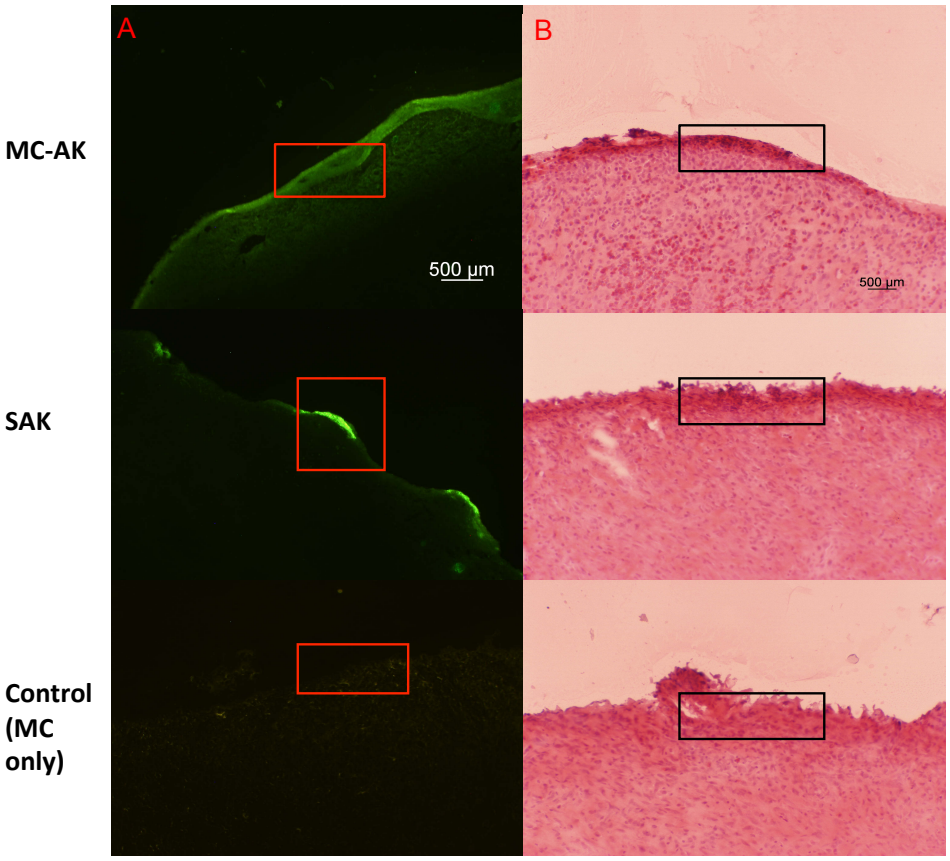

Figure 42: Tracing of GFP labelled keratinocytes and Hx & E staining in 3 treatment groups after 2 weeks
(A) Sections showing GFP positive keratinocytes within section surface in MC-AK and SAK, none in control group (red rectangle)
(B) Hx and E staining showing keratinocytes arranged in layers as early newly formed epidermis in MC-AK, and less uniform epithelium in SAK and granulation tissue in control groups (black rectangle) (x10 magnification, field width 3.6 mm)

GFP positive areas within the tissue sections were observed in the MCAK and SAK groups (figure 44a). These areas were located mainly on the surface of the wounds as seen on the surface of the sections (figure 44a, within red rectangle). The GFP +ve areas within the epidermis were more pronounced in the MCAK group compared to SAK group.

Tissue sections from all wounds were assessed for GFP content including the control group (MC only). MC only wounds showed very low levels of auto-fluorescence (figure 44A, lower left), whereas MCAK and SAK wounds showed significant GFP positive areas (figure 44a, top and middle left).

A macro application within Axiovision® software was used to measure the GFP positive areas within three random sections from each wound quadrant in the 3 groups.

Statistical analysis of the results was done using One Way Analysis of Variance on ranks (Kruskal-Wallis test). There was no statistically significant difference in GFP positive areas between the MCAK and SAK groups. The results indicated a comparable level of migration of GFP positive keratinocytes from microcarriers to wound bed between the two application methods.

Intact epithelium was not observed in any of the wounds at day 15 prior to animal termination. The wounds in the 3 treatment groups showed presence of granulation tissue covering the majority of the wound area within the wound chambers (figure 43, red tissue seen within PTFE chambers). The observation was confirmed by the findings of the Haematoxylin and Eosin (Hx & E) staining of tissue sections. There was no fully formed epithelium in any of the three groups; keratinocytes were arranged in flat even layers in the MCAK group (figure 44Bb, top). Observational assessment revealed the layers were less uniform in the SAK group with more irregular surface and absent in the control group (MC only) and replaced with granulation tissue (figure 44b, lower).

Immunohistochemical staining for K14 was positive in the MCAK and SAK groups and negative in the control group (figure 45a). A macro application within Axiovision® software was used to measure K14 positive areas (2 x 2 mm) within three random sections from each wound quadrant in the 3 groups selected by an independent assessor. The macro application was able to measure K14 positive areas within the wounds' sections after uploading a template of K14 positive section from normal pig skin initially. Statistical analysis of the results was done using One Way Analysis of Variance on ranks (Kruskal-Wallis test), and the p-value was <0.001. There was a statistically significant difference in K14 positive areas between the MCAK and SAK groups. The MCAK group had more positive K14 areas compared to the SAK group.

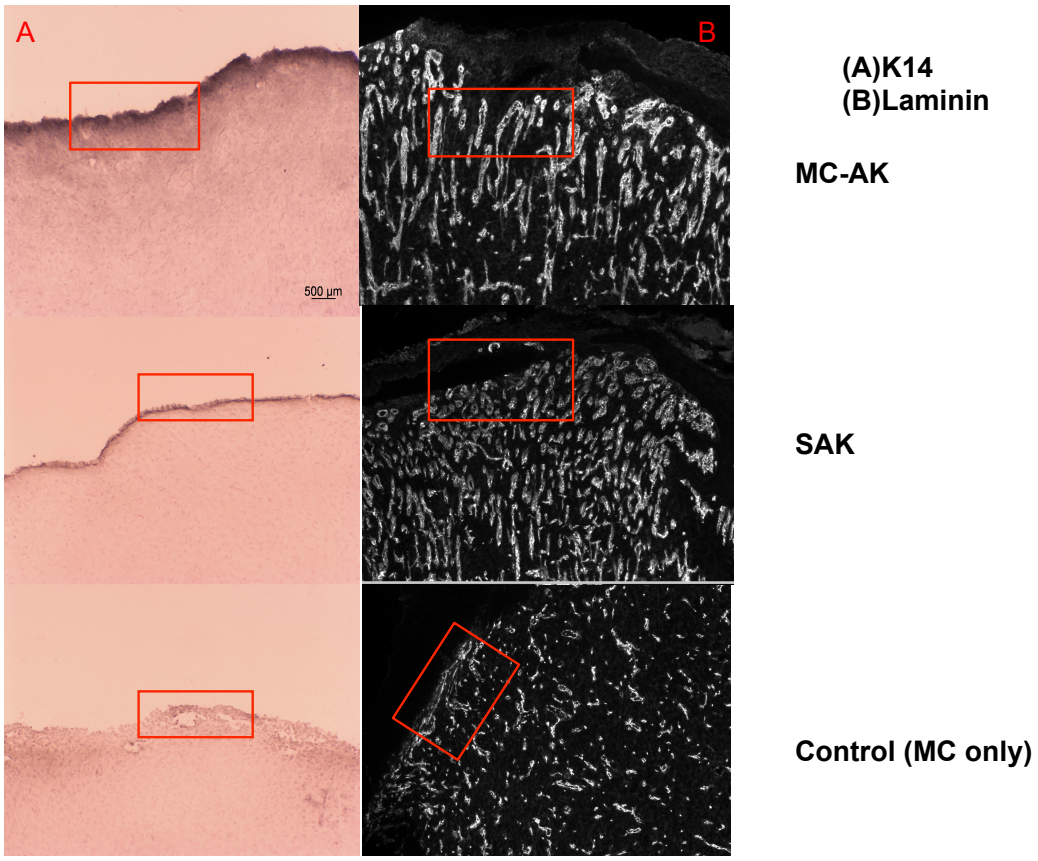

Figure 43: (A) K14 and (B) Laminin immuno-staining for 3 treatment groups
(A) K14 staining showing K14 positive keratinocytes (black colour) overlying the sections of MCAK and SAK (red rectangle)
(B) Laminin staining showing dense bundle distribution towards the surface of the section in the MCAK and SAK groups (right top and middle, red rectangle) compared to flat distribution within the same layer of the section in the control group (right lower, red rectangle) (x10 magnification, field width 3.6 mm)

Immunohistochemical staining for laminin showed striated distribution of bundles throughout the wound sections in the MCAK, SAK, and control groups (figure 45b). Observational assessment of the bundles' distribution revealed more dense distribution throughout the sections from the MCAK and SAK groups (figure 45b, upper and middle right) compared to the control group, where laminin bundles were more flat in upper layers of the sections (figure 45b, right lower). The bundles' density was denser towards the wound surface compared to the overall distribution in the granulation tissue of the control group (figure 45b, right column). No clearly formed basement membrane, which is characteristic of fully formed epithelium, was seen in any of the three groups. Collagen VII was negative in the 3 treatment groups indicating the lack of formation of basement membrane within mature epithelium.

There was no evidence of residual microcarriers within the tissue specimens by day 15 in the 3 treatment groups. The keratinocytes as evidenced by GFP positive areas migrated from the microcarriers to the wound surface in the MCAK and SAK groups.

Chapter 5: Investigation of wound healing and contraction rate of autologous keratinocytes on microcarriers, sprayed keratinocytes and widely meshed skin graft

5.1 Study objectives

The aim of this study was to investigate whether cultured autologous keratinocytes on microcarrier beads could reduce wound contraction in combination with widely meshed (6:1) split thickness skin graft (STSG). Their effect on wound contraction was compared with the combination of sprayed autologous keratinocytes and widely meshed STSG. Widely meshed STSG alone was used as a control. Wound contraction was assessed using serial measurements of the wound size using Visitrak™ at set time points. Epithelial regeneration and wound closure were assessed macroscopically using clinical observation and photography. Additionally, microscopic assessment using Haematoxylin and Eosin staining, and immunohistochemical staining for K14, collagen VII, and laminin was used to assess the rate of epithelial formation at 3 weeks.

5.2 Study design

Three pigs were used in this study as described in 2.3.1, and were admitted to NPIMR according to 2.3.2. In the first stage of the study, the animals were anaesthetised as described in 2.3.3, and one sheet of split skin graft measuring about 8 x 8 cm was harvested from the flank of each animal as described in 2.3.4.

The skin graft was wrapped in saline soaked gauze and transported back to the lab in porcine keratinocyte transport medium the same day. Porcine keratinocytes were isolated as described in 2.2.9, cultured as described in 2.2.10, and each flask was clearly labelled and kept in separate shelves in an incubator at 37°C. After keratinocyte expansion for one week, GFP labelling of porcine keratinocytes was undertaken as described in 2.2.14, repeated again in the same week, and the frequency of transduction calculated as described in 2.2.15. At the end of the second week, the flasks from each

animal were divided and keratinocytes from half the flasks were seeded on microcarriers as described in 2.2.16. The other flasks were maintained as described in 2.2.10 until cell harvest for application.

The keratinocytes on microcarriers remained in stirred culture for one week until 24 hours prior to wound application. Cells were counted using a haemocytometer after dissolving the beads using trypsin. Keratinocytes were harvested from the tissue culture flasks using trypsin and counted using haemocytometer. The cells were transferred to small Falcon® tubes in a concentration of 1 x 10^7 in each tube ready for spray application. The microcarriers seeded with keratinocytes were transferred to universal tubes, each containing 1 x 10^7 cells in total. The cells from both groups were stored in a cool bag overnight prior to application the next morning.

Three weeks after harvesting the skin grafts, (figure 46, representing wound allocations in one animal). There were 18 wounds in total; divided into 3 groups (6 wounds each) as follows;

Group 1	Microcarriers and autologous keratinocytes + STSG (6:1) ***[MCAK]***
Group 2	Sprayed autologous keratinocytes + STSG (6:1) ***[SAK]***
Group 3	STSG (6:1) only ***[Control]***

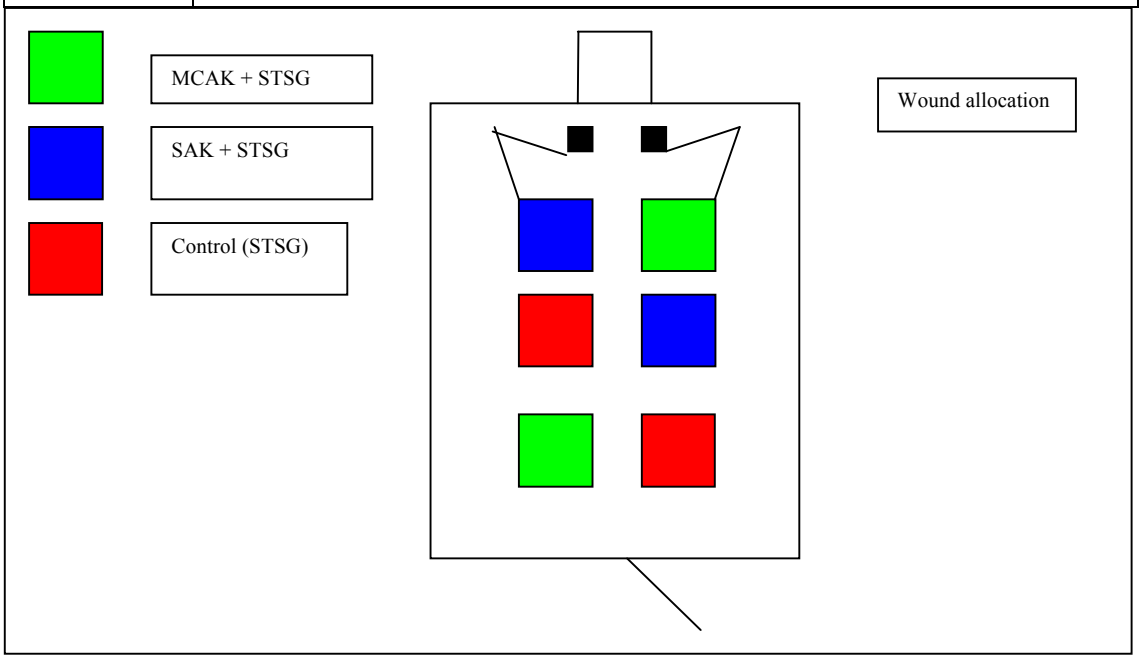

Figure 44: Wound allocation in one animal (Exp 2.10)
The other two animals had different wound allocations as all wounds were randomly assigned

Microcarriers and keratinocytes were applied using sterile pipettes on square wounds created as described in 2.3.6 covered with meshed Split thickness skin grafts (STSG) using Zimmer® mesher (figure 47). The sprayed keratinocytes were applied evenly using a sterile 5 ml syringe and a disposable sterile nozzle from a distance of about 10 cm. Wounds were dressed using Telfa clear® and Betadine soaked gauze as previously described.

Figure 45: Zimmer® mesher
The mesher is hand operated using a handle attached to the left side (not shown) and skin grafts are processed on plastic sheets depending on meshing ratio (manufacturer specific)

Dressings were changed under anaesthesia 4 days post-operative using the same dressings and photographs taken. The surface area of each wound was directly traced using Visitrak™ sheet, and the surface area measured on Visitrak™ device at each dressing change (figure 48) as described in 2.3.7.

Visitrak™ is a clinically validated and widely used method of wound surface area measurement, and has been shown to be an accurate tool in comparison with photography and Image J® analysis (Chang *et al.* 2011).

Further dressing changes were undertaken at day 8 and day 15 post-operatively, and the animals were terminated after three weeks (day 21) following treatment as described in 2.3.3. The wounds' surface areas were measured using Visitrak™ and photographs were

taken prior to wound excision. The wounds were excised full thickness and the specimens processed as described in 2.3.8.

Fresh frozen sections (15 μm) were examined for the presence of GFP labelled keratinocytes. Histological examination of the specimens was undertaken using Haematoxylin and Eosin as described in 2.4.1, and Immunohistochemistry for K14, collagen VII, and laminin was undertaken as described in 2.4.2.

Qualitative and quantitative assessment of wound contraction was undertaken using the serial photographs and the data from wound surface area assessment. Statistical analysis of the data was performed to compare wound contraction in the 3 treatment groups.

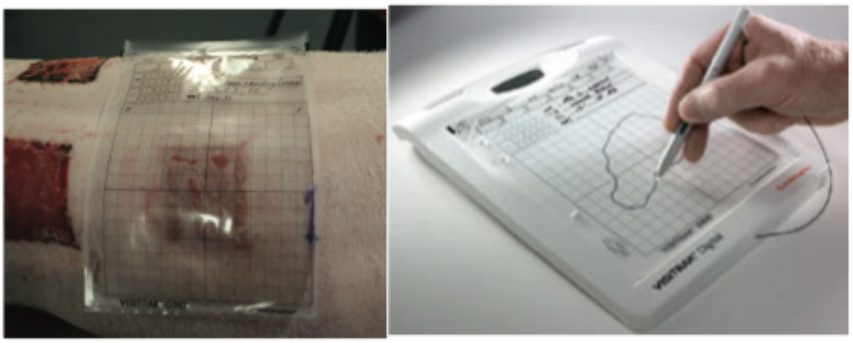

(A) Visitrak™ tracing sheet (B) Visitrak™ device

Figure 46: (A) Visitrak™ tracing sheet (B) Visitrak™ device.

(©http://global.smith-nephew.com/master/VISITRAK_PRODUCT_INFO_11079.htm)

(A) The wound edges are directly traced on the animal with an assistant keeping the sheet flat on the wound (B) The wound is then re-traced on Visitrak™ device to calculate wound area.
To maintain accuracy each wound was traced 3 times and an average area calculated

5.3 Results

5.3.1 Macroscopic qualitative assessment

During the three weeks course of the study, there were no wound complications in any of the three treatment groups. Following the initial harvesting of a small STSG) from

the flank of each animal for keratinocyte isolation, the donor healed two weeks later. Despite of the availability of the donor site for re-harvesting, the other flank was using for harvesting the widely meshed STSG (6:1).

Figure 49 demonstrates the appearance of the three treatment groups in dressing changes on days 4, 8, 15, and 21. On day 0 (STSG harvest and keratinocyte application), the STSG were spread carefully to cover all the entire surface area of each wound. On day 4, the meshed appearance of the STSG was partly lost on some areas of the wound in the three groups. This was attributed to the fragile nature of the thinly meshed STSG 6:1, the mobility of the animals in the post-operative period and the wounds' location on the animals' flanks. The partial loss of STSG occurred in the three groups in similar fashion, which ruled out any correlation to the type of treatment used.

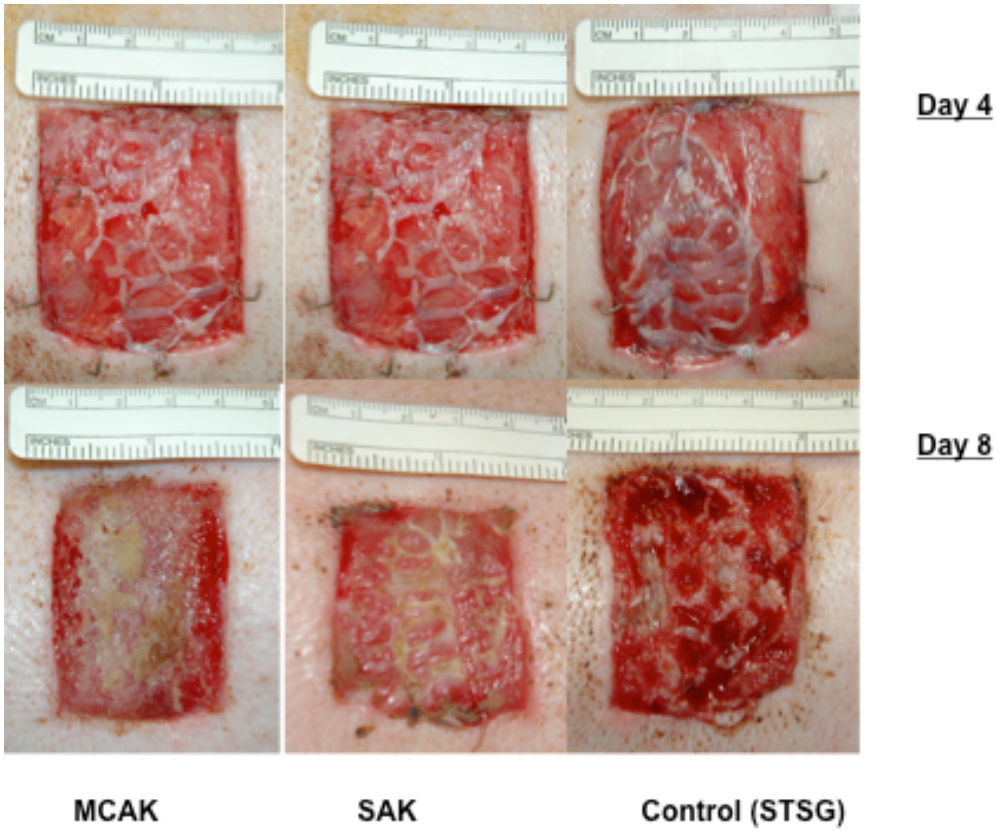

Figure 47: The 3 treatment groups days 4 and 8 (Exp 2.10)
From left to right; MCAK, SAK, and control (STSG) groups
Day 4 shows widely meshed STSG applied to the 3 treatment groups, day 8 shows signs of gradual wound healing (filling of the interstices of the meshed STSG) in the MCAK and SAK groups

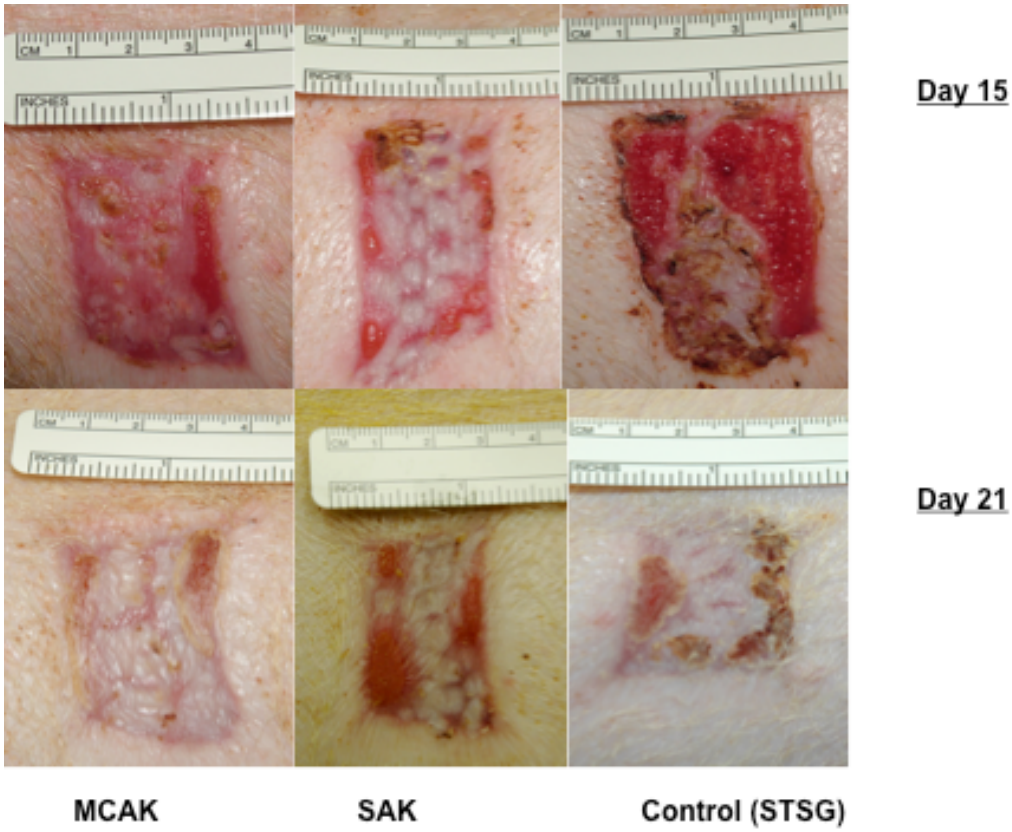

Figure 48: The 3 treatment groups Days 15 and 21 (Exp 2.10)
From left to right; MCAK, SAK, and Control groups
Day 15 shows minimal areas of granulation tissue in the MCAK and SAK groups compared to control group. Day 21 shows almost full wound healing (pattern of the interstices of the meshed STSG has disappeared). There is visible difference in the wound area seen between the 3 groups.

On day 8, the meshing pattern of the STSG was still apparent in the SAK and control groups, while less apparent in the MCAK group. On day 15, MCAK group showed signs of re-epithelisation of the full wound surface area. The SAK group still demonstrated the meshed pattern of the STSG and the control group showed areas of unhealed granulation tissue. On day 21, the wounds in the MCAK group were healed, the wounds in the SAK and control groups showed small areas of unhealed granulation tissue around the edges.

All the wounds were created using a template measuring 4 x 4 cm^2 to provide a standard wound surface area. A variation was noted in the measurement of the wound surface area between the three groups starting from day 4 (table 7). The variation (+ 2-4 cm^2) was noted in the three groups, the variation was attributed to the physiological wound edge movement prior to wound contraction. Due to the anatomical location of the wounds, the mobility of the skin edges probably led to retraction of the wound edges

prior to attachment to the underlying muscle layer during wound healing. The difference in mean wound surface area between the three groups on day 4 was minimal (less than 1 cm^2) (table 7). The variation was not statistically significant.

Day	MCAK		SAK		Control	
	Mean (cm^2)	SD	Mean (cm^2)	SD	Mean (cm^2)	SD
4	19.9	(1.1)	19.0	(0.9)	19.9	(0.6)
8	16.6	(1.7)	15.7	(1.2)	16.2	(1.8)
15	11.3	(0.5)	9.8	(0.8)	9.1	(0.6)
21	8.5	(0.6)	7.7	(0.5)	6.3	(0.4)

Table 7: Mean and Standard deviation wound surface area in the 3 groups

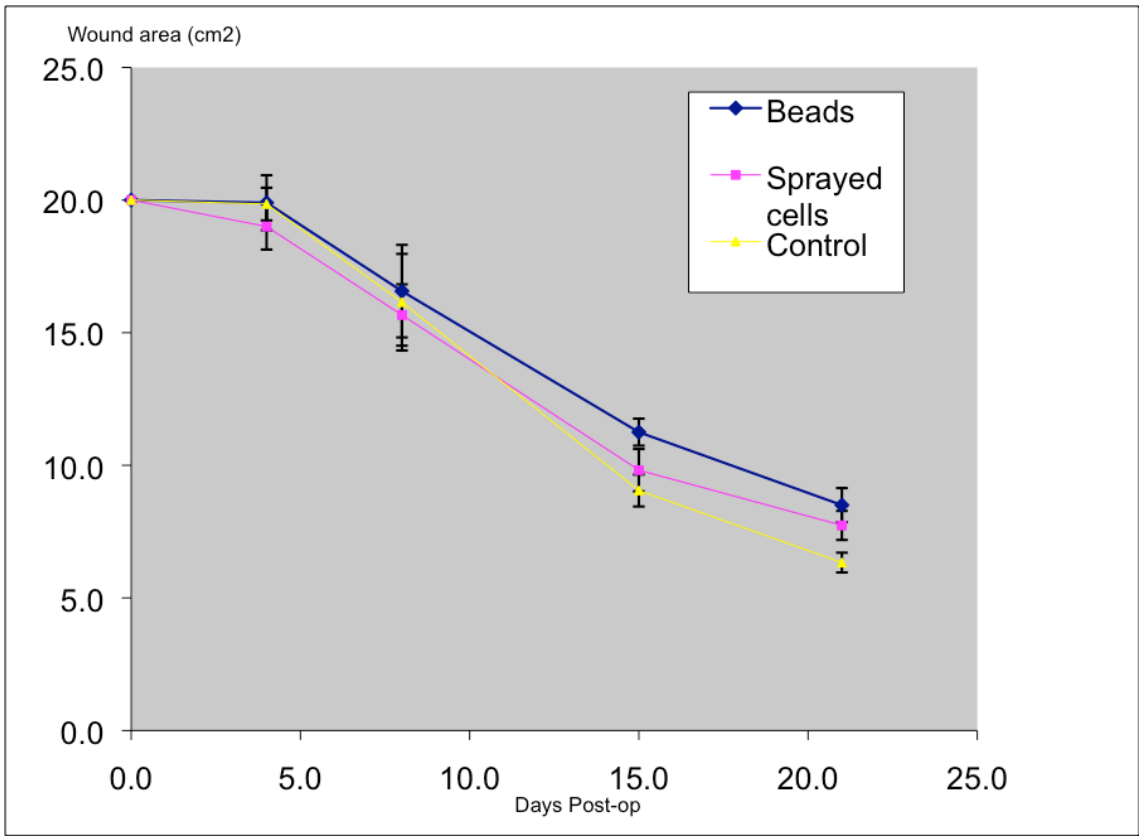

Figure 49: Graphical representation of wound contraction in wound surface area (Error bars refer to standard deviation)

On day 8 (table 7), the mean wound surface area in the three groups was similar with less than 0.5 cm^2 difference. Noticeably, all the 3 groups showed wound contraction of around 25% compared to the wound surface area on day 4.

On day 15 (table 7), a difference of 1.5-2.2 cm^2 in the mean wound surface area was noted between the MCAK group and the SAK and control groups. The MCAK group showed less wound contraction of 56.7% compared to 51.5% in the SAK group and 45.7% in the control group.

On day 21, the MCAK group showed wound contraction of 42.7% of the original wound surface area. The SAK group wound contraction was 40.5% and the control group wound contraction was 31.6% of the wound surface area. A difference of 11.1% in the wound contraction area was noted between the MCAK group and the control group by day 21 (figure 51).

The wounds in the MCAK group contracted more slowly than the SAK and control groups. The SAK group contracted slower than the control group. Significantly less wound contraction was found in wounds treated with MCAK (n = 6) than with STSG alone (n = 6) or SAK (n = 6) (***adjusted*** $p < 0.05$; Holm-Sidak post hoc test). Generally, all the wounds from the three groups were healed by day 21 despite the variation in the contraction of the wound area.

5.3.2 Histological and immunohistochemical analysis

Whole wounds were excised on day 21, following the termination of the animals.

At day 21 post-treatment, all wounds in the three groups displayed an intact epithelium. Fresh sections from both MCAK and SAK groups showed no GFP-positive cells despite full re-epithelialisation. This is due to the loss of the GFP after 2-3 weeks as previously discussed. Observational assessment of the Haematoxylin and Eosin staining of the three groups showed newly formed epithelium varying in arrangement and number of layers (figure 52). Both the MCAK and SAK groups showed a fully formed epithelium

arranged in layers resembling the architecture of normal porcine skin. The control group showed a thin layer of fragile epithelial cells corresponding to the nature of the thinly meshed STSG.

K14, a marker of proliferating basal keratinocytes, was expressed in all wounds (figure 53). The presence of K14 demonstrated the proliferation of keratinocytes in the MCAK and SAK groups to achieve epithelial closure in combination with STSG. The distribution of K14 in the MCAK and SAK groups was similar in pattern, with more pronounced multi-layered epithelium compared to the control group (figure 52).

Immunohistochemical staining for collagen VII was clearly positive in the three groups. In the MCAK group, collagen VII immuno-staining was more intense compared to the SAK and control groups (figure 53). The MCAK group demonstrated the formation of a well-developed basement membrane (figure 53-middle 2nd section) compared to the SAK and control groups.

The formation of basement membrane was an indication of the regeneration of intact epidermis in the three groups. The basement membrane appearance in the MCAK signified more developed epithelium compared to the SAK and control groups.

Immunohistochemical staining for Laminin was assessed using Fluorescein isothiocyanate (FITC), a fluorescent stain that binds strongly to DNA (figure 54). The three groups showed positive staining for laminin with a variation in the laminin distribution. The laminin distribution in the MCAK group was more uniform across the sections and condensed in the basement membrane and papillary dermis region. A similar pattern was seen in the SAK group with more condensation in the same area compared to the MCAK and control groups (figure 54).

The dense staining for laminin in the basement membrane and papillary dermis region could signal a more developed basement membrane in the SAK group compared to MCAK. The MCAK and SAK groups produced a distinctive pattern compared to the control group (figure 54).

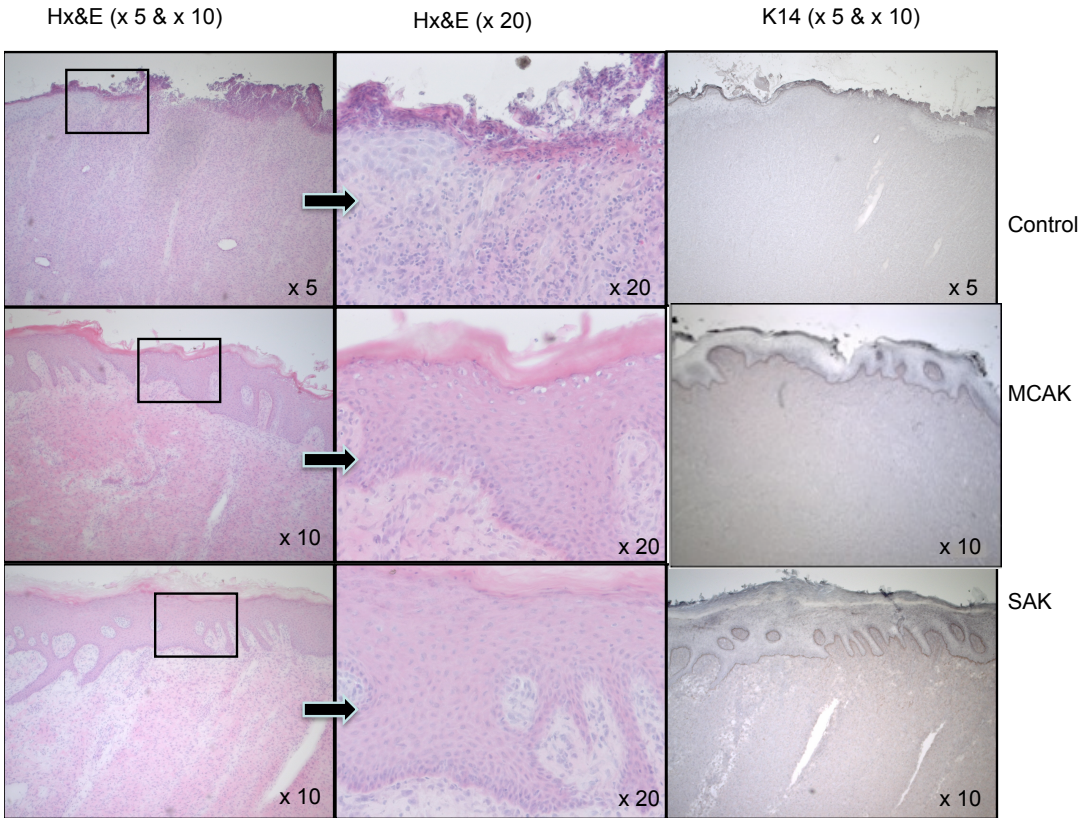

Figure 50: Hx & E and K14 immuno-labelling of the 3 groups
Hx & E staining x5 on the left, epidermis magnified x20 in the middle, and K14 staining on the right (positive staining dark black at the level of the epidermis) (x5 magnification-field width 7.2 mm, x10 magnification-field width 3.6 mm, and x20 magnification-field width 1.8 mm [middle column])

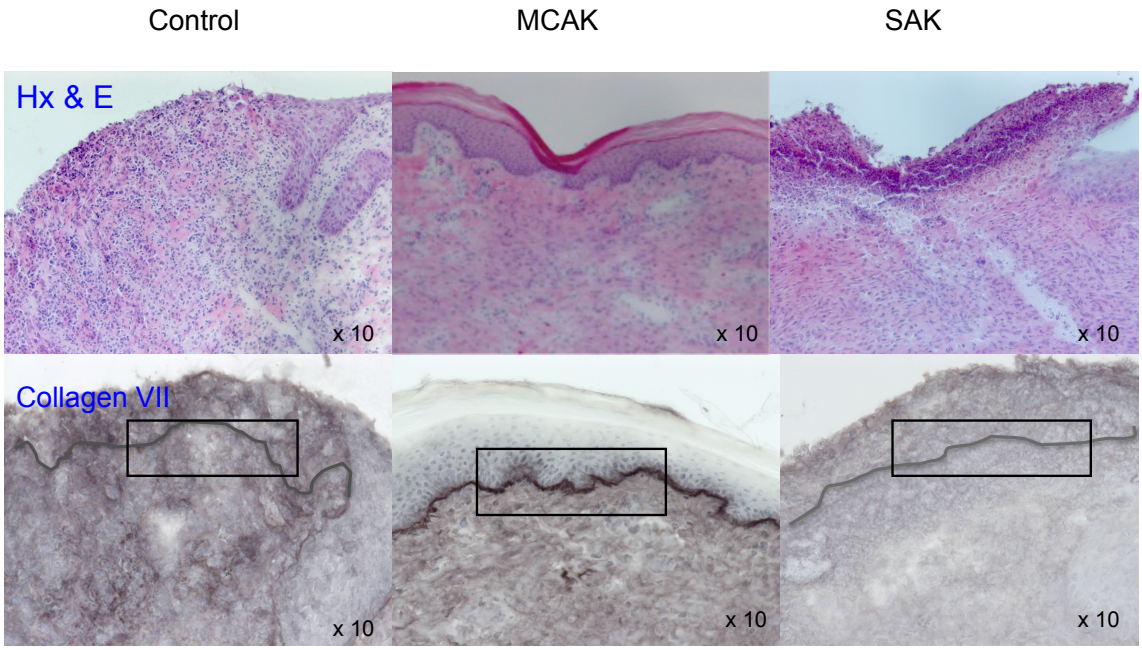

Collagen VII immuno-labelling is seen positive in the 3 groups, the MCAK group (middle column) is thicker compared to the SAK and control group

Figure 51: Hx & E staining and Collagen VII immuno-labelling of the 3 groups
Hx & E sections (top), with Collagen VII staining of the same sections (below). Positive staining for Collagen VII (Basement membrane) in the 3 groups (within the rectangle) (x10 magnification, field width 3.6 mm)

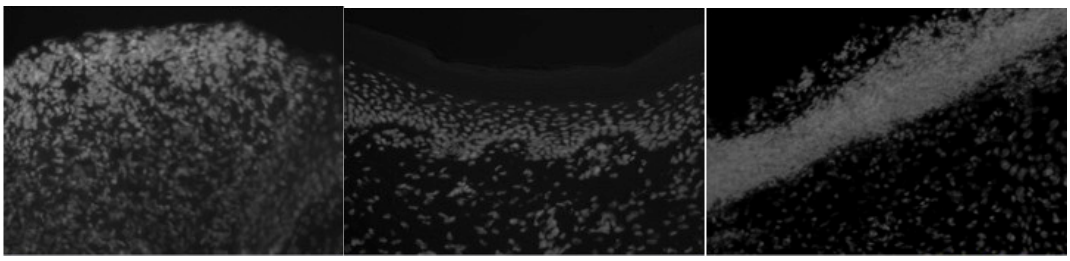

Figure 52: Laminin immuno-labelling (using FITC) in the 3 groups
Distribution of laminin in the control group (left) across the whole section compared to more uniform distribution within the papillary dermis in MCAK (middle) and SAK (right) [top of the section]. SAK showed denser distribution compared to MCAK (x10 magnification, field width 3.6 mm)

The laminin staining in the control group was less uniform and lacked dense distribution in the basement membrane and papillary dermis region (figure 54, left).

In conclusion, histological analysis of sections from the three groups demonstrated epithelial regeneration in all wounds examined. The quality of epithelium varied between the three groups with highly developed epithelium and basement membrane in the MCAK group. This could explain the variation in the wound contraction rate in the MCAK group compared to the SAK and control groups.

Chapter 6: Investigation of wound healing and contraction rate of allogeneic keratinocytes on microcarriers, sprayed keratinocytes and ultra-thin split skin graft on Integra® (Two stage dermal regeneration)

6.1 Study objectives

The aim of this study is to investigate whether cultured allogeneic keratinocytes on microcarrier beads can reduce wound contraction in combination with Integra® (dermal regeneration template). Their effect on wound contraction will be compared with the combination of sprayed allogeneic keratinocytes and Integra®. Ultra-thin split thickness skin graft (uSTSG) and Integra® will be used as a control, uSTSG will be used as it is sufficient to achieve wound closure in combination with Integra®. The area of wound contraction will be assessed using serial measurements of the wound size using Visitrak™ at set time points. Epithelial regeneration and wound closure will be assessed macroscopically using clinical observation and photography. Also microscopic assessment using Haematoxylin and Eosin staining, and immunohistochemical staining for K14, collagen VII, laminin, and α-SM actin will be used to assess the rate of epithelial formation and myofibroblast differentiation.

6.2 Study design

Three pigs were used in this study and prior to the beginning of the study; the animals as described in 2.3.1 were admitted to NPIMR according to 2.3.2.

In the first stage of the study, the animals were anaesthetised as described in 2.3.3, and three square-shaped wounds were created on the flank of each animal as described in 2.3.6. A piece of Integra® measuring 4 x 4 cm was inset in each wound using skin staples. One sheet of split skin graft measuring about 8-10 cm was harvested from each animal from the posterior part of the para-spinal area as described in 2.3.4. The wounds were dressed and wrapped in foam jackets as described before. The skin graft was

wrapped in saline soaked gauze and transported back to the lab in porcine keratinocyte transport medium the same day.

Porcine keratinocytes were isolated as described in 2.2.9, and cultured as described in 2.2.10. The flasks from each animal were clearly labelled and kept in separate shelves in an incubator at 37°C. After keratinocyte expansion for one week, GFP labelling of porcine keratinocytes was done as described in 2.2.14, repeated again in the same week and the frequency of transduction calculated as described in 2.2.15.

At the end of the second week, the flasks from each animal were divided and keratinocytes from half the flasks were seeded on microcarriers as described in 2.2.16, and the remaining flasks were maintained as described in 2.2.10. The keratinocytes on microcarriers remained in stirred culture for one week until 24 hours prior to application. The magnetic stirrer was stopped and the flask transferred to a tissue culture hood, where the culture medium was aspirated.

A cell count was undertaken after dissolving the beads using trypsin. Keratinocytes were harvested from the tissue culture flasks using trypsin, and cells counted. The cells were transferred to small Falcon® tubes in a concentration of 1 x 10^7 in each tube ready for spray application. The microcarriers seeded with keratinocytes were transferred to universal tubes, each containing 1 x 10^7 cells in total. The cells from both groups were stored in a cool bag overnight prior to application the next morning.

During the three weeks following the creation of the wounds and harvesting the skin grafts, two dressing changes at days 7 and 14 were performed under general anaesthesia. The wounds were dressed as described before and wrapped in foam jackets.

Three weeks after harvesting the skin grafts (Day 21), the animals were anaesthetised as described in (2.3.3). The silicone layer was removed from the surface of the Integra® to reveal a revascularised dermis and the skin staples were removed. The surface area of each wound was traced using Visitrak™ tracing sheet, and measured on Visitrak™ device as described in 2.3.7.

Treatments were randomised and applied to the wounds (figure 55), keratinocytes on microcarriers and sprayed keratinocytes were interchanged between the three pigs to provide allogeneic keratinocytes (Pig 1 to receive cells from Pig 2 and Pig 2 from Pig 3 etc). uSTSG was harvested from one flank using Zimmer® air dermatome (150-200 μm thick). The uSTSG was applied to the control wounds and secured with skin staples. There were 18 wounds in total; divided into 3 groups (6 wounds each) as shown in (figure 55).

Group 1	Microcarriers and allogeneic keratinocytes + Integra® ***[MCAlK]***
Group 2	Sprayed allogeneic keratinocytes + Integra® ***[SAlK]***
Group 3	uSTSG + Integra® ***[Control]***

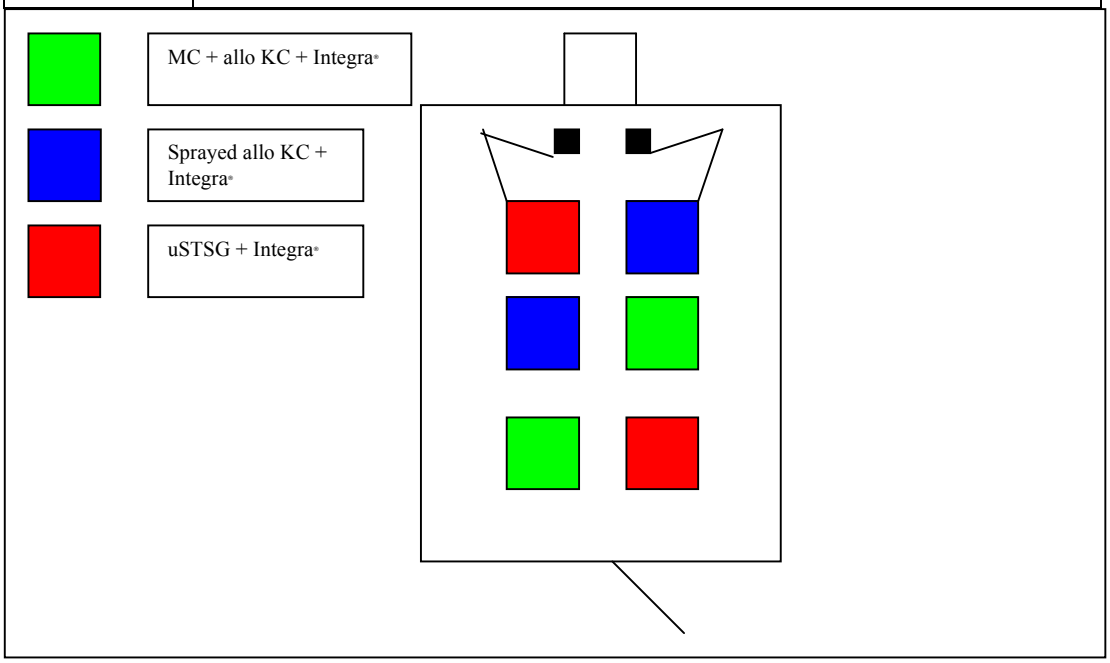

Figure 53: Wound allocation in one animal (Exp 3.10)
The wounds were allocated randomly and wound sites were different in the other 2 animals

Microcarriers and keratinocytes were applied using sterile pipettes. The sprayed keratinocytes were applied evenly using a sterile 5 ml syringe and a disposable sterile nozzle from a distance of about 10 cm. Wounds were dressed using Biobrane®, secured using skin staples, and dressed with Betadine soaked gauze as described before. Biobrane® was used to protect the allogenic keratinocytes rather than using Telfa Clear® as before. A dressing change was done under anaesthesia 7 days post-operative using the same dressings and photographs taken. Another dressing change was done under

anaesthesia on day 14 post-operative. Biobrane® was adhered to the wound surface after the dressing change on day 14 and was left undisturbed.

The animals were terminated three weeks (Day 21) following treatment as described in 2.3.3, Biobrane® was poorly adhered to the wound surface and was easily removed.

The wounds' surface areas were measured using Visitrak™ system and photographs were taken prior to wound excision. The wounds were excised along the edges including the full thickness of the skin and subcutaneous tissue. The tissue specimens were transferred back to the laboratory and the specimens processed as described in 2.3.6, and fresh sections were examined for the presence of GFP labelled keratinocytes. Histological examination of the specimens was done using Haematoxylin and Eosin as described in 2.4.1, and immunohistochemistry for K14, collagen VII, laminin, and α-SM actin was done as described in 2.4.2.

Qualitative and quantitative assessment of wound contraction was undertaken using the serial photographs and the data from wound surface area assessment. Statistical analysis of the data was performed to compare the overall wound contraction in the three treatment groups.

6.3 Results

6.3.1 Macroscopic qualitative assessment

During the six weeks course of the study, there were no wound complications in any of the three treatment groups. Following the initial harvesting of the STSG from the flank of each animal for keratinocyte isolation, the donor healed in two weeks. Dressing changes for Integra® over three weeks showed no wound infections or tissue rejection.

By day 21, the dermal template (Integra®) was completely vascularised and ready for treatment application.

Figure 56 demonstrates the development of the appearance of the MCAlK treatment group during the six weeks period. On day 0 (STSG harvest and Integra® application),

Integra® was inset using skin staples (figure 56a), the silicone layer was not visible prior to dermal layer vascularisation. On day 7 (figure 56b), there is no evidence of infection or collections beneath the silicone layer of Integra®. On day 21 (figure 56c), Integra® appeared well vascularised and the silicone layer removed in readiness for treatment applications. Following the application of MCAlK in (figure 56d), Biobrane® was applied and secured using staples to protect the wounds. During the next two dressing changes (figure 56e and f), there were no signs of wound infection and the Biobrane® was well adhered to the wound surface.

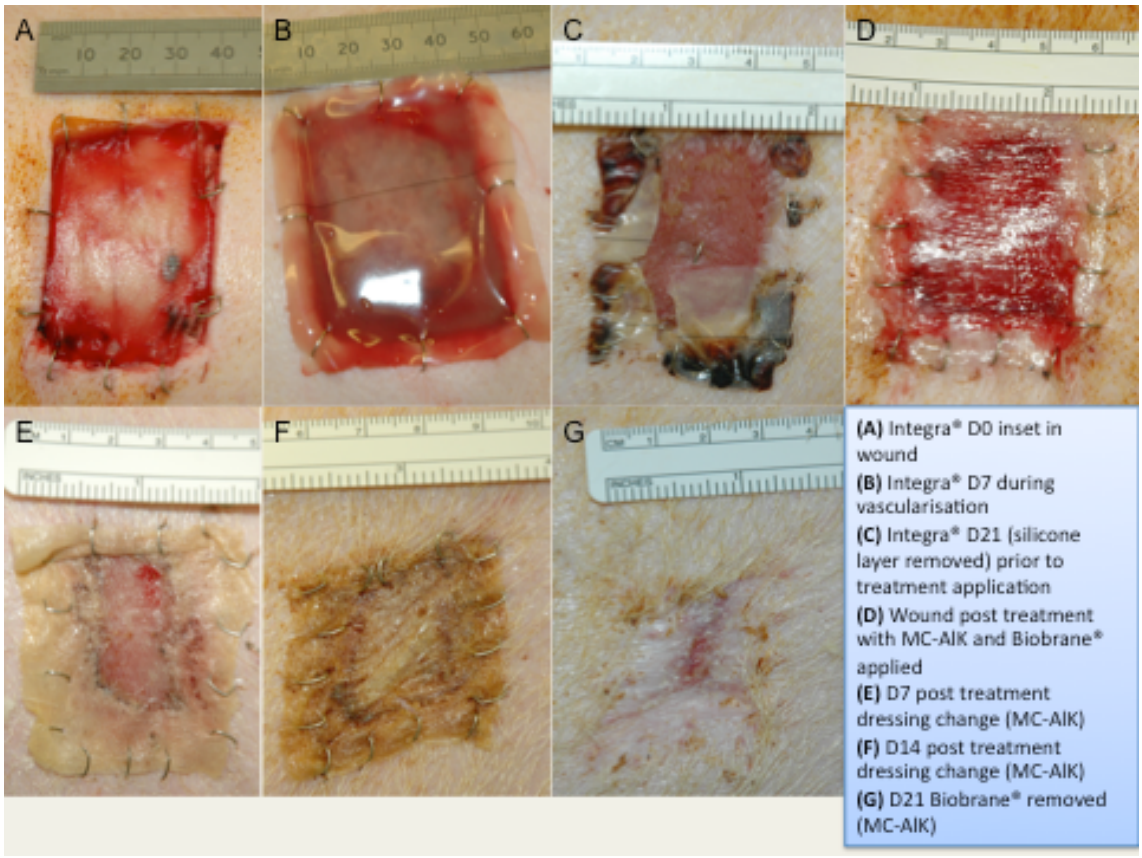

Figure 54: The MCAlK treatment group (A to C Integra® alone, D to G post treatment) [Exp 3.10]
The silicone layer covering Integra® was clearly visible at day 7 (B), Biobrane® was applied to the wounds post treatment day 21 (D), and was removed on day 21 (post treatment) prior to termination of the experiment

Between day 15 and day 21 post Integra® application during dressing changes, it was noted that vascularisation of Integra was complete in some wounds. Despite this observation, the silicone layer on all wounds was left intact.

On day 42 (experiment termination), following the removal of Biobrane®, all wounds in the three groups showed variation in epithelial closure (figure 57). MCAlK and SAlK groups' wounds had residual granulation tissue (figure 57a and b) compared to full epithelial closure in the control group (figure 57c). The control group was the only group to receive autologous cells in the form of uSTSG on Integra®.

Figure 55: Day 42 (Experiment termination)
The difference between the 3 treatment groups is shown at experiment termination where full epithelial closure was achieved in the control wounds (autologous uSTSG group)

All the wounds were created using a template measuring 4 x 4 cm^2 to provide a standard wound surface area. As seen in the previous study (chapter 5), the variation in the wound surface area (+ 2-4 cm^2) occurred early post operatively due to retraction of wound edges. This physiological stage precedes wound contraction as the wound surface area starts to decrease. The application of Integra® maintained the wound surface area at pre-contraction phase size for 3 weeks post application.

On day 21, the mean wound surface area in the three groups was similar with less than 1 cm^2 difference. On day 42, three weeks following treatment, a difference of less than 1 cm^2 in the mean wound surface area was noted between the MCAlK group and the SAlK. The control group showed the greatest contraction in wound area with a reduction in wound surface area from 18.88 (+/- 0.31) cm^2 to 3.6 (+/- 0.23) cm^2. The MCAlK group showed lower wound contraction with healed area of 33.7 % of the original wound area compared to 29.1% in the SAlK group and 19.1 % in the control group.

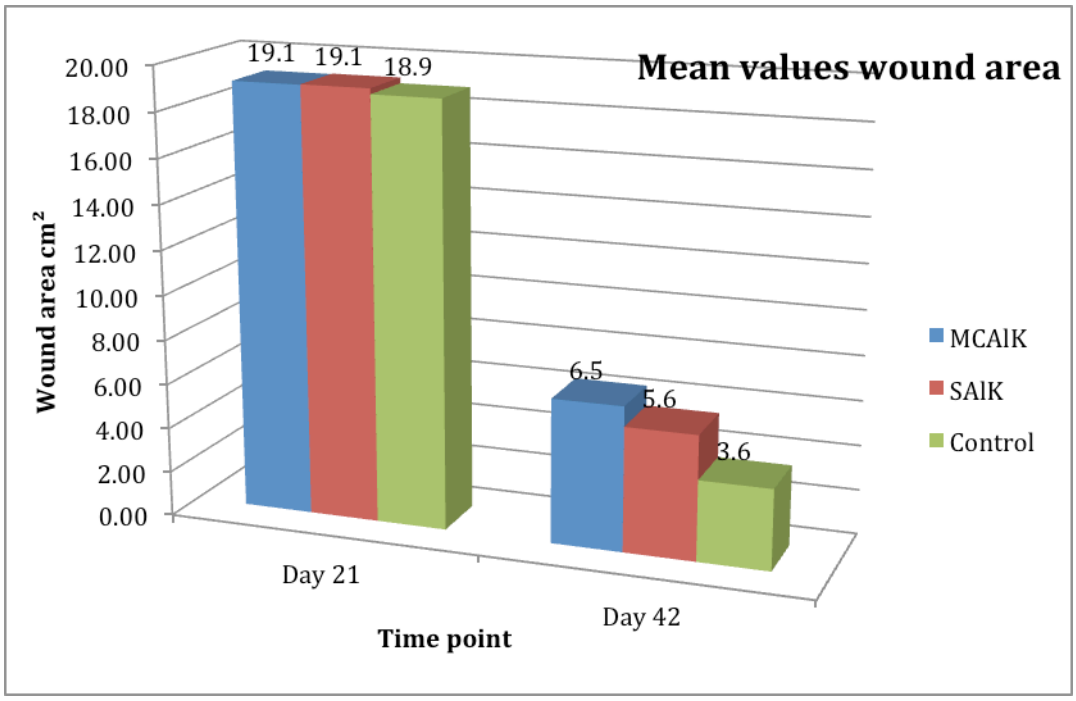

Figure 56: Graph representation of wound contraction in wound surface area (Days 21 and 42)

A difference of 14.6% in wound contraction area was noted between the MCAlK group and the control group by day 42. The MCAlK group wounds contracted less than the SAlK group, which contracted less than the control group (figure 58).

The wounds in the MCAlK group contracted slower than the SAlK and control groups, and the SAlK group contracted slower than the control group. Significantly less wound contraction was found in wounds treated with MCAlK (n = 6) than with uSTSG alone

(n = 6) or SAlK (n = 6) (adjusted $p < 0.05$; Holm-Sidak post hoc test). The control group wounds were healed by day 21 post treatment, the other two groups showed residual granulation tissue. Full epithelial closure did not occur despite the variation in wound area.

6.4.2 Histological and immunohistochemical analysis

The whole wounds were excised on day 42, following the termination of the animals. Fresh sections from both MCAlK and SAlK groups showed no GFP-positive cells in any of the wounds.

Haematoxylin and Eosin staining of the three groups showed newly formed epithelium varying in quality (figure 59). Both the MCAlK and SAlK groups showed an epithelium comparable to the control group but with reduced epidermis thickness. Both groups (MCAlK and SAlK) showed a residual thin layer of granulation tissue over the epithelium (figure 59b and c).

Immunohistochemical staining for collagen VII was positive in the three groups. In the MCAlK and SAlK groups, collagen VII immuno-staining was thicker compared to the control group (figure 59-middle column-Collagen VII). Both the MCAlK and SAlK groups demonstrated the formation of a well-developed basement membrane. The formation of basement membrane was an indication of the regeneration of intact epidermis. All wounds from the three groups showed distribution of K14, a marker of basal keratinocytes (figure 59-right column-K14).

The presence of K14 demonstrated the support provided by MCAlK and SAlK groups to wound healing in this animal model. The distribution of K14 in the MCAlK and SAlK groups was similar in pattern, and comparable to the control group.

The three groups showed positive staining for laminin with a variation in the laminin distribution (figure 60-left column). Immunohistochemical staining for laminin showed a more distinctive pattern in the SAlK group compared to MCAlK and control groups

(figure 60-middle). Laminin showed a more dense distribution across the sections compared to the more localised distribution in the basement membrane region in the other two groups.

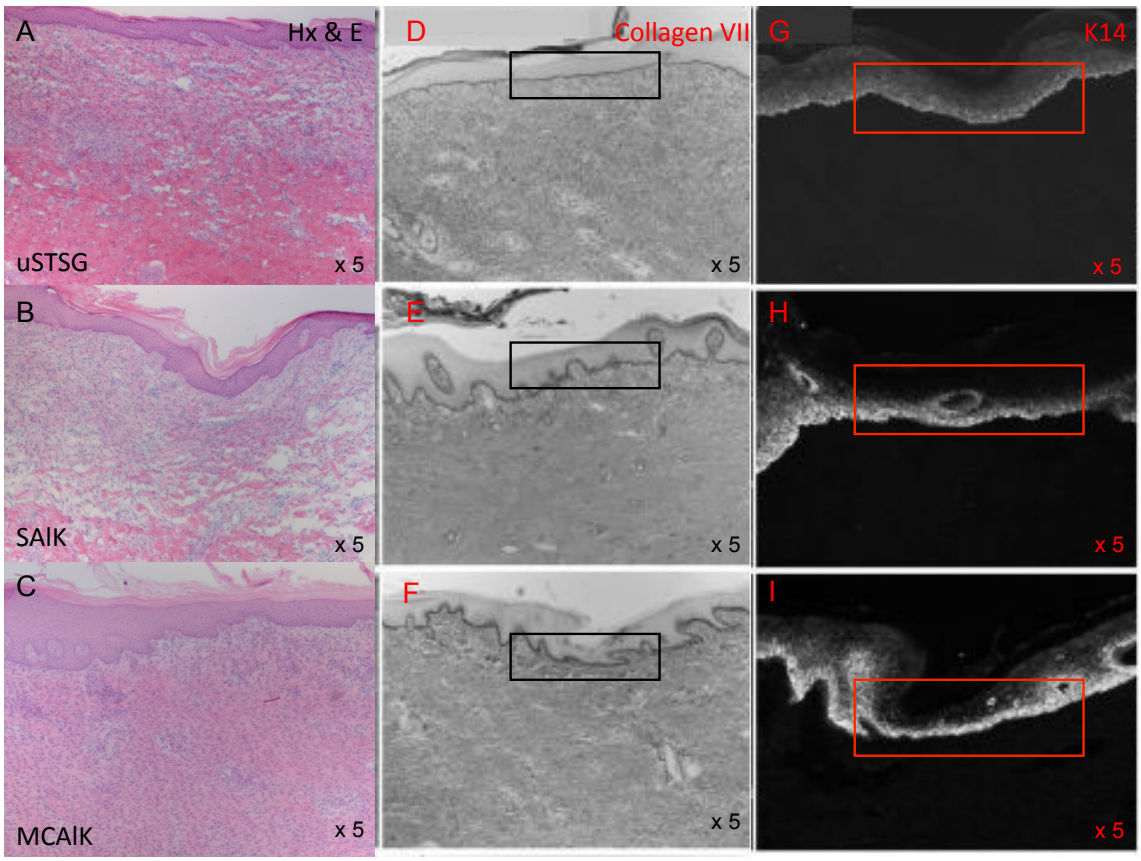

Figure 57: Hx & E, Collagen VII and K14 immuno-labelling of the 3 groups
(A) uSTSG, (B) SAlK, and (C) MCAlK, (D, E, and F) showing Collagen VII in the 3 groups with basement membrane positive staining (black rectangle). (G, H, and I) showing positive K14 staining in the epidermis in the 3 groups (red rectangle) (x5 magnification, field width 7.2 mm)

The laminin distribution in the MCAlK and control groups was more uniform across the sections and condensed in the basement membrane region. The dense staining for laminin in the basement membrane region could signal a mature basement membrane in the SAlK group compared to MCAlK and control groups.

Immunohistochemical staining for α-SMA was positive in the three groups demonstrating myofibroblast activity (figure 60-right column). A clear distribution pattern was seen in the control group where α-SMA was distributed in distinct areas deep within the dermo-epidermal junction (figure 60-top right within red rectangle).

The dermo-epidermal junction seen in more detail (x 20 magnification on the left) showed the difference in the distribution pattern between the 3 groups.

The myofibroblasts were arranged in flat-condensed arrays parallel to the dermal–epidermal junction compared to the other two groups.

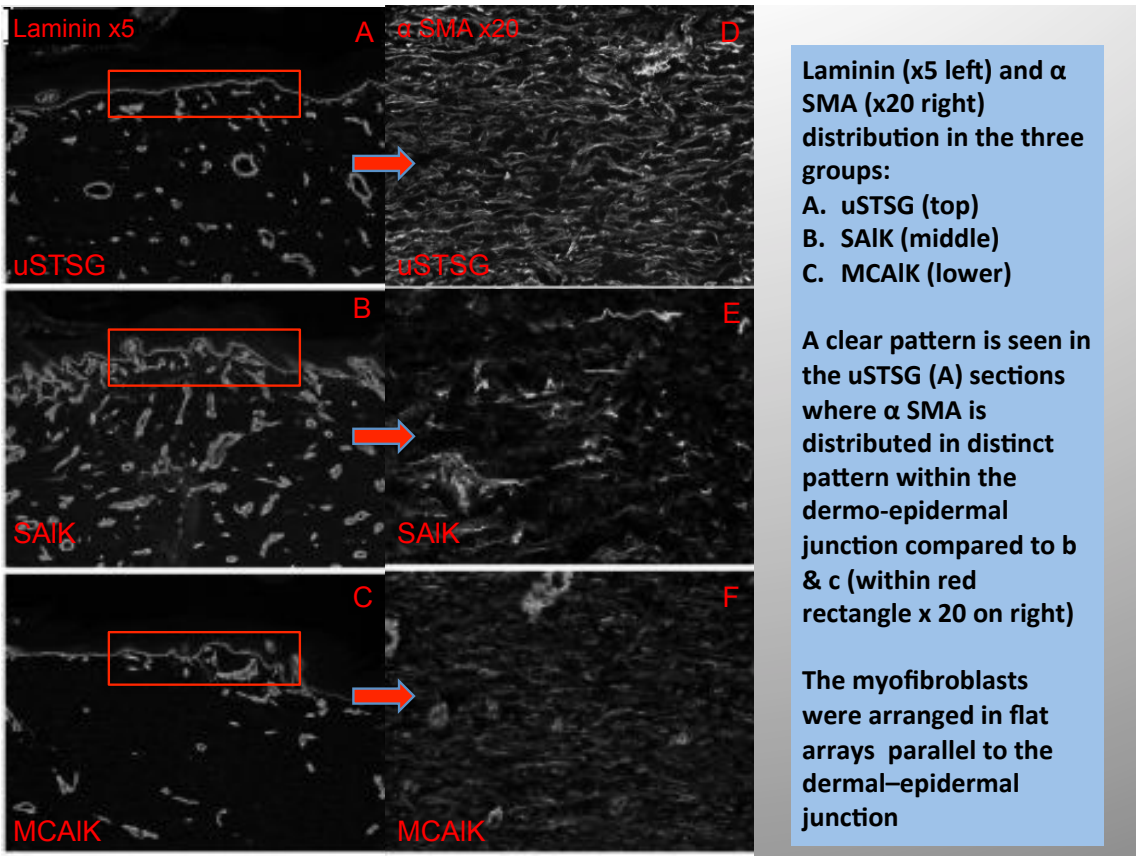

Figure 58: Laminin and α SMA immuno-labelling of the 3 groups
(A) uSTSG, (B) SAlK, and (C) MCAlK laminin staining x5 (left, field width 7.2 mm), and α-SMA x20 (right D, E, and F, field width 1.8 mm) where myofibroblast seen within the dermo-epidermal junction

In conclusion, histological analysis of sections from the three groups demonstrated epithelial regeneration in all the wounds examined. The quality of epithelium varied between the three groups as only the control group received autologous treatment (uSTSG). The control group demonstrated different myofibroblasts distribution through α-SMA immunolabelling. Both the MCAlK and SAlK groups showed re-epithelisation of wounds, which was comparable to the control group. This could be explained by epithelial migration from the wound edges to achieve closure rather than as a result of the allogeneic cells application.

Chapter 7: Investigation of wound healing and contraction rate of autologous keratinocytes and fibroblasts on microcarriers and sprayed keratinocytes on Integra® (Two stage dermal regeneration)

7.1 Study objectives

The aim of this study was to investigate whether cultured autologous keratinocytes and fibroblasts on microcarrier beads reduce wound contraction in combination with Integra® (dermal regeneration template). Their effect on wound contraction was compared with the combination of autologous keratinocytes on microcarriers and sprayed keratinocytes and Integra®. Wound contraction was assessed using serial measurements of the wound size using Visitrak™ at set time points. Epithelial regeneration and wound closure were assessed macroscopically using clinical observation and photography. Also microscopic assessment using Haematoxylin and Eosin staining, and immunohistochemical staining for K14, collagen VII, laminin, and α-SM actin was undertaken to assess the rate of epithelial formation and myofibroblast expression.

7.2 Study design

Three pigs were used in this study and prior to the beginning of the study; the animals as described in 2.3.1 were admitted to NPIMR according to 2.3.2.

In the first stage of the study, the animals were anaesthetised as described in 2.3.3. Three square-shaped wounds were created on the flank of each animal as described in 2.3.6. A piece of Integra® measuring 4 x 4 cm was inset in each wound using skin staples. One sheet of split skin graft measuring about 8-10 cm was harvested from each animal from the posterior part of the para-spinal area as described in 2.3.4.

The wounds were dressed and wrapped in foam jackets as described before, the skin graft was wrapped in saline soaked gauze and transported back to the lab the same day.

For two weeks following the creation of the wounds and harvesting of the skin grafts, one dressing change at day 7 was performed under general anaesthesia. The wounds were dressed as described before and wrapped in foam jackets.

Porcine keratinocytes were isolated as described in 2.2.9, and cultured as described in 2.2.10. Porcine fibroblasts were isolated as described in 2.2.11, and cultured as described in 2.2.12. The flasks from each animal were clearly labelled and kept in separate shelves in an incubator at 37°C. After keratinocyte and fibroblast expansion for one week, the flasks from each animal were divided and keratinocytes were seeded with fibroblasts (6:1) on microcarriers as described in 2.2.16.

Keratinocytes alone were seeded on microcarriers as described in 2.2.16 in a separate stirrer flask. The remaining tissue culture flasks were maintained as described in 2.2.10 until cell harvest for wound application.

The keratinocytes and fibroblasts, and keratinocytes alone on microcarriers remained in stirred culture for one week until 24 hours prior to wound application. The magnetic stirrer was stopped, the flasks transferred to a tissue culture hood and the culture medium aspirated. A cell count was undertaken after dissolving the beads using trypsin; keratinocytes were harvested from the tissue culture flasks using trypsin, and counted. The cells were transferred to small Falcon® tubes, 1 x 10^7 in each tube ready for cell spray application. The microcarriers seeded with keratinocytes and fibroblasts, and keratinocytes alone were transferred to universal tubes, each containing 1 x 10^7 cells in total. The count of each cell type in the keratinocyte fibroblast group was not undertaken. The cells from both groups were stored in a cool bag overnight prior to wound application the next morning.

Two weeks after harvesting the skin grafts (Day 14), the animals were anaesthetised as described in 2.3.3. The silicone layer was removed from the surface of the Integra® to reveal a vascularised dermal layer and the skin staples were removed. The surface area of each wound was traced using Visitrak™ tracing sheet, and the surface area measured

as described in 2.3.7. Treatments were applied to the wounds accordingly (figure 61). There were 18 wounds in total; divided into 3 groups (6 wounds each) as shown in (figure 61).

Group 1	Microcarriers and autologous keratinocytes-fibroblasts + Integra® ***[MCAK-FB]***
Group 2	Microcarriers and autologous keratinocytes + Integra® ***[MCAK]***
Group 3	Sprayed autologous keratinocytes + Integra® ***[SAK]***

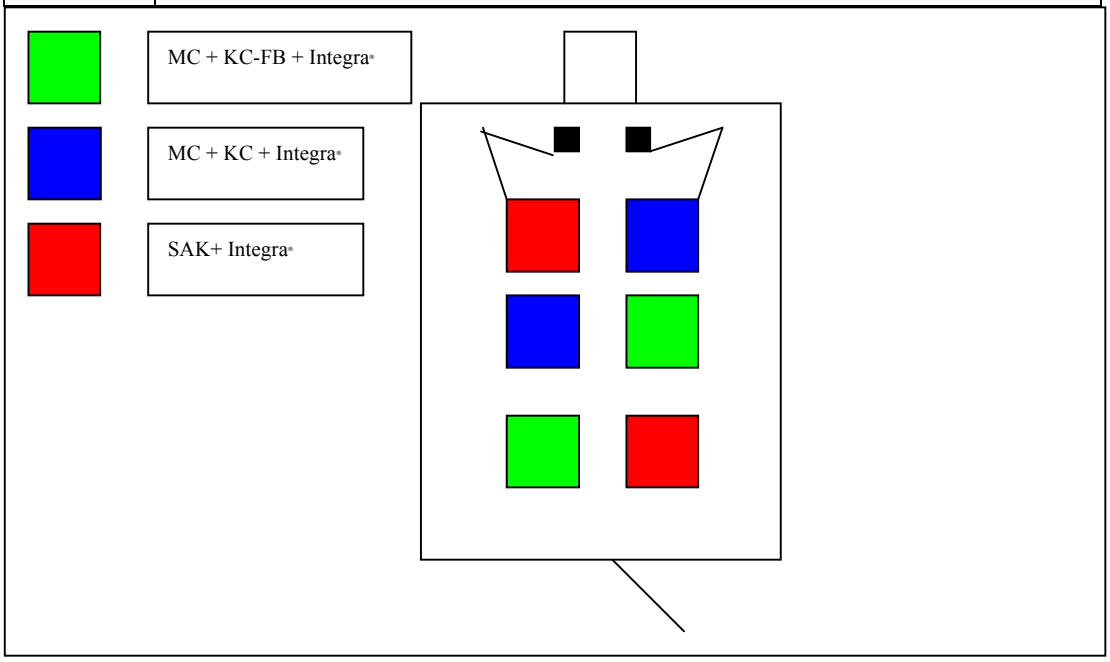

Figure 59: Wound allocation in one animal (Exp 4.10)
The wounds were randomly allocated and wound sites were different in the other 2 animals

Microcarriers and keratinocytes plus fibroblasts and keratinocytes alone were applied using sterile pipettes. The sprayed keratinocytes were applied evenly using a sterile 5 ml syringe and a disposable sterile nozzle from a distance of about 10 cm. Wounds were dressed using Telfa clear®, secured using skin staples, and dressed with Betadine soaked gauze as described before.

Dressing changes were performed under anaesthesia 7 and 14 days post-operatively. The animals were terminated three weeks (Day 21) following treatment as described in 2.3.3. The wound surface area was measured using Visitrak™ system and photographs

were taken prior to wound excision. The wounds were excised and the tissue specimens were processed as described in 2.3.6.

Histological examination of the specimens using Haematoxylin and Eosin was done as described in 2.4.1, and Immunohistochemistry for K14, collagen VII, laminin, and α-SM actin was undertaken as described in 2.4.2. Qualitative and quantitative assessment of wound contraction was undertaken using the serial photographs and the data from wound surface area measurement. The measurements were statistically analysed to compare wound contraction in the three treatment groups.

7.3 Results

7.3.1 Macroscopic qualitative assessment

During the course of the study, there was no wound infection in any of the three treatment groups. Following the harvesting of the STSG from the flank of each animal for keratinocyte and fibroblast isolation, the donor site healed in two weeks. The dressing changes for Integra® on day 7 showed no wound infection or tissue rejection.

By day 14, the dermal template (Integra®) was vascularised, well adhered to the wound and ready for the application of the treatment groups.

Figure 62 demonstrates the change in the appearance of the wounds from day 7, dressing change post application of Integra®, and day 14 pre and post treatment application. On day 7 (figure 62a), there was no evidence of infection or collection beneath the silicone layer of Integra®. On day 14 (figure 62b), Integra® was seen vascularised and well adhered with the silicone layer intact, (figure 62c) shows wounds post treatment applications with Telfa clear® applied.

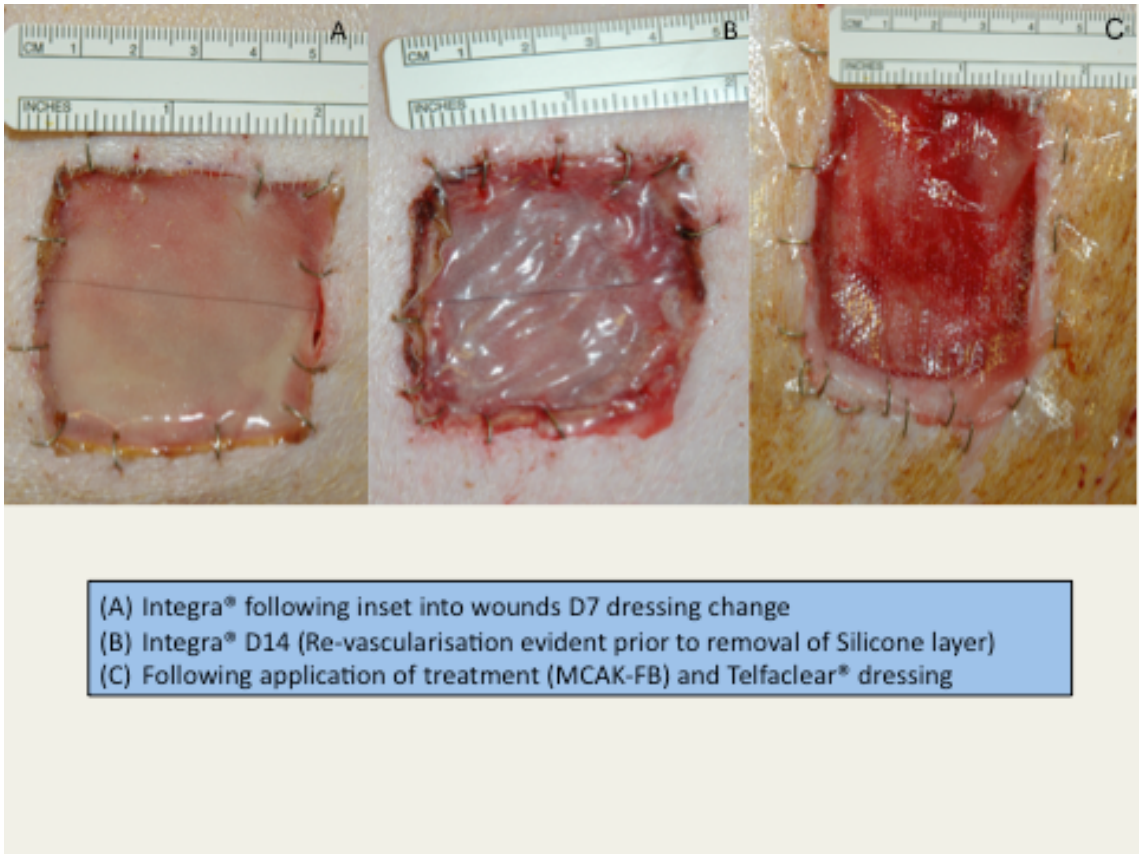

Figure 60: Wounds following Integra® inset D7 and D14 (Pre and Post-treatment)
(A) Day 7 following application of Integra®, the silicone layer started changing colour and was seen lifting off the wound by day 14 (B). (C) Wound following application of treatment (MCAK-FB)

The vascularisation of Integra® was complete two weeks post application with no reported complications. At the two dressing changes post treatment day 7 & 14 (figure 63), there was no sign of wound infection and granulation tissue was seen covering the wound surface.

On day 35 (experiment termination), all wounds in the three groups showed near to complete epithelial closure (figure 63-day 21). MCAK-FB and MCAK group wounds had small areas of residual granulation tissue (figure 63-day 21). The SAK group showed scabbing adherent to the granulation tissue compared to the other two groups (figure 63-day 21, bottom right).

On day 7, the mean wound surface area in the three groups was similar with less than 1 cm^2 difference. On day 21, three weeks following treatment, a difference of around 2 cm^2 in the mean wound surface area was noted between the MCAK-FB group and the MCAK and SAK groups.

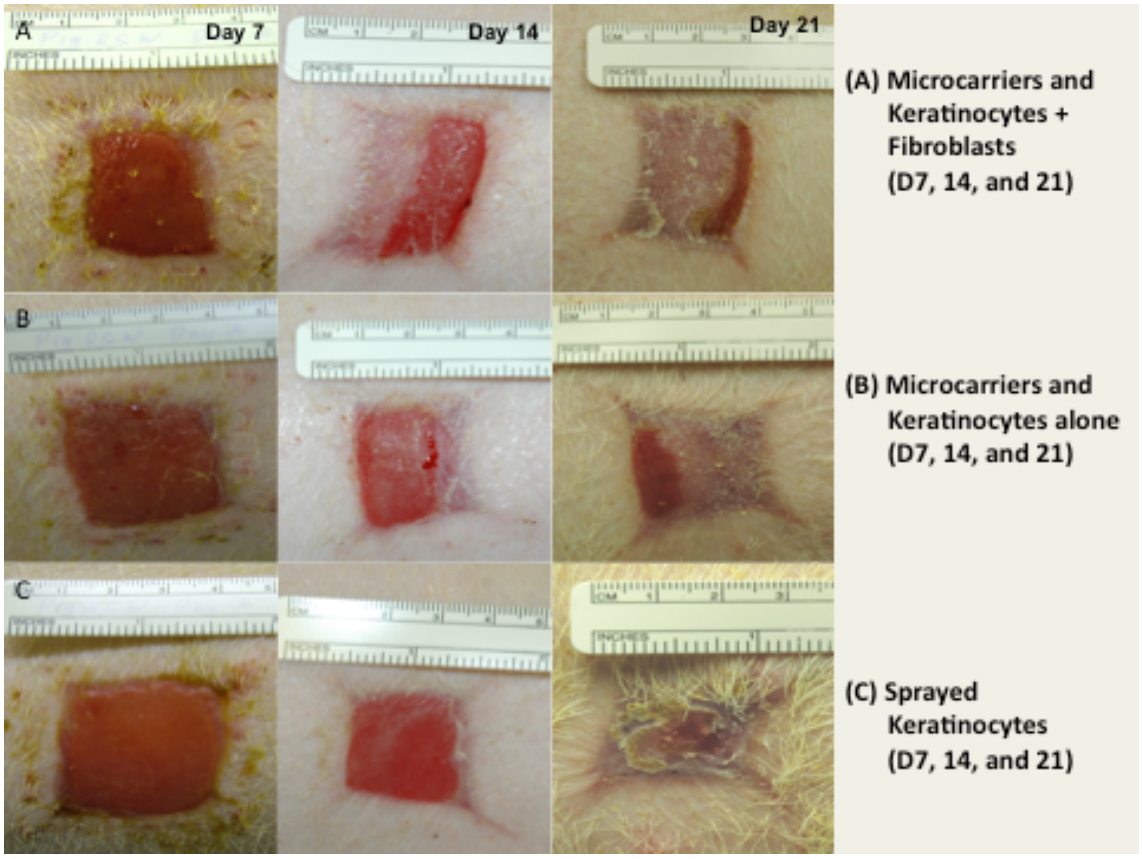

Figure 61: Wounds in the 3 treatment groups Days 7, 14, and 21 (Exp 4.10)
MCAK-FB (top), MCAK (middle), and SAK (lower) [left to right days 7, 14, and 21]
The area of the wound at day 21 was different comparing the 3 groups, where MCAK-FB group showed reduced wound contraction compared to MCAK and SAK

The SAK group showed the greatest wound contraction with a reduction in wound surface area from 19.5 (+/- 0.23) cm^2 to healed area measuring 9.1 (+/- 0.39) cm^2. The MCAK-FB group showed the lowest contraction in wound area; maintaining 56.8% compared to 47.6% in the MCAK group and 46.6% in the SAK group of the wound surface area.

A difference of 9.2% in wound area was noted between the MCAK-FB group and the MCAK group by day 21. The MCAK-FB group wounds contracted less than the MCAK group, which contracted less than the SAK group (figure 64).

The wounds in the MCAK-FB group contracted less than the MCAK and SAK groups, and the MCAK group contracted less than the SAK group. Significantly less wound contraction was found in wounds treated with MCAK-FB (n = 6) than with MCAK alone (n = 6) or SAK (n = 6) (adjusted $p < 0.05$; Holm-Sidak post hoc test). The wounds

from the 3 treatment groups were 90% healed by day 21-post treatment. Some wounds showed small areas of residual granulation tissue (< 10 % of wound surface area).

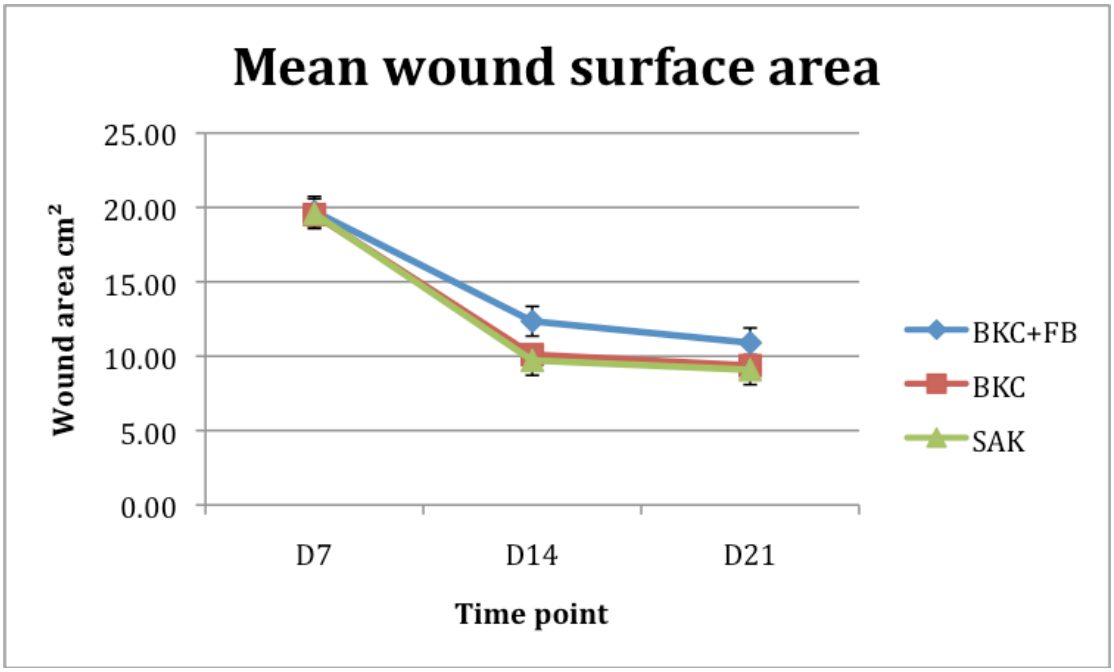

Figure 62: Graph representation of wound contraction in the 3 groups over 21 days (Error bars refer to standard deviation)

7.3.2 Histological and immunohistochemical analysis

The whole wounds were excised on day 21, following the termination of the animals.

At day 21 (3 weeks post-treatment), the wounds from the 3 groups displayed an intact epithelium. The wounds of the MCAK-FB and MCAK groups showed granulation tissue less than 10% of wound surface area, but were 90% healed.

Haematoxylin and Eosin staining of the three groups showed newly formed epithelium comparable in quality (figure 65). Both the MCAK-FB and SAK groups showed a well-stratified epithelium comparable to the MCAK group (figure 65b). The thickness of the epidermis in the MCAK was thinner compared to the thickness of the epidermis in the other 2 groups. This difference was observed in about 80-90% of the sections examined from all the wounds in the 3 groups. No clear explanation was found for that finding

despite previous studies demonstrating similar epidermis thickness between MCAK and SAK groups.

Immunohistochemical staining for collagen VII was positive in the three groups. The three groups demonstrated a well-developed basement membrane. The formation of the basement membrane confirmed the regeneration of an intact epidermis.

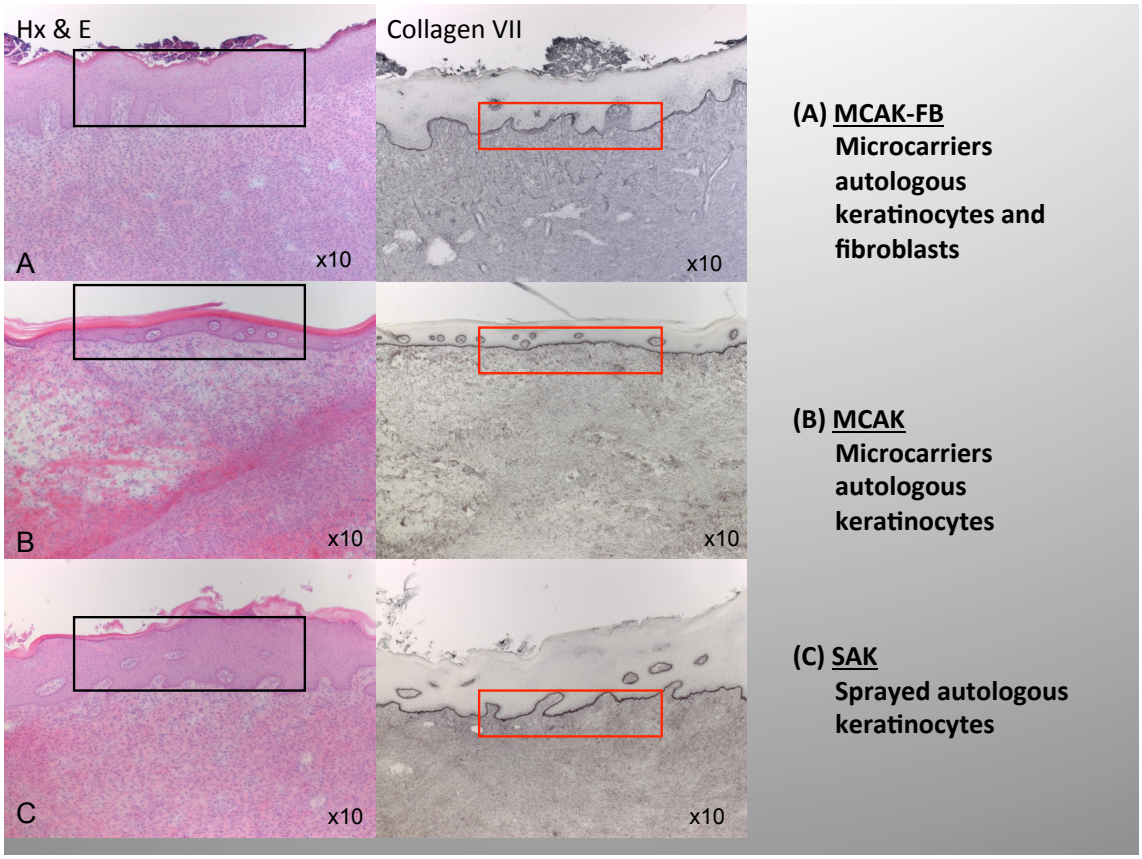

Figure 63: Hx & E and Collagen VII immuno-labelling of the 3 groups
(A) MCAK-FB, (B) MCAK, and (C) SAK. Left column: Hx & E staining with variable thickness of epidermis (black rectangle). Right column: Collagen VII staining for basement membrane (positive within red rectangle) (x10 magnification, field width 3.6 mm)

All wounds from the three groups showed comparable distribution of K14, a marker of basal keratinocytes (figure 66). The presence of K14 confirmed the regeneration of newly formed epithelium in the three treatment groups. The distribution of K14 in the MCAK-FB and SAK groups showed more intense staining possibly a thicker epithelium compared with the MCAK group, but similar to SAK. K14 staining findings regarding the thickness of epidermis were similar to findings from Haematoxylin and Eosin

staining previously. Both FITC and DAPI were undertaken to combine cellular staining (FITC) and nuclear staining (DAPI) together to illustrate clearly any variations between the 3 groups.

The three groups showed positive staining for laminin with a variation in the laminin distribution (figure 67). Immunohistochemical staining for laminin showed a more distinctive pattern in the MCAK-FB group compared with the MCAK and SAK groups (figure 67-bottom row).

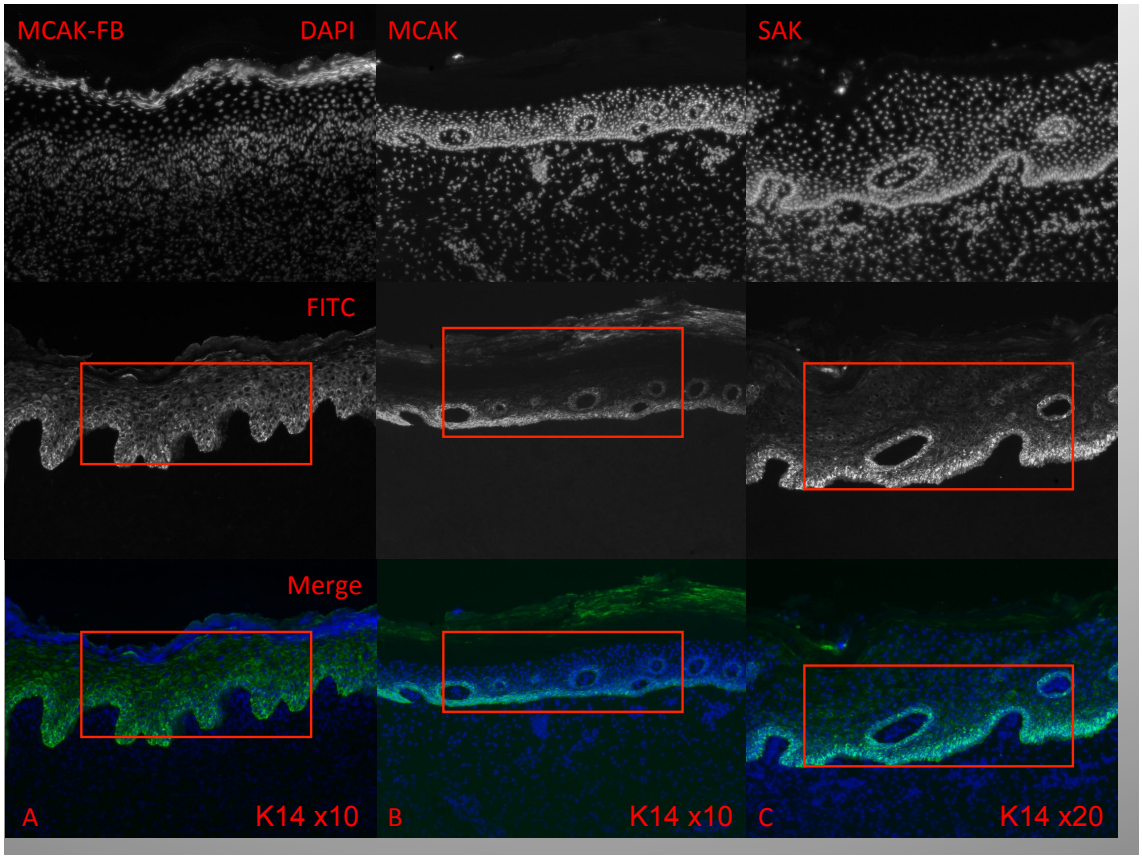

Figure 64: K14 immuno-labelling of the 3 groups
From left to right: (A) MCAK-FB, (B) MCAK, and (C) SAK. DAPI (nucleus staining-top), FITC (positive staining for epidermis shown in red rectangle) and below merge of both stains (x10 magnification-field width 3.6 mm, x20 magnification-field width 1.8 mm)

Laminin showed a more dense distribution in the basement membrane region in the MCAK-FB group compared with a generalised distribution across the sections in the MCAK and SAK groups (figure 67-bottom row). The laminin distribution in the MCAK-FB group was more uniform across the sections and condensed in the basement

membrane region. The dense laminin staining in the basement membrane region could possibly signal a mature basement membrane in the MCAK-FB group compared with the MCAK and SAK groups.

Immunohistochemical staining for α-SMA was positive in the three groups demonstrating myofibroblasts activity (figure 68). A clear distribution pattern was seen in the control group (uSTSG-chapter 6) where α-SMA is distributed in distinct areas deep within the dermo-epidermal junction and the papillary dermis (figure 68, left).

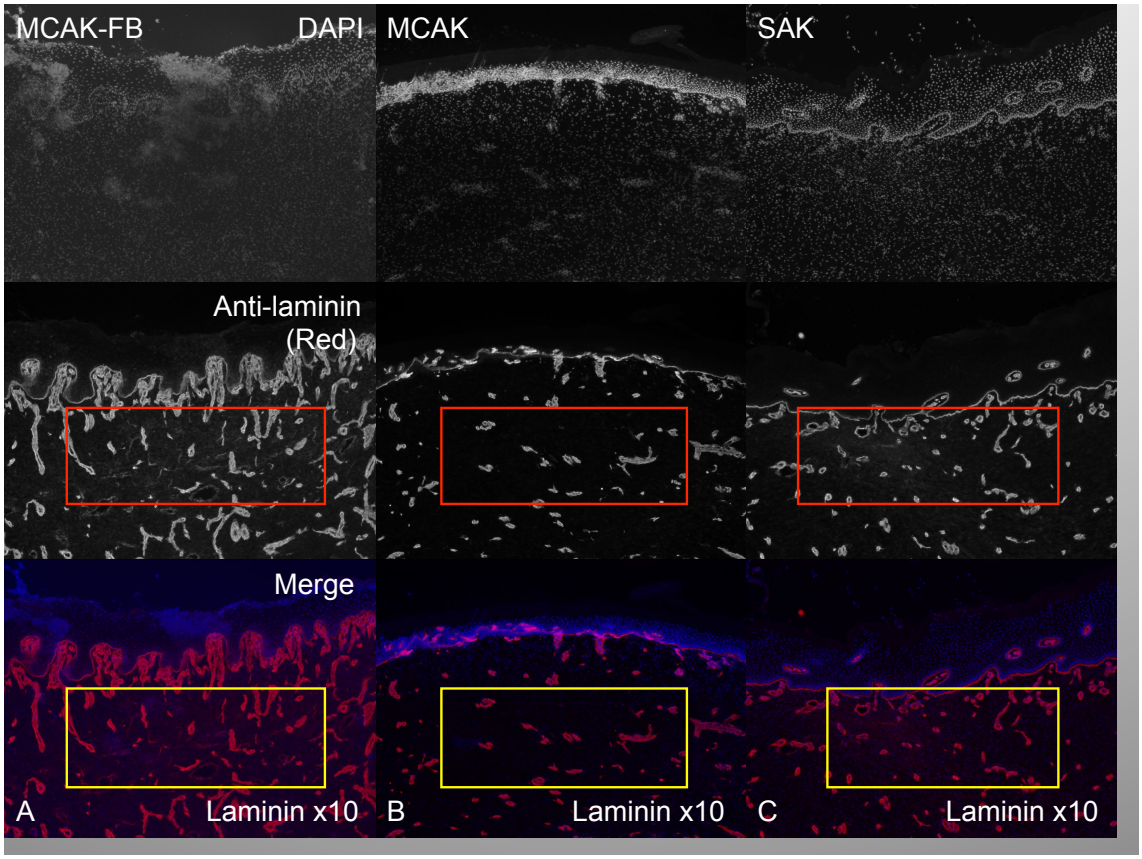

Figure 65: Laminin immuno-labelling of the 3 groups
From left to right: (A) MCAK-FB, (B) MCAK, and (C) SAK. DAPI (nucleus staining-top), Anti-laminin (dense distribution of laminin shown in red rectangle) and below merge of both stains (similar pattern within yellow rectangle) (x10 magnification, field width 3.6 mm)

Myofibroblasts were arranged in flat arrays parallel to the dermal–epidermal junction denoting higher activity compared with the three groups included in this study (figure 65-bottom row). The myofibroblast activity expressed in the control group (uSTSG) was a marker of increased wound contraction. This was reflected in the difference in wound surface area measurements after 21 days in the uSTSG group compared with the MCAK-FB, MCAK, and SAK groups included in this study.

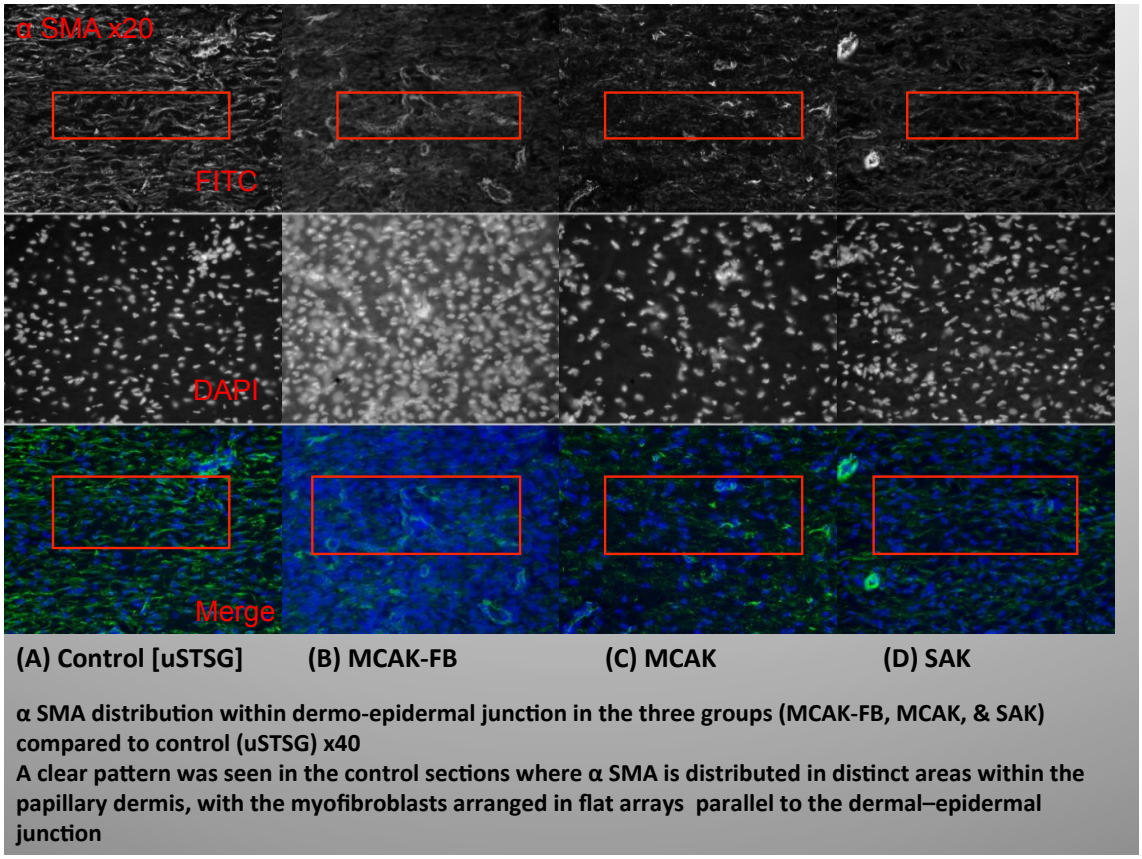

Figure 66: α-SMA immuno-labelling of the 3 groups
From left to right: (A) Control (uSTSG), (B) MCAK-FB, (C) MCAK, and (D) SAK (dermis shown) FITC staining (top), DAPI (nucleus staining-middle), and merge of both (below). Myofibroblasts distribution pattern in the 4 groups (within red rectangle) (x40 magnification, field width 0.9 mm)

In conclusion, histological analysis of sections from the three groups demonstrated epithelial regeneration in all the wounds examined. The quality of epithelium was comparable between the three groups with a variation in thickness only. Wound contraction in the MCAK-FB group was significantly less than the MCAK and SAK groups.

Chapter 8: Discussion

8.1 Discussion of *in vitro* studies

Microcarrier beads have been used to support cell culture for almost four decades and their use to support keratinocyte cell culture provides a novel tissue engineered approach to cutaneous wound repair. Viable cultured keratinocytes transferred on microcarriers to the wound bed can be used for skin replacement therapy in various conditions of skin loss or breakdown (Kim *et al.* 2005)

The availability of microcarriers from biodegradable materials, such as gelatin, paved the way for utilizing microcarriers in keratinocyte culture for skin replacement therapy. Recently, gelatin based microcarrier beads were used to support the growth of human keratinocytes *in vitro* without the need for 3T3 feeder cells (Borg *et al.* 2009). Also, gelatin beads were found to be degradable in 2-3 weeks when applied to chronic leg ulcers (Liu *et al.* 2004). Therefore, there are advantages for the use of gelatin microcarriers in keratinocyte cell culture.

Currently, there are two types of gelatin microcarrier beads commercially available for cell culture Cultispher G® and Cultispher S®. Cultispher S® has different size pores and due to the strength of the gelatin cross-linking is more resistant to mechanical stress in culture conditions. Cultispher G® in comparison has more uniform sized pores and is more suitable for culture of anchorage dependent cells. In the first *in vitro* study 3.1, two types of gelatin-based microcarrier beads were compared for maintaining keratinocyte cell culture and proliferation *in vitro*. Two types of cultures were used, static and stirred cultures, with quantitative and qualitative measurement of keratinocyte attachment and growth. Trypan blue was used to count keratinocytes on microcarrier beads stirred culture at set time points. The cell count was compared with keratinocytes count from standard culture flasks at identical time points.

Trypan blue is a widely used standard dye to assess cellular viability (Du Toit and Page 2009). The reactivity of Trypan blue is based on the fact that the chromophore is negatively charged and does not interact with the cell unless the cellular membrane is damaged. Therefore, all cells which exclude the dye are viable while cells which are blue in colour are non viable.

The choice of either Cultispher G® or Cultispher S® relied on a number of important factors. These factors included; keratinocytes attachment to the surface, supporting cell expansion in culture, biodegradability of the beads, their microstructure, and keratinocytes proliferation. Also microcarriers need to maintain keratinocyte proliferation *in vitro* to allow for the delivery of keratinocytes for *in vivo* applications.

Qualitative and quantitative assessments using MTT staining, acridine orange staining, Alamar Blue® assay, and Trypan blue cell count demonstrated that both Cultispher G® and S® microcarriers supported keratinocyte growth and expansion in rotator culture. Using Alamar Blue® reduction assay to assess keratinocytes proliferation, Cultispher G® produced marginally higher results. Results from both Cultispher S® and G® were compared using t-test, the results demonstrated 94% confidence interval, and the power was 0.04 (below the desired power of 0.8). The difference in the mean values of the two groups was not great enough to reject the possibility that the difference was due to random sampling variability. The difference was not statistically significant with a p value of 0.483. Therefore, the comparison of Cultispher S® and Cultispher G® found no significant differences, although Cultispher G® showed marginally higher rates of keratinocytes' expansion seen with Alamar Blue® assay.

In the assessment of keratinocyte cell count in microcarrier culture using Trypan blue, keratinocyte expansion on microcarriers was similar to conventional culture. Analysis of keratinocyte cell count using Trypan blue showed similar cell counts in traditional culture flasks and stirred microcarrier culture. The use of microcarriers did not have a

negative effect on keratinocyte expansion, and further studies were undertaken to explore potential advantages over traditional culture.

Therefore, in the second phase of the study, the decision to use Cultispher G® was based on the manufacturer's information sheet;

http://www.sigmaaldrich.com/catalog/DataSheetPage.do?brandKey=SIGMA&symbol=M9043 which states that the pores within the Cultispher G® microcarriers and their size are more uniform compared to Cultispher S®, despite Cultispher S® being more resistant to mechanical and thermal stress. Theoretically, the uniformity of Cultispher G® would be more suitable for stirred keratinocyte culture, and Cultispher G® was used in stirred culture. Keratinocytes cultured on microcarrier beads in agitated and stirred cultures produced similar results to previous *in vitro* studies reported in the literature (Bardouille *et al.* 2001, Abranches *et al.* 2007). The results from this study were similar to other reported studies highlighting the need for culture stirring when using microcarriers to maintain attachment of keratinocytes in culture. Culture stirring avoids microcarrier precipitation, the reduction of the surface area available for cellular attachment, and possibly degradation.

Trypan blue cell count results showed keratinocytes expansion on microcarriers was similar to conventional culture using culture flasks. Analysis of keratinocyte cell on days 6, 10, and 14, produced similar expansion rates comparing the two culture methods. The difference in cell count across the different time points was $< 0.5 \times 10^6$, with slightly higher count in traditional culture flasks. The results raised the question whether there was an advantage in using microcarriers for keratinocyte culture with no evidence of keratinocyte proliferation data available.

Despite the lack of supporting evidence for keratinocyte proliferation, keratinocyte attachment and expansion were demonstrated. The initial findings from the qualitative and quantitative assessments provided a platform for further investigations.

Human keratinocytes were used in this initial study to set a benchmark for further *in vitro* studies where porcine keratinocytes were used. The use of porcine keratinocytes in further *in vitro* studies aimed at investigating cell behaviour on microcarriers, prior to establishing whether further investigation in an *in vivo* animal model would be warranted. Keratinocyte expansion in culture supported further investigations into the biological fate of the microcarriers following wound application.

Since there was no sufficient data at that stage to proceed to an *in vivo* animal wound model, biodegradation of the microcarriers was investigated in a simulated environment. The transferral of keratinocytes and microcarriers from stirred culture to static culture flasks would provide an environment possibly resembling wound application. Porcine keratinocytes were used to assess the biodegradability of the microcarrier beads and keratinocytes attachment to the culture flask surface *in vitro*. Theoretically, Cultispher G® microcarriers are gelatin based and hence biodegradable when applied to *in vivo* wounds. The gelatin beads would degrade as a result of cellular interactions and tissue matrix remodelling during wound healing.

With future clinical applications in mind, the gelatin microcarriers would potentially biodegrade in the wound environment allowing keratinocyte migration. Ideally, the degradation would not produce infection or inflammatory reactions *in vivo.* Also keratinocytes would remain viable to differentiate and regenerate epithelial cover.

The use of static culture is unlikely to achieve successful outcomes using microcarriers, since the lack of culture agitation would not allow keratinocyte attachment to microcarriers. In addition, the possibility of microcarrier degradation in the static culture could not be excluded.

The results from the study 3.2, demonstrated that porcine keratinocytes migrated from microcarriers in culture flasks following degradation of the microcarriers. Porcine keratinocytes on Cultispher G® when seeded in tissue culture flasks, expanded to form colonies and the beads biodegraded without any adverse reactions. Porcine keratinocyte

expansion was maintained in the absence of culture infection or complications during the process of the degradation of the microcarriers *in vitro*. Keratinocyte cell attachment to the porous microcarrier surface was a reversible phenomenon allowing cellular migration when re-seeded into culture flasks. The lack of stirring within the culture allowed the microcarriers to precipitate and disintegrate within the culture medium. Hecht *et al*. (1997) used collagen-coated dextran microcarriers colonized with keratinocytes from human foreskin using a similar spinner flask culture technique. The colonized microcarriers were seeded into culture flasks and keratinocyte migration and proliferation were assessed. Immunohistological staining showed that keratinocytes migrated from microcarriers onto the surface of the flasks and proliferated to form a layer of epithelial cells. The results from section 3.2 were similar despite the lack of quantitative assessment of the proliferation of porcine keratinocytes following their attachment to the surface of the culture flask. No further qualitative assessment of proliferation was attempted as this would be investigated in the next studies primarily in spinner culture.

The process of microcarrier degradation in static culture in the presence of cultured keratinocytes could be due to either due to cellular enzymatic activity or other factors within the culture medium. The degradation process is difficult to fully assess and specify the role of different factors and cellular interactions contributing to its fulfilment.

Further assessment of keratinocyte cell attachment to the surface of the microcarriers was undertaken. The adhesion of cells to culture surfaces is fundamental to both traditional culture and to microcarriers culture. Freshly isolated animal cells of many types, and a few stable cell lines, fail to grow when they are suspended in fluid or in an agar gel (Stoker *et al.* 1968). If such cells make contact with a solid surface such as suitably treated plastic, however, they attach, spread and multiply. Their growth may be termed anchorage dependent (Stoker *et al.* 1968).

Keratinocyte proliferation is dependant among other factors, on adhesion to a suitable culture surface (Grinnell 1978) and microcarriers provide a suitable surface that enhances keratinocyte attachment (Grinnell and Minter 1978). Culture procedures affect the rate at which keratinocytes attach to culture surfaces. In microcarriers culture, the keratinocytes and the microcarrier beads are in a stirred suspension. An initial static period is required to allow for keratinocyte attachment prior to initiation of stirring.

Previous studies showed that keratinocytes attach to the surface of microcarriers when visualised using SEM and laser confocal microscopy (Bancel and Hu 1996, Borg *et al.* 2009). In these studies, the attachment of the keratinocytes to the microcarriers' surface was not complete as some pores were left empty. These studies highlighted a possible limitation of using Cultispher G® microcarriers for keratinocyte cell culture. The inability of keratinocytes to attach to all pores of the microcarriers could reduce the total surface area available for cell expansion within the culture.

In the study 3.3, the aim was to assess how porcine keratinocytes attach to the surface of gelatin microcarrier Cultispher G® using scanning electron microscopy (SEM). This would allow qualitative assessment of cellular attachment and the relation between keratinocytes and the porous surface of the gelatin microcarriers. SEM produces a rapid, direct, three-dimensional view of detailed surface structure over a distance of several centimetres with minimal preparation of tissue sample required (Salsbury and Clarke 1967).

The results demonstrated keratinocyte attachment to the entire surface of the microcarriers and cellular population of the pores. Keratinocyte attachment utilised all the available surface area on the microcarriers, with some overlap of the cell layers being observed. Keratinocytes attached to the microcarriers' surface and utilised the culture surface provided by the porous surface and total beads surface area within limited volume. Again, the advantage of utilising the limited space was clear when comparing with traditional flask cell culture.

The findings from this study were different from the findings of Bancel and Hu (1996) and Borg *et al.* (2009). Keratinocytes attached to the entire surface of the microcarriers as seen using SEM in our findings. This was difficult to explain as the seeding and culture protocol used in the study were according to the manufacturer's protocol and as described in Borg *et al.* (2009). The only modification was that the culture was left static for 48 hours rather than just 24 hours as described by Borg *et al.* (2009). The 48 hours period was chosen to allow an initial longer period for attachment of the keratinocytes to the microcarriers. In the early steps of keratinocytes culture on microcarriers, minimal attachment to the microcarriers was observed after 24 hours; hence the static period was changed successfully to 48 hours. This may help explain the difference between the findings reported here and those of Bancel and Hu (1996) and Borg et al. (2009).

The suitability of Cultispher G® gelatin microcarriers to support human and porcine keratinocyte cell culture was established from the previous studies. The next investigation looked into the use of 3T3 cells within porcine keratinocyte cell culture on microcarriers. The use of 3T3 mouse fibroblasts in keratinocyte cell culture is critical to support keratinocyte proliferation *in vitro*. The same is not necessarily applicable to keratinocyte cell culture on microcarriers.

The use of 3T3 feeder cells in keratinocyte cell culture is well established with the presence of murine fibroblasts within the culture supporting keratinocyte proliferation and colony formation (Navsaria *et al.* 1995). The use of microcarriers in human keratinocyte cell culture negates the use of 3T3 cells for keratinocyte cell culture (Borg *et al.* 2009, Bayram *et al.* 2005).

Several studies demonstrated human keratinocyte cell culture without 3T3 feeder cells on microcarrier beads following initial expansion (Katayama *et al.* 1987, Gorodetsky *et al.* 2004). Porcine keratinocytes and their cell culture and attachment to microcarriers without 3T3 cells could be possible as demonstrated with human keratinocytes and their

cell culture on microcarrier beads. The absence of 3T3 cells from the porcine keratinocyte microcarriers' culture has the potential to reduce infection, cost, culture maintenance, and produce a defined culture. However in this study, the initial expansion of keratinocytes included the addition of 3T3 cells to the culture, further keratinocyte expansion was assessed in the absence of 3T3 cells.

In the study 3.4, porcine keratinocytes were cultured in the absence and presence of 3T3 cells and the results compared. The results showed that microcarriers supported the proliferation of porcine keratinocytes in the presence or absence of 3T3 feeder cells in stirred culture. The primary expansion of keratinocytes was in culture flasks in the presence of 3T3 cells since the removal of 3T3 cells could not be negated despite several attempts to do so. Later, keratinocyte culture on microcarriers in stirred culture was achieved in the absence of 3T3 cells. Qualitative assessment using Acridine orange and MTT staining at various time points demonstrated porcine keratinocytes attachment and expansion. These findings were again similar to results reported by Borg *et al.* (2009), where initial expansion of keratinocytes was undertaken in the presence of murine 3T3 feeder cells. The possibility of keratinocyte expansion in defined media or without 3T3 cells prior to seeding on microcarriers requires further investigation, and was not undertaken. However, there are no reports up to date of porcine keratinocyte expansion on gelatin microcarriers in stirred culture in the absence of 3T3 cells.

The failure in the primary expansion of porcine keratinocytes in culture flasks without 3T3 cells emphasised the important role of 3T3 fibroblasts in the attachment of keratinocytes and initial expansion *in vitro*. Quantitative assessment using Trypan blue for cell counts at the same time points demonstrated comparable cell counts in culture with or without 3T3 cells. Keratinocyte cell count was slightly higher in the absence of 3T3 cells, averaging 1 to 3 x 10^6 higher than cell counts in the presence of 3T3 cells across 12 days. As cell count using Trypan blue included viable cells only, it was assumed that in culture flasks including keratinocytes and 3T3 cells, the count did not

include 3T3 cells. No significant differences in cell counts without 3T3 cells were noted from this study. Interpretation of these results needed to take into consideration the potential advantages of keratinocyte cell culture without 3T3 cells, even if cell counts were only comparable to traditional culture. Dispensing with the use of 3T3 cells in keratinocytes cell culture for clinical use remains a major advantage not only avoiding xenogenic cells presence within the culture, but also reducing infection, culture contamination, and maintenance requirements. The optimisation of stirred microcarrier culture is likely to improve keratinocyte expansion and cell population doubling in the future leading to culture up-scaling in a larger bio-reactor model.

Since, porcine keratinocyte expansion was achievable in stirred culture in the absence of 3T3 cells, subsequently porcine keratinocytes were cultured in the absence of 3T3 for further *in vivo* animal wound model studies.

Analysis of keratin expression supports the understanding of keratinocyte proliferation in mono-layered culture. In human and porcine epidermis, all basal keratinocytes synthesize Cytokeratins K5 and K14, and sometimes K15 and K17 (Sun *et al.* 1983). K14 is an epidermal keratin, which is paired with K5 and located in the proliferating basal cell layer of stratified squamous epithelium (Chu and Weiss 2002, Alam *et al.* 2011). K14 is a prototypic marker of dividing basal keratinocytes and helps in the maintenance of epidermal cell shape; it also provides resistance to mechanical stress.

Keratins K14 and K5 are considered biochemical markers of the stratified squamous epithelia, including epidermis (Moll *et al.* 1982, Sun *et al.* 1983, Coulombe *et al.* 1989). K14 and K5 are transcribed at a high level in epidermal proliferation; hence K14 gene assay can be used for assessment of epidermis-specific transcription (Sinha *et al.* 2000, Alam *et al.* 2011).

Keratin synthesis and expression *in vitro* is similar to *in vivo* expression and can be used to assess keratinocyte proliferation.

The availability of K14 antibody suitable for detection of K14 in pigs, made K14 immunohistochemical staining achievable compared to K5 (in which a suitable antibody was not available) in the porcine wound model used in this study. The pairing of K14/K5 can be used as a proliferation marker for basal epithelium (Purkis *et al.* 1990). Hence measurement of K14 mRNA was used to assess keratinocyte proliferation *in vitro* in this study. Quantitative assessment of K14 expression by porcine keratinocytes *in vitro* was done using total RNA isolation followed by real-time qualitative PCR (qPCR) of K14 mRNA using GAPDH was used as housekeeping gene.

MTT assay is a standard colorimetric assay measuring the activity of enzymes reducing MTT to formazan. It can be used for the assessment of cellular proliferation, including keratinocytes (Vistejnova *et al.* 2009, Peura *et al.* 2010, Lu *et al.* 2012). MTT assay was used to quantify cellular proliferation in the culture plotted against a standard curve of serial porcine keratinocyte cell counts. The MTT assay results were compared to the results of RNA isolation and RT-qPCR; also the results were used to calculate cell counts at different time points. The MTT assay results and keratinocyte cell counts demonstrated progressive increases in numbers along the study period, which verified keratinocyte expansion on microcarriers. The findings were similar to the results from the previous *in vitro* studies, which demonstrated keratinocyte expansion without clear evidence of cellular proliferation on microcarriers in stirred culture.

K14 expression was positive and relative expression to GAPDH demonstrated an increase in K14 expression from day 14 to day 21. The expression of K14 demonstrated relative porcine keratinocytes proliferation with positive phenotyping of basal epithelium-like cells. Atiyeh and Costagliola (2007) demonstrated that cultured epithelial autografts suffered poor graft take i.e. adherence in clinical practice. This was attributed to the high proportion of differentiated cells within the cultured epithelial autografts. These cells are unable to further proliferate following application to wounds resulting in poor take.

Since basal keratinocytes are mainly non-differentiated keratinocytes, the findings from the study 3.5 provided support of the use of stirred microcarrier culture for keratinocyte expansion and culture. The use of microcarriers stirred in culture provides an alternative source of expanded, non-differentiated keratinocytes for wound application, compared with traditional culture techniques. This assumes that the microcarriers delivered this way would degrade within the wound environment and have no adverse effect on the subsequent keratinocyte migration and proliferation.

In comparing the MTT assay and K14 expression results carried out in study 3.5, the MTT assay demonstrated cell expansion without keratinocyte proliferation; K14 expression on the other hand demonstrated relative keratinocyte proliferation. As K14 expression is mainly seen in basal epithelium, the proliferation was of basal-like keratinocytes phenotype within the stirred culture. This phenotype specific proliferation was not translated as a general keratinocyte population proliferation as shown by the MTT assay.

Human keratinocytes have been cultured in co-culture with autologous fibroblasts replacing feeder 3T3 cells (Jubin *et al.* 2011). The authors demonstrated that autologous porcine keratinocytes formed colonies and proliferated in the presence of autologous fibroblasts in two types of media. The ratio of keratinocytes to fibroblasts was 6:1, and fibroblasts did not overgrow the cultures, compared to ratios less than 6:1. This was in a similar manner to culture in the presence of lethally irradiated 3T3 cells.

The presence of autologous fibroblasts in culture may have a role in epithelial regeneration *in vivo*. Assessment of porcine keratinocyte proliferation in co-culture with autologous fibroblasts was essential prior to use in an animal model. Green Fluorescent Protein (GFP) labelling of porcine keratinocytes prior to seeding on microcarriers enabled their detection later using fluorescent microscopy.

In the study 3.6, lethally irradiated murine 3T3 feeder cells were replaced with autologous non-irradiated fibroblasts. Based on the results of Jubin *et al.* (2011), the

same ratio of 6:1 keratinocytes to fibroblasts was used in the study. Porcine keratinocytes were GFP labelled to allow qualitative assessment of their expansion within the co-culture with fibroblasts. The MTT assay was used for quantitative assessment comparing porcine keratinocytes culture and porcine keratinocytes fibroblasts co-culture.

The results demonstrated porcine keratinocyte expansion and attachment to microcarriers in the presence of autologous fibroblasts in stirred culture. The MTT assay results were slightly increased in keratinocytes fibroblasts co-culture compared to keratinocytes culture alone. The difference was not statistically significant with p value 0.357. The variation in the MTT assay results could be attributed to the presence of autologous fibroblasts, which were not irradiated compared to 3T3 cells. The results did not provide evidence of keratinocyte proliferation.

The fact remains that the use of microcarriers to support keratinocytes culture is a developing culture technique, which would require further optimisation to ensure keratinocytes proliferation *in vitro*. The use of microcarriers could provide an improved handling and delivery method for keratinocytes culture in the future with optimisation.

With similar keratinocytes expansion rates, the advantages of microcarriers culture would favour its use over conventional culture flask culture. The advantages include the large surface area to volume ratio offered by microcarriers and improved control of culture parameters (van Hemert *et al.* 1969). Reduced requirements for culture medium, labour, and less risk of contamination (since less handling of the cells in culture is usually required) are among other potential advantages.

The application of proliferating keratinocytes within cultured autografts would provide cells that are able to re-epithelialise skin defects. Therefore, further assessment of proliferation of keratinocytes within stirred culture is required to evaluate the efficiency of the culture method. Since keratinocyte proliferation is an important parameter when comparing keratinocyte culture on microcarriers with traditional culture methods.

The results from the previous *in vitro* studies demonstrated successful expansion and attachment of human and porcine keratinocytes on gelatin microcarriers in stirred culture. Keratinocytes attached easily to the porous surface of the microcarriers and expanded in the absence of 3T3 feeder cells. The limitations of the outcomes were clear, as the results did not provide clear evidence of keratinocytes proliferation on microcarriers *in vitro*. The limited evidence of keratinocytes proliferation was provided by K14 expression in study 3.5 demonstrating proliferation of basal-epithelium of non-differentiated keratinocytes.

8.2 Discussion of *in vivo* studies

Using traditional keratinocyte culture in culture flasks, cultured epithelial autografts (CEA) are harvested using dispase from the flasks and applied on wounds. Proliferating keratinocytes within the CEA continue to proliferate in the wound environment and re-epithelialise the wound bed. Cultured keratinocytes could be applied to the wound in a pre-confluent state, which improves survival and re-epithelialisation rates (Harris *et al.* 1998). Several methods have been described for the delivery of cultured keratinocytes to the wound bed for clinical application. Keratinocytes can be applied on a delivery membrane or in the form of cell suspension. The delivery membrane can be made of either synthetic or biological material, and the cell suspension can be delivered as a spray or droplet (Andree *et al.* 2001).

Chester, Balderson and Papini (2004) reported that the delivery of cultured keratinocytes as cell spray was more efficient in epithelial regeneration when compared to membrane delivery. *In vitro* comparisons of keratinocyte delivery methods have shown cell spray as more efficient when compared with other methods (Fredriksson *et al.* 2008). Keratinocyte cell delivery as cell spray provides higher cellular viability, adherence, and proliferation (Fredriksson *et al.* 2008). Application of cultured keratinocytes in a cell suspension or spray can accelerate epithelial formation (Magnusson *et al.* 2007, Wood *et al.* 2006). Based on these studies, cultured keratinocyte cell delivery as cell spray was chosen as the standard delivery method to compare with microcarriers in the *in vivo* animal studies.

In order to assess the rate of survival of keratinocytes on microcarriers and their possible role in wound re-epithelialisation, an animal wound model is required. An animal model should provide a similar wound environment mimicking clinical application in patients.

Montagna and Yun (1964) analysed pig skin sections from multiple anatomical sites to find an animal model similar to human skin. Their findings showed that the anatomy of

porcine skin was the most similar to humans. The choice of the porcine wound model was based on previous studies, which reported using the same model (Bevan *et al.* 1997, Ng *et al.* 1997, Grant *et al.* 2001). These studies showed good correlation between the porcine wound model and human wound healing. The findings indicated the suitability of this animal model for pre-clinical investigations of treatments for full-thickness wounds in humans, hence the pig wound model was chosen as the *in vivo* model.

The early efforts for creating an isolated wound chamber *in vivo* within an animal model included the use of intra-peritoneal diffusion chambers (Algire 1957, Algire *et al.* 1958). Later efforts included granuloma air pouches to study the effect of steroids on local tissue (Selye 1953). Cutaneous silicone implants were used to study wound healing following application of cultured keratinocytes (Worst *et al.* 1974). Kangesu *et al.* (1993b) further developed the silicone implants to produce polytetrafluoroethylene (PTFE) wound chambers for use in a pig wound model. PTFE is a per-fluorocarbon polymer compound commonly used as an alloplastic implant material. It is inert and non-adhesive when interacting with various tissues and it has been shown to be non-toxic to keratinocytes *in vitro* (Kangesu *et al.* 1993b). Kangesu *et al.* (1993a) later reported using the PTFE wound chambers successfully to assess keratinocyte growth following application of cultured keratinocytes on dermal defects.

From the above evidence, the decision to use the PTFE wound chambers in the pig wound model for assessment of keratinocyte growth and migration was taken. Porcine keratinocyte grown on Cultispher G® gelatin microcarrier beads were applied to full thickness wounds with PTFE chambers. This was compared with application of sprayed cultured keratinocytes using a standard spray nozzle. The fate and survival rate of the cultured keratinocytes were assessed to understand whether the cells would continue proliferation in the wound environment or not.

As the cultured keratinocytes migrate and become part of the newly formed epithelium, a cellular marker is required to identify the cells post transplantation. Ideally, the marker

should be stable and remain unchanged during cellular proliferation, and also resistant to the histological preparation of tissue samples. Retroviral labelling has been previously used in a porcine wound model to identify cultured keratinocytes (Ng *et al.* 1997, Bevan *et al.* 1997, Grant *et al.* 2001). In these studies, the lac Z gene was used as a cell marker, the main disadvantage was the gene required tissue processing to identify and as a result further histological staining was compromised. Green fluorescent protein (GFP) does not require tissue processing prior to cell identification hence is ideal to use as an initial assessment tool. Further histological staining is not affected and allows tissue processing to assess epithelium regeneration and wound healing. GFP retroviral labelling of porcine keratinocytes was chosen in this experiment as a marker for keratinocytes post wound application.

In addition to GFP tracing in tissue sections to investigate the survival rate of cultured keratinocytes, immunohistochemical staining for K14, laminin and collagen VII were used. K14, laminin, and collagen VII were used to assess the rate of epithelial formation and quality of the newly formed epithelium following cultured keratinocyte application.

The results from this study demonstrated that the application of keratinocytes on gelatin microcarriers in full thickness wound chambers led to keratinocyte migration and survival in a wound environment.

The choice of Cultispher G® microcarriers aimed to avoid complications such as foreign body reaction or granuloma formation as the microcarriers were biodegradable in comparison with non-biodegradable microcarriers. Other types of microcarrier beads such as PLGA [polylactic-co-glycolic acid] have been shown to remain with the tissues and resist resorption (Kim *et al.* 2005).

In the study in section 4, 3 treatment groups with 12 wounds in total, no wound infections or adverse reactions from the microcarriers' application were noted. The termination of this study was chosen at day 15 to trace the GFP labelling of the keratinocytes post application. Ng *et al.* (1997) showed that in a porcine wound model

with de-epithelialised dermis, cultured keratinocytes labelled with Lac Z gene were identified 3 weeks post application. Grant *et al.* (2001) and Svensjo *et al.* (2001) reported similar transduction rates at 8 days with the transduced cells in the differentiated layers of the epithelium and not the basal layer. The loss of Lac Z gene expression was noted to increase after day 8 with no identification of transduced cells (Svensjo *et al.* 2001). Also expression of GFP has been shown in retro-virally labelled cultured keratinocytes in an immuno-compromised nude mouse model (Spandau *et al.* 2000, Del Rio *et al.* 2002).

The porcine wound model used in this study was immuno-competent, and in this porcine model a loss of GFP expression was noted by 4 weeks despite a high transduction rate (Pfutzner *et al.* 2006). The loss of GFP expression could be related to the host immune response against the transgene expression (Lu and Ghazizadeh 2007). Therefore, 2 weeks represented an appropriate time point to trace GFP labelled keratinocytes within the wounds before the decline in GFP expression in 3-4 weeks. GFP positive areas were found at the surface of wounds in the MCAK and SAK groups confirming the survival of keratinocytes in the 2 groups. Statistical analysis of the intensity of GFP expression within 3 random sections in 2 x 2 mm area within the epidermis using macro application on Axiovision® software showed no difference between the 2 groups. There was no advantage to microcarrier delivery of keratinocytes over cell spray in regards to GFP expression. Collectively, Keratinocytes' application using microcarriers as a delivery method provided similar results to application using cell spray.

At day 15 when the study was terminated, no full epithelial coverage was noted macroscopically in any of the 3 groups. This can be attributed to the short study period and possibly the lack of dermal support to the cultured keratinocytes in a full thickness wound model. In this study, the lack of dermal support within the wound represented a challenge to the survival of the keratinocytes post wound application. The end target of

full wound re-epithelialisation was not the aim of this study, and was assessed in further studies utilising the same wound model.

The two groups microcarriers autologous keratinocytes and sprayed autologous keratinocytes (MCAK & SAK) showed positive immuno-staining for K14 and laminin. Collagen VII immuno-staining was negative in the two groups, and all immuno-staining for K14, laminin, and collagen VII was negative in the control group. Interpreting these results, statistical analysis of K14 staining in the MCAK and SAK groups showed more K14 positive areas in the MCAK group. The number of cells applied to each wound chamber in the 2 groups was 1×10^7 as confirmed by cell count following harvesting from tissue culture flasks.

Therefore, the keratinocytes in the MCAK group expressed a higher number of basal-like phenotype keratinocytes in the wound post application compared to the SAK group. This assumption relied on the statistical difference in K14 staining when comparing the two groups; understandably, the reliability of this method is limited. If available, retro-viral labelling of keratinocytes using a traceable vector *in vivo* would provide a more reliable method. The different cell handling methods in the 2 groups prior to wound application could possibly explain this finding. In the MCAK group, microcarriers seeded with keratinocytes were simply pipetted from the stirred culture to universals prior to pipetting on to the wound. In the SAK group, trypsin was used to harvest the cells from the culture flasks into a cell suspension prior to spray on the wound. The effect of trypsin use on keratinocyte migration or proliferation *in vivo* is unclear, but it could have produced a negative effect.

The positive expression of laminin as an early marker of basement membrane in the MCAK and SAK groups was interesting. In both groups, laminin expression showed a different pattern to the overall distribution in granulation tissue in the control group. Laminin expression in the form of a dense pattern concentrated towards the wound surface in the MCAK and SAK groups, demonstrated the potential to regenerate mature

epithelium on full thickness wounds. Whether this could ultimately be achieved remained unclear due to the lack of dermal support and the termination of the study at 15 days. Regeneration of epithelium in combination with various types of dermal replacement therapies was investigated in further studies.

Currie *et al.* (2003) compared the application of SAK and AK in fibrin glue to full thickness wounds in a porcine wound chamber model. The authors reported only approximately 25% of the wounds showed epithelial cover after 3 weeks of treatment. The findings from the study described in chapter 4 were similar, as wound healing was not achieved in the 2 weeks period.

Immuno-staining for collagen VII was negative in the 3 treatment groups, indicating the lack of a fully formed basement membrane within a mature epithelium. The findings confirmed the need for dermal replacement therapies to achieve full epithelial closure.

This study provided a proof of concept that gelatin microcarriers could be used to transfer autologous cultured keratinocytes to full thickness wounds *in vivo*. Keratinocyte cell culture on microcarriers in stirred culture had no negative effects on cell survival or expansion *in vivo*. Further studies were required to assess whether full epithelial closure is achievable using microcarriers for autologous keratinocyte culture and delivery.

Generally, cutaneous wounds heal through a process that combines migration of keratinocytes from the wound edges and wound contraction. Wound contraction develops through the differentiation of dermal fibroblasts to myofibroblasts and their contractile action on the extracellular matrix through expression of α SMA (Wipff *et al.* 2007). The differentiation of fibroblasts toward a myofibroblast phenotype is dependent on; mechanical tension, adhesion to extracellular matrix via integrin receptors, and stimulation by transforming growth factor beta (TGF-β) (Sharpe and Martin 2013). Wound contraction is an integral part of the process of wound healing; contraction of the wound edges provides wound closure and assists re-epithelialisation of the wound surface. Wound contraction in anatomical areas such as skin overlying joints leads to

the formation of "contractures" resulting in limitation of range of movement (Billingham and Medawar 1955, Parry *et al.* 2010). Scars resulting in contractures represent a major problem following skin loss after burn injuries or trauma. Contractures produce a functional deficit affecting patients' rehabilitation and return to pre-morbid levels of activity. Contractures are usually associated with decreased physical function, physical role limitation, bodily pain, and decreased vitality (Schneider *et al.* 2006). Scar contracture by definition is an impairment caused by replacement of skin with scar tissue of insufficient extensibility and length (Boyce *et al.* 2006b, Richard *et al.* 2009). Subsequently, contractures result in a loss of motion or tissue alignment of an associated joint or anatomical structure (Richard *et al.* 2009).

Different studies investigated the use of nonsurgical methods to prevent the development of scar contractures. The use of various physiotherapy protocols (Okhovatian and Zoubine 2007) or splinting techniques (Wust 2006, Obaidullah *et al.* 2005) have been described. Surgical techniques have also been described for the release of contractures, including the use of various flaps (Xie *et al.* 2012, Kim *et al.* 2012, Feng *et al.* 2010). Other techniques have also been described such as scar release (Kung *et al.* 2012, Grishkevich 2012, Daya 2008).

In utilising various flaps whether fascio-cutaneous or musculo-cutaneous, the aim is to replace the scarred tissue with more pliable tissue offering less restriction of movement. In case of scar release, different techniques are used to either lengthen the scar or reduce the tightness, to provide more skin mobility over the affected anatomical site.

It is understood that a wound left open will contract in a faster rate compared to another wound treated with a skin graft (Bertolami and Donoff 1979). Application of meshed skin grafts leads to poor quality scarring and formation of contractures when compared to split or full thickness skin grafts. Secondary contraction of skin grafts is more pronounced in split skin grafts due to the lack of dermis when compared to full thickness grafts. Another alternative is the use of dermal replacement therapies in

addition to skin grafting to reduce the formation of scar contractures. Alloderm®, dermal replacement product, was found to reduce post burn contractures over joints in combination with split skin grafts (Yim *et al.* 2010).

The process of wound contraction is produced through the contractile forces exerted by myofibroblasts during the normal process of wound healing (Gabbiani 1996). Myofibroblasts are a phenotype of differentiated fibroblasts developing in the maturation phase of wound healing (Hinz *et al.* 2007). The differentiation of fibroblasts occurs in response to mechanical stimuli and the release of transforming growth factor beta 1 (TGF-β1) (Gabbiani 2003, Hinz 2007). During the process of granulation tissue evolution, fibroblasts acquire smooth muscle (SM) cell features (Gabbiani *et al.* 1971). These features include the presence of cytoplasmic microfilament bundles, which are the source of the force producing wound contraction (Gabbiani 1981). This similarity with SM cells was confirmed when strips of granulation tissue were isolated and placed in a pharmacological bath. The granulation tissue contracted and relaxed under the influence of epinephrine, norepinephrine, and 5 hydroxy tryptamine producing contraction and relaxation similar to SM cells (Majno *et al.* 1971). The name myofibroblast was suggested to describe the modified and possibly contractile fibroblast (Gabbiani *et al.* 1972). Myofibroblasts have been shown to contain higher amounts of polymerized actin compared to normal fibroblasts *in vivo*.

Wound healing is significantly impaired in mouse models with an ablated myofibroblast differentiation pathway (Blumbach *et al.* 2010, Liu *et al.* 2010). Therefore, wound contraction is a part of the process of wound healing, but excessive contraction is an undesirable effect. Excessive myofibroblast activity within granulation tissue can lead to excessive scarring and contracture formation. The mechanism of wound contraction is not fully understood, but reducing the contraction rate can lead to improving the quality of scarring. It can also lead to preventing the development of contractures and their implications. Influencing the rate of wound contraction could lead to reducing the

formation of contractures across joint areas in particular leading to restoration of full range of motion.

Other models have been described to investigate wound contraction, Elsdale and Bard (1972) introduced a fibroblast-impregnated collagen gel model to study the behaviour of fibroblasts and myofibroblasts *in vitro*. This model has been extensively used to study wound contraction *in vitro* (Harrison *et al.* 2005) . The model used three-dimensional gels to induce morphological changes in fibroblast similar to *in vivo* changes (Elsdale and Bard 1972).

Harrison *et al.* (2006b) and Harrison and MacNeil (2008) reviewed the mechanisms behind wound contraction. Several theories were suggested to explain the process of wound contraction. Theories suggest that myofibroblasts either exert a pulling force or traction on collagen fibrils or extracellular matrix fibrils producing wound contraction. The pulling or traction force generates inward movement of the wound edges producing wound contraction and subsequent closure.

The widely accepted theory for wound contraction is that contraction is brought about by the differentiation of fibroblasts to myofibroblasts (Majno *et al.* 1971, Gabbiani *et al.* 1971). Fibroblast differentiation is accompanied by intrinsic expression of α-actin filament bundles (Welch *et al.* 1990). Myofibroblasts have contractile properties similar to smooth muscle cells and the sliding movement of the actin filaments results in cell adherence (Montandon *et al.* 1977). As a result of cell adherence, a compact cell mass develops producing contraction of granulation tissue followed by inward movement of the wound edges.

The need to provide better quality epidermal regeneration following application of cultured autologous keratinocytes resulted in a major shift. The use of undifferentiated single-cell suspensions and static carriers is currently recommended compared to differentiated cell sheets (Huss *et al.* 2007, Levine *et al.* 1977). As a result, a larger

proportion of the transplanted keratinocytes can contribute to epidermis regeneration compared to differentiated cells (Seland *et al.* 2011).

Biodegradable porous microcarriers 'Cultispher S®' provided an optimal matrix for the adhesion, migration and proliferation of epithelial cells (Gustafson *et al.* 2007, Huss *et al.* 2010). Seland *et al.* (2011) reported that grafting of 'Cultispher S®' microcarriers coated with cultured keratinocytes into full thickness wounds in athymic rats resulted in a thick epithelium. The regenerated epithelium was thicker and also substantial soft-tissue regeneration was noted compared to grafting with sheet-cultured keratinocytes.

Application of skin grafts on full thickness wounds reduces wound contraction and hypertrophic scarring (Walden *et al.* 2000). However, skin grafts undergo primary contraction following harvesting and secondary contraction following application on the wound bed. Secondary contraction results in contracture formation and poor cosmetic outcome (Walden *et al.* 2000). Combination therapies using skin grafting and cultured keratinocytes may have a role in reducing wound contraction. Other factors influencing wound contraction include; the wound bed and the skin graft thickness. Skin grafting on muscle fascia and full thickness skin grafts reduce wound contraction compared to mobile tissue and STSG (Corps 1969a, Corps 1969b).

A complex relationship exists between keratinocytes and fibroblasts during the process of wound contraction. Myofibroblast differentiation is influenced by keratinocyte differentiation during wound healing (Boyce *et al.* 1991). Full thickness skin grafts reduce myofibroblast differentiation and wound contraction compared to STSG (Corps 1969a). The use of keratinocytes on microcarriers or as cell spray could add more keratinocyte cell volume to STSG resulting in reduced wound contraction.

The measurement of the reduction in wound area over a period of time can quantify wound contraction *in vivo* (Lammers *et al.* 2011). This can be achieved through accurate measurements of wound area at different time points following the creation of a wound (Lammers *et al.* 2011). In the second *in vivo* study in chapter 5, the treatment

with MCAK and SAK, in conjunction with widely meshed STSG (6:1) was compared. Epithelial repair and wound contraction in both groups were compared with control using widely meshed STSG (6:1) alone. The use of the widely meshed STSG (6:1) was chosen, as it was unlikely to produce full epithelial wound closure due to the wide meshing pattern.

Understanding the role of wound contraction in wound healing and the factors influencing the process is important. The primary mechanism for full thickness wound healing in mammals is wound contraction (Billingham and Medawar 1955). The mechanical movement of the wound edges towards the centre of the wound along with keratinocyte migration achieves wound closure (Billingham and Medawar 1955).

Wound contraction may be prevented by covering the wound with a skin graft, thicker skin grafts reduce wound contraction more than thinner grafts (Billingham and Russell 1956). The use of full thickness skin graft to cover a granulating full thickness cutaneous defect inhibits contraction (Billingham and Russell 1956). Full thickness wounds treated with STSG have been shown to contract less than wounds left to heal by secondary intention (Sawhney and Monga 1970). The epidermal and dermal components within the STSG allow wound closure via keratinocytes migrating from the skin graft. In addition, keratinocyte migration from the wound edges and wound contraction help achieve epithelial closure. The use of keratinocytes on microcarriers could possibly replace the epidermal component of the STSG, while the widely meshed STSG could replace the dermal component.

In this study, the ability of MCAK or SAK to re-epithelialise the wound bed in conjunction with widely meshed STSG was investigated. This situation closely resembles clinical treatment regimes, where the lack of donor sites for STSG harvesting warrants wide skin graft meshing in combination with other treatments. In this study, the meshing procedure increased the surface area of the graft 6 times (6:1) and provided a thin STSG. The STSG alone was used as the control group in the study and the effect

on wound contraction following the application of MCAK and SAK on square full thickness wounds was assessed. The use of square wounds was to allow the natural process of wound edges' contraction, which would not be possible with the use of PTFE wound chambers. Inward migration of keratinocytes from the wound edges in combination with wound contraction through fibroblasts and myofibroblasts lead to wound healing. The two processes occur in tandem and none alone would achieve wound healing.

The use of keratinocytes cell suspensions in combination with STSG has been investigated previously. Keratinocytes cell suspensions provided the epidermal component, while the STSG provided the dermal component. Navarro *et al.* (2000) investigated the combination of cell suspensions and meshed skin grafts in a porcine wound model. More epithelial thickness and new vessel formation were noted in between the interstices of STSG in combination with cell suspensions compared to STSG alone (Navarro *et al.* 2000). Sprayed keratinocytes alone applied to full thickness wounds produced similar histological findings (Fraulin *et al.* 1998).

The results from the second *in vivo* study demonstrated the use of autologous keratinocytes on microcarriers in combination with thin meshed STSG produced a reduction in wound contraction. The MCAK group showed wound contraction of 42.7% compared to 40.5% in the SAK group and 31.6% in the control group after 21 days. The values represented percentage reduction in the wound surface over the study period. A difference of 11.1% in wound contraction was noted between the MCAK group and the control group by day 21. Therefore, the wounds in the MCAK group contracted less than the SAK and control groups. Significantly less wound contraction was noted in wounds treated with MCAK ($p < 0.05$; Holm-Sidak post hoc test).

All the wounds from the three treatment groups were healed by day 21 despite the variation in wound area contraction. Full epithelial closure was achieved in all three groups; the difference in the epithelial structure in the three groups was shown in

histological analysis. The epithelial structure was fully developed in the MCAK and SAK groups compared to the control group. Basement membrane formation was positive in the three treatment groups confirming epithelial closure. Basement membrane staining was more intense in the MCAK group compared to the SAK and control groups. The variation in the histological findings could be explained by the fragility of the thin STSG alone in the control group compared to the combination therapy with autologous keratinocytes in the other two groups. Application of keratinocytes on microcarriers produced a structured epithelium, basement membrane, and a reduction in wound contraction. Also application of keratinocytes on microcarriers improved epithelium quality compared with SAK. It is unclear whether this effect was a result of the difference in the culture and application methods of the two treatments or due to a different factor.

Noticeably animals possess a subcutaneous muscle layer "panniculus carnosus" enabling the skin to glide over deeper structures (Billingham and Medawar 1955). In humans, this muscular layer is absent and skin is attached to deeper structures. This difference in skin attachment between animals and humans allows extensive wound contraction in animals. In this study, wound closure was achieved in the three groups, despite the control group receiving widely meshed (6:1) STSG only. This can be attributed to the greater wound contraction ability in pigs compared to humans. It also highlighted the limitations of animal models for assessment of wound contraction compared to humans.

GFP positive cells were not seen in any of the sections from the three groups after 3 weeks. In similar studies, GFP labelled keratinocytes were not detectable after 3-4 weeks despite evidence that transplanted cells survived (Pfutzner *et al.* 2006, Lu and Ghazizadeh 2007).

From this study, it was possible to consider that the reduction in wound contraction was due to a change in the behaviour of fibroblasts or myofibroblasts. Their contraction

within the wound was reduced, although it is unclear how this effect was achieved. The reduction in wound contraction is considered a favourable outcome factor in a clinical setting where the limitation of skin mobility produces contractures and disability.

Nillesen *et al.* (2011) reported the use of acellular composite skin replacement consisting of porous dermal layer of collagen type I, elastin, dermatan sulphate, heparin, Fibroblast growth factor (FGF) 2, and vascular endothelial growth factor. The dermal scaffold had a thin epidermal layer of collagen type I, heparin and FGF7. This skin replacement therapy produced a delay in wound contraction when compared to Integra® and control wounds left to heal by secondary intention in a rat model up to 14 days. By day 28, there was significant wound contraction in all the treatment groups with no statistical difference in the wound area (Nillesen *et al.* 2011). FGF2 and 7, and vascular endothelial growth factor may have a role in reducing early wound contraction in a rat excisional wound model (Nillesen *et al.* 2011). The role of similar paracrine factors in the pig wound model remains a possibility requiring further investigation to understand their role and effect on wound contraction.

The interactions between keratinocytes and fibroblasts during the process of wound healing are complex (El Ghalbzouri *et al.* 2004, Le Poole and Boyce 1999). Andree *et al.* (2001) showed higher concentrations of transforming growth factor-β (TGF-β) in porcine wounds treated with sub-confluent keratinocyte suspensions compared to SAK and controls. Based on these results, there may be benefits from the combination of cell-based therapy with the application of STSG. The results from this study are consistent with our previous results comparing STSG and SAK treatments at Blond McIndoe Research Foundation (Reid *et al.* 2007).

In the second *in vivo* study, widely meshed STSG was used to support autologous keratinocytes in achieving epithelial closure. The treatment in combination with MCAK produced reduction in wound contraction. The presence of a different type of dermal support could possibly alter wound contraction. The use of dermal regeneration

template in combination with MCAK and its effect on wound contraction was investigated in the next study.

Allogeneic skin grafts showed signs of rejection in the porcine wound model 12 days following application (Richters *et al.* 2005). Allogeneic graft rejection in an immuno-competent host is usually mediated through activation of T lymphocyte cells as previously explained. Achauer *et al*. (1986) reported the use of cyclosporin for 2 years in a case with extensive burns to stop allograft rejection. No graft rejection was noted during the 2 years or following the gradual withdrawal of cyclosporin. Krupp *et al.* (1994) also reported the use of allografts in combination with Cyclosporin in a case report. Following the withdrawal of Cyclosporin, allografts were replaced with cultured autologous keratinocytes on allogeneic dermis. From these reports it is clear that the clinical role of allografts is limited to temporary wound cover, longer survival of allografts requires the use of immuno-suppressants.

However, in case of extensive burn injuries, this temporary cover is sometimes vital to patient survival. The use of allogeneic keratinocytes on microcarriers can possibly replace the use of cadaveric allografts, which is the current clinical standard. The disadvantages of cadaveric allograft use such as limited availability, transport, and storage could be avoided with the application of cultured allogeneic keratinocytes on microcarriers.

Integra®, dermal regeneration template (DRT) is composed of two layers; a bovine collagen-based dermal layer, and a temporary epidermal silicone sheet, which is removed following vascularisation of the dermal layer (Hansen *et al.* 2001). The dermal layer is composed of bovine type I collagen and shark chondroitin-6-sulphate, covered with a protective layer of nonporous silicone (Burke *et al.* 1981). The dermal layer is revascularised in 2-3 weeks providing a suitable wound bed for either ultra-thin skin grafting (150 μm) or cultured keratinocytes epidermal sheets.

Integra® was introduced as a treatment in burns surgery almost 30 years ago (Burke *et al.* 1981). In 1996, Integra® received U.S. Food and Drug Administration (FDA) approval for use as dermal regeneration template (Moiemen *et al.* 2006) and has been widely used since then. The role of Integra® in the treatment of major burns is to provide a temporary cover following the excision of burns. This provides valuable time for the next stage of epidermal cover during the vascularisation of the dermal component. In the meantime, physiological wound closure with minimising fluid loss helps to stabilise a critically ill patient. The use of Integra® has also been shown to reduce wound contraction in full thickness skin wounds (Reid *et al.* 2007).

The main disadvantages of the use of Integra® are its high cost and the possibility of wound infection (Nguyen *et al.* 2010). Due to the fact that the dermal component requires 2-3 weeks for vascularisation, Integra® is susceptible to bacterial infection during that period. General factors such as the immuno-compromised status of burns' patients and local wound conditions despite antibiotic cover play a major role.

Heimbach *et al.* (1988) in a multi-centre randomised controlled trial compared Integra®, autografts, allografts and xenografts. They reported Integra® as superior in wound healing time compared to other types of skin grafting. In two major studies by (Heimbach *et al.* 1988, Peck *et al.* 2002) no major complications or safety issues were reported following the use of Integra®. Both studies reported patient mortality, which was related to extensive burn injuries especially inhalational injuries. No patient mortality was attributed to the use of Integra® in either of the two studies.

In cases of extensive burn injuries and the lack of availability of skin graft donor sites, allografts can be used. Deceased donor allograft skin provides temporary cover of the burn wound in both partial thickness and full thickness skin loss. Allograft skin can also be used as a protective covering layer for widely meshed skin grafts (Alexander *et al.* 1981). The use of allografts improves wound healing, reduces heat and fluid loss, and improves scarring by restoring temporarily the protective role of the skin (Brychta *et al.*

2002). Allografts can also be applied as cultured epithelial sheets in the treatment of deep dermal burns (Brychta *et al.* 2002).

The disadvantages of allograft use include graft rejection and limited availability. Host rejection occurs after patients recover from the immuno-compromised status of the burn injury. The availability of allografts relies on tissue banks, and there is low risk of disease transmission. Ethical and cultural implications for donors and recipients also need to be considered (Burd and Chiu 2005).

The combination therapy of Integra® and allogeneic cultured keratinocytes has potential applications in severe cases of burn injuries or skin loss. The lack of available skin graft donor sites warrants exploring alternatives to autografts. The use of Integra® produces a vascularised bed supporting the application of cultured epithelial allografts and could prolong their survival.

Biobrane® is a biosynthetic dressing composed of a knitted nylon mesh that is bonded to a thin, silicone membrane and coated with porcine polypeptides (Hansen *et al.* 2001). Biobrane® has a variety of applications; it can be used as a temporary dressing for partial thickness burns or graft donor sites. It can be also used as a protective dressing over widely meshed split skin grafts initially to protect the fragile grafts from shearing. The design of Biobrane® allows its adherence to wounds and it can be trimmed away as wound healing progresses (Hansen *et al.* 2001). Biobrane® is considered an alternative to the use cadaveric allografts as it has similar properties to skin. Several studies established the safety and efficiency of Biobrane® as a temporary burn dressing (Gerding *et al.* 1990, Barret *et al.* 2000, Lal *et al.* 2000).

Biobrane® was also found to reduce wound contraction in full thickness wounds in rat animal model (Frank 1984, Frank *et al.* 1984). The reduction in wound contraction was a result of mechanical splinting rather than influencing myofibroblast activity (Frank *et al.* 1984). Therefore, the use of Biobrane® could provide a protective layer to either keratinocytes on microcarriers or as cell spray post wound application.

Alpha smooth muscle (α-SM) actin is important for myofibroblast contraction taking into consideration that α-SM actin is widely expressed in contractile cells such as myoepithelial or vascular SM cells. The main role of these cells is contraction, hence it likely myofibroblasts have a similar contractile role in wound healing.

α-SM actin has been suggested as the most significant marker of myofibroblasts (Sappino *et al.* 1990). The presence of myofibroblasts correlates with wound remodelling phase including wound contraction. Therefore, α-SM actin is the cell marker generally present in the myofibroblasts of normally healing granulation tissue (Gabbiani 2003). During the progression of the process of wound healing, fibroblasts acquire SM cell features; in the form of myofibroblasts capable of contraction (Desmouliere *et al.* 1993). Myofibroblasts appear temporarily in normal wound healing and more permanently in excessive fibrosis such as hypertrophic and keloid scarring (Desmouliere *et al.* 1995). The role of myofibroblasts in wound contraction was highlighted through research into foetal wound healing. In foetal wound healing, regeneration is the dominating process over scarring, and there is no appearance of myofibroblasts in fetal scar-less wound healing (Adzick and Lorenz 1994).

Wound scarring can be significantly reduced if epithelial closure is achieved within three weeks (Deitch *et al.* 1983, Deitch 1985, Cubison *et al.* 2006). Therefore achieving epithelial closure is a priority, and if it cannot be permanent, then temporary closure using allografts or cultured epithelial allografts is recommended. It could be possible for cultured allogeneic keratinocytes to survive longer following wound application in combination with dermal regeneration template. The potential for using microcarriers as a delivery method could also be explored along with possible effects on wound contraction.

In full thickness wound reconstruction, different types of dermal substitutes serve as a scaffold to support cellular migration and wound healing (Truong *et al.* 2005). Dermal

substitutes support re-epithelisation activity, which is achieved via a wide variety of additional treatments.

Some disadvantages to the use of Integra® in both clinical and experimental settings have been reported. Stern, McPherson and Longaker (1990) reported that 14.4% of human patients who received Integra® developed foreign body granuloma cells and eosinophil infiltration. Truong *et al.* (2005) demonstrated numerous foreign body granuloma cells in Integra® treated wounds in a nude mouse model. They attributed the findings to a reaction to the constituents of Integra®, which could delay the vascularisation process.

Overall as discussed before, the safety of Integra® and its effect in reducing wound healing time has been established (Heimbach *et al.* 1988). Also in previous work by our research group, Integra® was shown to reduce wound contraction (Reid *et al.* 2007). The combination therapy of Integra® and delivery of allogeneic cultured keratinocytes could have a future potential. As in the use of allografts, the concept of allogeneic cells could possibly postpone the need for immediate definitive treatment. Commercial products currently available include Cryoskin® (Altrika, Sheffield, United Kingdom), which can be provided on patient-by-patient basis in the UK. This is crucial, in cases of lack of available autografts or cultured autologous keratinocytes, to stabilise a critically ill patient temporarily. Several studies reported successfully the use of allogeneic cultured keratinocytes for treatment of chronic wound (Bayram *et al.* 2005, Martin *et al.* 2005) and recently a phase 2 randomised placebo-controlled multi-centre trial involving 205 patients (Kirsner *et al.* 2012). Allogeneic keratinocytes delivered to diabetic foot ulcers on Cytoline1™ microcarriers (polyethylene & silica) achieved wound healing in three weeks (Bayram *et al.* 2005).

The use of Biobrane® in the study in section 6 in combination with Integra® and allogeneic keratinocytes treatment was aimed at providing a protective and supportive layer to the cells. The concept of combining allogeneic keratinocytes with Biobrane®

has been previously reported in a rabbit wound model (Lin *et al.* 1993). Allogeneic keratinocytes irradiated prior to wound application on Biobrane® sheets completely resurfaced the wounds with by day 21 (Lin *et al.* 1993). This study showed that the use of allogeneic keratinocytes could generate epithelium leading to wound closure.

In this study, the use of allogeneic keratinocytes on microcarriers and as cell spray on Integra® was compared to a clinically standard treatment. The Integra® application followed by ultra-thin split thickness skin graft (uSTSG) application in 2-3 weeks is widely used in the treatment of full thickness burns' (Pham *et al.* 2007). No Biobrane® was applied to the control wounds, as there is no indication for Biobrane® use in combination with uSTSG.

Integra® was used as dermal replacement and to provide support to MCAlK and SAlK following wound application. As expected, the application of Integra® maintained the wound surface area up to day 21, when treatment was applied. It was noted from previous studies and discussed in chapter 5 that control wounds treated with widely meshed STSG alone were healed by day 21. Hence, the role of Integra® in reducing wound contraction and maintaining wound surface area can be assumed.

Notably the vascularisation of Integra® was complete around the second week post wound application. This finding is different from the manufacturer's recommendation for clinical application, which recommends 3 weeks for vascularisation: (http://integralife.com/products/pdfs/634199956311907893_IDRT_Treatment_Guidelines_ER3341.pdf)

It is possible that the rate of vascularisation of Integra® is different in the porcine wound model compared to humans. The use of Integra® with non-cultured cell suspension has been reported as a single stage procedure resulting in re-epithelisation (Wood *et al.* 2007). The rapid rate of vascularisation of the template in the porcine model contributed to the one stage wound closure (Wood *et al.* 2007).

Transplanted allogeneic skin to a healthy recipient would undergo a rejection process leading eventually to the destruction of the graft in around 14 days (Richters *et al.* 2005). The allograft rejection is mediated by activation of T cells, which can specifically destroy major histocompatibility complex–incompatible cells (Richters *et al.* 2005). Epidermal Langerhans cells initiate the rejection process, where they migrate from the skin graft to the recipient's draining lymph node of where activation of the T cells occur (Larsen *et al.* 1990). Dendritic cells within the dermis behave similarly producing further activation of the T cells (Richters *et al.* 1999). The use of cultured allogeneic keratinocytes lacking in Langerhans and dendritic cells has been reported (Phillips 1991). The use of allogeneic keratinocytes still does not produce permanent epithelium as graft rejection still occurs (Phillips 1991, Benichou *et al.* 2011). Following transplantation, the recipient T cells infiltrated the allogeneic graft or cultured epidermal sheets eventually causing rejection (Aubock *et al.* 1988). For definitive wound coverage, allogeneic cultured keratinocytes or grafts should be followed or combined with autologous cells or grafts.

The results from the third *in vivo* study showed the two groups MCAlK and SAlK wounds demonstrated epithelial closure 21 days following treatment application. Despite the presence of some residual granulation tissue, a satisfactory wound closure of more than 90% was achieved. These results were similar to the results reported by Lin *et al.* (1993) in a rabbit wound model using irradiated allogeneic keratinocytes on Biobrane®. The results regarding full epithelial closure unfortunately cannot be replicated in humans, unless the host is immuno-suppressed. The combination of Integra®, allogeneic keratinocytes, and Biobrane® could be considered an option in severe injuries where temporary coverage is required until permanent coverage is available.

The lack of GFP positive cells hinders the assessment of the origin of the newly formed epithelium in the MCAlK and SAlK groups. It is likely that wound healing in the two

groups was a result of epithelial migration from the wound edges rather than the allogeneic keratinocytes. The source of the keratinocytes contributing to wound healing in the MCAlK and SAlK groups was not clear. Keratinocytes migration from the wound edges was the likely explanation of how wound healing was achieved. Histological examination of the epithelium in the MCAlK and SAlK groups revealed similar quality to the control group. The combination treatments in the two groups played a role in promoting satisfactory wound closure comparable to autologous uSTSG use.

The application of Integra® maintained the wound surface area up to day 21, when treatment was applied. From the previous study in section 5, control wounds treated with widely meshed STSG were healed by day 21, demonstrating the role of Integra® in reducing wound contraction. In this study, the vascularisation of Integra was complete around the second week post application. In further studies, the application of treatments 2 weeks following Integra® was considered to reduce the possibility of wound infections.

The MCAlK group wounds' area contracted 14.6% of the original wound area less than the wounds in the control group by day 42. The MCAlK group wounds' area contracted 4.6% of the original wound area less than the wounds in the SAlK group. The variation in wound contraction could be possibly related to the use of microcarriers for allogeneic keratinocyte delivery. Significantly less wound contraction was found in wounds treated with MCAlK when compared with SAlK or uSTSG alone (adjusted $p < 0.05$; Holm-Sidak post hoc test).

In conclusion, there is a role for using allogeneic keratinocytes delivered on microcarriers in improving wound healing. The application of allogeneic keratinocytes on microcarriers in combination with Integra® and Biobrane® reduced wound contraction. The epithelial closure achieved in the MCAlK and SAlK groups is unlikely to be replicated in a clinical situation due to host rejection. The effect of autologous

keratinocytes with or without autologous fibroblasts delivered on microcarriers on wound contraction was assessed in the next study.

The interactions between keratinocytes and fibroblasts *in vivo* during the process of wound healing are fundamental for the maintenance of keratinocyte cell culture *in vitro*. Rheinwald and Green (1975b) demonstrated that keratinocyte growth in culture is dependent on interaction with fibroblasts. The use of murine 3T3 fibroblasts in keratinocyte cell culture was originally described by Rheinwald and Green (1975a). As an alternative, the use of human fibroblasts in keratinocyte cell culture was also reported (Limat *et al.* 1990). The expression of growth factors such as Transforming growth factor-beta 1 (TGF-β1) and Interleukin-6 (IL-6) is up-regulated during wound healing (Werner *et al.* 2007). TGF-β1 production by keratinocytes stimulates fibroblasts proliferation resulting in IL-6 up-regulation (Desmouliere *et al.* 1993). IL-6 in return stimulates keratinocyte proliferation and the keratinocyte-fibroblast interaction continues during wound healing (Grossman *et al.* 1989). The differentiation of fibroblasts to myofibroblasts is modulated by cytokines such as platelet-derived growth factor (PDGF) (Tingstrom *et al.* 1992). Skin substitutes containing fibroblasts demonstrated enhanced neovascularisation as fibroblasts expressed cytokines following application on wounds (Erdag and Sheridan 2004). Skin substitutes containing fibroblasts showed better graft take, less contraction and enhanced vascularisation (Erdag and Sheridan 2004, Demarchez *et al.* 1992).

Therefore, fibroblasts play an important role interacting with keratinocytes *in vitro* and *in vivo*. The interactions *in vivo* promote wound healing and result in optimum outcomes. Hence, the treatment of full thickness skin injuries with keratinocytes in the form of epidermal sheet grafts or cell spray could be improved by adding fibroblasts.

During the wound healing process, fibroblasts undergo migration from adjacent intact dermis to the fibrin clot at the site of skin injury (Yang *et al.* 2012). In response to growth factors such as TGF-β1, extracellular matrix (ECM), and mechanical wound

tension, fibroblasts differentiate into myofibroblasts (Webber *et al.* 2009). As previously discussed, myofibroblast expression of α-SMA plays an important role in wound contraction.

The co-culture of keratinocytes and fibroblasts demonstrated up-regulation of TGF-β1 expression, increased ECM deposition, and induced α-SMA expression in fibroblasts (Shephard *et al.* 2004b). Other studies have shown that keratinocytes suppressed the proliferation of co-cultured fibroblasts (Harrison *et al.* 2006a). The investigation of the interactions between keratinocytes and fibroblasts using monolayer culture *in vitro* may not be sufficient to study *in vivo* behaviour (Yang *et al.* 2012). The interactions between keratinocytes and fibroblasts are particularly evident in the late phase of wound healing during wound contraction and scar formation (Yang *et al.* 2012).

As discussed in the previous study, the use of Integra® dermal regeneration template reduced wound contraction in combination with allogeneic cultured keratinocytes. The use of full thickness skin grafts (FTSG) to cover wounds is known to reduce contraction (Rudolph 1980). Further studies using Electron microscopy demonstrated that FTSG did not influence myofibroblast populations or differentiation (Rudolph 1980, Vande Berg and Rudolph 1985). The application of FTSG led to myofibroblasts disappearing from the wound earlier than wounds without FTSG (Rudolph 1979, Vande Berg and Rudolph 1985). Artificial dermal substitutes and biomaterials aiming at restoring the dermis should ideally be enriched with keratinocytes and fibroblasts to resemble FTSG.

The possibility of application of fibroblasts in combination with dermal substitutes could have the potential to improve dermal regeneration. This in turn would lead to the reduction of wound contraction and improving the functional and aesthetic outcomes of skin replacement therapy compared with current available treatments. Worth noting that fibroblasts differentiation into myofibroblast is a part of the normal process of wound healing. Up to date, there are no available methods to control the number of fibroblasts differentiating into myofibroblasts.

The differentiation of fibroblasts to myofibroblasts *in vivo* is marked by an increase in the intracellular contractile capability of myofibroblasts (Rudolph and Woodward 1978). The effect of dermal substitutes on fibroblast differentiation and wound contraction requires further investigation. The combination of autologous keratinocytes and fibroblasts with Integra® could lead to epithelial closure and possibly influence wound contraction.

The *in vitro* replacement of murine 3T3 cells with human allogeneic fibroblasts (Sun *et al.* 2004) or irradiated human fibroblasts (Mujaj *et al.* 2010) has been described. Recent work by the Blond McIndoe Research Foundation demonstrated a ratio of 6:1 keratinocytes to fibroblasts produced the maximum cumulative population doubling (Jubin *et al.* 2011). The effect of fibroblasts on wound re-epithelisation has been shown in a porcine wound model (Peura *et al.* 2012). The results showed that fibroblast aggregate-derived paracrine mediators stimulated epidermal regeneration *in vivo* (Peura *et al.* 2012).

An important function of any potential skin substitute is to support the formation of an epidermal barrier restoring the physiological function of skin (Kempf *et al.* 2011). The need to restore the epidermal barrier remains a clinical priority, but the restoration of dermal architecture is also important (Klingenberg *et al.* 2010). Incorporating autologous cultured keratinocytes and fibroblasts within skin substitutes could potentially restore the epidermal and dermal skin architecture. Skin replacement therapy should ideally be able to reconstruct all layers of the skin including the epidermis and the dermis. The loss of the skin barrier function leads to a clinical challenge where restoration of the epidermal cover is a priority. Cultured epidermal sheet grafts provide an adequate treatment to restore the epidermis, but have many disadvantages. The fragility of the epidermal sheet grafts is mainly due to the lack of a dermal support within the grafts. Hence, combination therapy using cultured epidermal grafts and dermal replacements is recognised as an alternative approach (Heimbach *et al.* 1988).

Therefore, microcarriers could be used as a delivery method for autologous keratinocytes and fibroblasts in combination with Integra®. Other dermal replacements are available, but the use of Integra® has been shown to reduce wound contraction compared to STSG (Reid *et al.* 2007). In the assessment of *in vitro* porcine keratinocytes and fibroblasts co-culture in study 3.6, microcarriers supported keratinocytes fibroblasts co-culture *in vitro*. The effect of their application on the wound with regard to epithelial closure and wound contraction was assessed in the study in section 7.

In the study in section 6, allogeneic keratinocytes on microcarriers and cell spray were compared to the standard therapy of uSTSG and Integra®. Since the results from this control group on the same animal model were available, 3 treatment groups were allocated in this study. The results from the 3 treatment groups were compared to the control group from the previous study in section 6.

Dermal substitutes have been developed over the last 30 years (Burke *et al.* 1981). Integra® has been for many years the most widely used dermal substitute, but recently several new artificial dermal substitutes have been developed (Nguyen and Dickson 2006). Truong *et al.* (2005) compared different dermal substitutes in skin wound healing in a mouse model. All dermal substitutes were incorporated into the wound bed and wound contraction was decreased (Truong *et al.* 2005). A study comparing Integra® and Matriderm® in a rat model revealed no major differences in graft take rates or vascularisation (Schneider *et al.* 2009). Recently, five dermal substitutes including Integra® and Matriderm® were compared in a porcine wound model (Philandrianos *et al.* 2012). No major differences in wound healing or scar formation was found between the different dermal substitutes over a period of 6 months (Philandrianos *et al.* 2012).

The use of microcarriers to deliver cultured autologous keratinocytes and fibroblasts in combination with Integra® is a novel concept. Dermal substitutes such as Integra® provide a scaffold onto which keratinocytes can migrate and repair the injury (Truong *et*

al. 2005). The results of this study showed the application of autologous keratinocytes and fibroblasts on microcarriers produced epithelial closure. Histological analysis showed a developed epithelium and basement membrane as demonstrated by immuno-labelling of K14, Collagen VII and laminin.

The mechanism of differentiation of fibroblasts into myofibroblasts *in vitro* was reported to be cell density dependent (Masur *et al.* 1996) . Fibroblasts seeded at low density produced a cell culture population consisting of 70-80% myofibroblasts. In contrast, fibroblasts seeded at high density produced cultures with only 5-10% myofibroblasts (Masur *et al.* 1996). The challenge of keratinocyte fibroblast co-culture is that fibroblasts have the potential to expand at rates higher than keratinocytes. Fibroblasts rapid expansion in co-culture *in vitro* can lead to overtaking the culture and suppressing keratinocyte activity. The ratio of 6:1 as reported by Jubin *et al.* (2011) was used in this study for keratinocytes and fibroblasts culture on microcarriers. The low seeding density of fibroblasts could have contributed to less myofibroblast proliferation *in vivo*. It is worth noting that this was a purely theoretical assumption as no keratinocyte to fibroblast cell count in the MCAK-FB group was undertaken prior to wound application.

Kempf *et al*. (2011) reported the use of a denatured collagen microfiber scaffold seeded with human fibroblasts and keratinocytes for skin grafting. The scaffold was biocompatible, biodegradable, and delivered human fibroblasts and keratinocytes in an *in vivo* mouse model. The combined delivery of keratinocytes and fibroblasts in skin substitutes is more preferable than the delivery of keratinocytes alone. Theoretically, the combination of keratinocytes and fibroblasts can allow the regeneration of the epidermis and the dermis hence restoring the skin architecture.

During the late phase of wound healing, cellular interactions are dominated by keratinocyte-fibroblast interactions (Werner *et al.* 2007). The wound-healing environment changes from an inflammatory phase to the formation of granulation

tissue. The formation of a new basement membrane zone in the neo-epithelium is a result of the interactions between keratinocytes and fibroblasts (El Ghalbzouri *et al.* 2004). The composition of the basement membrane and its formation can also influence keratinocytes phenotype (El Ghalbzouri *et al.* 2004). Shephard *et al.* (2004a) analysed fibroblast responses to keratinocyte-derived stimuli in a comparative study. The authors compared mRNA expression of fibroblasts in monoculture with the fibroblasts co-cultured with keratinocytes. Fibroblasts differentiated into myofibroblasts as shown by a time-dependent increase of α-SMA-positive mesenchymal cells (Shephard *et al.* 2004a). The expression data showed that several genes characteristic of TGF-β1 signalling were upregulated. Physical factors such as mechanical tension exerted by the wound edges play an important role in fibroblast differentiation. Shephard *et al.* (2004b) reported that fibroblasts differentiate into myofibroblasts after 1-2 days in co-culture with keratinocytes compared to control cultures of fibroblasts alone.

Ideally, the interactions between keratinocytes and fibroblasts during wound healing should be replicated following the application of skin replacements. Therefore, skin substitutes should comprise keratinocytes and fibroblasts applied together in an attempt to replicate physiological wound healing.

Several studies assessed wound healing using artificial dermal substitutes *in vivo* using a porcine model (Butler *et al.* 1999, Myers *et al.* 2007, Haslik *et al.* 2010). The studies assessed different modalities of dermal substitutes in combination with epidermal substitutes such as keratinocyte seeding, cultured epithelial autografts, and skin grafts. In a recent study, Philandrianos *et al.* (2012) compared five different dermal substitutes in a porcine wound model. The authors used 4 x 4 cm^2 square wounds in a porcine animal model identical to the wound model in this body of work. The authors argued that all of the five dermal substitutes (Integra®, Renoskin®, Matriderm®, Proderm®, and Hyalomatrix®) had long term scar quality as good as a skin graft alone. Hence, the authors questioned the rationale behind using artificial dermal substitutes if the resulting

scarring and wound healing is comparable with skin grafts alone. Taking into consideration the findings from this study, there are real advantages for the use of artificial dermal substitutes. Artificial dermal substitutes are used clinically when there is no available donor site for skin grafting or in anatomical areas where dermal support is required in addition to skin grafting.

In extensive cases of skin loss, the first stage application of dermal substitutes temporarily restores the physiological barrier functions of the skin. Integra® has a silicone layer that prevents fluid and tissue fluid loss from the wounds while vascularisation takes place. This allows time for cultured keratinocytes delivered on microcarriers or as epithelial autografts or cell spray to be ready. Therefore, artificial dermal substitutes continue to have an important role in the treatment of trauma and burns patients.

In this study, a difference of 9.2 % in wound contraction area was noted between the MCAK-FB group and the MCAK group by day 21-post treatment. The reduction in wound contraction in MCAK-FB group could be partly explained by the presence of fibroblasts compared to MCAK and SAK groups. The three groups (MCAK-FB, MCAK, and SAK) had reduced myofibroblast activity demonstrated by a reduction in α-SMA expression compared with uSTSG and Integra® (used as control). The reduction in myofibroblast activity was not related to the use of microcarriers for cell delivery as SAK showed similar picture. The difference in wound contraction could be explained by the difference in laminin and α SMA distribution in the MCAK-FB and the other 3 groups including the standard treatment combination of uSTSG and Integra®.

The reduction in wound contraction in the MCAK-FB and MCAK groups compared to SAK provided evidence of an advantage to using microcarriers as delivery method. Using microcarriers to deliver keratinocytes and fibroblasts facilitated efficient cellular integration into the wound, hence enhancing wound healing and reducing contraction. Lamme *et al.* (2000) reported that the use of autologous fibroblasts in conjunction with

acellular dermis reduced contraction in porcine full-thickness wounds. The reduction in wound contraction was accompanied by a reduction in αSMA-positive myofibroblasts (Lamme *et al.* 2000). The results from the study in chapter 7 showed a reduction in αSMA-positive cells in wounds treated with keratinocytes alone or keratinocytes with fibroblasts. Interpreting these results, it can be assumed that the addition of a cellular component in the form of autologous keratinocytes with or without fibroblasts led to a reduction in the contraction of healing wounds.

The number of cells transplanted to the wound bed has a direct effect on wound contraction (Lamme *et al.* 2000). Further studies using variable cell counts on microcarriers are needed to establish whether the same effect can be replicated using microcarriers. The reduction in wound contraction discussed in chapter 7 could be a result of the combination of keratinocytes and fibroblasts or simply the effect of increased cell populations within the wound.

A significant reduction in wound contraction occurred using microcarriers to deliver keratinocytes or keratinocytes with fibroblasts in combination with Integra®. Similar to the findings reported by Lamme *et al.* (2000), the presence of additional cells in the granulation tissue possibly reduced the need for cells to migrate from the wound margins. This is a process that would normally bring them into contact with the signals necessary for myofibroblast differentiation. It is also conceivable that keratinocytes or keratinocytes with fibroblasts delivered on microcarriers can reduce wound contraction more than cells delivered in suspension. This could potentially be due to keratinocytes being damaged during process of harvesting from tissue culture flasks. The results from the study in chapter 7 support this assumption since wounds treated with cells on microcarriers contracted approximately 10% less than those treated with sprayed cells.

The reduction in wound contraction area is a significant outcome following the application of keratinocytes and fibroblasts on microcarriers. Reducing wound contraction can clinically reduce the incidence of development of contractures.

In conclusion, the possibility of application of a skin replacement therapy capable of reducing wound contraction is promising. Further studies are required to assess keratinocytes and fibroblasts interactions on microcarriers in combination with or without different dermal replacements *in vivo*.

8.3 Conclusion

The studies described in this body of work assessed the culture of human and porcine keratinocytes on gelatin microcarriers *in vitro* and *in vivo*. The studies also assessed the effect of application of porcine keratinocytes on microcarriers on wound contraction *in vivo*. This work presented the results of experiments to test the effects of microcarriers in culture and delivery of keratinocytes using a porcine model for full-thickness wounds.

The traditional culture of human keratinocytes in culture flasks remains time consuming and expensive. Modifications to the standard keratinocyte cell culture *in vitro* can be introduced to reduce time and costs. Also the application of cultured epithelial autografts (CEA) *in vivo* is known to have disadvantages such as fragility and poor take. Hernon *et al.* (2006) reported the primary take of CEA at 45% in one burns unit over ten-year period. Other problems highlighted included the delay in treatment delivery and poor handling *in vivo* due to fragility. In comparison, keratinocytes seeded on microcarriers can be applied directly on the wound bed, as gelatin microcarriers are biodegradable hence improving the handling of cultured keratinocytes. Fragility and wound breakdown in the long-term require further assessment in a clinical model.

In the *in vitro* investigations, results showed the ability of gelatin microcarriers 'Cultispher G®' to support keratinocyte expansion *in vitro* in static and stirred culture. Analysis of microcarriers seeded with keratinocytes using SEM demonstrated that the cells attached to the entire surface of the microcarriers.

Liu *et al.* (2006) demonstrated successfully the use of porcine gelatin microcarrier beads for human fibroblast culture for mass production of autologous living dermal equivalents. Borg *et al*. (2009) demonstrated that the use of microcarriers for keratinocyte cell culture eliminated the need for feeder cells. The use of microcarriers also facilitated the development of an improved keratinocyte cell culture compared with traditional flask culture. In our *in vitro* studies, the results from comparing two types of

microcarriers showed similar findings, where 3T3 feeder cells were initially used in the microcarrier keratinocyte cell culture. In later *in vitro* studies, porcine keratinocyte expansion on microcarriers was achieved in the absence of 3T3 feeder cells. Dispensing with the use of 3T3 cells for the initial expansion of porcine keratinocytes was not achieved and remains a challenge.

When seeded in static culture, porcine keratinocytes migrated from the surface of the microcarriers to tissue culture flasks and reached confluence. Cultispher G® microcarriers biodegraded within the culture medium without affecting keratinocyte expansion and subsequently confluence. This finding was similar to previous work by Malda *et al*. (2003), Chun *et al.* (2004), and Chung *et al.* (2008), which demonstrated the biodegradability of microcarriers for chondrocyte cell culture. Kim *et al.* (2005) and Gustafson *et al.* (2007) demonstrated the biodegradability of microcarriers for keratinocyte cell culture.

Further studies were undertaken since the initial *in vitro* studies did not demonstrate keratinocytes proliferation on microcarriers. Quantitative assessment of porcine keratinocyte proliferation on microcarrier beads was performed using MTT assay, RNA isolation and real-time quantitative PCR. K14 was used as a marker for porcine keratinocyte proliferation. MTT assay results showed a progressive increase in cell count demonstrating porcine keratinocyte expansion. K14 assay results showed an increase in K14 expression demonstrating keratinocyte proliferation.

The results from this study demonstrated keratinocyte-specific proliferation on microcarriers, which was not shown in the earlier *in vitro* studies. The earlier *in vitro* studies demonstrated keratinocytes attachment and expansion in microcarriers static and stirred culture without clear evidence of proliferation.

Further assessment of *in vitro* porcine keratinocytes and fibroblasts co-culture on microcarrier beads was performed with future clinical application in mind. The results demonstrated porcine keratinocytes expansion in the presence of autologous fibroblasts.

Autologous fibroblasts optimised growth and expansion conditions within the microcarriers stirred culture in a similar form to 3T3 feeder cells. The use of the autologous fibroblasts dispensed the use of 3T3 feeder cells within the microcarrier stirred culture.

The initial expansion of keratinocytes in static culture in the presence of 3T3 feeder cells continued to be necessary due to problems with the initial attachment in culture following isolation. Replicating the results reported by Jubin *et al.* (2011) for human keratinocytes microcarriers culture using porcine keratinocytes would require further investigations to negate the use of 3T3 cells.

Further studies investigating the secretion and availability of growth factors, matrix proteins, and the interaction between keratinocytes and fibroblasts are required. Also, further studies are required to dispense with the use of 3T3 feeder cells for the primary expansion of keratinocytes. The *in vitro* results despite their limitations signalled the possibility of investigating the use of microcarriers in an *in vivo* animal model.

In conclusion, the *in vitro* results demonstrated that microcarrier keratinocytes culture is likely to have some benefits over traditional culture methods. The results highlighted the future possibility of *in vivo* application of autologous keratinocytes and autologous fibroblasts following successful co-culture. The utilisation of the keratinocyte microcarrier culture in clinical use requires further investigation in an *in vivo* animal wound model. The application of autologous fibroblasts and keratinocytes could potentially have significant benefits in the treatment of skin loss providing an alternative to the fragile cultured epidermal grafts.

Another area where microcarriers keratinocyte culture might have an impact is wound contraction. A significant amount of wound contraction occurs during the process of wound healing and excessive wound contraction may result in the development of contractures. The role of keratinocytes and keratinocytes-fibroblasts co-culture on microcarriers in reducing wound contraction was investigated in the *in vivo* studies.

Several methods have been described for the delivery of cultured keratinocytes to the wound bed for clinical application. *In vitro* comparisons of keratinocyte delivery methods have shown cell spray as more efficient when compared with other methods (Fredriksson *et al.* 2008). Based on these studies, cultured keratinocyte cell delivery as cell spray was chosen as the standard delivery method to compare with microcarriers in the *in vivo* animal model. Previous studies showed good correlation between the porcine wound model and human wound healing. Hence the pig wound model was chosen as the *in vivo* wound model in further studies.

Excessive wound contraction beyond the physiological process of wound healing leads to the development of wound contractures. A very close relationship exists between the time required for achieving wound healing and wound contracture formation. Wound healing within 3 weeks produces less scarring and contracture formation (Deitch *et al.* 1983, Cubison *et al.* 2006). Therefore, early clinical identification of full thickness skin injuries requiring either skin grafting or skin replacement therapy is important. Also providing the treatment within the first 3 weeks following the injury and achieving wound healing is critical. Hence, the availability of cultured keratinocytes for cell-based therapy as early as possible within this limited time frame is essential to provide the necessary treatment. The utilisation of microcarriers for keratinocyte cell culture can provide keratinocytes for wound application within the time frame of 3 weeks, hence reducing scarring and contracture formation.

Currently, standard keratinocyte cell culture for clinical use involves cell culture in tissue culture flasks and repeated cell passages. Keratinocytes are passaged several times to maintain the cells in a sub-confluent state until clinical application. Sub-confluent keratinocytes have been shown to facilitate better epithelial repair than cells grown to confluent sheets (Desai *et al.* 1991). Keratinocytes within confluent sheets demonstrate change from a proliferative to a differentiated phenotype with reduced

quality of wound repair (Desai *et al.* 1991). In comparison the use of microcarrier culture showed sufficient amounts of proliferative sub-confluent cells at low passage.

In the first *in vivo* experiment, the survival of GFP labelled keratinocytes following application on full thickness wounds was investigated. The study was terminated at two weeks to investigate the fate of the GFP transduced cells. As expected, epithelial closure was not achieved in the 2 weeks period, as a minimal period of 3 weeks is required to achieve full epithelial healing. Histological analysis of wound sections showed GFP-positive cells primarily in the superficial wound regions after 2 week. These results were consistent with previous work done at the Blond McIndoe Research Foundation (Ng *et al.* 1997), and results reported by (Vogt *et al.* 1994). Histological analysis of the wounds showed mainly dense granulation tissue, which was consistent with previous work (Currie *et al.* 2003). The use of PTFE wound chambers prevented keratinocyte migration from the wound edges, which in turn prevented epidermal regeneration by keratinocytes migration. Any epidermal cover, if any, would have been a result of either MCAK or SAK applied within the wound chamber.

The lack of epidermal cover could be related to the absence of dermal replacement therapy in combination with cultured keratinocytes application or simply due to the two-week study period. Both MCAK and SAK groups showed early signs of basement membrane regeneration and recreation of multi-layer architecture compared to lack of these features in the control group. These results also demonstrated the biocompatibility of the gelatin 'Cultispher G®' microcarriers in the porcine model, as no adverse reactions to the beads or wound infections were noted.

The initial *in vitro* studies showed the migration of keratinocytes from the surface of microcarriers to culture flasks, the first *in vivo* study demonstrated the same effect *in vivo*. The hypothesis was keratinocytes migration and proliferation *in vivo* would replicate the *in vitro* behaviour with microcarriers presence and subsequent degradation having no influence on the process. Keratinocyte cell culture on microcarriers in stirred

culture had no negative effects on cell survival or proliferation *in vivo*. The comparison between using microcarriers for keratinocyte culture and application, and sprayed keratinocytes showed comparable results. Despite not achieving full epithelial closure in the two groups, the advantages of the microcarrier culture were further explored in the next studies. Further *in vivo* studies were undertaken to assess achieving full epithelial closure using microcarrier delivered autologous keratinocyte.

In further *in vivo* studies, full epithelial closure and the effect on wound contraction, using MCAK in combination with STSG (Split thickness skin graft) was investigated.

The use of keratinocytes cell suspensions in combination with STSG has been investigated previously. Keratinocytes cell suspensions provided the epidermal component, while the STSG provided the dermal component. Fraulin *et al.* (1998) and Navarro *et al.* (2000) reported no difference in wound contraction rate following the use of cell suspension in combination with meshed STSG. Based on these studies, epithelial closure can be achieved using SAK and meshed STSG. Hence, in chapter 5, MCAK and SAK were compared in combination with widely meshed STSG (6:1), while using widely meshed STSG as control in square wounds without chambers.

It is worth noting that both these studies used non-cultured keratinocytes for wound application. The application of cultured keratinocytes has been reported to produce significant wound re-epithelialisation when compared with non cultured keratinocytes (Svensjo *et al.* 2001). The results from chapter 5 showed similar findings to the afore-mentioned study. The results showed that the addition of keratinocytes, as MCAK or SAK, had a clear effect on wound healing, particularly in relation to wound contraction.

Wound contraction was significantly less after treatment with MCAK or SAK compared to wounds treated with STSG alone. This lower wound contraction could be due to the keratinocytes themselves or their expression of paracrine factors. The results from this study are consistent with our previous results comparing STSG and SAK treatments at Blond McIndoe Research Foundation (Reid *et al.* 2007). The presence of paracrine

factors may reduce myofibroblast differentiation and therefore reduce wound contraction. Identifying these factors and quantifying their effect on wound contraction would require an *in vivo* model replicating the wound environment.

In the study described in chapter 5, there was no evidence of GFP-labelled cells persisting at 21 days in wounds treated with GFP-labelled MCAK or SAK. These results are again consistent with previous studies that have shown that GFP expression does not persist beyond two weeks (Kirsch *et al.* 2003, Pfutzner *et al.* 2006, Lu and Ghazizadeh 2007). Previous studies have shown that expression of transfected marker genes in the porcine *in vivo* model is lost in keratinocytes integrating in more basal layers of the neo-epithelium (Vogt *et al.* 1994). The results from chapter 5 are similar and support the above-mentioned findings from these previous studies as no GFP expression by keratinocytes was detected after 3 weeks.

Histological analysis showed the quality of epithelial repair was consistent between the MCAK and SAK groups. It is difficult to define the contribution of exogenous cells to wound re-epithelialisation due to the inability to trace GFP-labelled keratinocytes. It is still a possibility that keratinocytes within either MCAK or SAK did not survive within the wound environment. The fact that wounds within both the MCAK and SAK groups showed mature epithelium and less contraction compared to STSG alone makes this less likely. Also even in the presence of the widely meshed STSG, epithelial closure was unlikely within the 3-week period relying on endogenous keratinocyte migration alone.

However, due to the lack of supporting evidence about long-term survival, the reduction in wound contraction could be an effect of keratinocytes application method or the cells themselves. The use of microcarriers as a delivery method for keratinocytes or simply the addition of the exogenous keratinocytes could have produced the reduction in wound contraction.

In the third *in vivo* animal study in chapter 6, the use of the dermal substitute Integra® in combination with allogeneic keratinocytes on microcarriers or as cell spray was

investigated. Both groups were compared to the standard clinical application of Integra® and ultra-thin STSG; treatments in the 3 groups were done as two-stage procedures. The decision to use allogenic keratinocytes was a replication of the clinical use of allografts particularly in the management of extensive burn injuries.

In this study, the use of allogeneic cells facilitated epithelial wound closure of comparable quality to that of wounds treated with autologous cells or uSTSG. No GFP positive cells were found in any of the wounds from the MCAlK or SAlK groups. Epithelial closure was achieved in a comparable fashion to the control group where autologous keratinocytes were applied as ultra-thin STSG. Certainly, the inability to trace the keratinocytes post wound application hinders the assessment of the origin of the newly formed epithelium.

Hammond *et al.* (1987) demonstrated that cultured allogeneic sheet grafts survived longer than non-cultured allogeneic grafts in a mouse model. Their findings were mainly attributed to the loss of Langerhans cells in culture, which are involved in the graft rejection process as previously discussed. LaFrance and Armstrong (1999) reported that allogeneic fibroblasts delivered to partial-thickness porcine wounds on poly-(L-lactide) microcarriers were well tolerated. Also, allogeneic cells were beneficial in the treatment of chronic wounds, such as recalcitrant leg ulcers, when combined with the commercial product Apligraf® (Falanga and Sabolinski 1999).

It is likely that wound healing in the two groups (MCAlK and SAlK) was a result of epithelial migration from the wound edges rather than the allogeneic keratinocytes. Histological examination of the epithelium in the MCAlK and SAlK groups revealed similar quality epithelium to the control group. The combination treatments in the two groups played a role in promoting satisfactory wound closure comparable to autologous uSTSG use.

The “take” of cultured epithelial autografts is improved by the presence of a dermal layer (Chester *et al.* 2004, Cuono *et al.* 1986). In the study described in chapter 6,

Integra® was used as dermal replacement and to provide support to MCAlK and SAlK following wound application. As expected, the application of Integra® maintained the wound surface area up to day 21, when treatment was applied. It was noted from previous studies and discussed in chapter 5 that control wounds treated with widely meshed STSG alone were healed by day 21. Hence, the role of Integra® in reducing wound contraction and maintaining wound surface area can be assumed. It was difficult to accurately assess whether the reduction of wound contraction was a result of microcarriers use as a delivery vehicle or other variables within the wound environment. There is possibly a role for using allogeneic keratinocytes delivered on microcarriers for the improvement of wound healing. The application of allogeneic keratinocytes on microcarriers in combination with Integra® and Biobrane® reduced wound contraction, even though the mechanism is unclear. The epithelial closure achieved in the MCAlK and SAlK groups is unlikely to be replicated in a clinical situation due to graft rejection in immuno-competent humans.

The effect of autologous keratinocytes and fibroblasts delivered on microcarriers on wound contraction was assessed in chapter 7. Integra® is usually used as dermal replacement reference treatment in comparing new artificial dermal products (Druecke *et al.* 2004). Therefore in the study described in chapter 7, the effect of autologous keratinocytes and fibroblasts on microcarriers in combination with Integra® on wound contraction was investigated. As the results from the control group on the same animal model were available, 3 treatment groups were allocated in this study, MCAK-FB, MCAK, and SAK. The results from the 3 treatment groups were compared to the control group from the study in chapter 6 (Integra® and ultra-thin STSG).

A reduction in αSMA-positive cells in wounds treated with keratinocytes alone or keratinocytes with fibroblasts was demonstrated. Interpreting these results, it can be assumed that the addition of a cellular component in the form of autologous

keratinocytes with or without fibroblasts led to a reduction in the contraction of healing wounds.

The number of cells transplanted to the wound bed has a direct effect on wound contraction (Lamme *et al.* 2000). Further studies using variable cell counts on microcarriers are needed to establish whether the same effect can be replicated using microcarriers. The reduction in wound contraction observed in chapter 7 could be a result of the combination of keratinocytes and fibroblasts or simply the effect of increased cell populations within the wound.

A significant reduction in wound contraction occurred using microcarriers to deliver keratinocytes or keratinocytes with fibroblasts in combination with Integra®. Similar to the findings reported by Lamme *et al.* (2000), the presence of additional cells in the granulation tissue possibly reduced the need for cells to migrate from the wound margins. This is a process that would normally bring them into contact with the signals necessary for myofibroblast differentiation. It is also conceivable that keratinocytes or keratinocytes with fibroblasts delivered on microcarriers can reduce wound contraction more than cells delivered in suspension. This could potentially be due to keratinocytes being damaged during process of harvesting from tissue culture flasks. The results from the study in chapter 7 support this assumption since wounds treated with cells on microcarriers contracted approximately 10% less than those treated with sprayed cells.

The reduction in wound contraction may represent a small percentage, but the clinical significance of the change in wound contraction is valuable. A small reduction in wound contraction can possibly prevent contracture formation. The formation of skin contractures can lead to impairment of function and limitations of ranges of movement. Significant improvements in function, particularly over joints, can be achieved when contracture formation is avoided.

It is arguable that microcarriers could offer a better method of delivery for keratinocytes and fibroblasts when compared with cell spray despite the lack of strong evidence, the

advantages of microcarriers culture over the traditional culture in tissue culture flasks required for cell spray were discussed in the *in vitro* studies.

In conclusion, both the *in vitro* and *in vivo* studies collectively demonstrated that the use of microcarriers in culture and delivery of keratinocytes and/or fibroblasts had many advantages. The use of microcarriers allowed the transfer of cells to the wound bed without the use of trypsin for cell harvest. Avoiding the use of trypsin could enhance the ability of the cultured keratinocytes to re-epithelialise the wound and generate neo-epithelium. The handling and application of microcarriers and keratinocytes or fibroblasts was similar to sprayed cell application. There were no major technical difficulties associated with the application of microcarriers and cultured cells on porcine wound model. The inert characteristics of the microcarriers achieved the delivery of cultured cells to the wound bed with minimal impact on the keratinocytes or the wound environment. The reduction in contraction achieved using microcarriers for culture and delivery of keratinocytes represented a highly desirable outcome in the treatment of full-thickness wounds.

The findings from this work were significant as they highlighted a real potential for clinical benefit to patients sustaining large full-thickness wounds. Microcarrier-keratinocyte culture could be used to reconstruct and restore the function of the epidermis in combination with dermal replacement therapies. Potentially, the use of microcarriers could be modulated to reduce wound contraction, guide the regeneration of epidermis, and the interactions between cells responsible for wound contraction. The early provision of viable keratinocytes supported by a dermal component is likely to be conducive to a less contractile myofibroblast phenotype resulting in reduced wound contraction.

Finally, microcarriers clearly have great potential in skin tissue engineering applications. Microcarriers can be used in expansion of keratinocytes and fibroblasts and investigation of cellular differentiation in culture. This can be achieved in an

efficient culture method that saves cost and space needed for culture. Therefore, microcarriers could be considered a very useful tool for skin regeneration research and future clinical application. In the near future, microcarriers could play an important role in clinical restoration of skin barrier following burn injuries and trauma.

Through a better understanding of the mechanisms behind wound contraction, new treatment modalities to reduce wound contraction can be developed. Any minimal reduction in wound contraction resulting in avoiding contracture formation could have a significant improvement in patients' lives following extensive skin loss injuries.

8.4 Assessment of hypotheses

8.2.1 Human and pig keratinocytes will attach to microcarrier beads *in vitro* and proliferate under *in vitro* culture conditions

This hypothesis is supported

8.2.2 Cultured autologous pig keratinocytes on microcarrier beads will migrate from the microcarrier beads and integrate into neo-epithelium when applied to porcine full thickness wounds

This hypothesis is partly supported

8.2.3 Green fluorescent protein is a long-term retroviral genetic marker in cultured pig keratinocytes on microcarrier beads when applied to full thickness wounds

This hypothesis is rejected

8.2.4 Cultured autologous pig keratinocytes on microcarrier beads will form permanent epithelium when applied to full thickness wounds

This hypothesis is partly supported

8.2.5 Cultured autologous pig keratinocytes on microcarrier beads will reduce wound contracture when applied to full thickness wounds in combination with widely meshed split skin graft

This hypothesis is supported

8.2.6 Cultured allogeneic pig keratinocytes on microcarrier beads in combination with two-stage artificial dermal regeneration template and artificial skin replacement will produce epithelial closure when applied to full thickness wounds

This hypothesis is partly supported

8.2.7 Cultured allogeneic pig keratinocytes on microcarrier beads in combination with two-stage artificial dermal regeneration template and artificial skin replacement will reduce wound contracture when applied to full thickness wounds

This hypothesis is supported

8.2.8 Cultured autologous pig keratinocytes and fibroblasts on microcarrier beads in combination with two-stage artificial dermal regeneration template will form a permanent functional epithelium when applied to full thickness wounds

This hypothesis is partly supported

8.2.9 Cultured autologous pig keratinocytes and fibroblasts on microcarrier beads in combination with two-stage artificial dermal regeneration template will reduce wound contraction in full thickness wounds

This hypothesis is supported

8.5 Future research

Continuous development of the methods used for keratinocyte culture is needed to improve their availability for clinical application. Efficient cell culture techniques, higher productivity and media free from animal products are all areas for future development.

The number of cells produced should increase for the same cost and in a similar space improving cost efficiency, along with more robust culture methods. If possible the number of patient interventions in term of cell applications should be minimised reducing labour hours and infection rates.

Future research in the field of keratinocyte cell culture continues to be challenging and more *in vivo* wound models are required. The aspects for improvement include for example, culture productivity, co-culture of keratinocytes and fibroblasts, and delivery methods to the wound.

Further research may look at different types of materials for microcarrier beads such as cellulose or poly D, L-lactic-co-glycolic acid (PLGA), or possibly growing cells without pre-expansion. The newly developed materials ideally should be biodegradable and biologically inert. Improvements such as the usage of defined mediums and robust application techniques could be achieved in the future.

The interactions between keratinocytes on microcarriers and dermal replacement template "Integra®" shown in the previous studies are interesting. There are different types of artificial dermis available commercially, and further research is now required to explore the benefits of their use with MCAK in various *in vivo* wound models. These studies comparing the various types of artificial dermis would explore epithelial regeneration and the effect on wound contraction.

There is evidence suggesting that myofibroblast differentiation is controlled by keratinocytes through paracrine growth factors (Shephard *et al.* 2004b). Further studies are required to investigate their mechanism of action and possibly the development of

similar molecules *in vitro*. The balance between keratinocytes and fibroblasts during wound healing needs to be explored *in vivo*. The main aim would be to produce stable neo-epithelium without wound contracture formation.

There have been several attempts to combine autologous cultured keratinocytes and dermal substitutes (Boyce *et al.* 2006b). Despite these attempts, there is no true replacement for skin including sweat glands, hair follicles, and nerve endings. The development of such off the shelf product may be still years away, but the possibility of combining keratinocytes, fibroblasts, and dermal replacement may be a first step.

Another area of future research is the modification of allogeneic keratinocytes during culture prior to wound application. This modification could be in the form of inhibition of the allogeneic keratinocytes from inducing a host immune response, and possibly reducing time required for keratinocytes in culture. This achievement could open the horizon for scaling-up *in vitro* keratinocyte cell culture without relying on conventional culture methods.

Another area of potential development is targeting the complex interactions between various growth factors and cytokines in wound healing using biological therapies. The majority of the biological therapies primarily aim to reduce hypertrophic or keloid scarring such as TGF-β antagonists, basic fibroblast growth factor, and Rho-associated kinase inhibitors (Sharpe and Martin 2013).

The use of microcarrier beads for keratinocyte cell culture and delivery is a relatively new area of research, which is rapidly expanding. The results from the studies in this thesis may pave the way for a randomised controlled clinical trial in the near future.

Publications and presentations from thesis:

9.1 Publications

1. Comparative analysis of two types of gelatin microcarrier beads for the culture of keratinocytes *in vitro*

   M Eldardiri, K Jubin, J Roxburgh, and JR Sharpe. *EWMA Journal 2010, Volume 10 no 2 (p. 5-11)*

2. Microcarriers and Their Potential in Tissue Regeneration

   Y Martin, M Eldardiri, DJ Lawrence-Watt, and JR Sharpe. Tissue Engineering*: Part B, Volume 17, Number 1, 2011 (p. 71-80)*

3. Wound Contraction Is Significantly Reduced by the Use of Microcarriers to Deliver Keratinocytes and Fibroblasts in an i*n vivo* Pig Model of Wound Repair and Regeneration

   M Eldardiri, Y Martin, J Roxburgh, DJ Lawrence-Watt, and JR Sharpe. Tissue Engineering*: Part A, Volume 18, Numbers 5 and 6, 2012 (p. 587-597)*

9.2 Presentations

International

1. 'Culture and delivery of autologous keratinocytes on micro-carrier beads for cutaneous repair'

   M Eldardiri, Y Martin and J Sharpe

   Poster in (TERMIS-EU) Tissue Engineering and Regenerative Medicine International Society-European chapter meeting, Galway, Ireland (June 2010)

2. 'Microcarrier beads for the culture of Keratinocytes *in vitro*, what's next?'

   M Eldardiri, K Jubin, J Roxburgh, and J Sharpe

   Presentation in (EUPRAS) European Association of Plastic Surgeons meeting, Rhodes, Greece (September 2009)

3. ‘Microcarrier beads for the culture of Keratinocytes, an *in vivo* model’

   M Eldardiri, K Jubin, J Roxburgh, and J Sharpe

   Presentation in (TERMIS) Tissue Engineering and Regenerative Medicine International Society meeting, Seoul, South Korea (August 2009)

4. ‘*In vitro* analysis of two types of microcarrier beads for the culture of keratinocytes ’

   M Eldardiri, K Jubin, J Roxburgh, and J Sharpe

   Poster Presentation in 5th Joint meeting of (ETRS & WHS) European Tissue Repair Society and Wound Healing Society), Limoges, France (July 2009)

5. ‘Comparative analysis of two types of microcarrier beads for culture of keratinocytes *in vitro*’

   M Eldardiri, K Jubin, J Roxburgh, and J Sharpe

   Presentation in (EWMA) European Wound management association 19th annual meeting, Helsinki, Finland (May 2009)

National

1. ‘The combination of Integra and autologous keratinocytes-fibroblasts reduce wound contraction in full thickness wound animal model’

   M Eldardiri, Y Martin, Judy Roxburgh, and J Sharpe

   Presentation in (BAPRAS) British Association of Plastic Reconstructive and Aesthetic Surgeons Summer meeting, Newcastle (July 2012)

2. ‘Autologous keratinocytes and fibroblasts delivered on microcarriers in combination with Integra reduce wound contraction *in vivo* porcine model’

   Y Martin, M Eldardiri, and J Sharpe

   Presentation in (TCES) Tissue and Cell Engineering Society meeting, Leeds University (July 2011)

3. ‘Culture and delivery of autologous keratinocytes on micro-carrier beads, an *in vitro* and *in vivo* model’

   M Eldardiri, Y Martin, and J Sharpe

   Poster in (TCES) Tissue Culture and Engineering Society meeting, Manchester (July 2010)

4. ‘Culture and delivery of autologous keratinocytes on micro-carrier beads for cutaneous repair *in vivo* animal model’

   M Eldardiri, Y Martin and J Sharpe

   Presentation in (BAPRAS) British Association of Plastic Reconstructive and Aesthetic Surgeons summer meeting, Sheffield (June 2010)

5. ‘Autologous keratinocytes on micro-carrier beads for cutaneous repair; a step forward?’

   M Eldardiri, Y Martin and J Sharpe

   Presentation in Douglas Murray Prize annual meeting (National West Midlands Plastic Surgery day) Birmingham (October 2009)

References

Abranches, E, Bekman, E, Henrique, D & Cabral, J M (2007) Expansion of mouse embryonic stem cells on microcarriers. *Biotechnol Bioeng,* 96**,** 1211-21.

Achauer, B M, Hewitt, C W, Black, K S, Martinez, S E, Waxman, K S, Ott, R A & Furnas, D W (1986) Long-term skin allograft survival after short-term cyclosporin treatment in a patient with massive burns. *Lancet,* 1**,** 14-5.

Adzick, N S & Lorenz, H P (1994) Cells, matrix, growth factors, and the surgeon. The biology of scarless fetal wound repair. *Ann Surg,* 220**,** 10-8.

Alam, H, Sehgal, L, Kundu, S T, Dalal, S N & Vaidya, M M (2011) Novel function of keratins 5 and 14 in proliferation and differentiation of stratified epithelial cells. *Mol Biol Cell,* 22**,** 4068-78.

Alexander, J W, MacMillan, B G, Law, E & Kittur, D S (1981) Treatment of severe burns with widely meshed skin autograft and meshed skin allograft overlay. *J Trauma,* 21**,** 433-8.

Algire, G H (1957) Diffusion-chamber techniques for studies of cellular immunity. *Ann N Y Acad Sci,* 69**,** 663-7.

Algire, G H, Borders, M L & Evans, V J (1958) Studies of heterografts in diffusion chambers in mice. *J Natl Cancer Inst,* 20**,** 1187-1201.

Andreassi, A, Bilenchi, R, Biagioli, M & D'Aniello, C (2005) Classification and pathophysiology of skin grafts. *Clin Dermatol,* 23**,** 332-7.

Andree, C, Reimer, C, Page, C P, Slama, J, Stark, B G & Eriksson, E (2001) Basement membrane formation during wound healing is dependent on epidermal transplants. *Plast Reconstr Surg,* 107**,** 97-104.

Athari, A, Unthan-Fechner, K, Schwartz, P & Probst, I (1988) Adult rat hepatocyte microcarrier culture. Comparison to the conventional dish culture system. *In Vitro Cell Dev Biol,* 24**,** 1085-91.

Atiyeh, B S & Costagliola, M (2007) Cultured epithelial autograft (CEA) in burn treatment: three decades later. *Burns,* 33**,** 405-13.

Aubock, J, Irschick, E, Romani, N, Kompatscher, P, Hopfl, R, Herold, M, Schuler, G, Bauer, M, Huber, C & Fritsch, P (1988) Rejection, after a slightly prolonged survival time, of Langerhans cell-free allogeneic cultured epidermis used for wound coverage in humans. *Transplantation,* 45**,** 730-7.

Bancel, S & Hu, W S (1996) Confocal laser scanning microscopy examination of cell distribution in macroporous microcarriers. *Biotechnol Prog,* 12**,** 398-402.

Bardouille, C, Lehmann, J, Heimann, P & Jockusch, H (2001) Growth and differentiation of permanent and secondary mouse myogenic cell lines on microcarriers. *Appl Microbiol Biotechnol,* 55**,** 556-62.

Baron, P, Traber, L D, Traber, D L, Nguyen, T, Hollyoak, M, Heggers, J P & Herndon, D N (1994) Gut failure and translocation following burn and sepsis. *J Surg Res,* 57**,** 197-204.

Barret, J P, Dziewulski, P, Ramzy, P I, Wolf, S E, Desai, M H & Herndon, D N (2000) Biobrane versus 1% silver sulfadiazine in second-degree pediatric burns. *Plast Reconstr Surg,* 105**,** 62-5.

Battal, M N, Hata, Y, Matsuka, K, Ito, O, Matsuda, H, Yoshida, Y & Kawazoe, T (1996) Reduction of progressive burn injury by a stable prostaglandin I2 analogue, beraprost sodium (Procylin): an experimental study in rats. *Burns,* 22**,** 531-8.

Baxter, C R (1993) Management of burn wounds. *Dermatol Clin,* 11**,** 709-14.

Baxter, C R & Shires, T (1968) Physiological response to crystalloid resuscitation of severe burns. *Ann N Y Acad Sci,* 150**,** 874-94.

Bayram, Y, Deveci, M, Imirzalioglu, N, Soysal, Y & Sengezer, M (2005) The cell based dressing with living allogenic keratinocytes in the treatment of foot ulcers: a case study. *Br J Plast Surg,* 58**,** 988-96.

Benichou, G, Yamada, Y, Yun, S H, Lin, C, Fray, M & Tocco, G (2011) Immune recognition and rejection of allogeneic skin grafts. *Immunotherapy,* 3**,** 757-70.

Bertolami, C & Donoff, R B (1979) The effect of full-thickness skin grafts on the actomyosin content of contracting wounds. *J Oral Surg,* 37**,** 471-6.

Bettex-Galland, M, Slongo, T, Hunziker, T, Wiesmann, U & Bettex, M (1988) Use of cultured keratinocytes in the treatment of severe burns. *Z Kinderchir,* 43**,** 224-8.

Bevan, S, Woodward, B, Ng, R L, Green, C & Martin, R (1997) Retroviral gene transfer into porcine keratinocytes following improved methods of cultivation. *Burns,* 23**,** 525-32.

Billingham, R E, Brent, L & Medawar, P B (1955) Acquired tolerance of skin homografts. *Ann N Y Acad Sci,* 59**,** 409-16.

Billingham, R E & Medawar, P B (1955) Contracture and intussusceptive growth in the healing of extensive wounds in mammalian skin. *J Anat,* 89**,** 114-23.

Billingham, R E & Russell, P S (1956) Studies on wound healing, with special reference to the phenomenon of contracture in experimental wounds in rabbits' skin. *Ann Surg,* 144**,** 961-81.

Blight, A, Mountford, E M, Cheshire, I M, Clancy, J M & Levick, P L (1991) Treatment of full skin thickness burn injury using cultured epithelial grafts. *Burns,* 17**,** 495-8.

Blumbach, K, Zweers, M C, Brunner, G, Peters, A S, Schmitz, M, Schulz, J N, Schild, A, Denton, C P, Sakai, T, Fassler, R, Krieg, T & Eckes, B (2010) Defective granulation tissue formation in mice with specific ablation of integrin-linked kinase in fibroblasts - role of TGFbeta1 levels and RhoA activity. *J Cell Sci,* 123**,** 3872-83.

Borg, D J, Dawson, R A, Leavesley, D I, Hutmacher, D W, Upton, Z & Malda, J (2009) Functional and phenotypic characterization of human keratinocytes expanded in microcarrier culture. *J Biomed Mater Res A,* 88**,** 184-94.

Borlongan, C V, Saporta, S & Sanberg, P R (1998) Intrastriatal transplantation of rat adrenal chromaffin cells seeded on microcarrier beads promote long-term functional recovery in hemiparkinsonian rats. *Exp Neurol,* 151**,** 203-14.

Boyce, S T (1996) Cultured skin substitutes: a review. *Tissue Eng,* 2**,** 255-66.

--- (1998) Skin substitutes from cultured cells and collagen-GAG polymers. *Med Biol Eng Comput,* 36**,** 791-800.

--- (2001) Design principles for composition and performance of cultured skin substitutes. *Burns,* 27**,** 523-33.

Boyce, S T, Anderson, B A & Rodriguez-Rilo, H L (2006a) Quantitative assay for quality assurance of human cells for clinical transplantation. *Cell Transplant,* 15**,** 169-74.

Boyce, S T, Christianson, D J & Hansbrough, J F (1988) Structure of a collagen-GAG dermal skin substitute optimized for cultured human epidermal keratinocytes. *J Biomed Mater Res,* 22**,** 939-57.

Boyce, S T, Foreman, T J, English, K B, Stayner, N, Cooper, M L, Sakabu, S & Hansbrough, J F (1991) Skin wound closure in athymic mice with cultured human cells, biopolymers, and growth factors. *Surgery,* 110**,** 866-76.

Boyce, S T & Hansbrough, J F (1988) Biologic attachment, growth, and differentiation of cultured human epidermal keratinocytes on a graftable collagen and chondroitin-6-sulfate substrate. *Surgery,* 103**,** 421-31.

Boyce, S T, Kagan, R J, Greenhalgh, D G, Warner, P, Yakuboff, K P, Palmieri, T & Warden, G D (2006b) Cultured skin substitutes reduce requirements for harvesting of skin autograft for closure of excised, full-thickness burns. *J Trauma,* 60**,** 821-9.

Braverman, I M & Keh-Yen, A (1981) Ultrastructure of the human dermal microcirculation. III. The vessels in the mid- and lower dermis and subcutaneous fat. *J Invest Dermatol,* 77**,** 297-304.

Brychta, P, Adler, J, Rihova, H, Suchanek, I, Kaloudova, Y & Koupil, J (2002) Cultured epidermal allografts: Quantitative evaluation of their healing effect in deep dermal burns. *Cell Tissue Bank,* 3**,** 15-23.

Burd, A & Chiu, T (2005) Allogenic skin in the treatment of burns. *Clin Dermatol,* 23**,** 376-87.

Burke, J F, Yannas, I V, Quinby, W C, Jr., Bondoc, C C & Jung, W K (1981) Successful use of a physiologically acceptable artificial skin in the treatment of extensive burn injury. *Ann Surg,* 194**,** 413-28.

Butler, C E, Yannas, I V, Compton, C C, Correia, C A & Orgill, D P (1999) Comparison of cultured and uncultured keratinocytes seeded into a collagen-GAG matrix for skin replacements. *Br J Plast Surg,* 52**,** 127-32.

Caruso, D M, Gregory, M W & Schiller, W R (1996) The use of skin from a monozygotic twin combined with cultured epithelial autografts as coverage for a large surface area burn: a case report and review of the literature. *J Burn Care Rehabil,* 17**,** 432-4.

Caruso, D M, Schuh, W H, Al-Kasspooles, M F, Chen, M C & Schiller, W R (1999) Cultured composite autografts as coverage for an extensive body surface area burn: case report and review of the technology. *Burns,* 25**,** 771-9.

Chang, A C, Dearman, B & Greenwood, J E (2011) A comparison of wound area measurement techniques: visitrak versus photography. *Eplasty,* 11**,** e18.

Chen, R, Curran, S J, Curran, J M & Hunt, J A (2006) The use of poly(l-lactide) and RGD modified microspheres as cell carriers in a flow intermittency bioreactor for tissue engineering cartilage. *Biomaterials,* 27**,** 4453-60.

Cherksey, B D, Sapirstein, V S & Geraci, A L (1996) Adrenal chromaffin cells on microcarriers exhibit enhanced long-term functional effects when implanted into the mammalian brain. *Neuroscience,* 75**,** 657-64.

Chester, D L, Balderson, D S & Papini, R P (2004) A review of keratinocyte delivery to the wound bed. *J Burn Care Rehabil,* 25**,** 266-75.

Choi, Y S, Park, S N & Suh, H (2008) The effect of PLGA sphere diameter on rabbit mesenchymal stem cells in adipose tissue engineering. *J Mater Sci Mater Med,* 19**,** 2165-71.

Chu, P G & Weiss, L M (2002) Keratin expression in human tissues and neoplasms. *Histopathology,* 40**,** 403-39.

Chun, K W, Yoo, H S, Yoon, J J & Park, T G (2004) Biodegradable PLGA microcarriers for injectable delivery of chondrocytes: effect of surface modification on cell attachment and function. *Biotechnol Prog,* 20**,** 1797-801.

Chung, H J, Kim, I K, Kim, T G & Park, T G (2008) Highly open porous biodegradable microcarriers: in vitro cultivation of chondrocytes for injectable delivery. *Tissue Eng Part A,* 14**,** 607-15.

Chung, H J & Park, T G (2009) Injectable cellular aggregates prepared from biodegradable porous microspheres for adipose tissue engineering. *Tissue Eng Part A,* 15**,** 1391-400.

Clowes, G H, Lund, C C & Levenson, S M (1943) The surface treatment of burns : A comparison of results of tannic acid, silver nitrate, triple dye, and vaseline or boric ointment as surface treatments in 150 cases. *Ann Surg,* 118**,** 761-79.

Compton, C C (1992) Current concepts in pediatric burn care: the biology of cultured epithelial autografts: an eight-year study in pediatric burn patients. *Eur J Pediatr Surg,* 2**,** 216-22.

Corps, B V (1969a) The effect of graft thickness, donor site and graft bed on graft shrinkage in the hooded rat. *Br J Plast Surg,* 22**,** 125-33.

--- (1969b) Wound contracture in the hooded rat in relation to skin tension lines and depth of injury. *Br J Plast Surg,* 22**,** 44-7.

Coulombe, P A, Kopan, R & Fuchs, E (1989) Expression of keratin K14 in the epidermis and hair follicle: insights into complex programs of differentiation. *J Cell Biol,* 109**,** 2295-312.

Cubison, T C, Pape, S A & Parkhouse, N (2006) Evidence for the link between healing time and the development of hypertrophic scars (HTS) in paediatric burns due to scald injury. *Burns,* 32**,** 992-9.

Cuono, C, Langdon, R & McGuire, J (1986) Use of cultured epidermal autografts and dermal allografts as skin replacement after burn injury. *Lancet,* 1**,** 1123-4.

Currie, L J, Martin, R, Sharpe, J R & James, S E (2003) A comparison of keratinocyte cell sprays with and without fibrin glue. *Burns,* 29**,** 677-85.

Daya, M (2008) Clinical experience and analysis of length gain with the use of seven-flap plasty in burn contractures. *Burns,* 34**,** 1022-6.

Deitch, E A (1985) A policy of early excision and grafting in elderly burn patients shortens the hospital stay and improves survival. *Burns Incl Therm Inj,* 12**,** 109-14.

Deitch, E A, Wheelahan, T M, Rose, M P, Clothier, J & Cotter, J (1983) Hypertrophic burn scars: analysis of variables. *J Trauma,* 23**,** 895-8.

Del Rio, M, Larcher, F, Serrano, F, Meana, A, Munoz, M, Garcia, M, Munoz, E, Martin, C, Bernad, A & Jorcano, J L (2002) A preclinical model for the analysis of genetically modified human skin in vivo. *Hum Gene Ther,* 13**,** 959-68.

Demarchez, M, Hartmann, D J, Regnier, M & Asselineau, D (1992) The role of fibroblasts in dermal vascularization and remodeling of reconstructed human skin after transplantation onto the nude mouse. *Transplantation,* 54**,** 317-26.

Demetriou, A A, Levenson, S M, Novikoff, P M, Novikoff, A B, Chowdhury, N R, Whiting, J, Reisner, A & Chowdhury, J R (1986a) Survival, organization, and function of microcarrier-attached hepatocytes transplanted in rats. *Proc Natl Acad Sci U S A,* 83**,** 7475-9.

Demetriou, A A, Reisner, A, Sanchez, J, Levenson, S M, Moscioni, A D & Chowdhury, J R (1988) Transplantation of microcarrier-attached hepatocytes into 90% partially hepatectomized rats. *Hepatology,* 8**,** 1006-9.

Demetriou, A A, Whiting, J F, Feldman, D, Levenson, S M, Chowdhury, N R, Moscioni, A D, Kram, M & Chowdhury, J R (1986b) Replacement of liver function in rats by transplantation of microcarrier-attached hepatocytes. *Science,* 233**,** 1190-2.

Desai, M H, Mlakar, J M, McCauley, R L, Abdullah, K M, Rutan, R L, Waymack, J P, Robson, M C & Herndon, D N (1991) Lack of long-term durability of cultured keratinocyte burn-wound coverage: a case report. *J Burn Care Rehabil,* 12**,** 540-5.

Desmouliere, A, Geinoz, A, Gabbiani, F & Gabbiani, G (1993) Transforming growth factor-beta 1 induces alpha-smooth muscle actin expression in granulation tissue myofibroblasts and in quiescent and growing cultured fibroblasts. *J Cell Biol,* 122**,** 103-11.

Desmouliere, A, Redard, M, Darby, I & Gabbiani, G (1995) Apoptosis mediates the decrease in cellularity during the transition between granulation tissue and scar. *Am J Pathol,* 146**,** 56-66.

Druecke, D, Lamme, E N, Hermann, S, Pieper, J, May, P S, Steinau, H U & Steinstraesser, L (2004) Modulation of scar tissue formation using different dermal regeneration templates in the treatment of experimental full-thickness wounds. *Wound Repair Regen,* 12**,** 518-27.

Du Toit, D F & Page, B J (2009) An in vitro evaluation of the cell toxicity of honey and silver dressings. *J Wound Care,* 18**,** 383-9.

Ebanks, J P, Koshoffer, A, Wickett, R R, Schwemberger, S, Babcock, G, Hakozaki, T & Boissy, R E (2011) Epidermal Keratinocytes from Light vs. Dark Skin Exhibit Differential Degradation of Melanosomes. *J Invest Dermatol*.

Ehrlich, H P (2004) Understanding experimental biology of skin equivalent: from laboratory to clinical use in patients with burns and chronic wounds. *Am J Surg,* 187**,** 29S-33S.

El Ghalbzouri, A, Hensbergen, P, Gibbs, S, Kempenaar, J, van der Schors, R & Ponec, M (2004) Fibroblasts facilitate re-epithelialization in wounded human skin equivalents. *Lab Invest,* 84**,** 102-12.

Elsdale, T & Bard, J (1972) Collagen substrata for studies on cell behavior. *J Cell Biol,* 54**,** 626-37.

Erdag, G & Sheridan, R L (2004) Fibroblasts improve performance of cultured composite skin substitutes on athymic mice. *Burns,* 30**,** 322-8.

Falanga, V & Sabolinski, M (1999) A bilayered living skin construct (APLIGRAF) accelerates complete closure of hard-to-heal venous ulcers. *Wound Repair Regen,* 7**,** 201-7.

Farmer, A W, Franks, W R, Young, D M, Maxmen, M & Chasmar, L R (1955) Effect of early excision of experimental burns. *Br J Plast Surg,* 7**,** 289-302.

Feng, C H, Yang, J Y, Chuang, S S, Huang, C Y, Hsiao, Y C & Lai, C Y (2010) Free medial thigh perforator flap for reconstruction of the dynamic and static complex burn scar contracture. *Burns,* 36**,** 565-71.

Foster, M A, Moledina, J & Jeffery, S L (2011) Epidemiology of U.K. military burns. *J Burn Care Res,* 32**,** 415-20.

Frank, D H (1984) Plastic surgery-important advances in clinical medicine: biobrane-a synthetic skin substitute. *West J Med,* 141**,** 234-5.

Frank, D H, Brahme, J & Van de Berg, J S (1984) Decrease in rate of wound contraction with the temporary skin substitute biobrane. *Ann Plast Surg,* 12**,** 519-24.

Fraulin, F O, Bahoric, A, Harrop, A R, Hiruki, T & Clarke, H M (1998) Autotransplantation of epithelial cells in the pig via an aerosol vehicle. *J Burn Care Rehabil,* 19**,** 337-45.

Fredriksson, C, Kratz, G & Huss, F (2008) Transplantation of cultured human keratinocytes in single cell suspension: a comparative in vitro study of different application techniques. *Burns,* 34**,** 212-9.

Freed, L E, Vunjak-Novakovic, G & Langer, R (1993) Cultivation of cell-polymer cartilage implants in bioreactors. *J Cell Biochem,* 51**,** 257-64.

Frodin, T & Skogh, M (1984) Measurement of transepidermal water loss using an evaporimeter to follow the restitution of the barrier layer of human epidermis after stripping the stratum corneum. *Acta Derm Venereol,* 64**,** 537-40.

Frondoza, C, Sohrabi, A & Hungerford, D (1996) Human chondrocytes proliferate and produce matrix components in microcarrier suspension culture. *Biomaterials,* 17**,** 879-88.

Gabbiani, G (1981) The myofibroblast: a key cell for wound healing and fibrocontractive diseases. *Prog Clin Biol Res,* 54**,** 183-94.

--- (1996) The cellular derivation and the life span of the myofibroblast. *Pathol Res Pract,* 192**,** 708-11.

--- (2003) The myofibroblast in wound healing and fibrocontractive diseases. *J Pathol,* 200**,** 500-3.

Gabbiani, G, Hirschel, B J, Ryan, G B, Statkov, P R & Majno, G (1972) Granulation tissue as a contractile organ. A study of structure and function. *J Exp Med,* 135**,** 719-34.

Gabbiani, G, Ryan, G B & Majne, G (1971) Presence of modified fibroblasts in granulation tissue and their possible role in wound contraction. *Experientia,* 27**,** 549-50.

Gangemi, E N, Gregori, D, Berchialla, P, Zingarelli, E, Cairo, M, Bollero, D, Ganem, J, Capocelli, R, Cuccuru, F, Cassano, P, Risso, D & Stella, M (2008) Epidemiology and risk factors for pathologic scarring after burn wounds. *Arch Facial Plast Surg,* 10**,** 93-102.

Gerding, R L, Emerman, C L, Effron, D, Lukens, T, Imbembo, A L & Fratianne, R B (1990) Outpatient management of partial-thickness burns: Biobrane versus 1% silver sulfadiazine. *Ann Emerg Med,* 19**,** 121-4.

Giard, D J, Thilly, W G, Wang, D I & Levine, D W (1977) Virus production with a newly developed microcarrier system. *Appl Environ Microbiol,* 34**,** 668-72.

Girdner, J (1881) Skin grafting with graft taken from the dead subjec. *Med Rec (NY),* 20**,** 119-20.

Gorodetsky, R, Vexler, A, Levdansky, L & Marx, G (2004) Fibrin microbeads (FMB) as biodegradable carriers for culturing cells and for accelerating wound healing. *Methods Mol Biol,* 238**,** 11-24.

Gottschaldt, K M & Vahle-Hinz, C (1981) Merkel cell receptors: structure and transducer function. *Science,* 214**,** 183-6.

Grant, I, Ng, R L, Woodward, B, Bevan, S, Green, C & Martin, R (2001) Demonstration of epidermal transfer from a polymer membrane using genetically marked porcine keratinocytes. *Burns,* 27**,** 1-8.

Green, H (1978) Cyclic AMP in relation to proliferation of the epidermal cell: a new view. *Cell,* 15**,** 801-11.

Grinnell, F (1978) Cellular adhesiveness and extracellular substrata. *Int Rev Cytol,* 53**,** 65-144.

Grinnell, F & Minter, D (1978) Attachment and spreading of baby hamster kidney cells to collagen substrata: effects of cold-insoluble globulin. *Proc Natl Acad Sci U S A,* 75**,** 4408-12.

Grishkevich, V M (2012) Ankle dorsiflexion postburn scar contractures: Anatomy and reconstructive techniques. *Burns*.

Grossman, R M, Krueger, J, Yourish, D, Granelli-Piperno, A, Murphy, D P, May, L T, Kupper, T S, Sehgal, P B & Gottlieb, A B (1989) Interleukin 6 is expressed in high levels in psoriatic skin and stimulates proliferation of cultured human keratinocytes. *Proc Natl Acad Sci U S A,* 86**,** 6367-71.

Gustafson, C J, Birgisson, A, Junker, J, Huss, F, Salemark, L, Johnson, H & Kratz, G (2007) Employing human keratinocytes cultured on macroporous gelatin spheres to treat full thickness-wounds: an in vivo study on athymic rats. *Burns,* 33**,** 726-35.

Hammond, E J, Ng, R L, Stanley, M A & Munro, A J (1987) Prolonged survival of cultured keratinocyte allografts in the nonimmunosuppressed mouse. *Transplantation,* 44**,** 106-12.

Han, S, McBride, D J, Losert, W & Leikin, S (2008) Segregation of type I collagen homo- and heterotrimers in fibrils. *J Mol Biol,* 383**,** 122-32.

Hansen, S L, Voigt, D W, Wiebelhaus, P & Paul, C N (2001) Using skin replacement products to treat burns and wounds. *Adv Skin Wound Care,* 14**,** 37-44; quiz 45-6.

Harris, P A, Leigh, I M & Navsaria, H A (1998) Pre-confluent keratinocyte grafting: the future for cultured skin replacements? *Burns,* 24**,** 591-3.

Harrison, C A, Dalley, A J & Mac Neil, S (2005) A simple in vitro model for investigating epithelial/mesenchymal interactions: keratinocyte inhibition of fibroblast proliferation and fibronectin synthesis. *Wound Repair Regen,* 13**,** 543-50.

Harrison, C A, Gossiel, F, Bullock, A J, Sun, T, Blumsohn, A & Mac Neil, S (2006a) Investigation of keratinocyte regulation of collagen I synthesis by dermal fibroblasts in a simple in vitro model. *Br J Dermatol,* 154**,** 401-10.

Harrison, C A, Gossiel, F, Layton, C M, Bullock, A J, Johnson, T, Blumsohn, A & MacNeil, S (2006b) Use of an in vitro model of tissue-engineered skin to investigate the mechanism of skin graft contraction. *Tissue Eng,* 12**,** 3119-33.

Harrison, C A & MacNeil, S (2008) The mechanism of skin graft contraction: an update on current research and potential future therapies. *Burns,* 34**,** 153-63.

Haslik, W, Kamolz, L P, Manna, F, Hladik, M, Rath, T & Frey, M (2010) Management of full-thickness skin defects in the hand and wrist region: first long-term experiences with the dermal matrix Matriderm. *J Plast Reconstr Aesthet Surg,* 63**,** 360-4.

Hecht, J, Hoefter, E A, Haraida, S, Nerlich, A, Hartinger, A, Muhlbauer, W & Dimoudis, N (1997) [Cultivated keratinocytes on micro-carriers: in vitro studies of a new carrier system]. *Handchir Mikrochir Plast Chir,* 29**,** 101-6.

Heimbach, D, Luterman, A, Burke, J, Cram, A, Herndon, D, Hunt, J, Jordan, M, McManus, W, Solem, L, Warden, G & et al. (1988) Artificial dermis for major burns. A multi-center randomized clinical trial. *Ann Surg,* 208**,** 313-20.

Hernon, C A, Dawson, R A, Freedlander, E, Short, R, Haddow, D B, Brotherston, M & MacNeil, S (2006) Clinical experience using cultured epithelial autografts leads to an alternative methodology for transferring skin cells from the laboratory to the patient. *Regen Med,* 1**,** 809-21.

Hinz, B (2007) Formation and function of the myofibroblast during tissue repair. *J Invest Dermatol,* 127**,** 526-37.

Hinz, B, Phan, S H, Thannickal, V J, Galli, A, Bochaton-Piallat, M L & Gabbiani, G (2007) The myofibroblast: one function, multiple origins. *Am J Pathol,* 170**,** 1807-16.

Hong, S J, Yu, H S & Kim, H W (2009) Tissue engineering polymeric microcarriers with macroporous morphology and bone-bioactive surface. *Macromol Biosci,* 9**,** 639-45.

Howard, G A, Turner, R T, Puzas, J E, Nichols, F & Baylink, D J (1983) Bone cells on microcarrier spheres. *JAMA,* 249**,** 258-9.

Huss, F R, Junker, J P, Johnson, H & Kratz, G (2007) Macroporous gelatine spheres as culture substrate, transplantation vehicle, and biodegradable scaffold for guided regeneration of soft tissues. In vivo study in nude mice. *J Plast Reconstr Aesthet Surg,* 60**,** 543-55.

Huss, F R, Nyman, E, Bolin, J S & Kratz, G (2010) Use of macroporous gelatine spheres as a biodegradable scaffold for guided tissue regeneration of healthy dermis in humans: an in vivo study. *J Plast Reconstr Aesthet Surg,* 63**,** 848-57.

Isik, S, Sahin, U, Ilgan, S, Guler, M, Gunalp, B & Selmanpakoglu, N (1998) Saving the zone of stasis in burns with recombinant tissue-type plasminogen activator (r-tPA): an experimental study in rats. *Burns,* 24**,** 217-23.

Jackson, D M (1953) The diagnosis of the depth of burning. *Br J Surg,* 40**,** 588-96.

Janzekovic, Z (1970) A new concept in the early excision and immediate grafting of burns. *J Trauma,* 10**,** 1103-8.

Jubin, K, Martin, Y, Lawrence-Watt, D J & Sharpe, J R (2011) A fully autologous co-culture system utilising non-irradiated autologous fibroblasts to support the expansion of human keratinocytes for clinical use. *Cytotechnology,* 63**,** 655-62.

Kadler, K E, Holmes, D F, Trotter, J A & Chapman, J A (1996) Collagen fibril formation. *Biochem J,* 316 (Pt 1)**,** 1-11.

Kangesu, T, Navsaria, H A, Manek, S, Fryer, P R, Leigh, I M & Green, C J (1993a) Kerato-dermal grafts: the importance of dermis for the in vivo growth of cultured keratinocytes. *Br J Plast Surg,* 46**,** 401-9.

Kangesu, T, Navsaria, H A, Manek, S, Shurey, C B, Jones, C R, Fryer, P R, Leigh, I M & Green, C J (1993b) A porcine model using skin graft chambers for studies on cultured keratinocytes. *Br J Plast Surg,* 46**,** 393-400.

Katayama, H, Itami, S, Koizumi, H & Tsutsui, M (1987) Epidermal cell culture using Sephadex beads coated with denatured collagen (cytodex 3). *J Invest Dermatol,* 88**,** 33-6.

Kauvar, D S, Wolf, S E, Wade, C E, Cancio, L C, Renz, E M & Holcomb, J B (2006) Burns sustained in combat explosions in Operations Iraqi and Enduring Freedom (OIF/OEF explosion burns). *Burns,* 32**,** 853-7.

Kempf, M, Miyamura, Y, Liu, P Y, Chen, A C, Nakamura, H, Shimizu, H, Tabata, Y, Kimble, R M & McMillan, J R (2011) A denatured collagen microfiber scaffold seeded with human fibroblasts and keratinocytes for skin grafting. *Biomaterials,* 32**,** 4782-92.

Khan, A A, Rawlins, J, Shenton, A F & Sharpe, D T (2007) The Bradford Burn Study: the epidemiology of burns presenting to an inner city emergency department. *Emerg Med J,* 24**,** 564-6.

Kim, K S, Kim, E S, Hwang, J H & Lee, S Y (2012) Medial sural perforator plus island flap: A modification of the medial sural perforator island flap for the reconstruction of postburn knee flexion contractures using burned calf skin. *J Plast Reconstr Aesthet Surg,* 65**,** 804-9.

Kim, S S, Gwak, S J, Choi, C Y & Kim, B S (2005) Skin regeneration using keratinocytes and dermal fibroblasts cultured on biodegradable microspherical polymer scaffolds. *J Biomed Mater Res B Appl Biomater,* 75**,** 369-77.

Kimmel, M, Darzynkiewicz, Z & Staiano-Coico, L (1986) Stathmokinetic analysis of human epidermal cells in vitro. *Cell Tissue Kinet,* 19**,** 289-304.

Kirsch, P, Hafner, M, Zentgraf, H & Schilling, L (2003) Time course of fluorescence intensity and protein expression in HeLa cells stably transfected with hrGFP. *Mol Cells,* 15**,** 341-8.

Kirsner, R S, Marston, W A, Snyder, R J, Lee, T D, Cargill, D I & Slade, H B (2012) Spray-applied cell therapy with human allogeneic fibroblasts and keratinocytes for the treatment of chronic venous leg ulcers: a phase 2, multicentre, double-blind, randomised, placebo-controlled trial. *Lancet,* 380**,** 977-85.

Klingenberg, J M, McFarland, K L, Friedman, A J, Boyce, S T, Aronow, B J & Supp, D M (2010) Engineered human skin substitutes undergo large-scale genomic reprogramming and normal skin-like maturation after transplantation to athymic mice. *J Invest Dermatol,* 130**,** 587-601.

Ko, M S & Marinkovich, M P (2010) Role of dermal-epidermal basement membrane zone in skin, cancer, and developmental disorders. *Dermatol Clin,* 28**,** 1-16.

Krupp, S, Wiesner, L, Krstic, R, Pescia, G & Winistorfer, B (1994) Mid-term results with cultured epidermal autografts, allogenic skin transplants and cyclosporin A medication. *Burns,* 20**,** 15-20.

Kung, T A, Jebson, P J & Cederna, P S (2012) An individualized approach to severe elbow burn contractures. *Plast Reconstr Surg,* 129**,** 663e-73e.

LaFrance, M L & Armstrong, D W (1999) Novel living skin replacement biotherapy approach for wounded skin tissues. *Tissue Eng,* 5**,** 153-70.

Lal, S, Barrow, R E, Wolf, S E, Chinkes, D L, Hart, D W, Heggers, J P & Herndon, D N (2000) Biobrane improves wound healing in burned children without increased risk of infection. *Shock,* 14**,** 314-8; discussion 318-9.

Lamme, E N, Van Leeuwen, R T, Brandsma, K, Van Marle, J & Middelkoop, E (2000) Higher numbers of autologous fibroblasts in an artificial dermal substitute improve tissue regeneration and modulate scar tissue formation. *J Pathol,* 190**,** 595-603.

Lammers, G, Verhaegen, P D, Ulrich, M M, Schalkwijk, J, Middelkoop, E, Weiland, D, Nillesen, S T, Van Kuppevelt, T H & Daamen, W F (2011) An overview of methods for the in vivo evaluation of tissue-engineered skin constructs. *Tissue Eng Part B Rev,* 17**,** 33-55.

Lao, L, Tan, H, Wang, Y & Gao, C (2008) Chitosan modified poly(L-lactide) microspheres as cell microcarriers for cartilage tissue engineering. *Colloids Surf B Biointerfaces,* 66**,** 218-25.

Larsen, C P, Steinman, R M, Witmer-Pack, M, Hankins, D F, Morris, P J & Austyn, J M (1990) Migration and maturation of Langerhans cells in skin transplants and explants. *J Exp Med,* 172**,** 1483-93.

Le Poole, I C & Boyce, S T (1999) Keratinocytes suppress transforming growth factor-beta1 expression by fibroblasts in cultured skin substitutes. *Br J Dermatol,* 140**,** 409-16.

Leigh, I M, Purkis, P E, Navsaria, H A & Phillips, T J (1987) Treatment of chronic venous ulcers with sheets of cultured allogenic keratinocytes. *Br J Dermatol,* 117**,** 591-7.

Leon-Villapalos, J, Eldardiri, M & Dziewulski, P (2010) The use of human deceased donor skin allograft in burn care. *Cell Tissue Bank,* 11**,** 99-104.

Levine, D W, Wong, J S, Wang, D I & Thilly, W G (1977) Microcarrier cell culture: new methods for research-scale application. *Somatic Cell Genet,* 3**,** 149-55.

Limat, A, Hunziker, T, Boillat, C, Noser, F & Wiesmann, U (1990) Postmitotic human dermal fibroblasts preserve intact feeder properties for epithelial cell growth after long-term cryopreservation. *In Vitro Cell Dev Biol,* 26**,** 709-12.

Lin, S D, Chai, C Y, Lai, C S & Chou, C K (1993) Allogeneic microskin grafting of rabbits' skin wounds. *Burns,* 19**,** 208-14.

Liu, J Y, Hafner, J, Dragieva, G & Burg, G (2006) A novel bioreactor microcarrier cell culture system for high yields of proliferating autologous human keratinocytes. *Cell Transplant,* 15**,** 435-43.

Liu, J Y, Hafner, J, Dragieva, G, Seifert, B & Burg, G (2004) Autologous cultured keratinocytes on porcine gelatin microbeads effectively heal chronic venous leg ulcers. *Wound Repair Regen,* 12**,** 148-56.

Liu, S, Xu, S W, Blumbach, K, Eastwood, M, Denton, C P, Eckes, B, Krieg, T, Abraham, D J & Leask, A (2010) Expression of integrin beta1 by fibroblasts is required for tissue repair in vivo. *J Cell Sci,* 123**,** 3674-82.

Livak, K J & Schmittgen, T D (2001) Analysis of relative gene expression data using real-time quantitative PCR and the 2(-Delta Delta C(T)) Method. *Methods,* 25**,** 402-8.

Lu, W, Yu, J, Zhang, Y, Ji, K, Zhou, Y, Li, Y, Deng, Z & Jin, Y (2012) Mixture of fibroblasts and adipose tissue-derived stem cells can improve epidermal morphogenesis of tissue-engineered skin. *Cells Tissues Organs,* 195**,** 197-206.

Lu, Z & Ghazizadeh, S (2007) Loss of transgene following ex vivo gene transfer is associated with a dominant Th2 response: implications for cutaneous gene therapy. *Mol Ther,* 15**,** 954-61.

Mackenzie, J C (1969) Ordered structure of the stratum corneum of mammalian skin. *Nature,* 222**,** 881-2.

Macmillan, B G (1958) Early excision of more than twenty-five percent of body surface in the extensively burned patient; an evaluation. *AMA Arch Surg,* 77**,** 369-75.

Macmillan, B G & Artz, C P (1957) A planned evaluation of early excision of more than twenty-five per cent of the body surface in burns. *Surg Forum,* 7**,** 88-93.

MacNeil, S (2007) Progress and opportunities for tissue-engineered skin. *Nature,* 445**,** 874-80.

Magnusson, M, Papini, R P, Rea, S M, Reed, C C & Wood, F M (2007) Cultured autologous keratinocytes in suspension accelerate epithelial maturation in an in vivo wound model as measured by surface electrical capacitance. *Plast Reconstr Surg,* 119**,** 495-9.

Majno, G, Gabbiani, G, Hirschel, B J, Ryan, G B & Statkov, P R (1971) Contraction of granulation tissue in vitro: similarity to smooth muscle. *Science,* 173**,** 548-50.

Malda, J, Kreijveld, E, Temenoff, J S, van Blitterswijk, C A & Riesle, J (2003) Expansion of human nasal chondrocytes on macroporous microcarriers enhances redifferentiation. *Biomaterials,* 24**,** 5153-61.

Marcusson, J A, Lindgren, C, Berghard, A & Toftgard, R (1992) Allogeneic cultured keratinocytes in the treatment of leg ulcers. A pilot study. *Acta Derm Venereol,* 72**,** 61-4.

Martin, B R, Sangalang, M, Wu, S & Armstrong, D G (2005) Outcomes of allogenic acellular matrix therapy in treatment of diabetic foot wounds: an initial experience. *Int Wound J,* 2**,** 161-5.

Martin, Y, Eldardiri, M, Lawrence-Watt, D J & Sharpe, J R (2011) Microcarriers and their potential in tissue regeneration. *Tissue Eng Part B Rev,* 17**,** 71-80.

Masur, S K, Dewal, H S, Dinh, T T, Erenburg, I & Petridou, S (1996) Myofibroblasts differentiate from fibroblasts when plated at low density. *Proc Natl Acad Sci U S A,* 93**,** 4219-23.

Meignier, B (1979) Cell culture on beads used for the industrial production of foot-and-mouth disease virus. *Dev Biol Stand,* 42**,** 141-5.

Mered, B, Albrecht, P & Hopps, H E (1980) Cell growth optimization in microcarrier culture. *In Vitro,* 16**,** 859-65.

Moiemen, N S, Vlachou, E, Staiano, J J, Thawy, Y & Frame, J D (2006) Reconstructive surgery with Integra dermal regeneration template: histologic study, clinical evaluation, and current practice. *Plast Reconstr Surg,* 117**,** 160S-174S.

Moll, R, Franke, W W, Schiller, D L, Geiger, B & Krepler, R (1982) The catalog of human cytokeratins: patterns of expression in normal epithelia, tumours and cultured cells. *Cell,* 31**,** 11-24.

Montagna, W & Yun, J S (1964) The skin of the domestic pig. *J Invest Dermatol,* 42**,** 11-21.

Montandon, D, D'Andiran, G & Gabbiani, G (1977) The mechanism of wound contraction and epithelialization: clinical and experimental studies. *Clin Plast Surg,* 4**,** 325-46.

Mowlem, R (1952) Skin homografts. *Med Illus,* 6**,** 552-5.

Mujaj, S, Manton, K, Upton, Z & Richards, S (2010) Serum-free primary human fibroblast and keratinocyte coculture. *Tissue Eng Part A,* 16**,** 1407-20.

Myers, S R, Partha, V N, Soranzo, C, Price, R D & Navsaria, H A (2007) Hyalomatrix: a temporary epidermal barrier, hyaluronan delivery, and neodermis induction system for keratinocyte stem cell therapy. *Tissue Eng,* 13**,** 2733-41.

Navarro, F A, Stoner, M L, Park, C S, Huertas, J C, Lee, H B, Wood, F M & Orgill, D P (2000) Sprayed keratinocyte suspensions accelerate epidermal coverage in a porcine microwound model. *J Burn Care Rehabil,* 21**,** 513-8.

Navsaria, H A, Myers, S R, Leigh, I M & McKay, I A (1995) Culturing skin in vitro for wound therapy. *Trends Biotechnol,* 13**,** 91-100.

Ng, R L, Woodward, B, Bevan, S, Green, C & Martin, R (1997) Retroviral marking identifies grafted autologous keratinocytes in porcine wounds receiving cultured epithelium. *J Invest Dermatol,* 108**,** 457-62.

Nguyen, D Q & Dickson, W A (2006) A review of the use of a dermal skin substitute in burns care. *J Wound Care,* 15**,** 373-6.

Nguyen, D Q, Potokar, T S & Price, P (2010) An objective long-term evaluation of Integra (a dermal skin substitute) and split thickness skin grafts, in acute burns and reconstructive surgery. *Burns,* 36**,** 23-8.

Nillesen, S T, Lammers, G, Wismans, R G, Ulrich, M M, Middelkoop, E, Spauwen, P H, Faraj, K A, Schalkwijk, J, Daamen, W F & van Kuppevelt, T H (2011) Design and in vivo evaluation of a molecularly defined acellular skin construct: reduction of early contraction and increase in early blood vessel formation. *Acta Biomater,* 7**,** 1063-71.

Obaidullah, Ullah, H & Aslam, M (2005) Figure-of-8 sling for prevention of recurrent axillary contracture after release and skin grafting. *Burns,* 31**,** 283-9.

Okhovatian, F & Zoubine, N (2007) A comparison between two burn rehabilitation protocols. *Burns,* 33**,** 429-34.

Ong, Y S, Samuel, M & Song, C (2006) Meta-analysis of early excision of burns. *Burns,* 32**,** 145-50.

Parry, I, Walker, K, Niszczak, J, Palmieri, T & Greenhalgh, D (2010) Methods and tools used for the measurement of burn scar contracture. *J Burn Care Res,* 31**,** 888-903.

Peck, M D, Kessler, M, Meyer, A A & Bonham Morris, P A (2002) A trial of the effectiveness of artificial dermis in the treatment of patients with burns greater than 45% total body surface area. *J Trauma,* 52**,** 971-8.

Pelle, E, Mammone, T, Maes, D & Frenkel, K (2005) Keratinocytes act as a source of reactive oxygen species by transferring hydrogen peroxide to melanocytes. *J Invest Dermatol,* 124**,** 793-7.

Peura, M, Kaartinen, I, Suomela, S, Hukkanen, M, Bizik, J, Harjula, A, Kankuri, E & Vuola, J (2012) Improved skin wound epithelialization by topical delivery of soluble factors from fibroblast aggregates. *Burns,* 38**,** 541-50.

Peura, M, Siltanen, A, Saarinen, I, Soots, A, Bizik, J, Vuola, J, Harjula, A & Kankuri, E (2010) Paracrine factors from fibroblast aggregates in a fibrin-matrix carrier enhance keratinocyte viability and migration. *J Biomed Mater Res A,* 95**,** 658-64.

Pfutzner, W, Joari, M R, Foster, R A & Vogel, J C (2006) A large preclinical animal model to assess ex vivo skin gene therapy applications. *Arch Dermatol Res,* 298**,** 16-22.

Pham, C, Greenwood, J, Cleland, H, Woodruff, P & Maddern, G (2007) Bioengineered skin substitutes for the management of burns: a systematic review. *Burns,* 33**,** 946-57.

Philandrianos, C, Andrac-Meyer, L, Mordon, S, Feuerstein, J M, Sabatier, F, Veran, J, Magalon, G & Casanova, D (2012) Comparison of five dermal substitutes in full-thickness skin wound healing in a porcine model. *Burns*.

Phillips, T J (1991) Cultured epidermal allografts--a temporary or permanent solution? *Transplantation,* 51**,** 937-41.

Pianigiani, E, Ierardi, F, Cherubini Di Simplicio, F & Andreassi, A (2005) Skin bank organization. *Clin Dermatol,* 23**,** 353-6.

Pineau, N, Bernerd, F, Cavezza, A, Dalko-Csiba, M & Breton, L (2008) A new C-xylopyranoside derivative induces skin expression of glycosaminoglycans and heparan sulphate proteoglycans. *Eur J Dermatol,* 18**,** 36-40.

Powell, D W, Mifflin, R C, Valentich, J D, Crowe, S E, Saada, J I & West, A B (1999) Myofibroblasts. I. Paracrine cells important in health and disease. *Am J Physiol,* 277**,** C1-9.

Prunieras, M (1979) Recent advances in epidermal cell cultures. *Arch Dermatol Res,* 264**,** 243-7.

Prunieras, M, Delescluse, C & Regnier, M (1976) The culture of skin. A review of theories and experimental methods. *J Invest Dermatol,* 67**,** 58-65.

Prunieras, M, Regnier, M, Fougere, S & Woodley, D (1983) Keratinocytes synthesize basal-lamina proteins in culture. *J Invest Dermatol,* 81**,** 74s-81s.

Purkis, P E, Steel, J B, Mackenzie, I C, Nathrath, W B, Leigh, I M & Lane, E B (1990) Antibody markers of basal cells in complex epithelia. *J Cell Sci,* 97 (Pt 1)**,** 39-50.

Reid, M J, Currie, L J, James, S E & Sharpe, J R (2007) Effect of artificial dermal substitute, cultured keratinocytes and split thickness skin graft on wound contraction. *Wound Repair Regen,* 15**,** 889-96.

Rennekampff, H O, Hansbrough, J F, Kiessig, V, Abiezzi, S & Woods, V, Jr. (1996) Wound closure with human keratinocytes cultured on a polyurethane dressing overlaid on a cultured human dermal replacement. *Surgery,* 120**,** 16-22.

Rheinwald, J G & Green, H (1975a) Formation of a keratinizing epithelium in culture by a cloned cell line derived from a teratoma. *Cell,* 6**,** 317-30.

--- (1975b) Serial cultivation of strains of human epidermal keratinocytes: the formation of keratinizing colonies from single cells. *Cell,* 6**,** 331-43.

--- (1977) Epidermal growth factor and the multiplication of cultured human epidermal keratinocytes. *Nature,* 265**,** 421-4.

Richard, R, Baryza, M J, Carr, J A, Dewey, W S, Dougherty, M E, Forbes-Duchart, L, Franzen, B J, Healey, T, Lester, M E, Li, S K, Moore, M, Nakamura, D, Nedelec, B, Niszczak, J, Parry, I S, Quick, C D, Serghiou, M, Ward, R S, Ware, L & Young, A (2009) Burn rehabilitation and research: proceedings of a consensus summit. *J Burn Care Res,* 30**,** 543-73.

Richters, C D, Hoekstra, M J, du Pont, J S, Kreis, R W & Kamperdijk, E W (2005) Immunology of skin transplantation. *Clin Dermatol,* 23**,** 338-42.

Richters, C D, van Gelderop, E, du Pont, J S, Hoekstra, M J, Kreis, R W & Kamperdijk, E W (1999) Migration of dendritic cells to the draining lymph node after allogeneic or congeneic rat skin transplantation. *Transplantation,* 67**,** 828-32.

Ronfard, V, Broly, H, Mitchell, V, Galizia, J P, Hochart, D, Chambon, E, Pellerin, P & Huart, J J (1991) Use of human keratinocytes cultured on fibrin glue in the treatment of burn wounds. *Burns,* 17**,** 181-4.

Roosterman, D, Goerge, T, Schneider, S W, Bunnett, N W & Steinhoff, M (2006) Neuronal control of skin function: the skin as a neuroimmunoendocrine organ. *Physiol Rev,* 86**,** 1309-79.

Ross, J A & Hulbert, K F (1940) Treatment of Burns by Silver Nitrate, Tannic Acid, and Gentian Violet. *Br Med J,* 2**,** 702-703.

Rudolph, R (1979) Location of the force of wound contraction. *Surg Gynecol Obstet,* 148**,** 547-51.

--- (1980) Contraction and the control of contraction. *World J Surg,* 4**,** 279-87.

Rudolph, R & Woodward, M (1978) Spatial orientation of microtubules in contractile fibroblasts in vivo. *Anat Rec,* 191**,** 169-81.

Salsbury, A J & Clarke, J A (1967) New method for detecting changes in the surface appearance of human red blood cells. *J Clin Pathol,* 20**,** 603-10.

Saporta, S, Borlongan, C, Moore, J, Mejia-Millan, E, Jones, S L, Bonness, P, Randall, T S, Allen, R C, Freeman, T B & Sanberg, P R (1997) Microcarrier enhanced survival of human and rat fetal ventral mesencephalon cells implanted in the rat striatum. *Cell Transplant,* 6**,** 579-84.

Sappino, A P, Schurch, W & Gabbiani, G (1990) Differentiation repertoire of fibroblastic cells: expression of cytoskeletal proteins as marker of phenotypic modulations. *Lab Invest,* 63**,** 144-61.

Sato, K, Kang, W H, Saga, K & Sato, K T (1989) Biology of sweat glands and their disorders. I. Normal sweat gland function. *J Am Acad Dermatol,* 20**,** 537-63.

Sawhney, C P & Monga, H L (1970) Wound contraction in rabbits and the effectiveness of skin grafts in preventing it. *Br J Plast Surg,* 23**,** 318-21.

Schneider, J, Biedermann, T, Widmer, D, Montano, I, Meuli, M, Reichmann, E & Schiestl, C (2009) Matriderm versus Integra: a comparative experimental study. *Burns,* 35**,** 51-7.

Schneider, J C, Holavanahalli, R, Helm, P, Goldstein, R & Kowalske, K (2006) Contractures in burn injury: defining the problem. *J Burn Care Res,* 27**,** 508-14.

Schone, G (1906) Bruns Beitr KIin Chir. 61**,** 1.

Seland, H, Gustafson, C J, Johnson, H, Junker, J P & Kratz, G (2011) Transplantation of acellular dermis and keratinocytes cultured on porous biodegradable microcarriers into full-thickness skin injuries on athymic rats. *Burns,* 37**,** 99-108.

Selye, H (1953) Use of granuloma pouch technic in the study of antiphlogistic corticoids. *Proc Soc Exp Biol Med,* 82**,** 328-33.

Serra, M, Brito, C, Leite, S B, Gorjup, E, von Briesen, H, Carrondo, M J & Alves, P M (2009) Stirred bioreactors for the expansion of adult pancreatic stem cells. *Ann Anat,* 191**,** 104-15.

Sharpe, J R & Martin, Y (2013) Strategies Demonstrating Efficacy in Reducing Wound Contraction. *Adv Wound Care (New Rochelle),* 2**,** 167-175.

Shephard, P, Hinz, B, Smola-Hess, S, Meister, J J, Krieg, T & Smola, H (2004a) Dissecting the roles of endothelin, TGF-beta and GM-CSF on myofibroblast differentiation by keratinocytes. *Thromb Haemost,* 92**,** 262-74.

Shephard, P, Martin, G, Smola-Hess, S, Brunner, G, Krieg, T & Smola, H (2004b) Myofibroblast differentiation is induced in keratinocyte-fibroblast co-cultures and is antagonistically regulated by endogenous transforming growth factor-beta and interleukin-1. *Am J Pathol,* 164**,** 2055-66.

Shima, M, Seino, Y, Tanaka, H, Kurose, H, Ishida, M, Yabuuchi, H & Kodama, H (1988) Microcarriers facilitate mineralization in MC3T3-E1 cells. *Calcif Tissue Int,* 43**,** 19-25.

Shupp, J W, Nasabzadeh, T J, Rosenthal, D S, Jordan, M H, Fidler, P & Jeng, J C (2010) A review of the local pathophysiologic bases of burn wound progression. *J Burn Care Res,* 31**,** 849-73.

Sinha, S, Degenstein, L, Copenhaver, C & Fuchs, E (2000) Defining the regulatory factors required for epidermal gene expression. *Mol Cell Biol,* 20**,** 2543-55.

Slominski, A, Wortsman, J, Paus, R, Elias, P M, Tobin, D J & Feingold, K R (2008) Skin as an endocrine organ: implications for its function. *Drug Discov Today Dis Mech,* 5**,** 137-144.

Sommar, P, Pettersson, S, Ness, C, Johnson, H, Kratz, G & Junker, J P (2010) Engineering three-dimensional cartilage- and bone-like tissues using human dermal fibroblasts and macroporous gelatine microcarriers. *J Plast Reconstr Aesthet Surg,* 63**,** 1036-46.

Spandau, D F, Marques, M, Bierhuizen, M, Wagemaker, G, Hurwitz, S, Pei, Y, Breese, R & Travers, J B (2000) Use of enhanced green fluorescent protein to monitor retroviral-mediated gene therapy in human keratinocytes. *Exp Dermatol,* 9**,** 252-7.

Stern, R, McPherson, M & Longaker, M T (1990) Histologic study of artificial skin used in the treatment of full-thickness thermal injury. *J Burn Care Rehabil,* 11**,** 7-13.

Stoker, M, O'Neill, C, Berryman, S & Waxman, V (1968) Anchorage and growth regulation in normal and virus-transformed cells. *Int J Cancer,* 3**,** 683-93.

Sullivan, T P, Eaglstein, W H, Davis, S C & Mertz, P (2001) The pig as a model for human wound healing. *Wound Repair Regen,* 9**,** 66-76.

Sun, T, Higham, M, Layton, C, Haycock, J, Short, R & MacNeil, S (2004) Developments in xenobiotic-free culture of human keratinocytes for clinical use. *Wound Repair Regen,* 12**,** 626-34.

Sun, T T, Eichner, R, Nelson, W G, Vidrich, A & Woodcock-Mitchell, J (1983) Keratin expression during normal epidermal differentiation. *Curr Probl Dermatol,* 11**,** 277-91.

Svensjo, T, Yao, F, Pomahac, B & Eriksson, E (2001) Autologous keratinocyte suspensions accelerate epidermal wound healing in pigs. *J Surg Res,* 99**,** 211-21.

Tanner, J C, Jr., Vandeput, J & Olley, J F (1964) The mesh skin graft. *Plast Reconstr Surg,* 34**,** 287-92.

Thiersch, J (1886) On skin grafting. *Verhandl2nd Deutsch Ges Chir,* 15**,** 17-20.

Tingstrom, A, Heldin, C H & Rubin, K (1992) Regulation of fibroblast-mediated collagen gel contraction by platelet-derived growth factor, interleukin-1 alpha and transforming growth factor-beta 1. *J Cell Sci,* 102 (Pt 2)**,** 315-22.

Tobin, D J (2006) Biochemistry of human skin--our brain on the outside. *Chem Soc Rev,* 35**,** 52-67.

Truong, A T, Kowal-Vern, A, Latenser, B A, Wiley, D E & Walter, R J (2005) Comparison of dermal substitutes in wound healing utilizing a nude mouse model. *J Burns Wounds,* 4**,** e4.

Tsao, M C, Walthall, B J & Ham, R G (1982) Clonal growth of normal human epidermal keratinocytes in a defined medium. *J Cell Physiol,* 110**,** 219-29.

van den Berg, L M, de Jong, M A, Witte, L D, Ulrich, M M & Geijtenbeek, T B (2011) Burn injury suppresses human dermal dendritic cell and Langerhans cell function. *Cell Immunol*.

van Hemert, P, Kilburn, D G & van Wezel, A L (1969) Homogeneous cultivation of animal cells for the production of virus and virus products. *Biotechnol Bioeng,* 11**,** 875-85.

van Osch, G J, Brittberg, M, Dennis, J E, Bastiaansen-Jenniskens, Y M, Erben, R G, Konttinen, Y T & Luyten, F P (2009) Cartilage repair: past and future--lessons for regenerative medicine. *J Cell Mol Med,* 13**,** 792-810.

van Wezel, A L (1967) Growth of cell-strains and primary cells on micro-carriers in homogeneous culture. *Nature,* 216**,** 64-5.

--- (1976) The large-scale cultivation of diploid cell strains in microcarrier culture. Improvement of microcarriers. *Dev Biol Stand,* 37**,** 143-7.

Vande Berg, J S & Rudolph, R (1985) Cultured myofibroblasts: a useful model to study wound contraction and pathological contracture. *Ann Plast Surg,* 14**,** 111-20.

Vardaxis, N J, Brans, T A, Boon, M E, Kreis, R W & Marres, L M (1997) Confocal laser scanning microscopy of porcine skin: implications for human wound healing studies. *J Anat,* 190 (Pt 4)**,** 601-11.

Vinatier, C, Mrugala, D, Jorgensen, C, Guicheux, J & Noel, D (2009) Cartilage engineering: a crucial combination of cells, biomaterials and biofactors. *Trends Biotechnol,* 27**,** 307-14.

Vistejnova, L, Dvorakova, J, Hasova, M, Muthny, T, Velebny, V, Soucek, K & Kubala, L (2009) The comparison of impedance-based method of cell proliferation monitoring with commonly used metabolic-based techniques. *Neuro Endocrinol Lett,* 30 Suppl 1**,** 121-7.

Vodicka, P, Smetana, K, Jr., Dvorankova, B, Emerick, T, Xu, Y Z, Ourednik, J, Ourednik, V & Motlik, J (2005) The miniature pig as an animal model in biomedical research. *Ann N Y Acad Sci,* 1049**,** 161-71.

Vogt, P M, Thompson, S, Andree, C, Liu, P, Breuing, K, Hatzis, D, Brown, H, Mulligan, R C & Eriksson, E (1994) Genetically modified keratinocytes transplanted to wounds reconstitute the epidermis. *Proc Natl Acad Sci U S A,* 91**,** 9307-11.

Voigt, M, Schauer, M, Schaefer, D J, Andree, C, Horch, R & Stark, G B (1999) Cultured epidermal keratinocytes on a microspherical transport system are feasible to reconstitute the epidermis in full-thickness wounds. *Tissue Eng,* 5**,** 563-72.

Walden, J L, Garcia, H, Hawkins, H, Crouchet, J R, Traber, L & Gore, D C (2000) Both dermal matrix and epidermis contribute to an inhibition of wound contraction. *Ann Plast Surg,* 45**,** 162-6.

Warfel, A H, Thorbecke, G J & Belsito, D V (1993) Langerhans cells as outposts of the dendritic cell system. *Adv Exp Med Biol,* 329**,** 469-80.

Watsky, M A, Weber, K T, Sun, Y & Postlethwaite, A (2010) New insights into the mechanism of fibroblast to myofibroblast transformation and associated pathologies. *Int Rev Cell Mol Biol,* 282**,** 165-92.

Webber, J, Meran, S, Steadman, R & Phillips, A (2009) Hyaluronan orchestrates transforming growth factor-beta1-dependent maintenance of myofibroblast phenotype. *J Biol Chem,* 284**,** 9083-92.

Welch, M P, Odland, G F & Clark, R A (1990) Temporal relationships of F-actin bundle formation, collagen and fibronectin matrix assembly, and fibronectin receptor expression to wound contraction. *J Cell Biol,* 110**,** 133-45.

Werner, S, Krieg, T & Smola, H (2007) Keratinocyte-fibroblast interactions in wound healing. *J Invest Dermatol,* 127**,** 998-1008.

Williamson, J S, Snelling, C F, Clugston, P, Macdonald, I B & Germann, E (1995) Cultured epithelial autograft: five years of clinical experience with twenty-eight patients. *J Trauma,* 39**,** 309-19.

Wipff, P J, Rifkin, D B, Meister, J J & Hinz, B (2007) Myofibroblast contraction activates latent TGF-beta1 from the extracellular matrix. *J Cell Biol,* 179**,** 1311-23.

Wissemann, K W & Jacobson, B S (1985) Pure gelatin microcarriers: synthesis and use in cell attachment and growth of fibroblast and endothelial cells. *In Vitro Cell Dev Biol,* 21**,** 391-401.

Wong, V W, Sorkin, M, Glotzbach, J P, Longaker, M T & Gurtner, G C (2011) Surgical approaches to create murine models of human wound healing. *J Biomed Biotechnol,* 2011**,** 969618.

Wood, F M, Kolybaba, M L & Allen, P (2006) The use of cultured epithelial autograft in the treatment of major burn injuries: a critical review of the literature. *Burns,* 32**,** 395-401.

Wood, F M, Stoner, M L, Fowler, B V & Fear, M W (2007) The use of a non-cultured autologous cell suspension and Integra dermal regeneration template to repair full-thickness skin wounds in a porcine model: a one-step process. *Burns,* 33**,** 693-700.

Worst, P K, Valentine, E A & Fusenig, N E (1974) Formation of epidermis after reimplantation of pure primary epidermal cell cultures from perinatal mouse skin. *J Natl Cancer Inst,* 53**,** 1061-4.

Wu, Y J, Parker, L M, Binder, N E, Beckett, M A, Sinard, J H, Griffiths, C T & Rheinwald, J G (1982) The mesothelial keratins: a new family of cytoskeletal proteins identified in cultured mesothelial cells and nonkeratinizing epithelia. *Cell,* 31**,** 693-703.

Wust, K J (2006) A modified dynamic mouth splint for burn patients. *J Burn Care Res,* 27**,** 86-92.

Xie, F, Wang, J, Li, Q, Zhou, S, Zan, T, Gu, B & Liu, K (2012) Resurfacing large skin defects of the face and neck with expanded subclavicular flaps pedicled by the thoracic branch of the supraclavicular artery. *Burns*.

Yang, L, Hashimoto, K, Tohyama, M, Okazaki, H, Dai, X, Hanakawa, Y, Sayama, K & Shirakata, Y (2012) Interactions between myofibroblast differentiation and epidermogenesis in constructing human living skin equivalents. *J Dermatol Sci,* 65**,** 50-7.

Yim, H, Cho, Y S, Seo, C H, Lee, B C, Ko, J H, Kim, D, Hur, J, Chun, W & Kim, J H (2010) The use of AlloDerm on major burn patients: AlloDerm prevents post-burn joint contracture. *Burns,* 36**,** 322-8.

Zaroff, L I, Mills, W, Jr., Duckett, J W, Jr., Switzer, W E & Moncrief, J A (1966) Multiple uses of viable cutaneous homografts in the burned patient. *Surgery,* 59**,** 368-72.

Zawacki, B E (1974) Reversal of capillary stasis and prevention of necrosis in burns. *Ann Surg,* 180**,** 98-102.

Zhang, X, Deng, Z, Wang, H, Yang, Z, Guo, W, Li, Y, Ma, D, Yu, C, Zhang, Y & Jin, Y (2009) Expansion and delivery of human fibroblasts on micronized acellular dermal matrix for skin regeneration. *Biomaterials,* 30**,** 2666-74.